PROJETO Energia
Heliotérmica

Concentrated Solar Power

Fundamentals, Technology and Economics

Lecturer: Dr.-Celso Eduardo Lins de Oliveira
Prepared by: Prof. Dr.-Ing. Olaf Goebel

February 2016

PROJETO Energia Heliotérmica

Universidade de São Paulo – USP

FZEA USP

Pirassununga, February 15 to 19, 2016

2015/2016 CSP EM FOCO

cooperação alemã
DEUTSCHE ZUSAMMENARBEIT

Por meio da:

giz Deutsche Gesellschaft für Internationale Zusammenarbeit (GIZ) GmbH

Content of the Course

Learning Targets

Students attending this course shall learn how to:

1) Investigate and judge the solar resource at a site
2) Prepare a concept design of a CSP plant
3) Simulate the energy yield of a CSP plant with given solar irradiation data
4) Perform a site selection for a CSP project
5) Calculate electricity generation cost of a CSP plant

Introduction:

Reasons for Using Solar Energy

Two Reasons for the Utilization of Renewable Energies

1) Fossil Fuels are running out. Remaining ‘production’ time:
   - oil: 40 years*
   - natural gas: 40 years*
   - coal: 200 years*

*static reach

2) The “Greenhouse Effect”
   - Burning fuel generates CO_2
   - CO_2 reflects infrared radiation
   - The Planet has “closed windows” and heats up
   - Climate starts to change

The Problem of Depleting Fossil Energy Resources

- Fuels are the ‘blood’ of modern economy
- Fuels become scarce
- Fuels become more expensive (oil price increased sixfold 2001 to 2008)
  (The current low of oil prices is expected to last not very much longer)
- Only rich countries can afford to buy fuels
- Poor countries will have no chance for Development
- Conflicts will arise for the access to the fuel sources (Iraq)

- Renewable Energies will ease these problems!

Regional Distribution of Oil Reserves

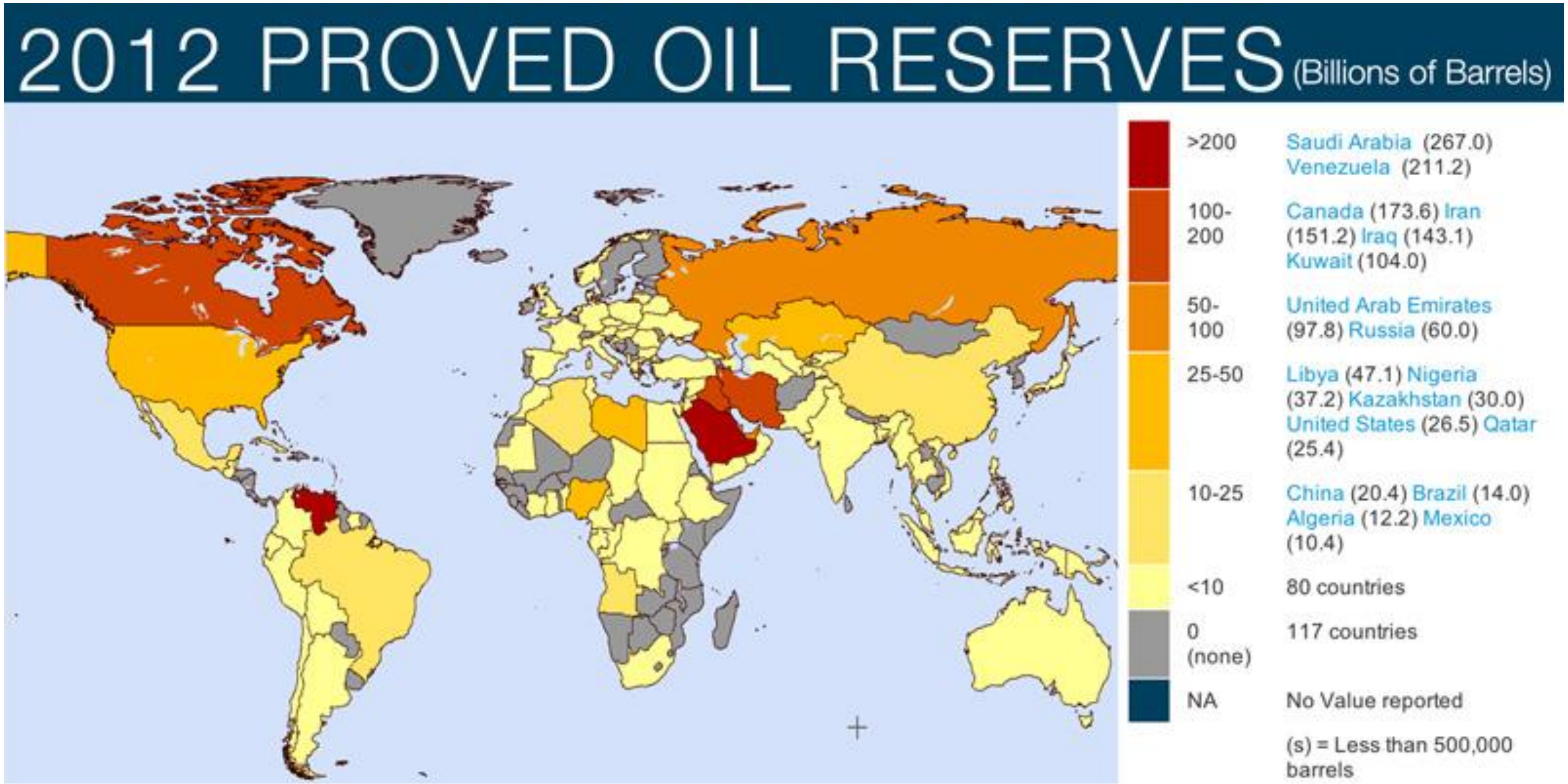

Source: zion oil&gas

Regional Distribution of Oil Reserves

Reserves by Region, end-2011

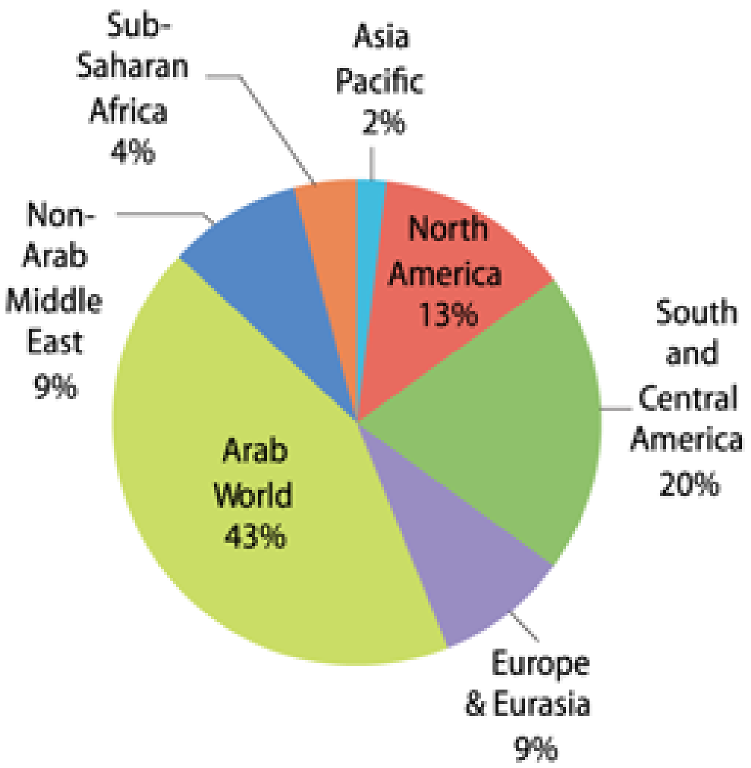

Production by Region, 2011

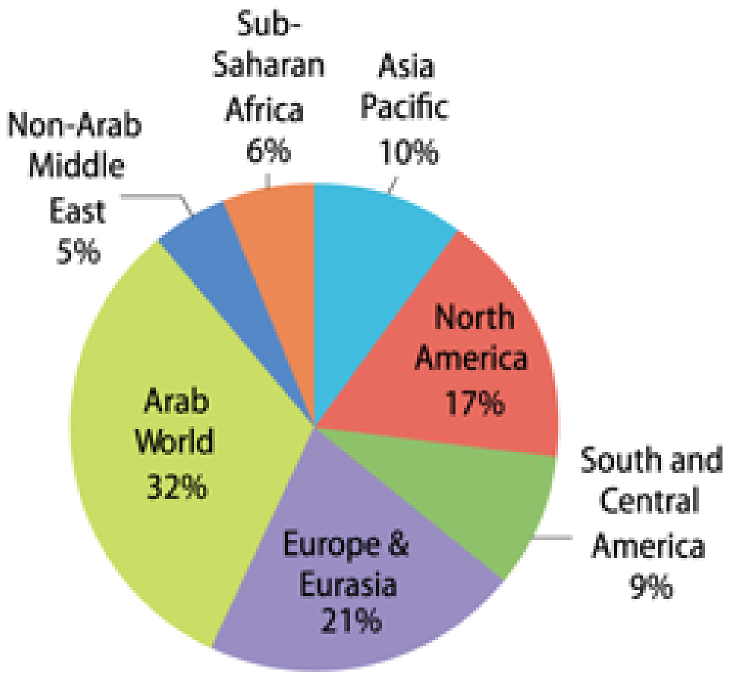

World Crude Oil Production 1930 - 2012

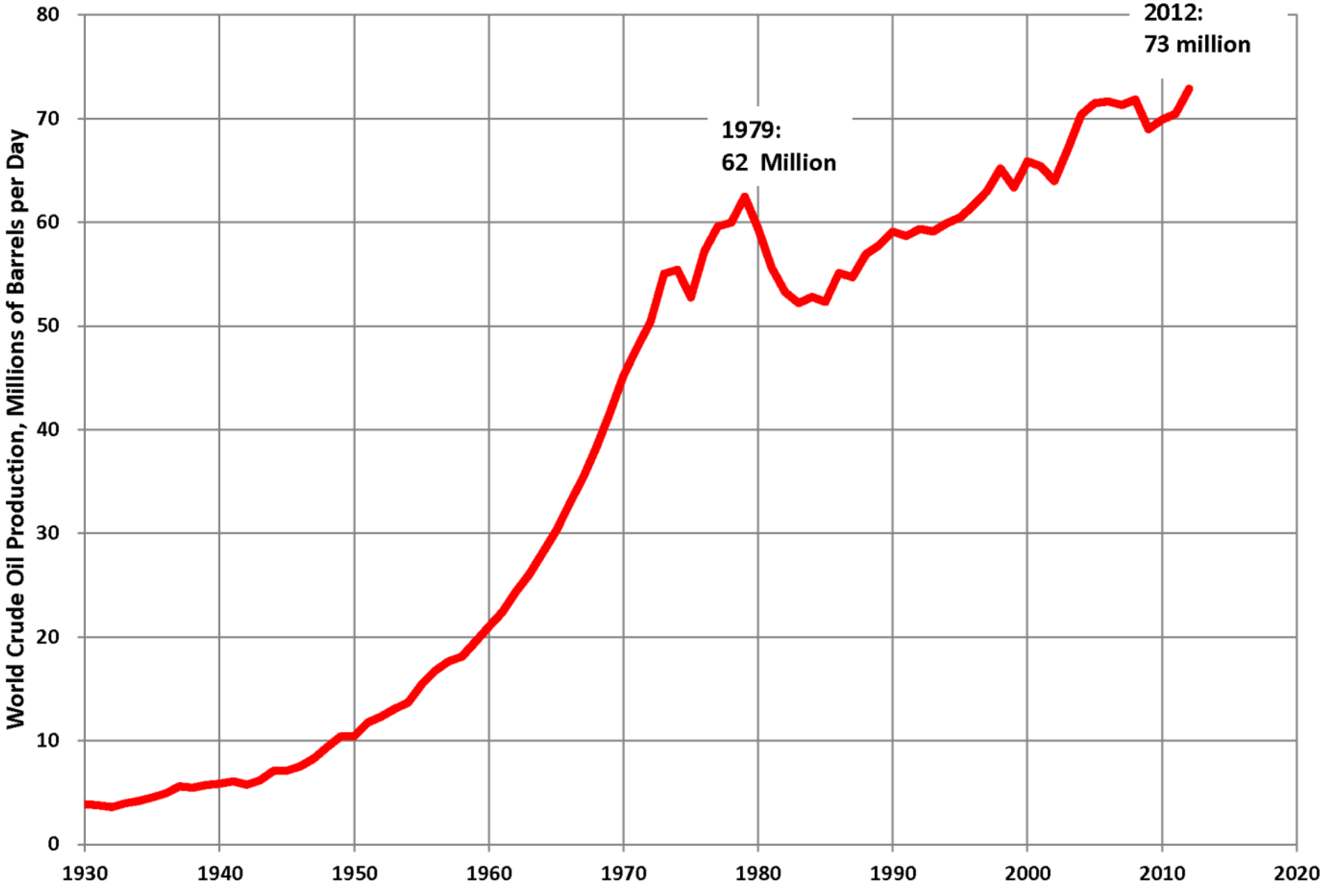

Source: Wikipedia: https://en.wikipedia.org/wiki/Peak_oil

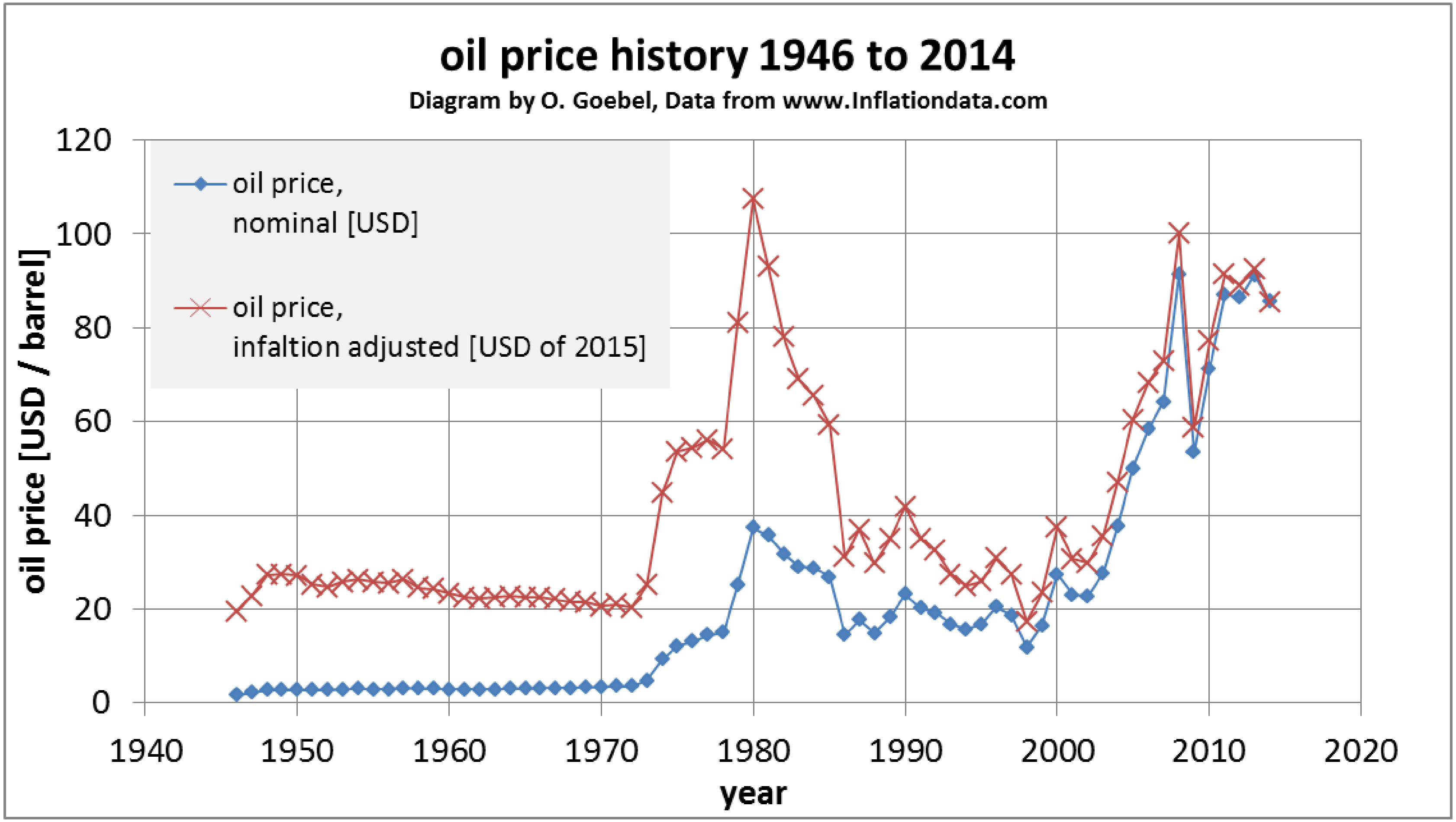
oil price history 1946 to 2014
Diagram by O. Goebel, Data from www.Inflationdata.com
oil price, nominal [USD]
oil price, infaltion adjusted [USD of 2015]
oil price [USD / barrel]
0
20
40
60
80
100
120
1940
1950
1960
1970
1980
1990
2000
2010
2020
year

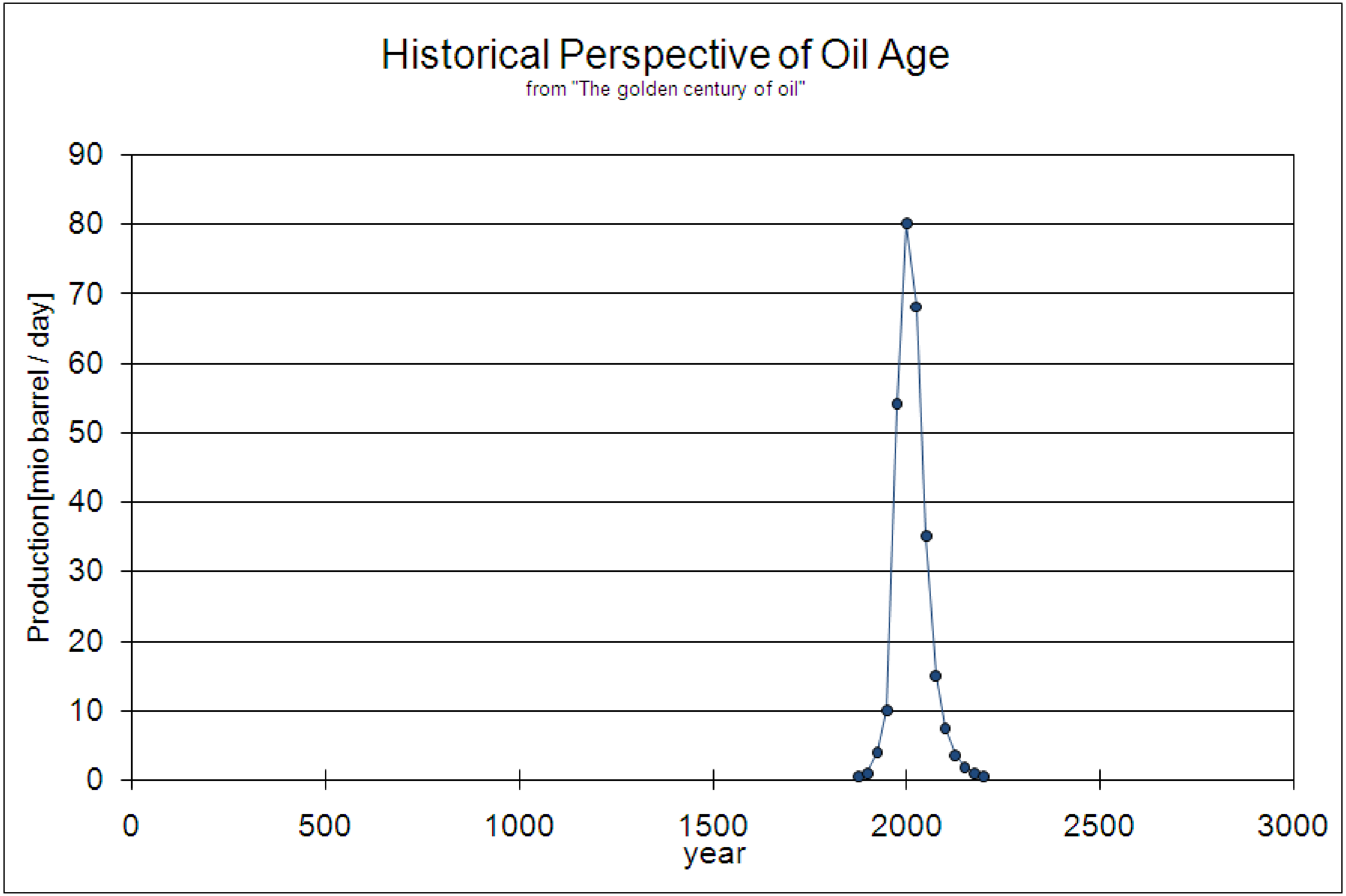

Historical Perspective of Oil Age

from "The golden century of oil"

Greenhouse Effect 1/6

- **The natural CO_2 circuit**

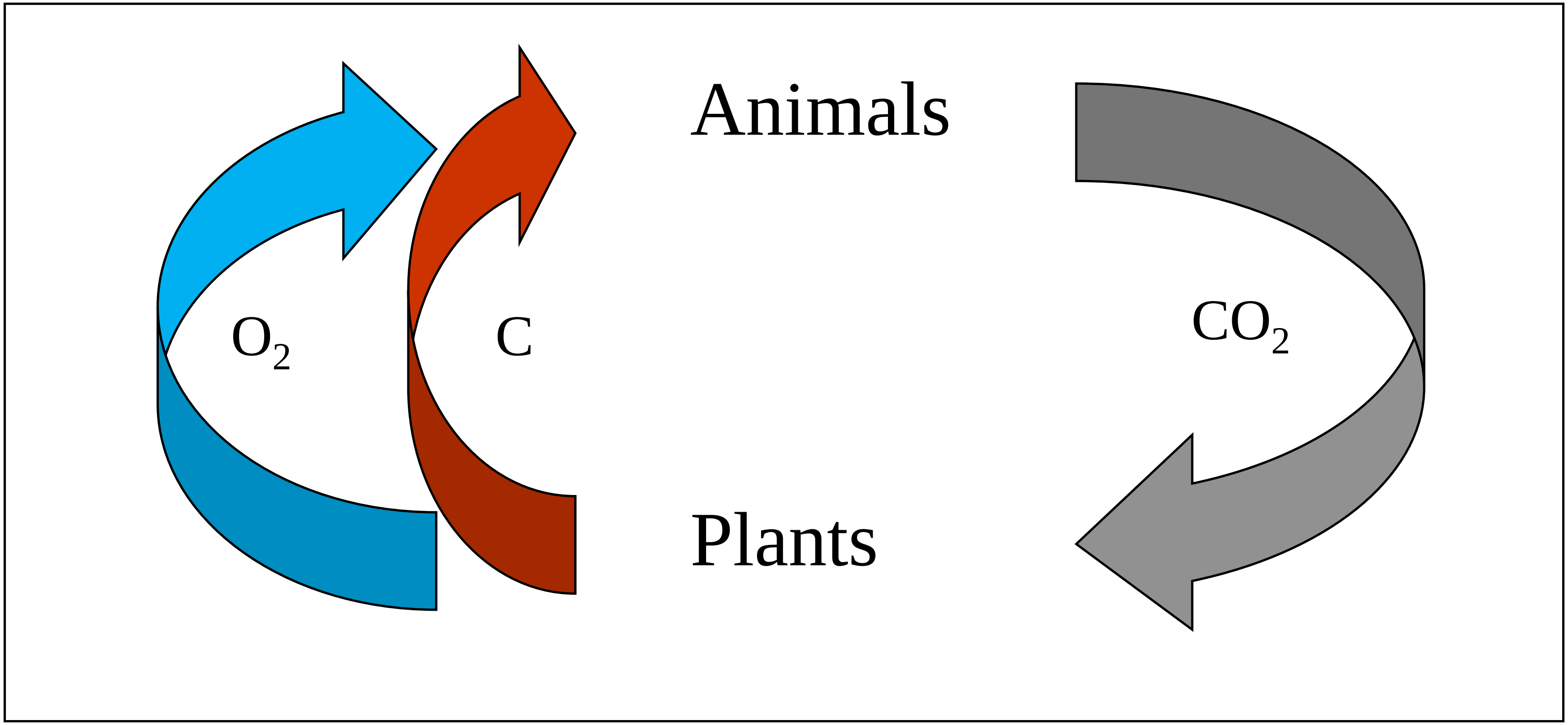

Greenhouse Effect 2/6

- Today’s CO_2 “Circuit”

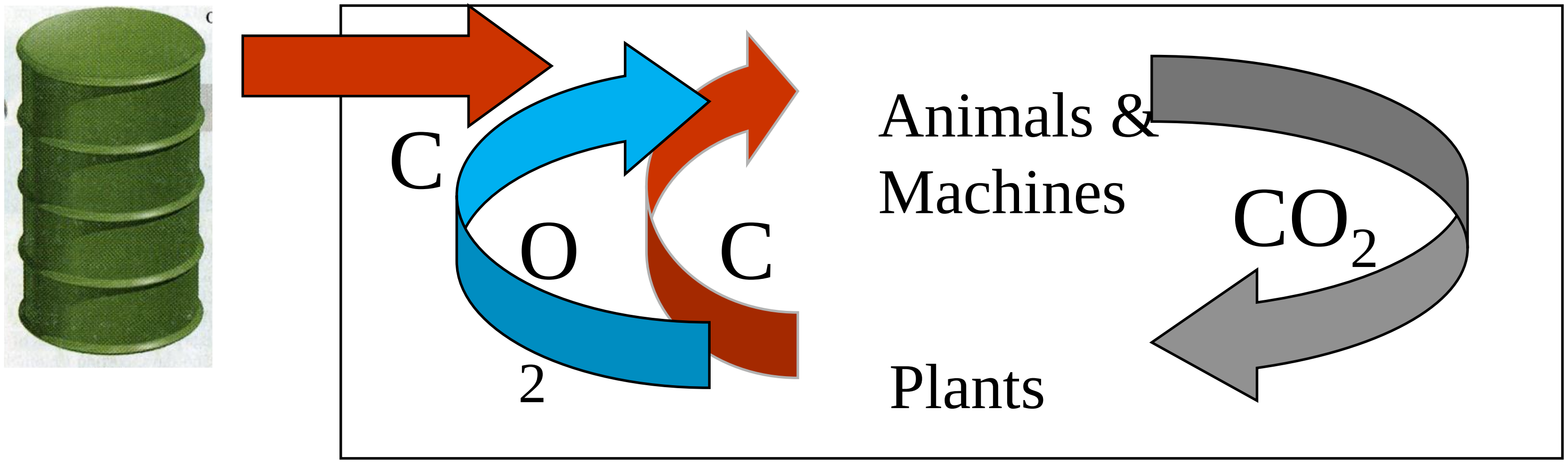

- Today machines generate much more CO_2 than animals
- C (carbon) is added to the circuit by burning fossil fuels
- Plant population on Earth is reduced (cutting of rain forest)

Greenhouse Effect 3/6

- Rising CO_2 content of our atmosphere

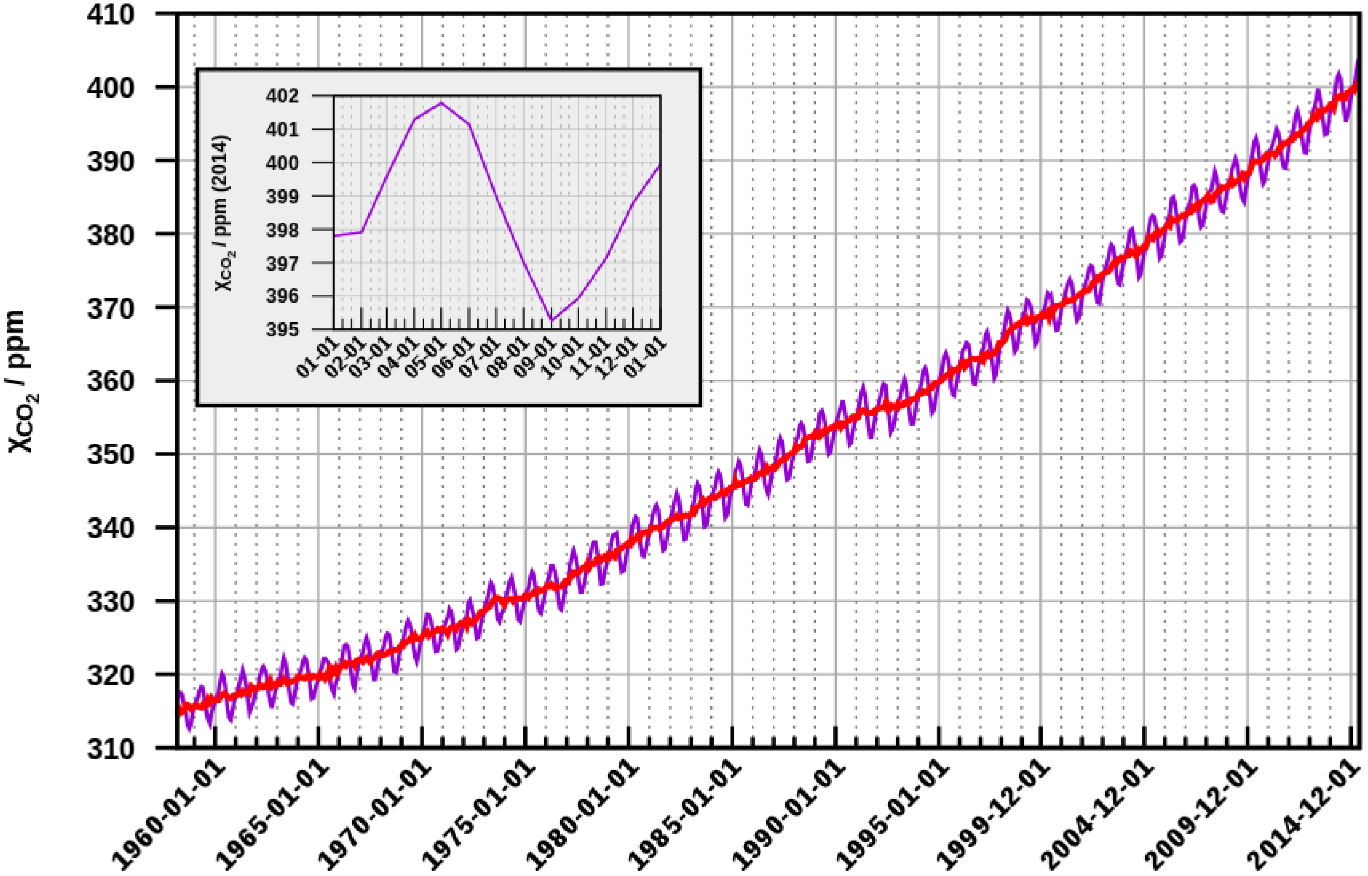

Source:https://de.wikipedia.org/wiki/Keeling-Kurve#/media/File:Mauna_Loa_Carbon_Dioxide.svg

PROJETO Energia Heliotérmica

Greenhouse Effect 4/6

- Rising CO_2 content of our atmosphere

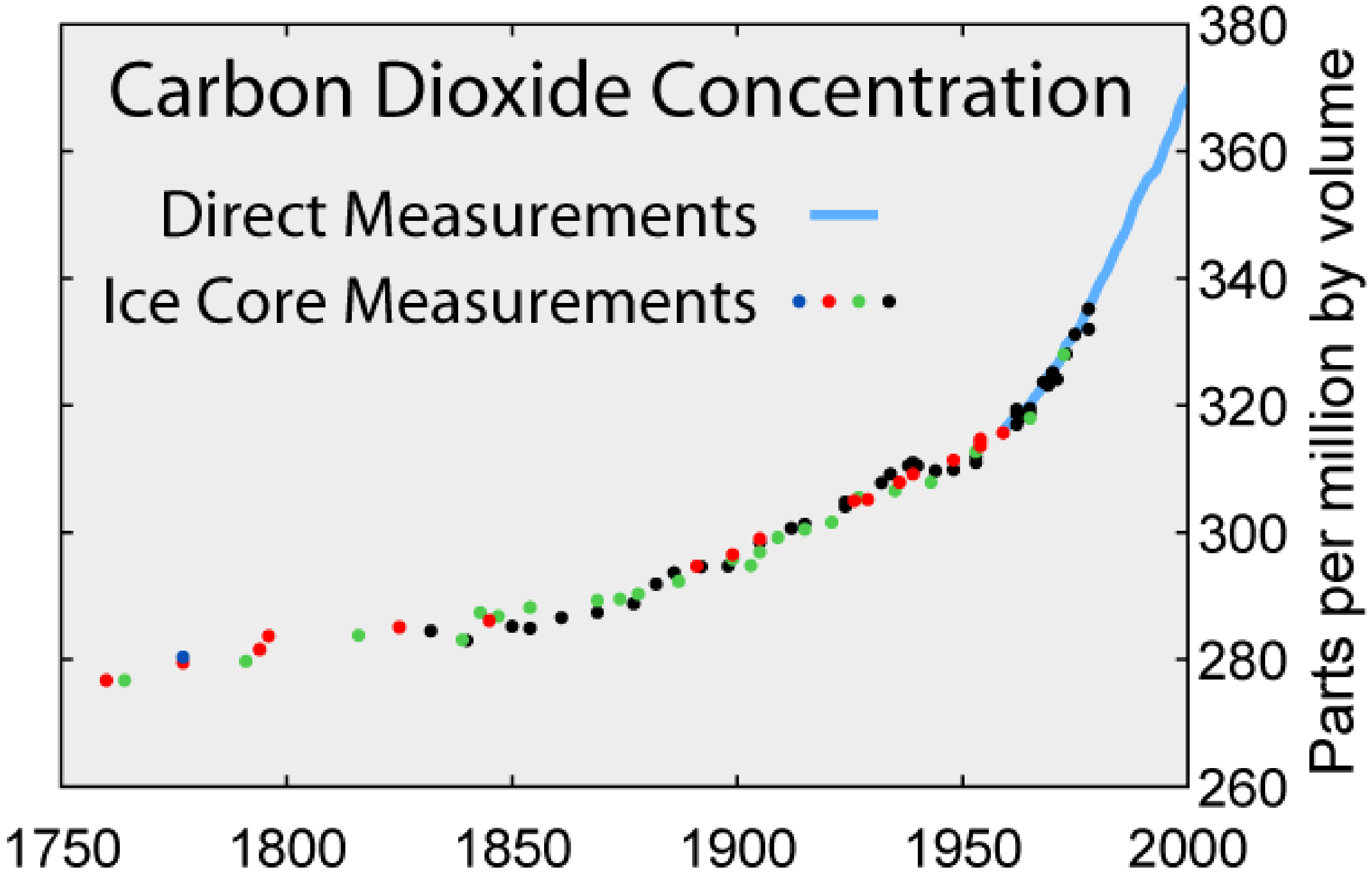

Source: Windows to the Universe

Greenhouse Effect 5/6

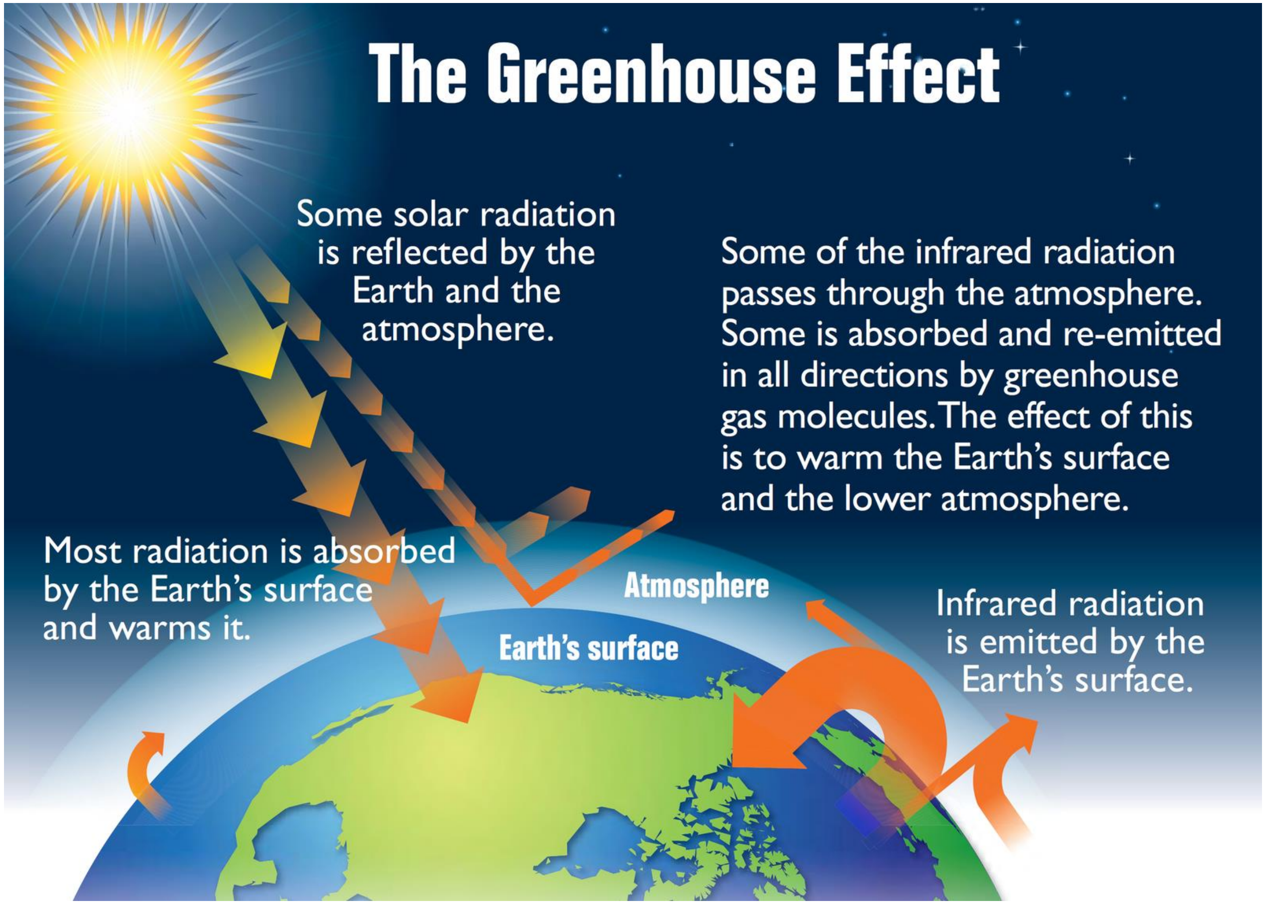

https://commons.wikimedia.org/wiki/File:Earth%27s_greenhouse_effect_(US_EPA,_2012).png

Greenhouse Effect 6/6

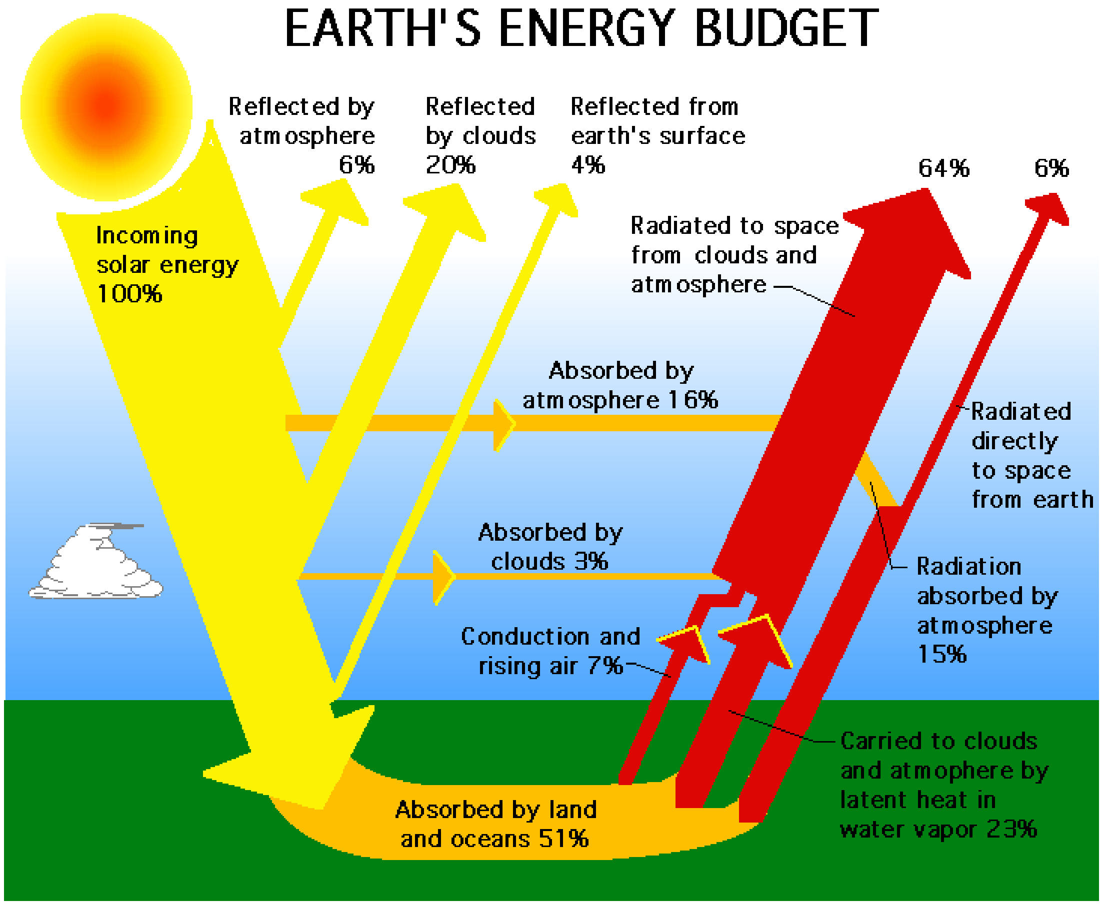

The Basics of Solar Irradiation

Solar Irradiation is an Electro-Magnetic Wave

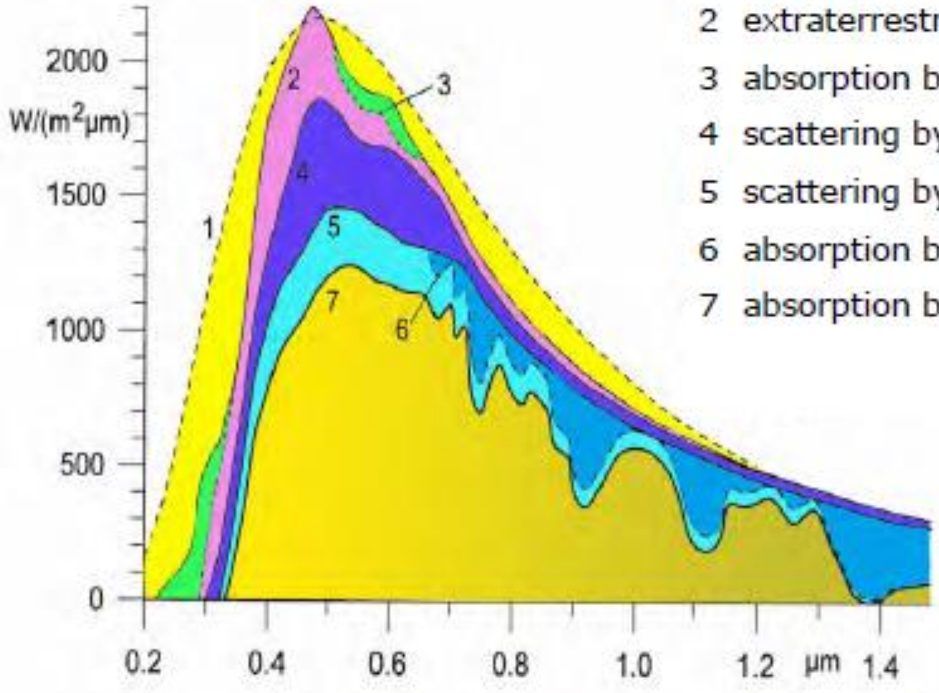

1 Planck curve T=5780 K at mean sun-earth distance

2 extraterrestrial solar spectrum

3 absorption by O_3

4 scattering by O_2 und N_2

5 scattering by aerosols

6 absorption by H_2O vapor

7 absorption by aerosols

UV radiation:	0.01 - 0.39 µm, ~ 7 %
Visible Spectrum:	0.39 – 0.75 µm, ~ 46 %
Near infrared:	0.75 – 2.5 µm, ~ 47 %

www.volker-quaschning.de/articles/fundamentals1/index.php

Solar Irradiation

- The sun irradiates a power (Luminosity of the sun, L) of:
- L = 3.846 * 10^{26} W
- The average distance between earth and sun (called "Astronomical Unit", AU) is:
- AU = 149.6 million km
- The flux density of the solar irradiation, I at this distance is:
- I = $\frac{L}{AU^2 * 4 * \pi} = \frac{3.846 * 10^{26} W}{(149.6 * 10^9 m)^2 * 4 * \pi} = \frac{3.846 * 10^{26} W}{2.8124 * 10^{23} m^2} = 1367 \frac{W}{m^2}$
- In reality this value is not constant over the year, due to the eccentricity of the earth's orbit around the sun

The Eccentricity of the Earth’s Orbit and resulting variation of Solar Irradiation, I

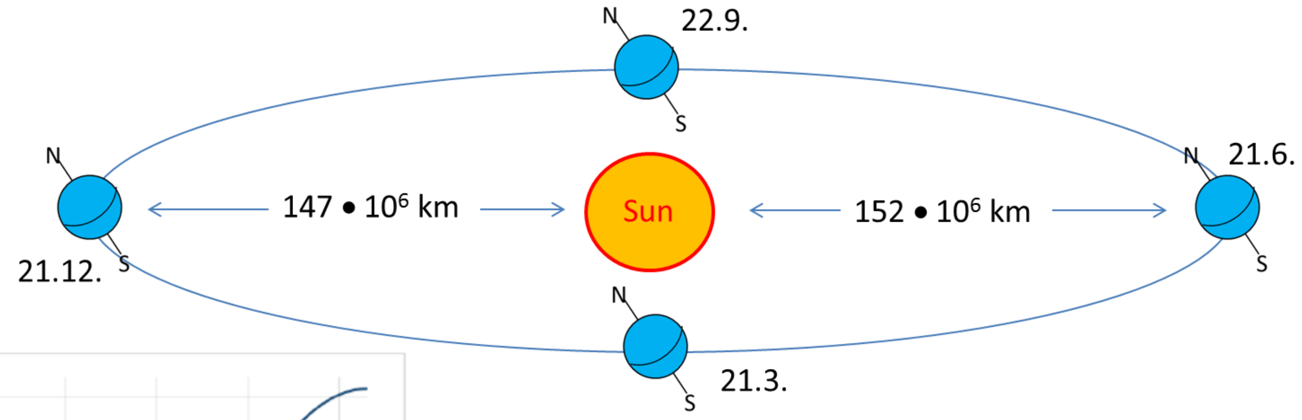

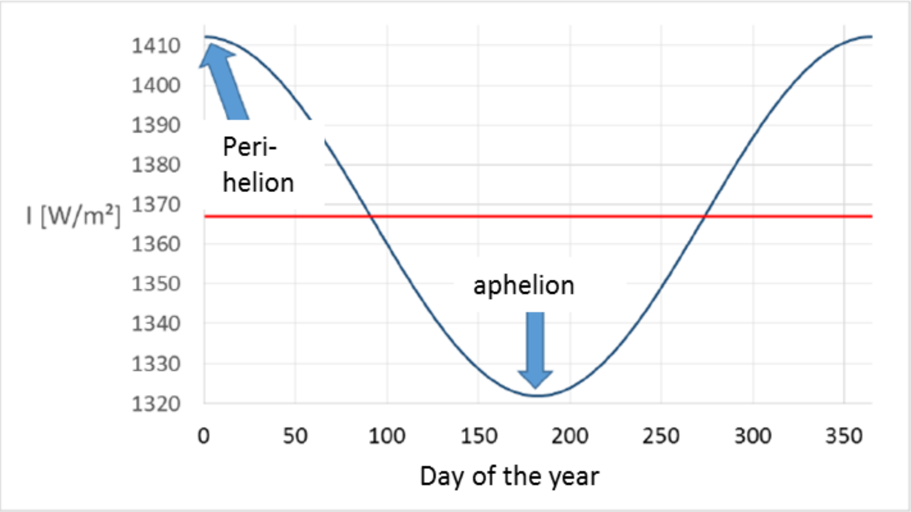

Source: Vorlesung „Nutzung Solarer Strahlungsenergie“ Universität Kassel

The Tilt of the Earth Axis Against the Ecliptic Plane

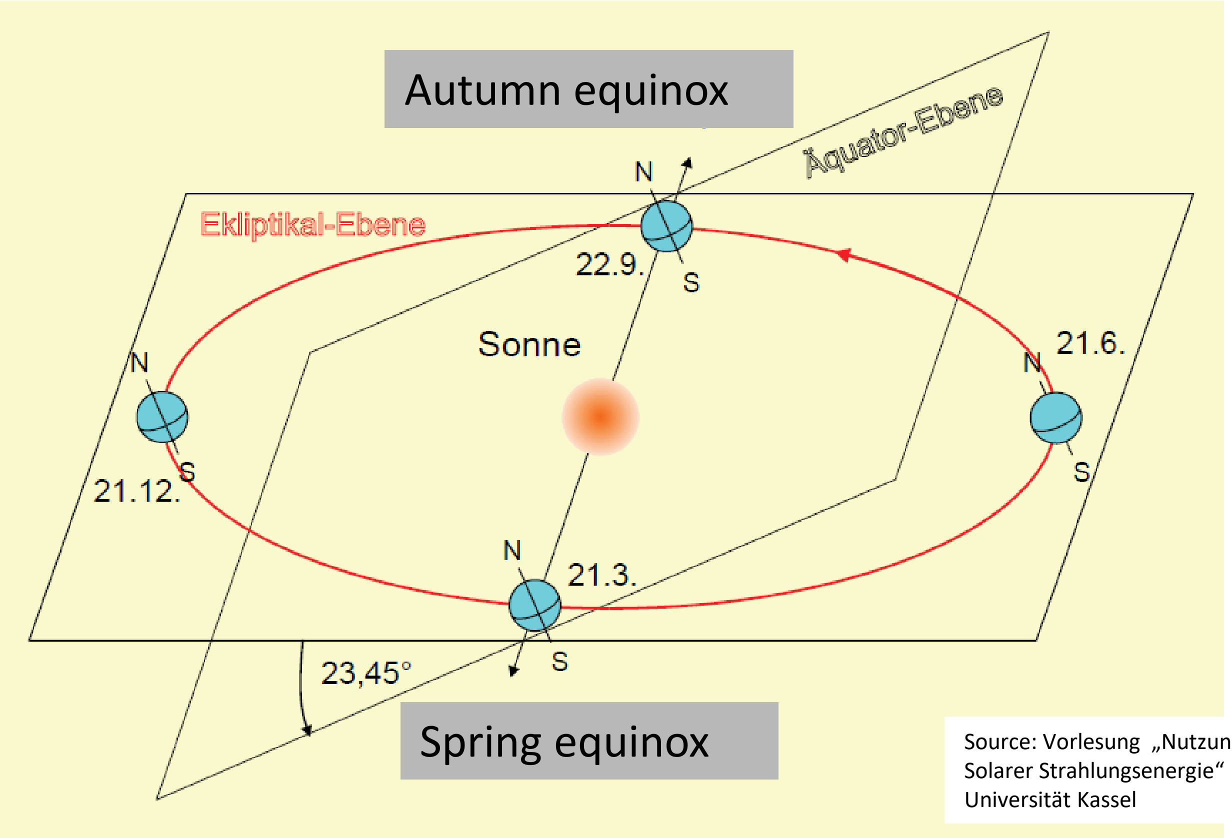

Source: Vorlesung „Nutzung Solarer Strahlungsenergie“ Universität Kassel

Reason for the Seasons

- The seasons are caused by the tilt of the earth's axis (and not by the distance earth – sun)
- The declination angle, δ can be calculated with the equation below

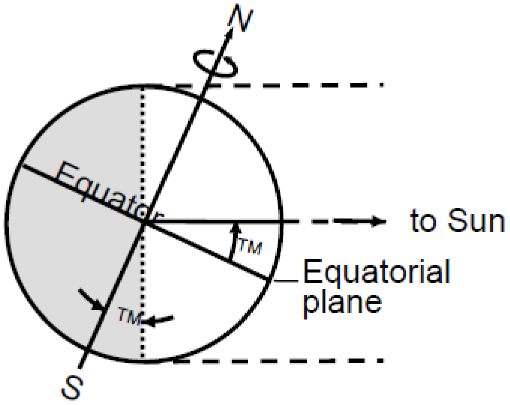

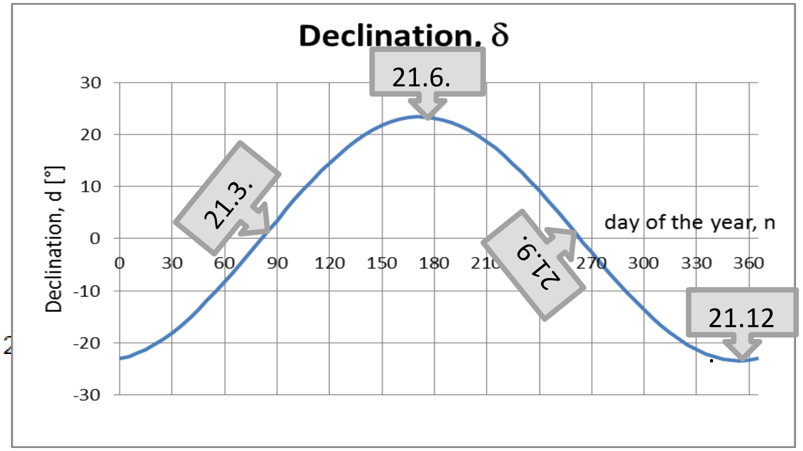

Declination angle $\delta = 23.45°$

Variation of the declination angle:

$$\delta = 23.45 * \sin [360 / 365 * (284 + n)]$$

with n = day of the year

δ_{max} = the tilt angle of earth's axis = 23.45°

Source: Duffie Beckman

Reduction of Solar Irradiation Along its Way Through the Atmosphere

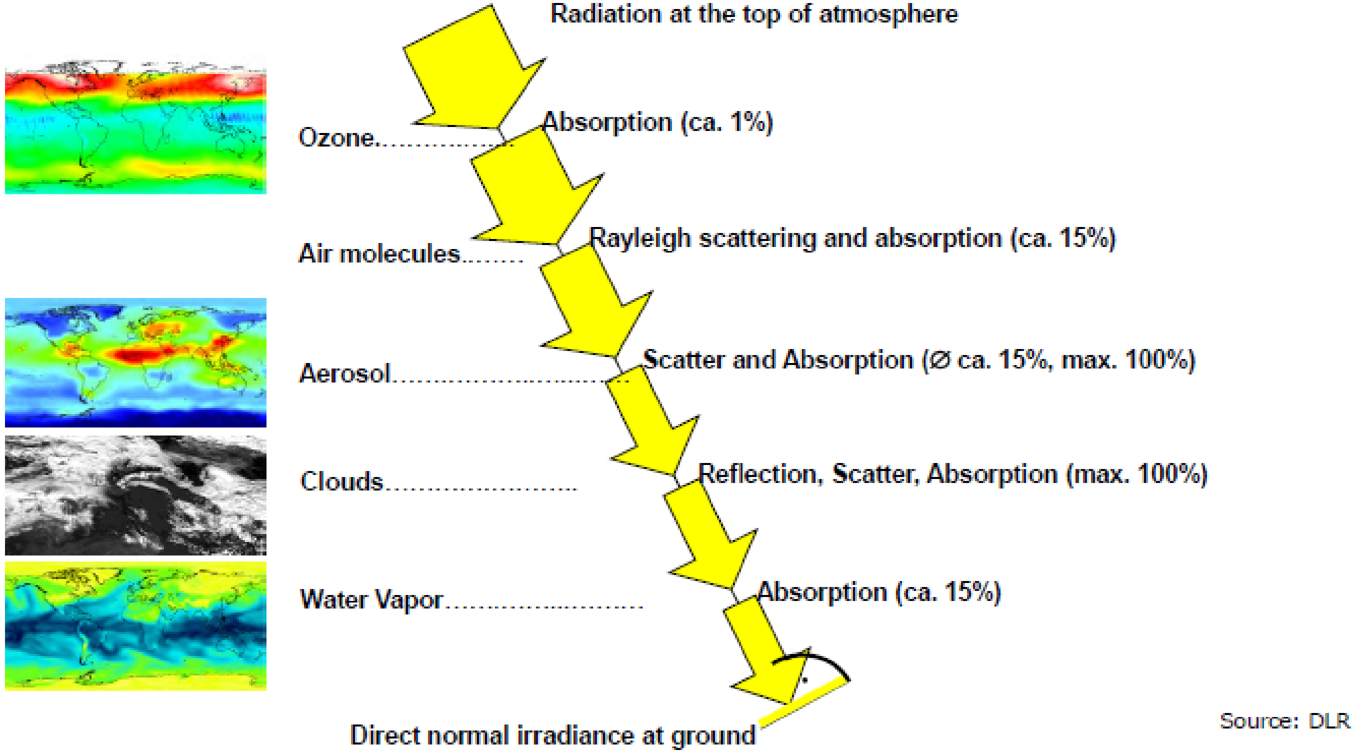

Radiation at the top of atmosphere

Ozone……………… Absorption (ca. 1%)

Air molecules……. Rayleigh scattering and absorption (ca. 15%)

Aerosol…………………………. Scatter and Absorption (∅ ca. 15%, max. 100%)

Clouds…………………… Reflection, Scatter, Absorption (max. 100%)

Water Vapor……………………. Absorption (ca. 15%)

Direct normal irradiance at ground

Source: DLR

The Definition of (Relative) Air Mass, AM

- The (relative) air mass, AM describes the multiple of path length through the atmosphere compared to the shortest way (perpendicular to the ground)
- AM = 1 / sin ε   ε = elevation angle

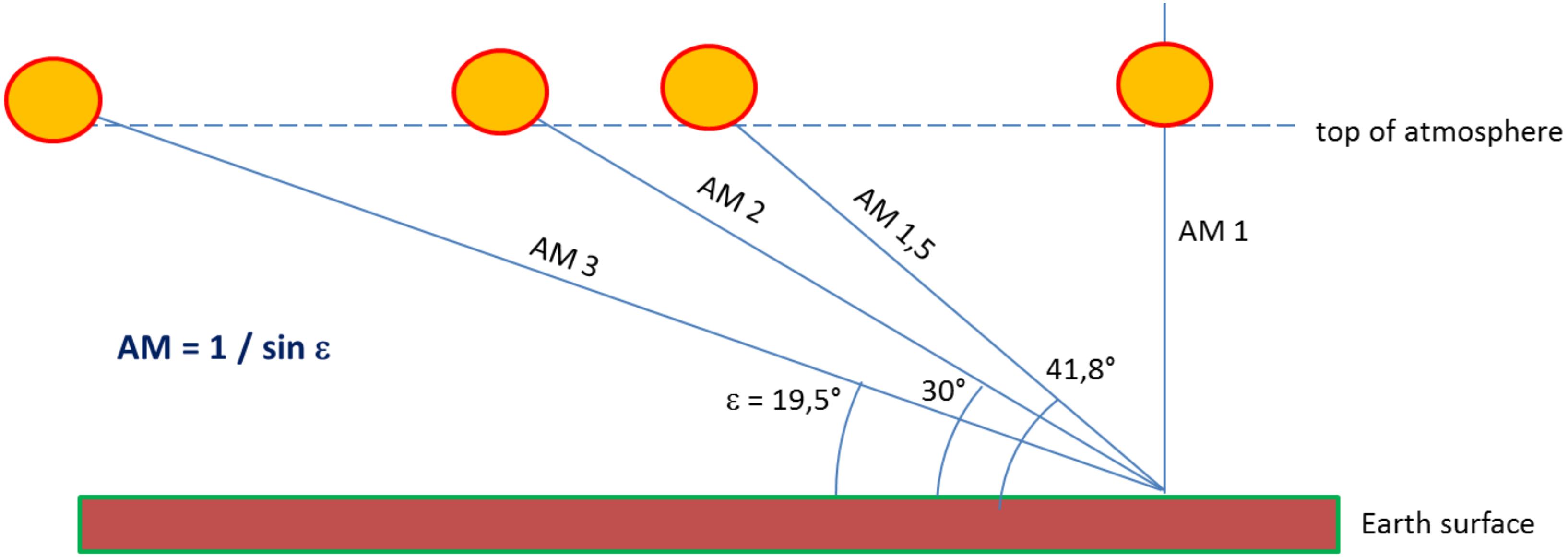

Radiative Transfer in the Atmosphere

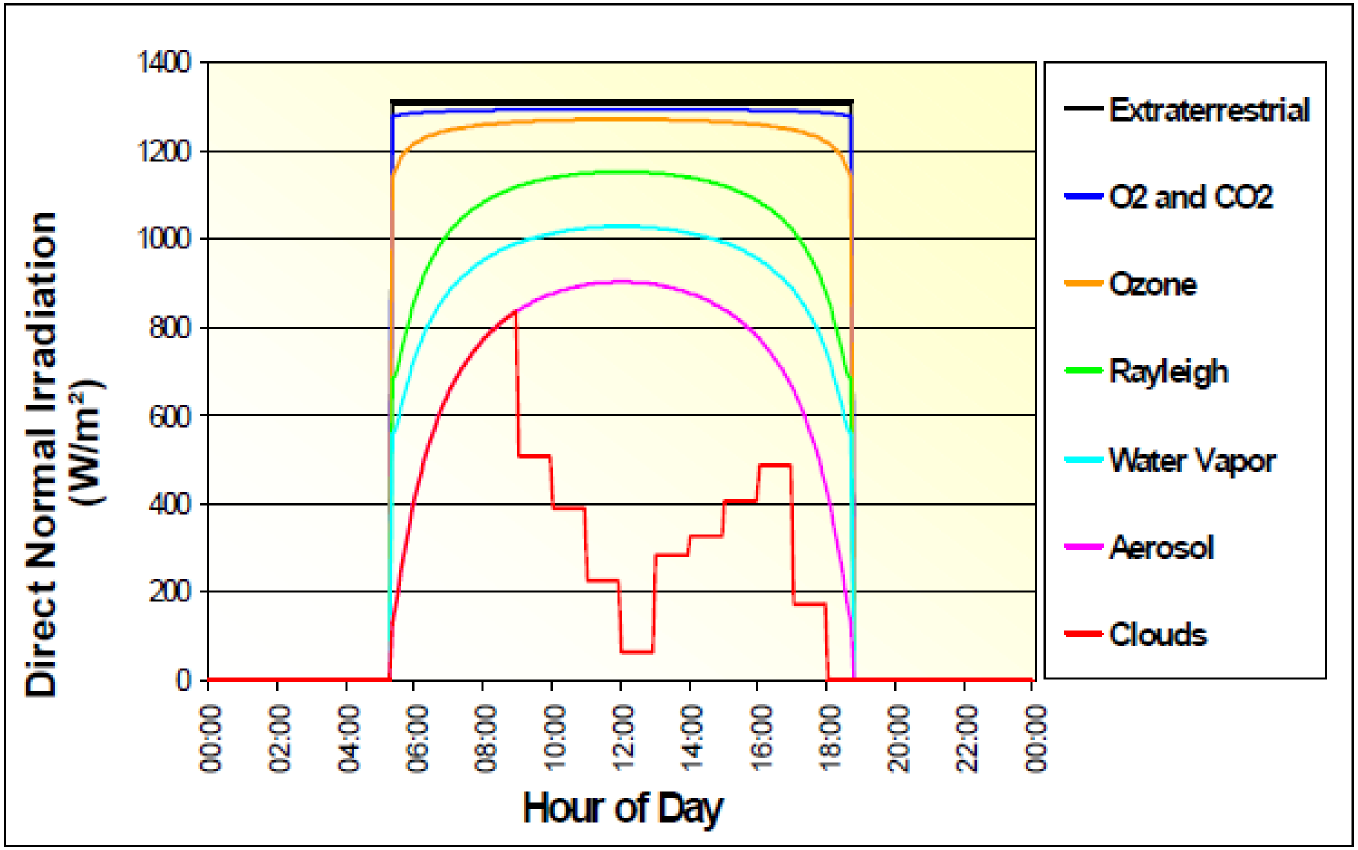

Source: Masdar / CSP Services

Atmospheric Extinction Mechanisms

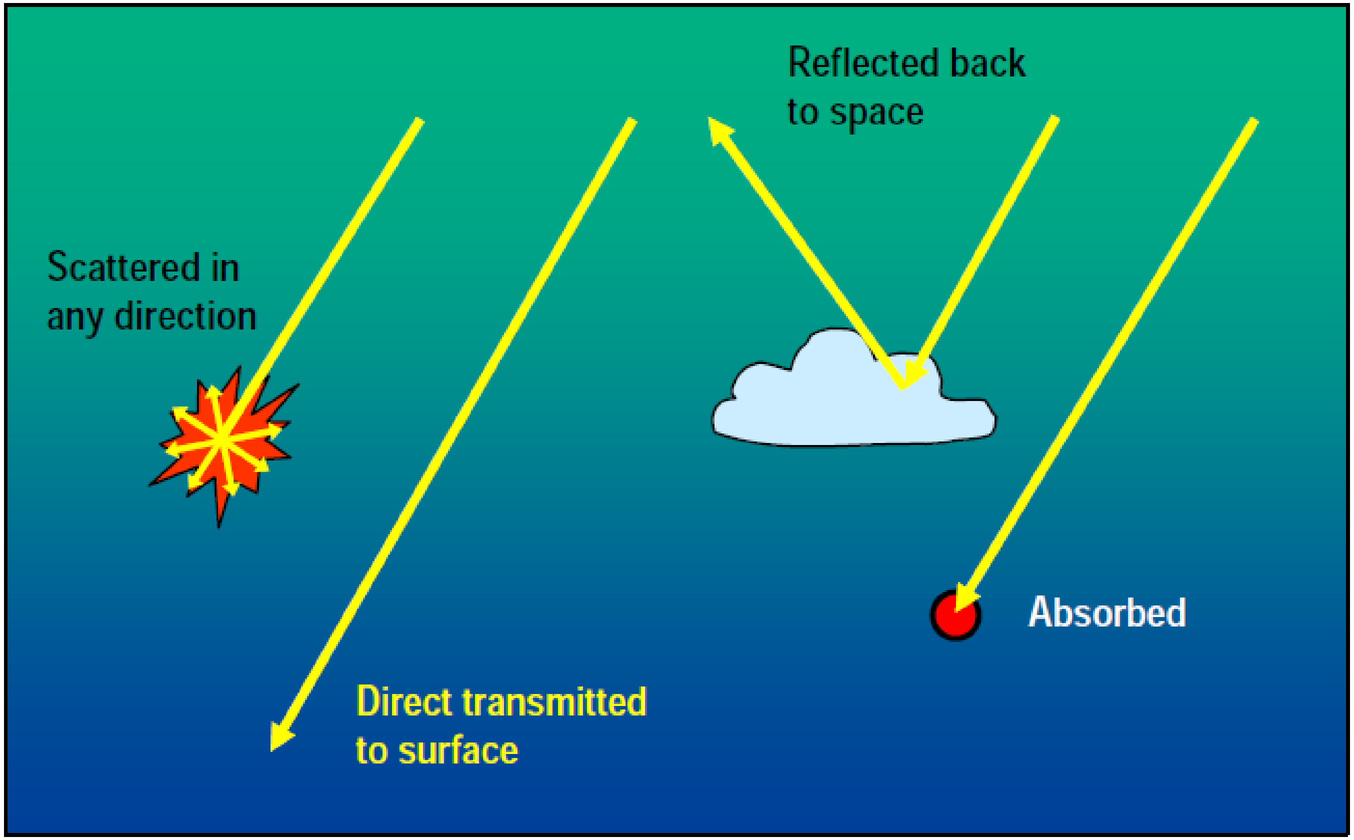

Source: Masdar / CSP Services

Different Scattering Mechanisms

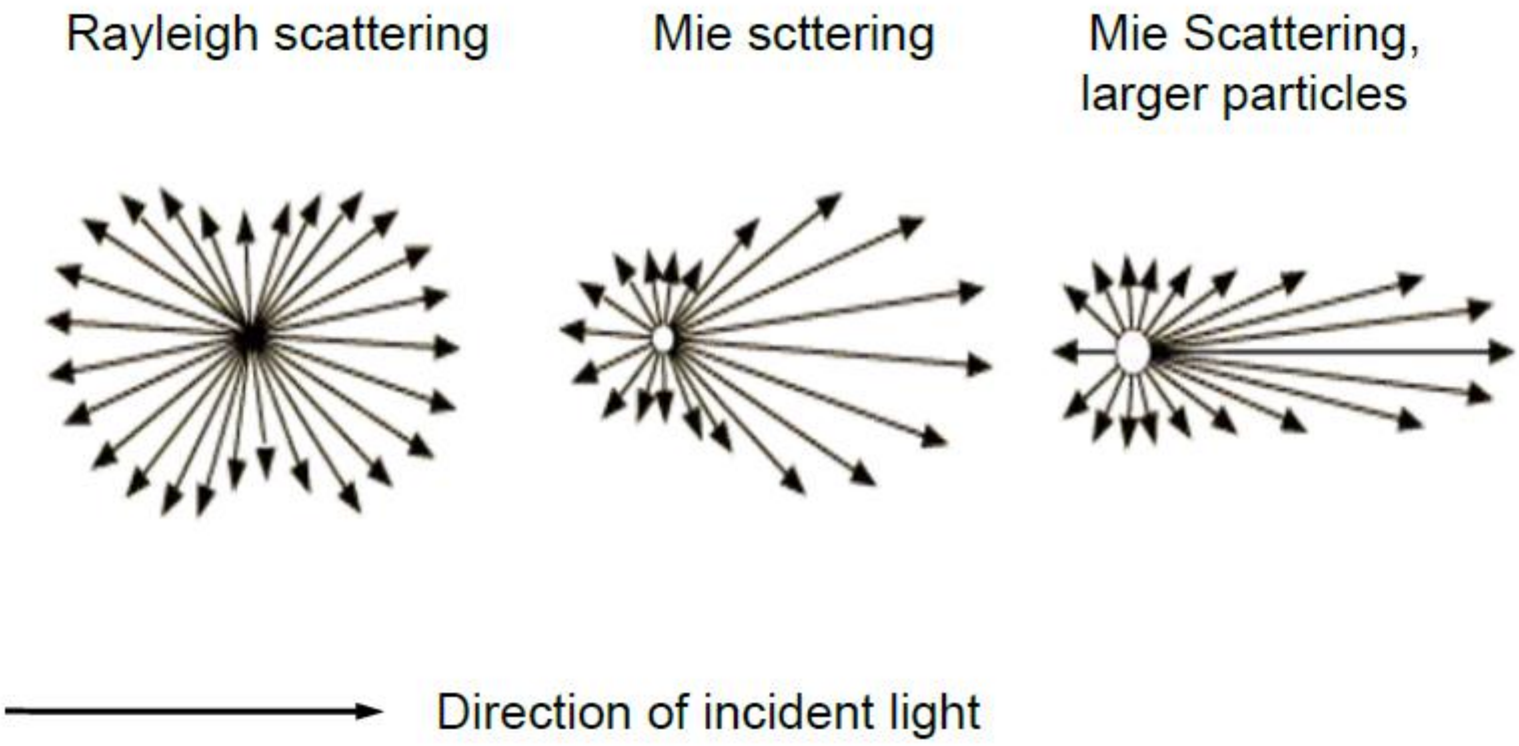

Source: Masdar / CSP Services

Direct and Diffuse Irradiation

- Due to the above mentioned scattering mechanisms two different types of irradiation are measured on the Earth’s surface:
- Direct Irradiation and
- Diffuse Irradiation
- The Direct Irradiation comes directly from the direction where the sun is
- The Diffuse Irradiation comes from all directions above the horizon
- The sum of both is called Global Irradiation

Inclined Irradiation is less dense at a Horizontal Surface [kW / m²]

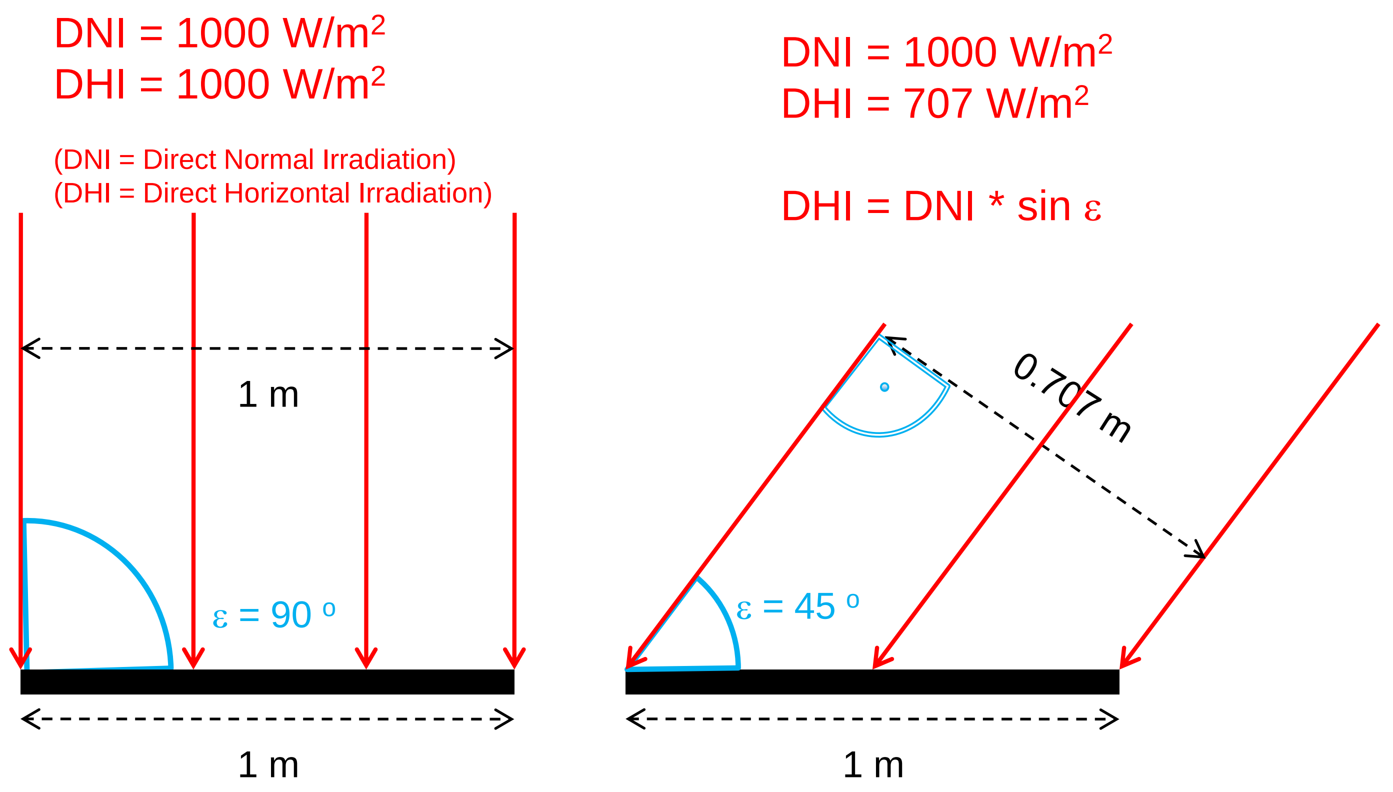

DNI = 1000 W/m²
DHI = 1000 W/m²

(DNI = Direct Normal Irradiation)
(DHI = Direct Horizontal Irradiation)

DNI = 1000 W/m²
DHI = 707 W/m²

DHI = DNI * sin ε

Horizontal or Normal

- We also distinguish on what target we receive the Irradiation:
- Horizontal surface (Letter “H” at 2nd position)
- Surface Normal to Direct Beam (Letter “N” at 2nd position)
- $\mathrm{DHI} = \mathrm{DNI} * \sin \varepsilon$ (ε, “epsilon” is the elevation angle of the sun)
- If there is Diffuse Irradiation in addition to the Direct Irradiation (which is always the case), then the Global Horizontal Irradiation (GHI) is: $\mathrm{GHI} = \mathrm{DHI} + \mathrm{DIF}$
- DIF = Diffuse Irradiation

Global Horizontal Irradiation, GHI

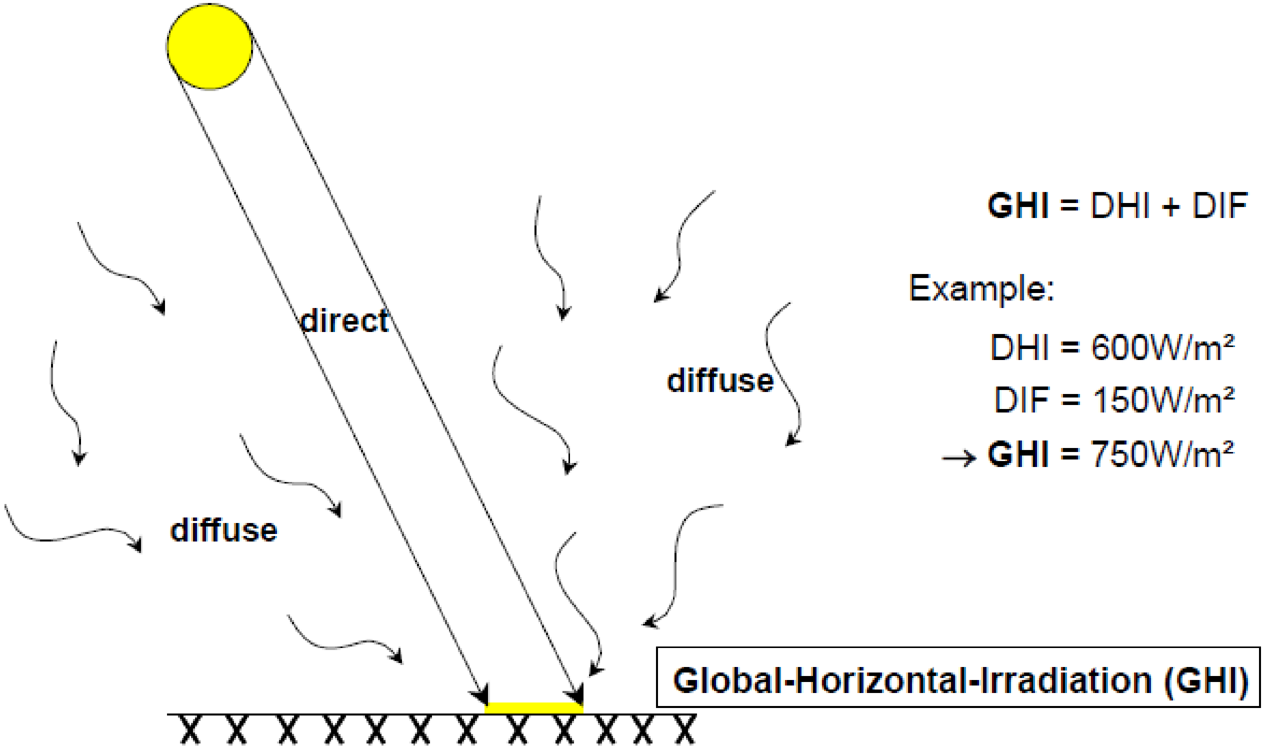

GHI = DHI + DIF

Example:

DHI = 600W/m²

DIF = 150W/m²

→ **GHI** = 750W/m²

Source: Masdar / CSP Services

Measured DNI and GHI in Madinat Zayed, Abu Dhabi, UAE

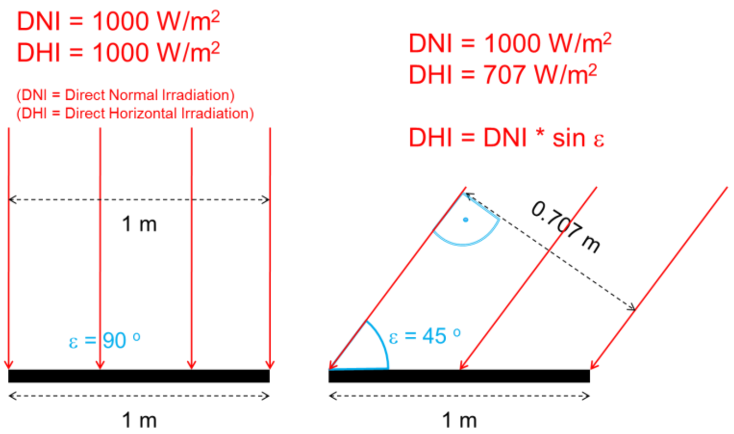

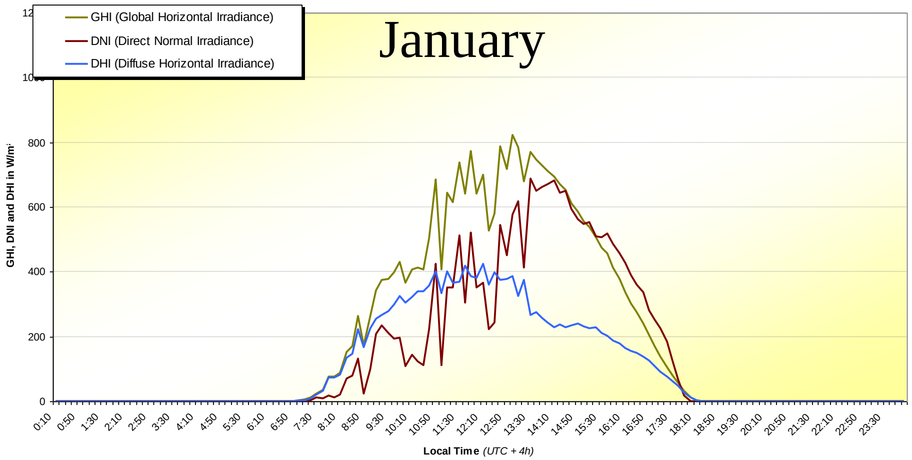

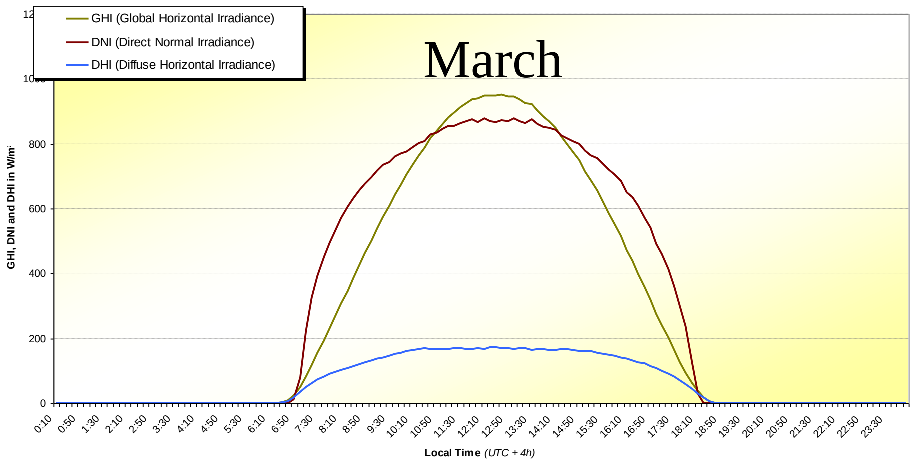

The diagrams show:

- GHI (Global Horizontal Irradiation)
- DNI (Direct Normal Irradiation)
- DHI (Diffuse Horizontal Irradiation)

Here it is important to note the difference between ”Horizontal“ and “Normal“ ! “Horizontal“ is the flux density on a horizontal plane, while “Normal“ is the flux density on a plane normal to the direct beam.

Conversion from “Normal“ to “Horizontal“:

- DHI = DNI * sin (Elevation Angle, ε)

The Elevation Angle, ε is the angle of the sun above the horizon. At low ε the flux density on a horizontal plan is much smaller than on the plane perpendicular to the direct beam. Note the Diagram for March, where DNI is much higher than GHI in the morning and evening.

Attention: Because the letter “D” stands for “Direct” and “Diffuse” as well, there is potential for confusion.

Direct + Diffuse = Global (only for the same plane!)

PROJETO Energia Heliotérmica

Measured Irradiation Madinat Zayed 27.2.2012

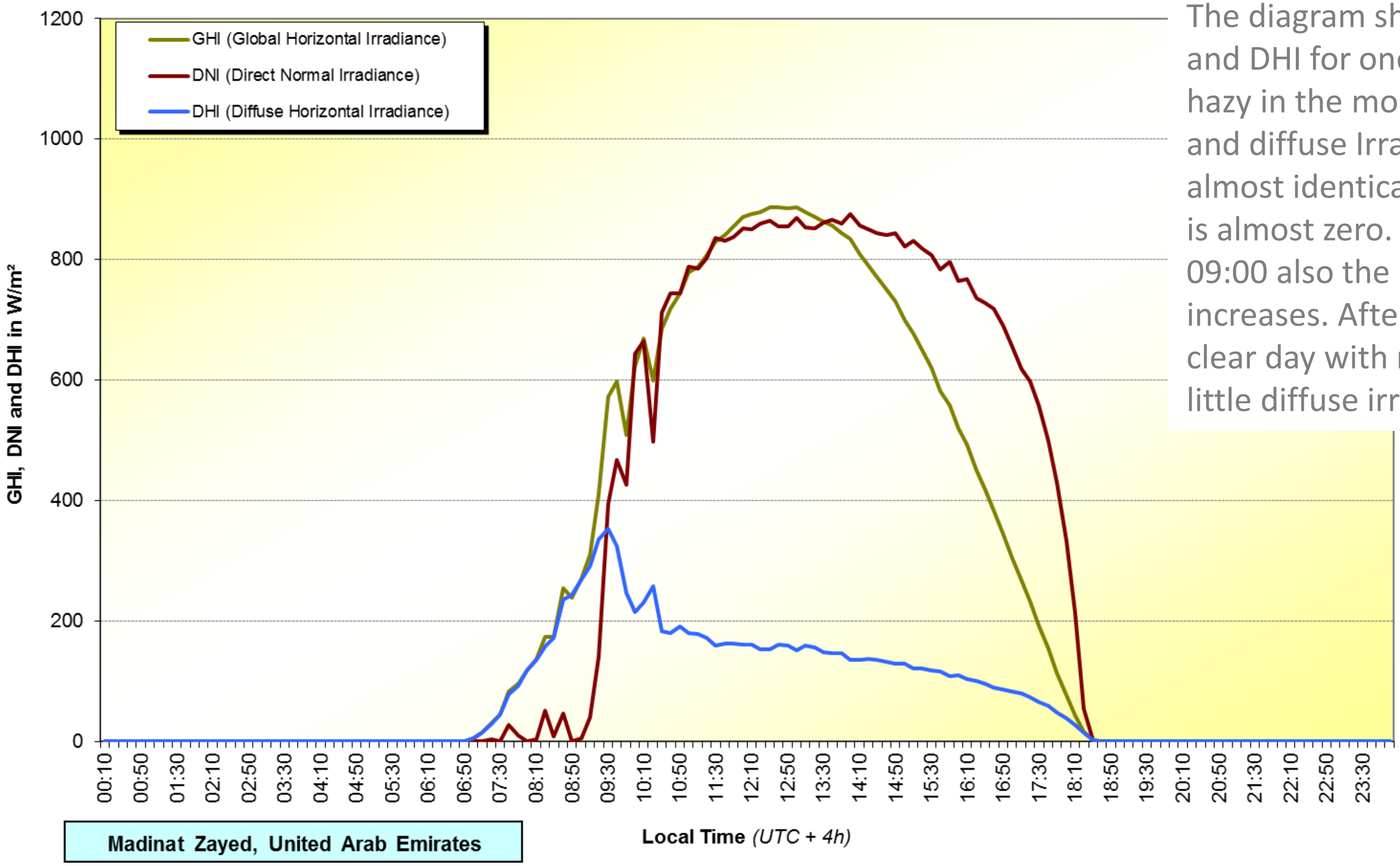

The diagram shows GHI, DNI and DHI for one day. It is hazy in the morning. Global and diffuse Irradiation are almost identical, while DNI is almost zero. Only after 09:00 also the DNI increases. After that, it is a clear day with relatively little diffuse irradiation.

Sun‘s diameter and distance from Earth

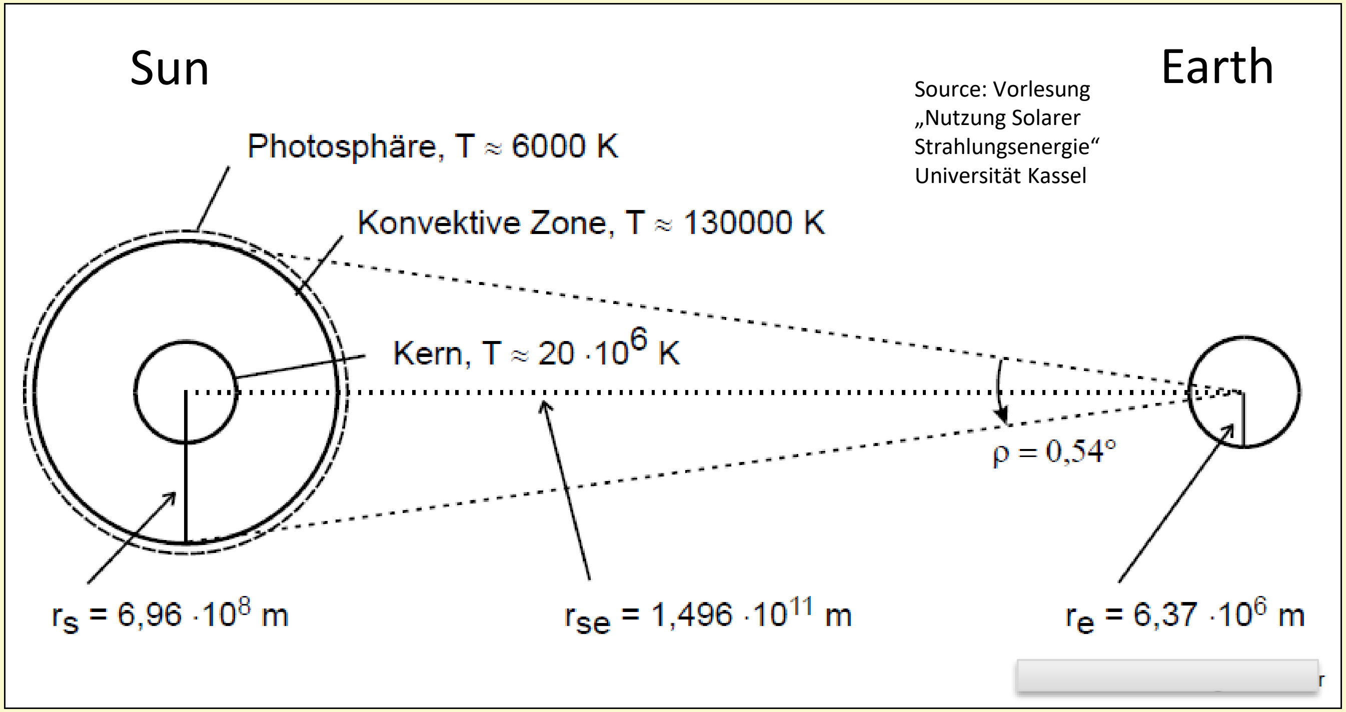

Source: Vorlesung „Nutzung Solarer Strahlungsenergie“ Universität Kassel

Comparing dimensions: Sun is a ball of 20 m diameter, then Earth is a ball of 18 cm and both balls are 2 km apart.

Time Zones

- The Earth rotates from west to east with a frequency of one revolution per 24 hours.
- This is a rotation speed of 15° per hour or 1° per four minutes.
- Each degree of longitude experiences solar noon (sun passing the plane of the degree of longitude) at a different point in time.
- In order to have the solar noon close to 12:00 local time, different time zones have been defined.
- The middle degree of longitude of each time zone is a number which is a multiple of 15°.
- Time zones are described by their time difference to Greenwich Mean Time (GMT), also called United Time Coordinated, UTC
- Central Europe e.g. is GMT + 1h
- The eastern part of Brazil e.g. is GMT – 3 h.

Time Zones

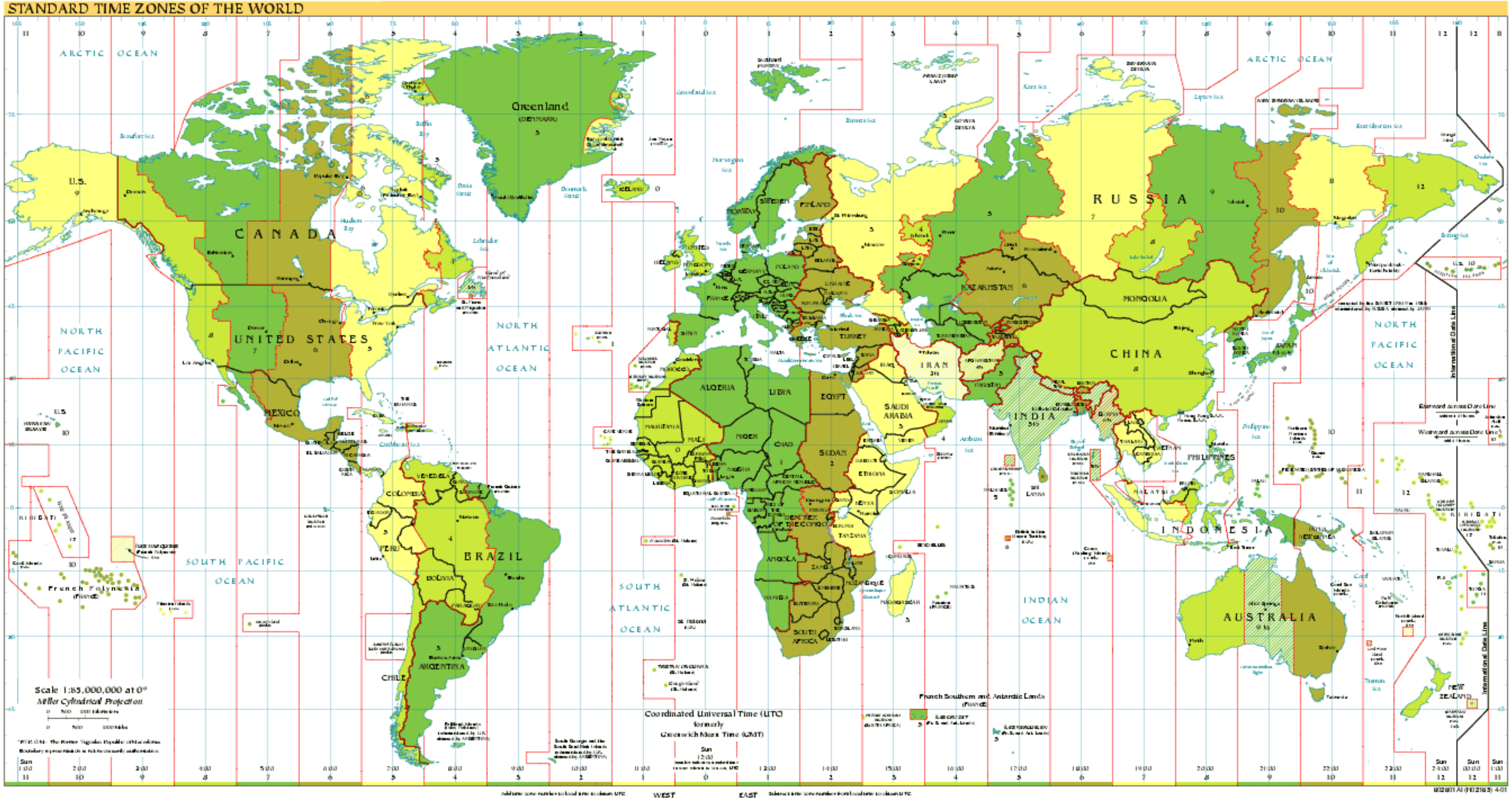
STANDARD TIME ZONES OF THE WORLD
ARCTIC OCEAN
Greenland (DENMARK)
CANADA
UNITED STATES
RUSSIA
CHINA
MONGOLIA
KAZAKHSTAN
INDIA
IRAN
SAUDI ARABIA
ALGERIA
LIBYA
EGYPT
SUDAN
BRAZIL
ARGENTINA
CHILE
AUSTRALIA
INDONESIA
PHILIPPINES
NORTH PACIFIC OCEAN
NORTH ATLANTIC OCEAN
SOUTH PACIFIC OCEAN
SOUTH ATLANTIC OCEAN
INDIAN OCEAN
Coordinated Universal Time (UTC) formerly Greenwich Mean Time (GMT)
International Date Line
Scale 1:85,000,000 at 0°
Miller Cylindrical Projection
WEST
EAST

Solar Time vs. Local Time

- On a degree of longitude which is a center of a time zone, solar time and local time coincide.
- East of the center of a time zone solar noon occurs before 12:00 local time and west of it, it occurs later than 12:00.
- The difference is 4 minutes per each degree distance to the center of the relevant time zone.
- Example:
- Berlin L=13.4°E, center of time zone: L=15°
- Difference = 1.6° west
- => solar noon is 1.6°· 4min/° = 6.4 minutes after 12:00 = 12:06':24''
- Brasilia: L=48.0°W, ct. of time zone: L=45°W; solar noon = 12:12:00
- *Note: In some countries in summer the clock is put 1 hr forward*

Two Additional Variations

- The time for solar noon as calculated on the previous page is only correct in annual average.
- On a concrete date it can be up to 14 minutes later or up to 16 minutes earlier.
- This is caused by two different mechanisms:

  1) The tilt of the Earth's axis against the ecliptic plane

  2) The Eccentricity of the Earth's orbit around the sun
- Mechanism 1) is rather difficult to explain:

  When the rotation of the earth's axis is projected onto the ecliptic plane, this projection is faster than the earth's rotation at some positions of the earth along its orbit around the sun, and at some positions it is slower.

Solar Time Variation due to Tilt

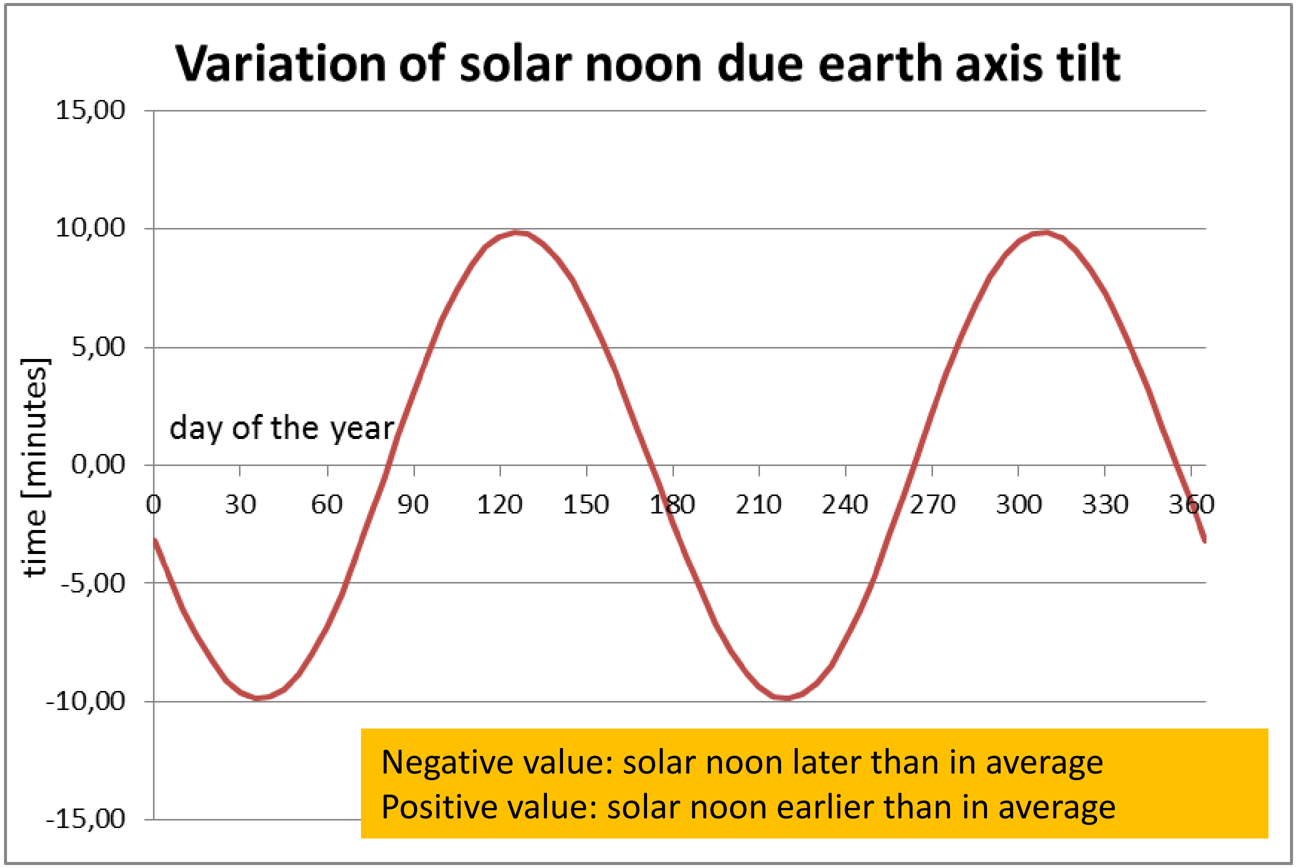

Negative value: solar noon later than in average
Positive value: solar noon earlier than in average

Variation due to Eccentricity

- The Earth’s orbit around the sun is not circular.
- Average distance sun – earth: 149.6 * 10^6 km
- Maximum distance sun – earth: 152.1 * 10^6 km
- Minimum distance sun – earth: 147.1 * 10^6 km

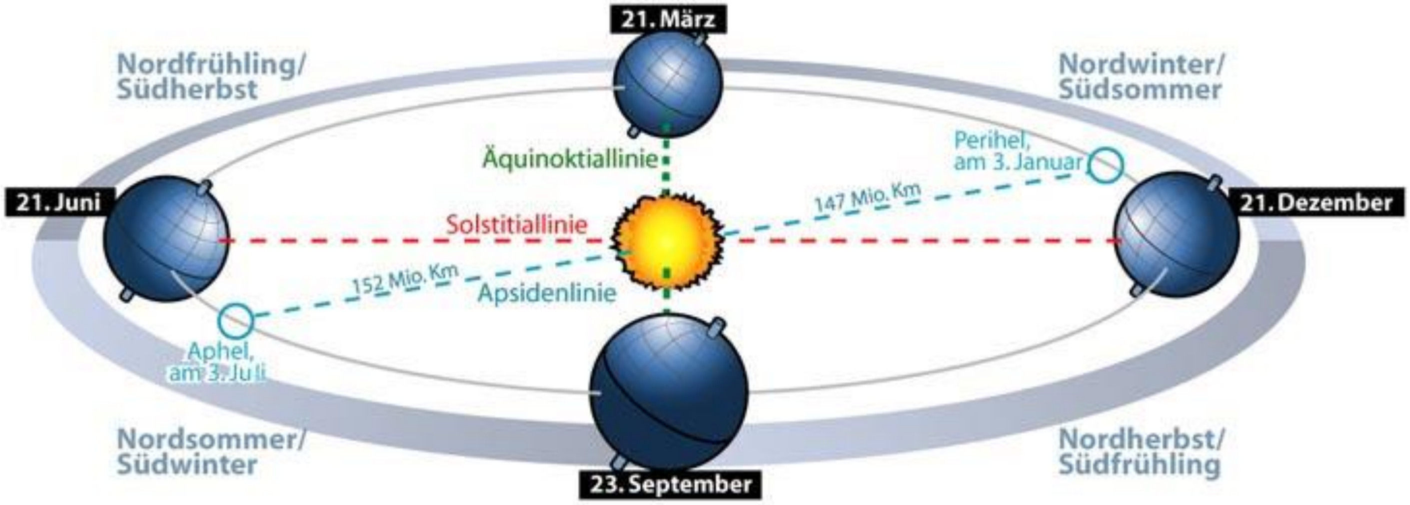

Source: Wikipedia

Variation due to Eccentricity

- The sidereal length of a day is 23:56:04
- The remaining 3min and 56 sec are needed to complete one revolution in relation to the sun
- Due to the eccentricity of the earth's orbit the angle travelled by earth per day changes (fast at Perihelion, slow at Aphelion).
- Therefor 24h are not enough top catch up with the sun in December, while it is more than enough in June.

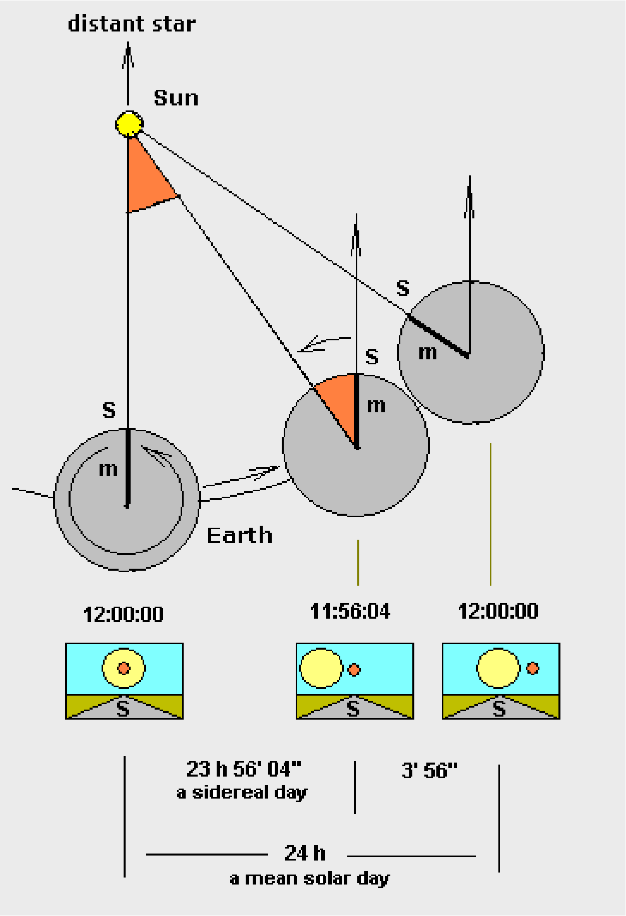

Source: Wikipedia

Solar Time Variation due to Eccentricity

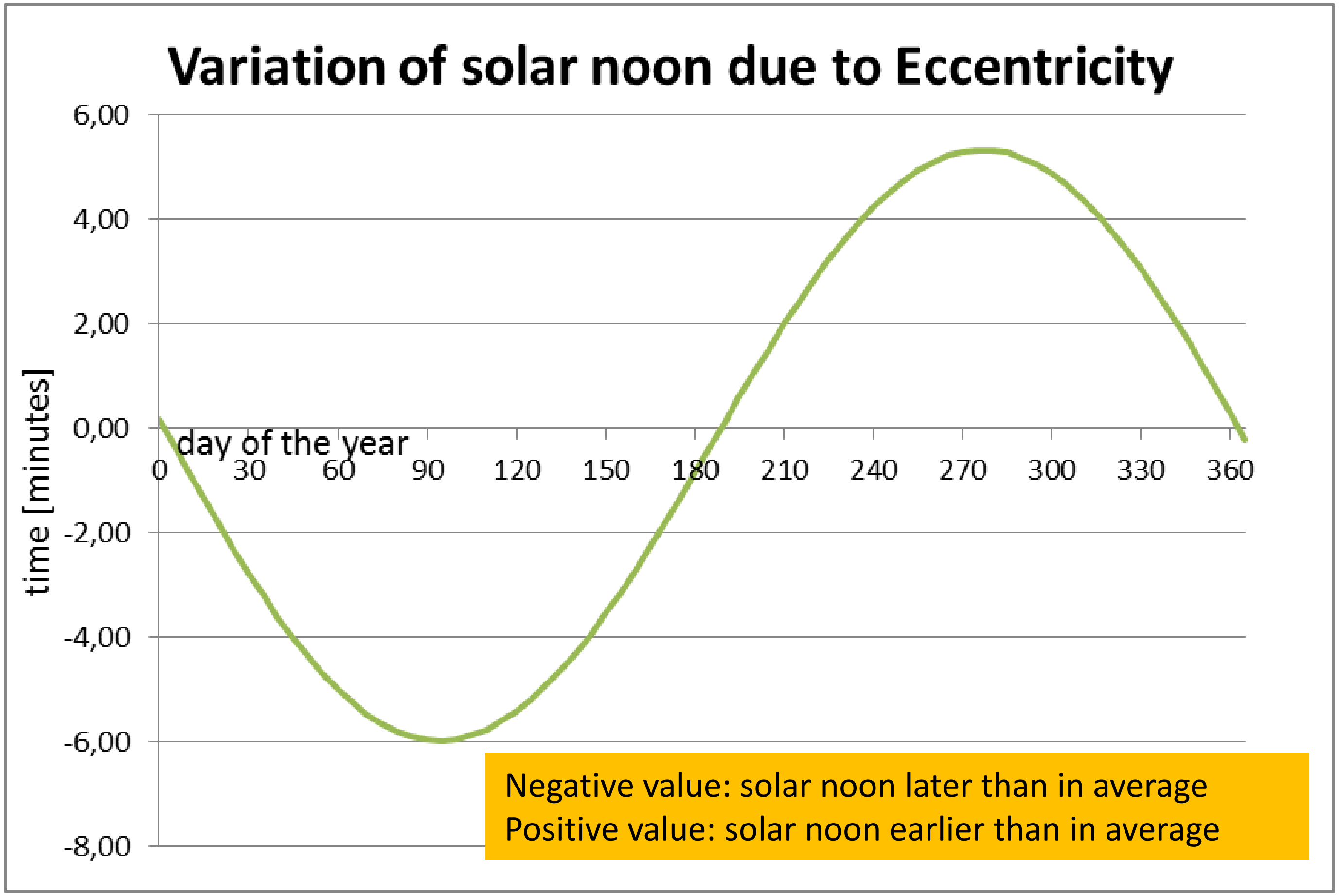

Negative value: solar noon later than in average
Positive value: solar noon earlier than in average

Solar Time Variation due to Both Effects Together

- The following equation describes both effects together:
- E=229,2*(0,000075+0,001868*cos(B)-0,032077*sin(B)-0,014615*cos(2B)-0,04089*sin(2B))
- With: B=(n-1)*360/365 n = the number of the day of the year E in [minutes]

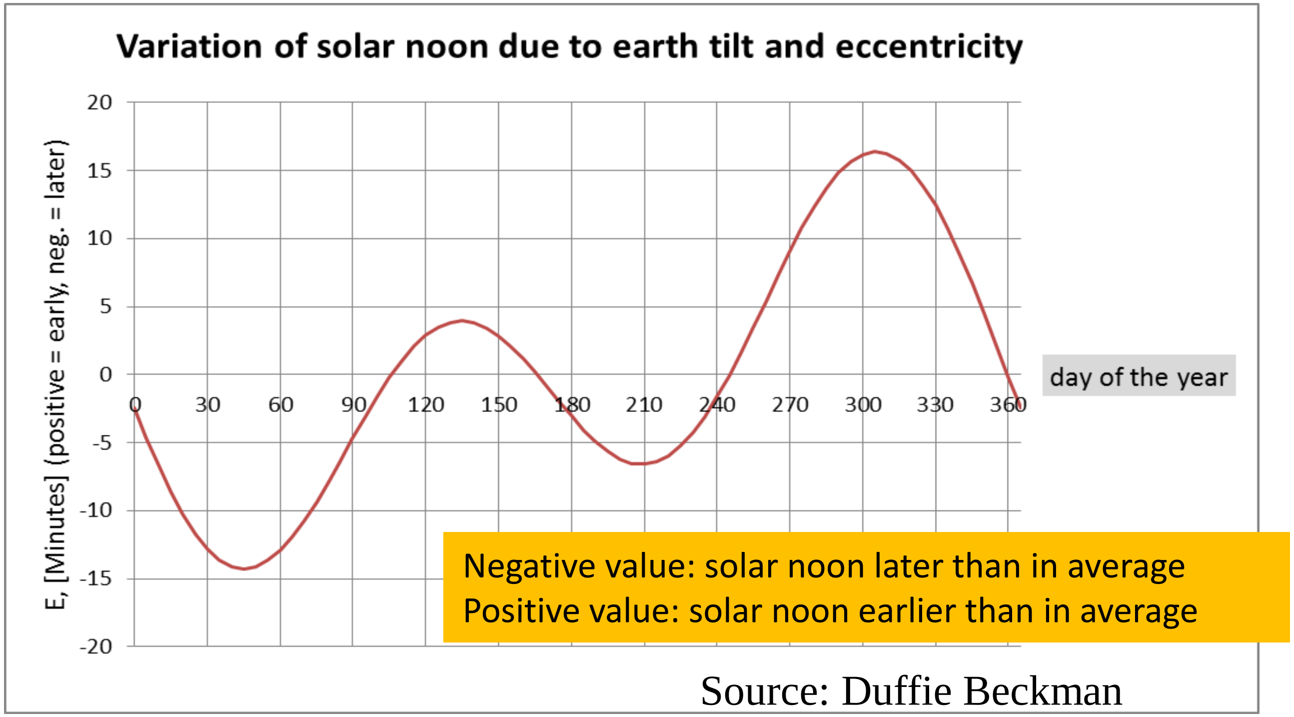

Variation of solar noon due to earth tilt and eccentricity

Negative value: solar noon later than in average
Positive value: solar noon earlier than in average

Source: Duffie Beckman

Describing the Sun's Position

α= Azimuth Angle*
ε = Elevation Angle

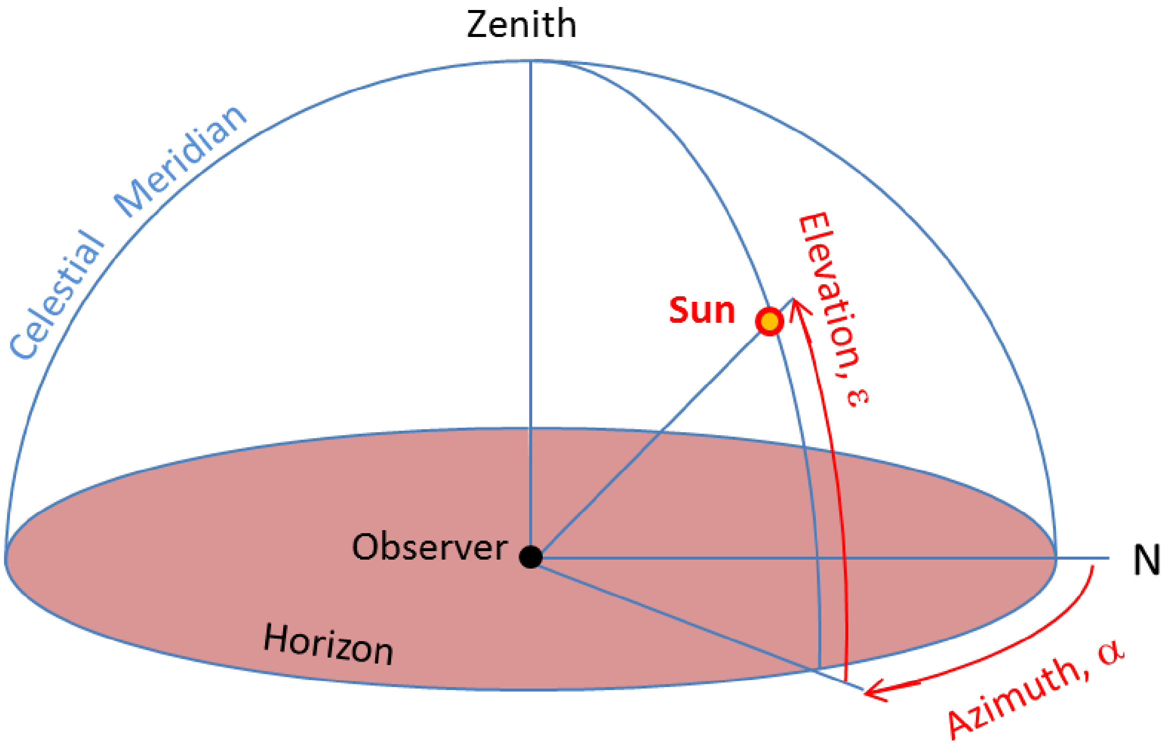

* Attention: α can also be defined with South = 0°
** Celestial Meridial = the actual degree of longitude of the observer

Knowing the Sun‘s Position

The elevation, ε and the azimuth, α can be calculated for every day of the year and hour of the day with the following equations:

$$\varepsilon = \arcsin(\sin\varphi * \sin\delta + \cos\varphi * \cos\delta * \cos\omega)$$

$$\alpha = \arcsin(\cos\delta * \sin\omega / \cos\varepsilon)$$

The calculation of α is not finished with this equation. It needs to be determined in which quadrant the sun is located. Depending on the quadrant 90° may need to be added or subtracted. Further details can be found in: Duffie Beckman: “Solar Engineering”

With:

- φ = degree of latitude
- δ = declination of the day
- ω = hour angle *(zero at noon, negative before noon, positive after noon)*

$\omega = h_{pm}*15$ (examples: 3 pm => $\omega = 45°$; 9 am = -3pm => $\omega = -45°$)

Solar Position Diagram Brasilia

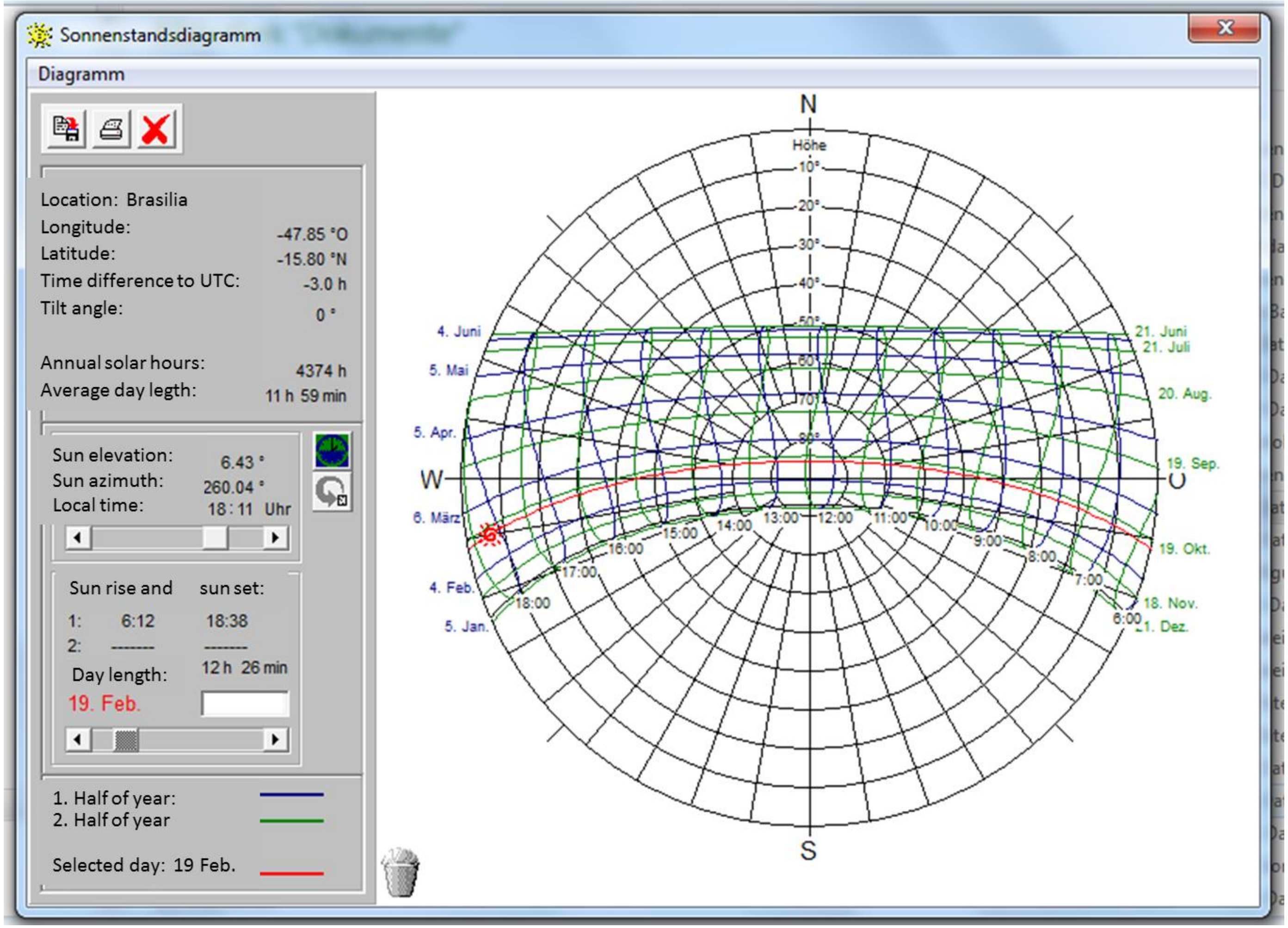

Location: Brasilia
Longitude: -47.85 °O
Latitude: -15.80 °N
Time difference to UTC: -3.0 h
Tilt angle: 0 °

Annual solar hours: 4374 h
Average day legth: 11 h 59 min

Sun elevation: 6.43 °
Sun azimuth: 260.04 °
Local time: 18 : 11 Uhr

Sun rise and	sun set:
1: 6:12	18:38
2: --------	--------
Day length:	12 h 26 min
19. Feb.	

1. Half of year: 🟦
2. Half of year 🟩

Selected day: 19 Feb. 🟥

Source: Sun Orb, Programm der Ruhr Uni Bochum, Lehrstuhl für Nukleare und Neue Energiesysteme (English translation by Prof. O. Goebel)

Knowing the Sun‘s Position

Knowing the sun‘s position is important for Solar Engineering, especially in CSP, because:

- The CSP Solar Collectors have to follow the sun, and hence their tracking mechanisms has to be programmed, knowing the sun’s position at any day of the year at any hour of the day.
- Also for PV plants with fixed modules, the sun’s position has to be known in order to avoid shadowing of the modules at certain times of the day / year.

Solar Resource Maps

- Solar Resource Maps show the quantity of the solar resource for certain regions of the world (or the whole world)
- Usually they show either GHI or DNI *(map below: GHI)*
- Common units are: average annual flux density [W/m²] or annual / daily sum [kWh/(m² a)]

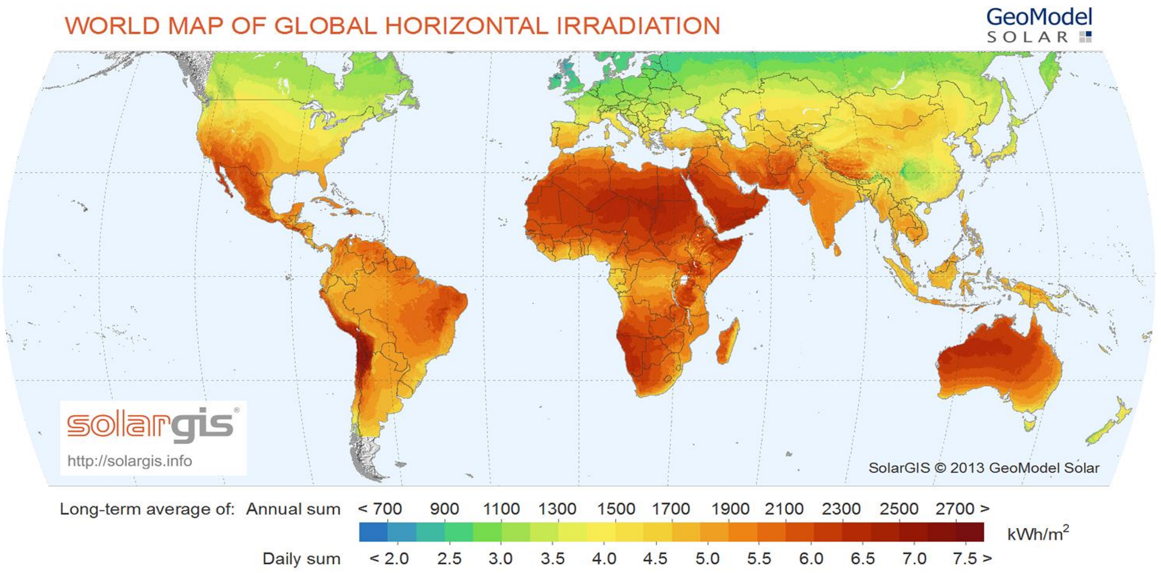

Solar Resource Maps

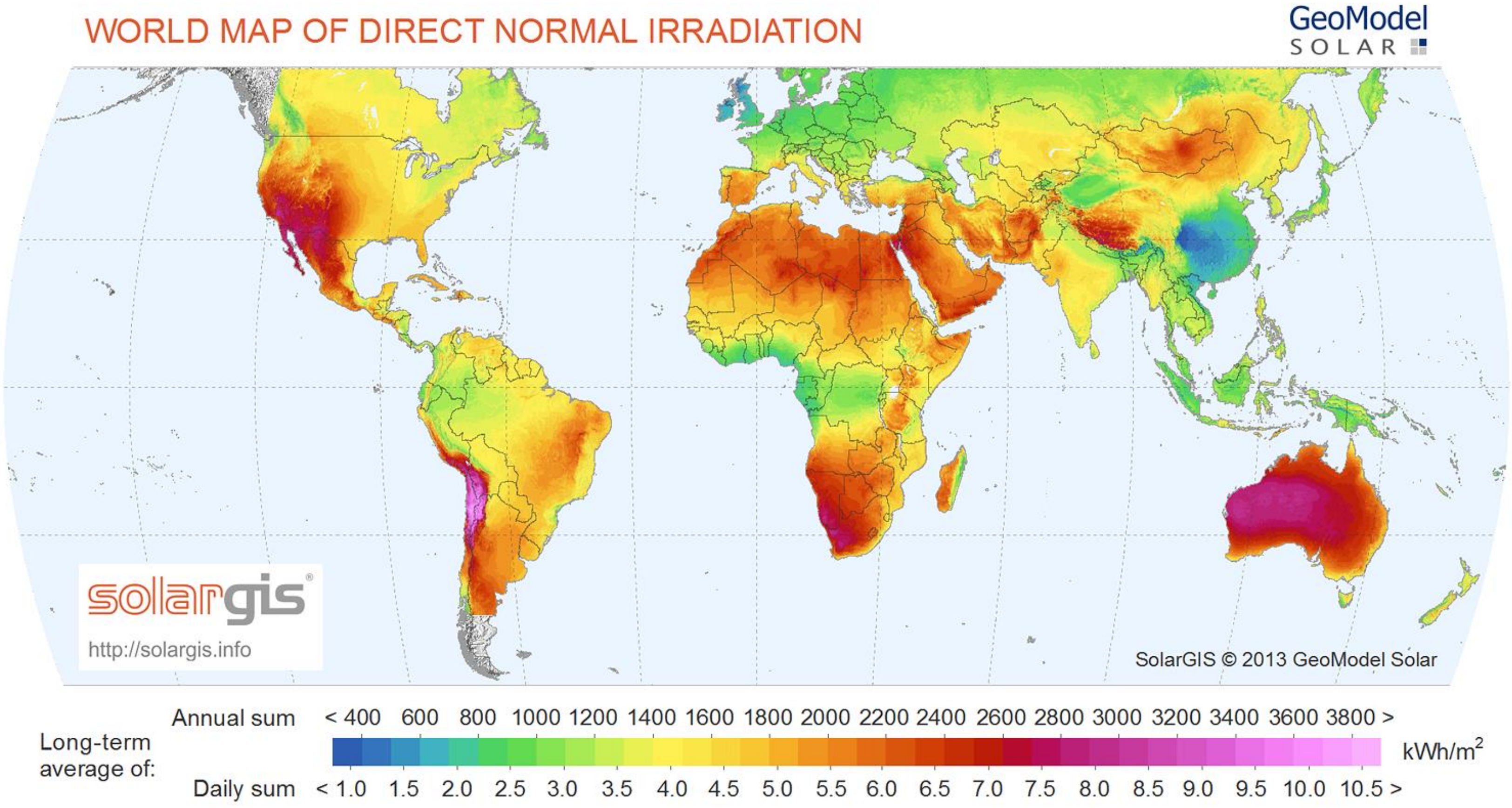

Solar Resource Maps

GHI Map of Latin America

Solar Resource Maps

DNI Map of Latin America

Attention:

- DNI maps are often generated from Satellite data only. They have a high degree of uncertainty (up to 12%), unless they are calibrated against ground based measurements.
- Satellite based data tend to overestimate the DNI resource!

Annual sums of Solar Irradiation

- Good solar sites offer annual sums of solar irradiation of 2400 kWh/(m² a) and more. (This is true for DNI and GHI as well).
- Considering, that one barrel of oil has an energy content of 1600 kWh, this is equivalent to 1.5 barrels of oil per m² each year!
- A very important number in energy engineering is the energy content of oil:
  - 10 kWh / Liter (36 MJ / Liter)
  - 11,7 kWh / kg (42 MJ / kg)

The Energetic Potential of Solar Energy

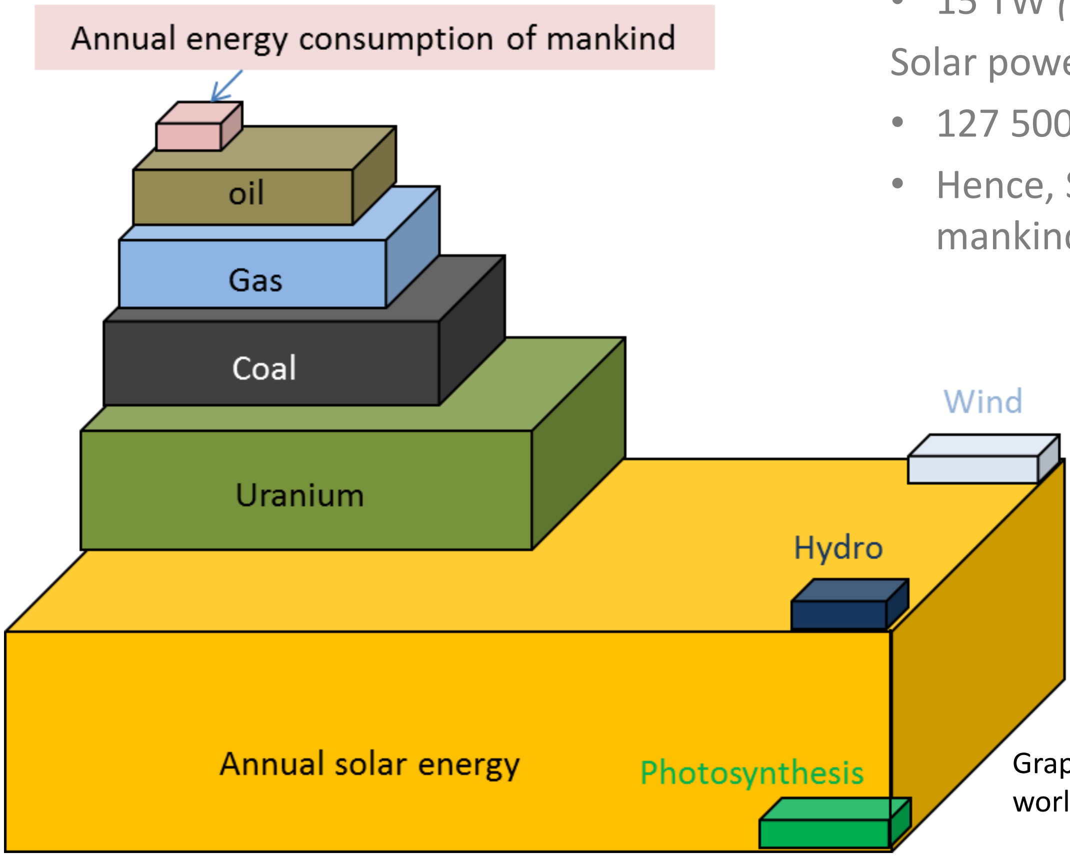

Mankind’s power Consumption:

- 15 TW *(www.IEA.org)*

Solar power on earth disk:

- 127 500 TW $(6371\ km)^2 * \pi * 1\ kW/m^2 = 127.5 * 10^{12}\ kW$
- Hence, Solar power is 8500 times bigger than mankind’s power consumption

In other words:

The energy the earth receives in one hour from the sun is equivalent to the energy demand of mankind in one year.

Graphik by Prof. O. Goebel using data from IEA, world energy outlook

The Energetic Potential of Solar Energy

Practical Potential of Solar Energy:

- The theoretical potential of solar energy is in practice reduced by:
  - weather
  - non suitable sites (oceans and mountains)
  - efficiency of conversion systems are below 100%
- Theses effects alone reduce the theoretical potential by a factor of 100: remaining factor is: 8 000 / 100 = 80
- A more detailed analysis shows some further reductions
- However, solar energy has the potential to satisfy all energy demand of mankind several times, even under the most pessimistic assumptions.

Solar Irradiation, Summary

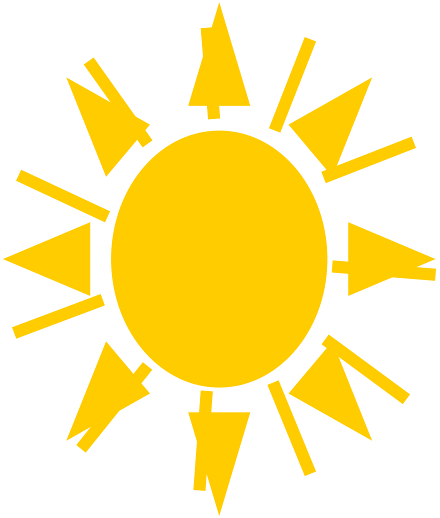

Solar Flux Density:

- Outside of earth’s atmosphere: 1367 W / m^2
- At sea level at a clear day:
  - **1000 W / m^2 or 1 kW / m^2** (1.36 HP / m^2)

- Sun shine hours up to 4000 h / a at good sites
- Received **energy** up to 2600 kWh / m^2 a at very good sites

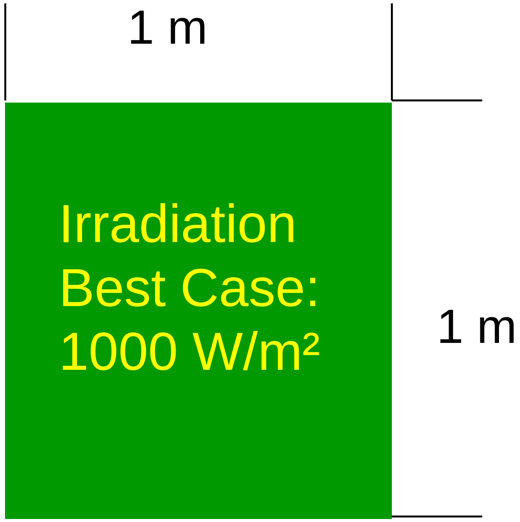

Irradiation
Best Case:
1000 W/m^2

Measuring Solar Irradiation

Measuring Solar Irradiation

- **Global Irradiation = Diffuse Irradiation + Direct Irradiation**
- Global Irradiation is measured with a Pyranometer

- Direct Irradiation is measured with a Pyrheliometer or with two Pyranometers, where one of them is covered with a Shadow Band.

- Important for CSP: Only Direct Irradiation can be concentrated.

Rotating Shadowband Pyranometer, RSP

- Low maintenance requirement
- Measures Direct, Diffuse and Global Irradiation
- Less accurate than Pryheliometer

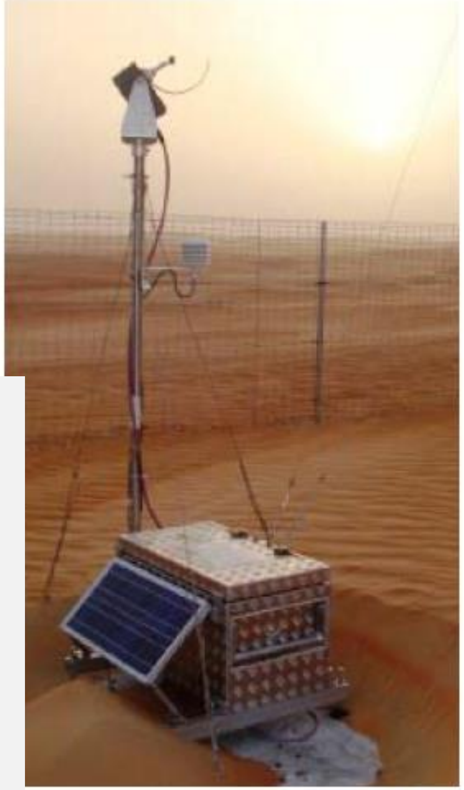

The shadow band rotates periodically (usually every 30 s) around the sensor., such that it is temporarily shaded and able to measure Diffuse Irradiation., while it measures Global Irradiation when not shaded. By subtracting the Diffuse from the Global Irradiation, the Direct Irradiation can be calculated.

Seite 23

Rotating Shadowband Pyranometer, RSP

The shadow band rotates periodically (usually every 30 s) around the sensor., such that it is temporarily shaded and able to measure Diffuse Irradiation., while it measures Global Irradiation when not shaded. By subtracting the Diffuse from the Global Irradiation, the Direct Irradiation can be calculated.

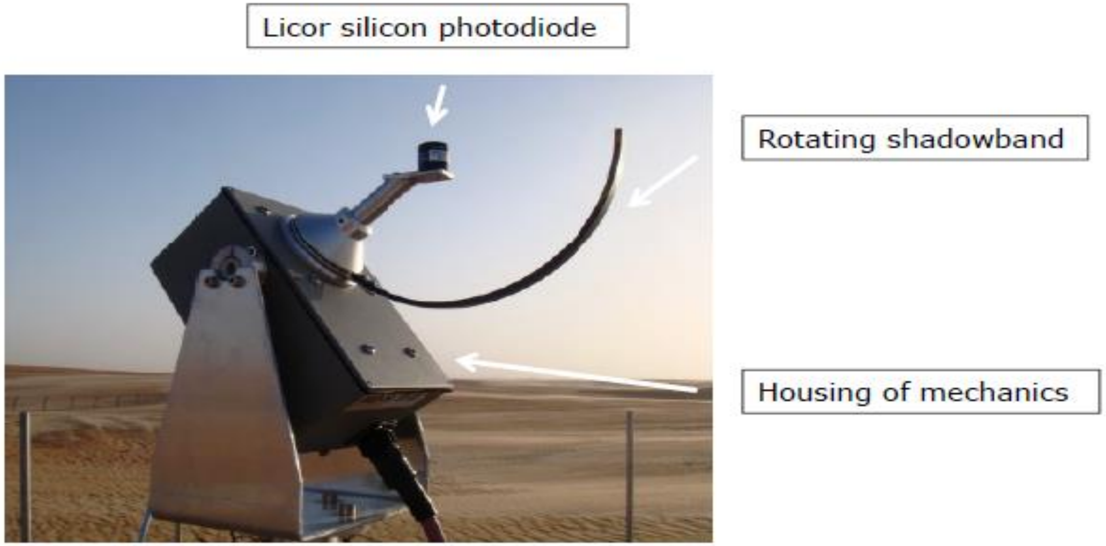

Rotating Shadowband Pyranometer, RSP

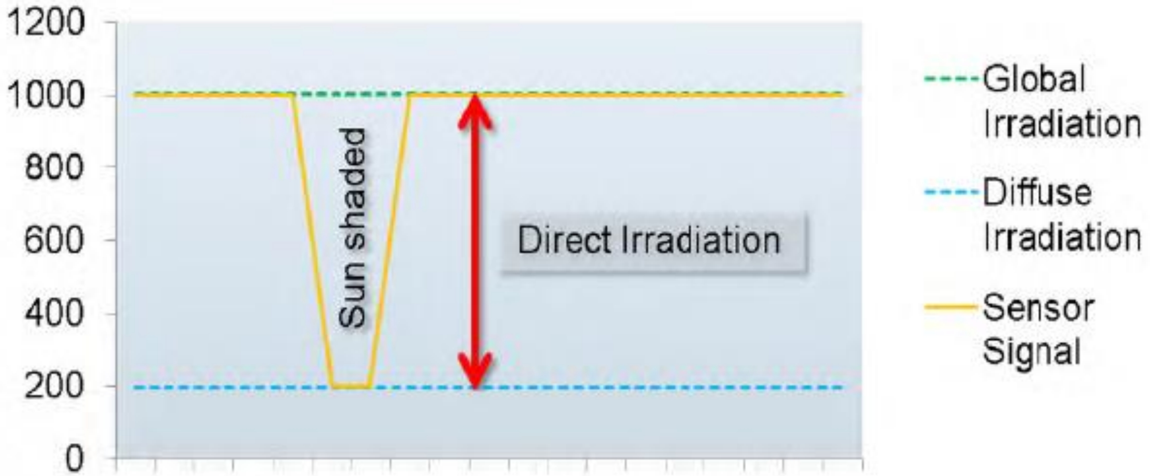

Simplified sensor signal during shadow band rotation:
once per minute, rotation lasts about 1.5 seconds

Source: Solar Millennium AG

High Precision Measuring Station

Pyrheliometer and Pyranometer on sun tracker

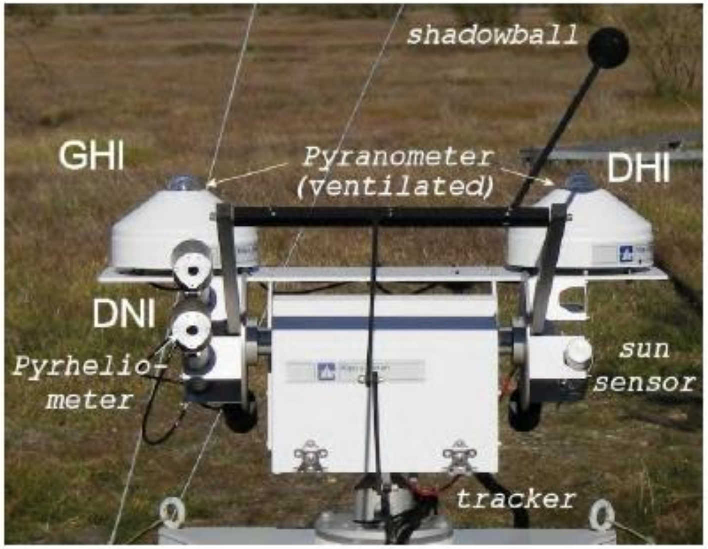

Advantages:

\+ high accuracy (1 to 2%)

\+ separate sensors for GHI, DNI and DHI

(cross-check through redundancy)

Disadvantages:

- high acquisition costs
- high maintenance costs
- high susceptibility for soiling
- high power demand
  (grid connection required)

CSP Services

4th Sfera Summer School, Hornberg Castle, 2013 - 31

Soiling Characteristics of Pyrheliometer vs. RSP

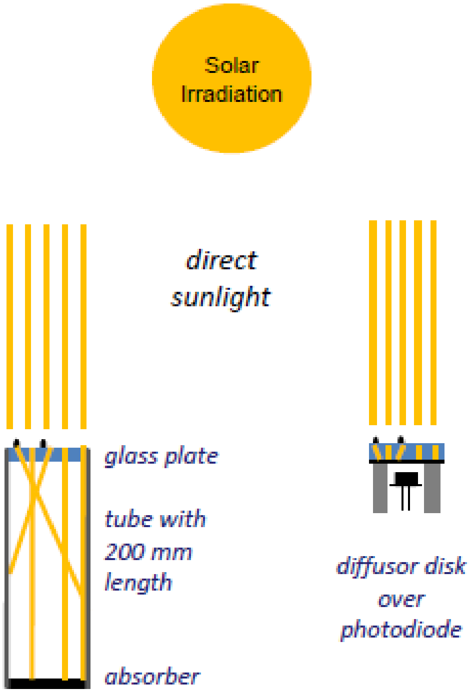

Pyrheliometer

RSP sensor head

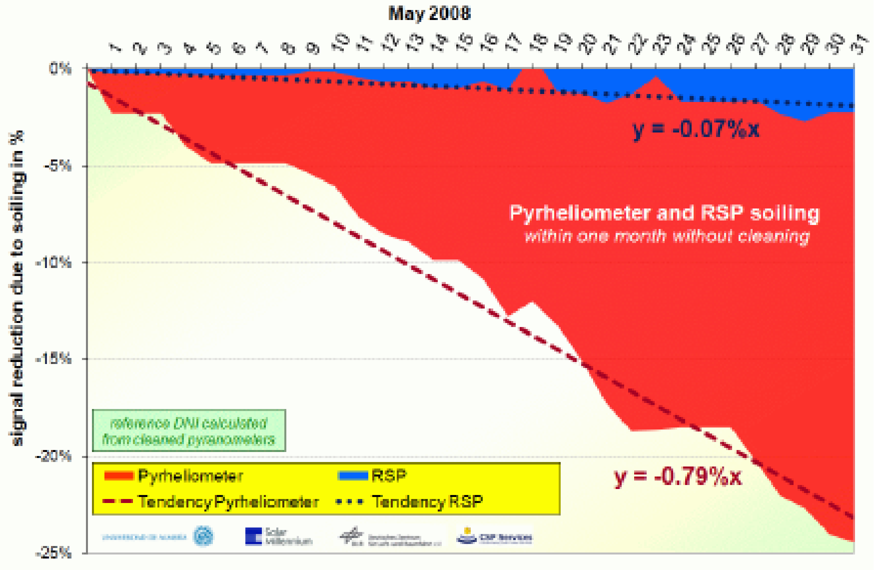

Measuring the Solar Resource

- When evaluating a site for solar projects, the solar resource is estimated initially without on site measurements. Reason: Time and money
- With some existing measuring stations in the area:
  - Interpolation of the existing data for the candidate site
  - Attention: Interpolation not possible if there are weather influencing barriers between the meteo stations (e.g. mountain ranges).
- Without existing measuring stations in the area:
  - Utilization of Satellite Data
- These non site based data should be available for a period of at least 5 years, in order to have a representative long term average value. The longer the period, the more reliable is the average value.

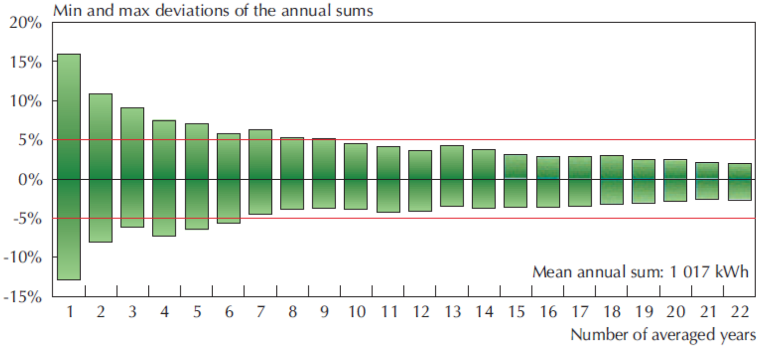

Note: The bottom figure shows the deviations from long-term average GHI of the moving averages across 1 to 22 years.

Sources: Datasource: DWD GHI Data from 1937 to 2003 (top); Volker Quaschning, DLR/Hoyer-Klick et al. *2010 (bottom).*

Measuring the Solar Resource

Using existing measurements from the region 1/2

Measurements of the solar resource are conducted by the following institutions:

1. **National Meteorological Institutes**
2. **Airports**

Warning: The quality of the solar data is often not good. Many meteorological institutes and airports mainly pay attention to temperature, air pressure, humidity and wind speed. Solar Irradiation is often measured with a glass ball only.

Measuring the Solar Resource

Using existing measurements from the region 2/2

Measurements of the solar resource are conducted by the following institutions:

3. **Research Institutes**
   - Here it is possible to obtain high quality data. Besides the budget for proper measuring equipment, here is also available the necessary knowledge for operation & maintenance of the equipment.

4. **Project Developer**
   - If there are already some solar power plants (of a certain minimum capacity) in the area, then there have been conducted respective measuring campaigns. There are cases where the project developers are willing to sell the data, and there are cases where they are not willing to do so.
   - From existing solar power plants in the area also some other relevant information can be obtained (e.g. about Storms, Soiling, Vandalism), if the developer cooperates.

Measuring the Solar Resource Satellite Based Measurements

- It is possible to calculate (or better: estimate) the solar resource at the earth’s surface from the information measured by meteorological satellites.
- The algorithms used in that process are dependent on calibration with ground based measurements. Therefore satellite based solar resource measurements without such calibration are rather imprecise. *(Example: Shams 1)*
- DNI is more difficult to derive than GHI.
- Uncertainty at DNI:
  - Without ground based calibration in the region: up to +/- 15%
  - With ground based calibration in the region: approx. +/- 5%
- Uncertainty at GHI:
  - Without ground based calibration in the region: up to +/- 10%
  - With ground based calibration in the region: approx. +/- 3 to 4%

Satellite based Data are available from DLR (German Aerospace Center, www.dlr.de), from NASA and from other space R&D Institutions

Measuring the Solar Resource Ground Based Measurements

- In case a site has been positively evaluated by non site based investigations (nearby site data or Satellite), then site based solar resource measurement is initiated.
- On site measurement shall last at least one year.
- Sites of solar power plants are often located in remote locations.
- Therefore data transmission shall be done via cell phone network.
- The cleaning of the sensors (RSP approx. 1x per week) needs to be organized. For this task a person living near to the site shall be trained and contracted. Attention: The cleaning has to be conducted according to a well defined plan, and the execution shall be well documents. (Keep in mind the importance of the data for the evaluation of the project site!)

Measuring the Solar Resource:

Correlating Data from the Two Sources

- Once on site data will be available for one complete year, then they shall be correlated with the non site based long term data.
- Concretely: The year for which we have both, the on site measurements and the long term data (the overlap period) is used to calibrate the long term data for the candidate site. This way the long term average value of the site is obtained.
- Example:
  - The long term average annual sum of DNI for the site according to Satellite data is 2200 kWh/(m^2 a).
  - In the overlap period the Satellite showed 2100 kWh/(m^2 a) and the on site measurement showed 2000 kWh/(m^2 a)
  - Then the long term average value of 2200 kWh/(m^2 a) is corrected with the factor of 2000 / 2100, and hence the corrected value is 2095 kWh/(m^2 a)

Measuring the Solar Resource:

The TMY (Typical Meteorological Year)

- With the above mentioned method the long term average value for the site is available.
- However, the annual sum of DNI [kWh / (m^2 a)] is not sufficient for the simulation model which calculates the annual energy yield. For this purpose hourly values (or better10 minutes values) are required.
- If we would simply average each hourly value of several years we would eliminate the dynamic of the weather. However, this dynamic is needed for a realistic simulation of the plant behavior.
- Solution: We take the hourly values (or 10 minutes values) of the ground based data and correlate them with the long term average of the monthly sums of DNI.

Measuring the Solar Resource:

The TMY (Typical Meteorological Year)

Example of a GHI measurement of January 1st for 5 different years

The average curve does not show the dynamic of the years 2007 and 2011.

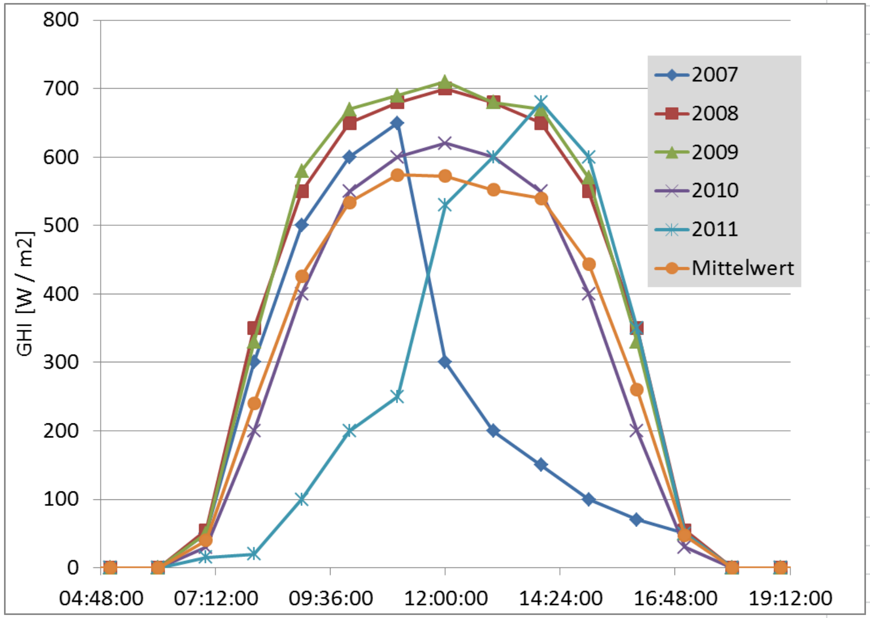

		GHI über 5 Jahre gemessen [W / m^2]					
Tag	**Uhrzeit**	**2007**	**2008**	**2009**	**2010**	**2011**	**Mittelwert**
01. Jan	00:00	0	0	0	0	0	0
	01:00	0	0	0	0	0	0
	02:00	0	0	0	0	0	0
	03:00	0	0	0	0	0	0
	04:00	0	0	0	0	0	0
	05:00	0	0	0	0	0	0
	06:00	0	0	0	0	0	0
	07:00	50	55	50	30	15	40
	08:00	300	350	330	200	20	240
	09:00	500	550	580	400	100	426
	10:00	600	650	670	550	200	534
	11:00	650	680	690	600	250	574
	12:00	300	700	710	620	530	572
	13:00	200	680	680	600	600	552
	14:00	150	650	670	550	680	540
	15:00	100	550	570	400	600	444
	16:00	70	350	330	200	350	260
	17:00	50	55	50	30	50	47
	18:00	0	0	0	0	0	0
	19:00	0	0	0	0	0	0
	20:00	0	0	0	0	0	0
	21:00	0	0	0	0	0	0
	22:00	0	0	0	0	0	0
	23:00	0	0	0	0	0	0
02. Jan	00:00	0	0	0	0	0	0

Measuring the Solar Resource Describing the uncertainty

- In case the energy yield calculations based on the TMY are satisfactory, then the site is declared as positive (at least from the solar resource point of view).
- For an objective judgment, the uncertainty of the TMY shall be described. For this task the uncertainties of all components involved in the process (measuring instruments, satellite data, correlation method, number of years of long term data) are combined by relevant statistical methods.
- The resulting overall uncertainty is then expressed as a σ–value in the Gaussian Equation.

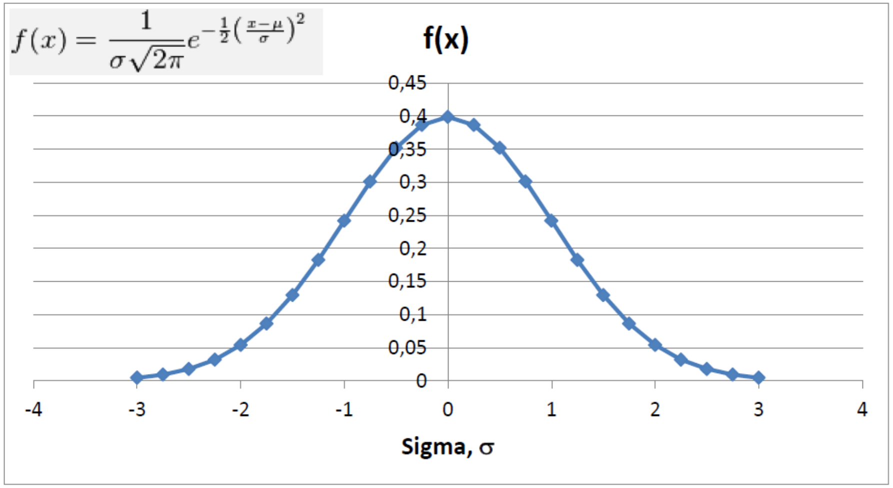

$$f(x) = \frac{1}{\sigma\sqrt{2\pi}} e^{-\frac{1}{2}\left(\frac{x-\mu}{\sigma}\right)^2}$$

Gaussian Curve with Median = 0 and σ=1

Measuring the Solar Resource Describing the uncertainty

- Is has to be calculated which percentage of deviation from the calculated value of the annual DNI sum represents 1σ.

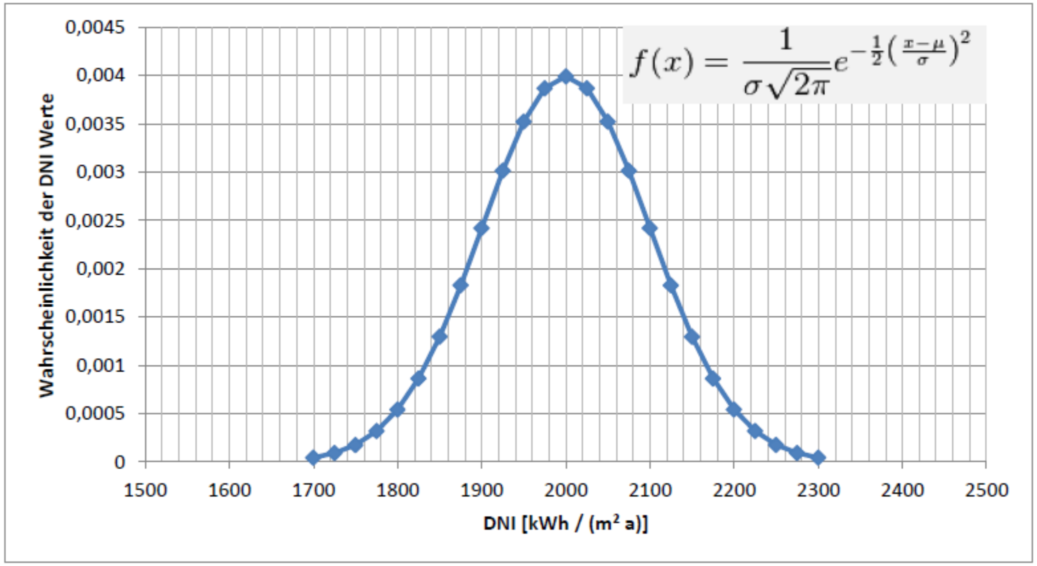

- Example:
- The long term average value of the DNI calculation is 2000 kWh/(m^2 a), and 1σ is 5% or here 100 kWh/(m^2 a). Then the average minus 1σ =1900 kWh/(m^2 a) and the average plus 1σ =2100 kWh/(m^2 a)

Measuring the Solar Resource Describing the uncertainty

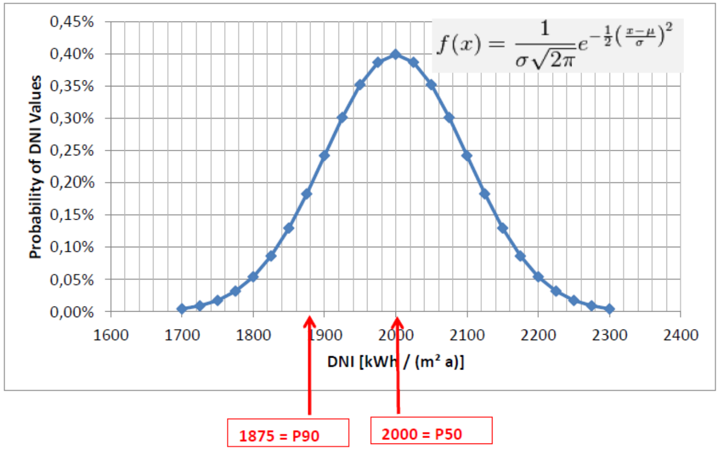

1875 = P90

2000 = P50

Show Example with P50 = 2000 kWh/(m^2 a) and 1σ = 5%.

- 68,27 % of all values are located in the interval +/- 1 σ around the average value,
- 95,45 % of all values are located in the interval +/- 2 σ around the average value,
- 99,73 % of all values are located in the interval +/- 3 σ around the average value.

Investment bankers use the term P-Value to describe uncertainty (P = probability)

- P50 (0σ) means that 50% of the possible values are higher than the P50 value and 50% are lower. P 50 is the most probable value.
- P90 (-1,25σ) means that 90% of the possible values are higher than the P90 value and 10% are lower.
- For the assessment of the creditworthiness of a project the banks want to know the P50, P75 and the P90 value of the DNI annual sum. (Or better directly the energy yield [GWh$_{el}$/a] calculated with these DNI values.)

The Principles of CSP Technology and Overview of different CSP Technologies on the Market

Classification of Solar Energy Technologies

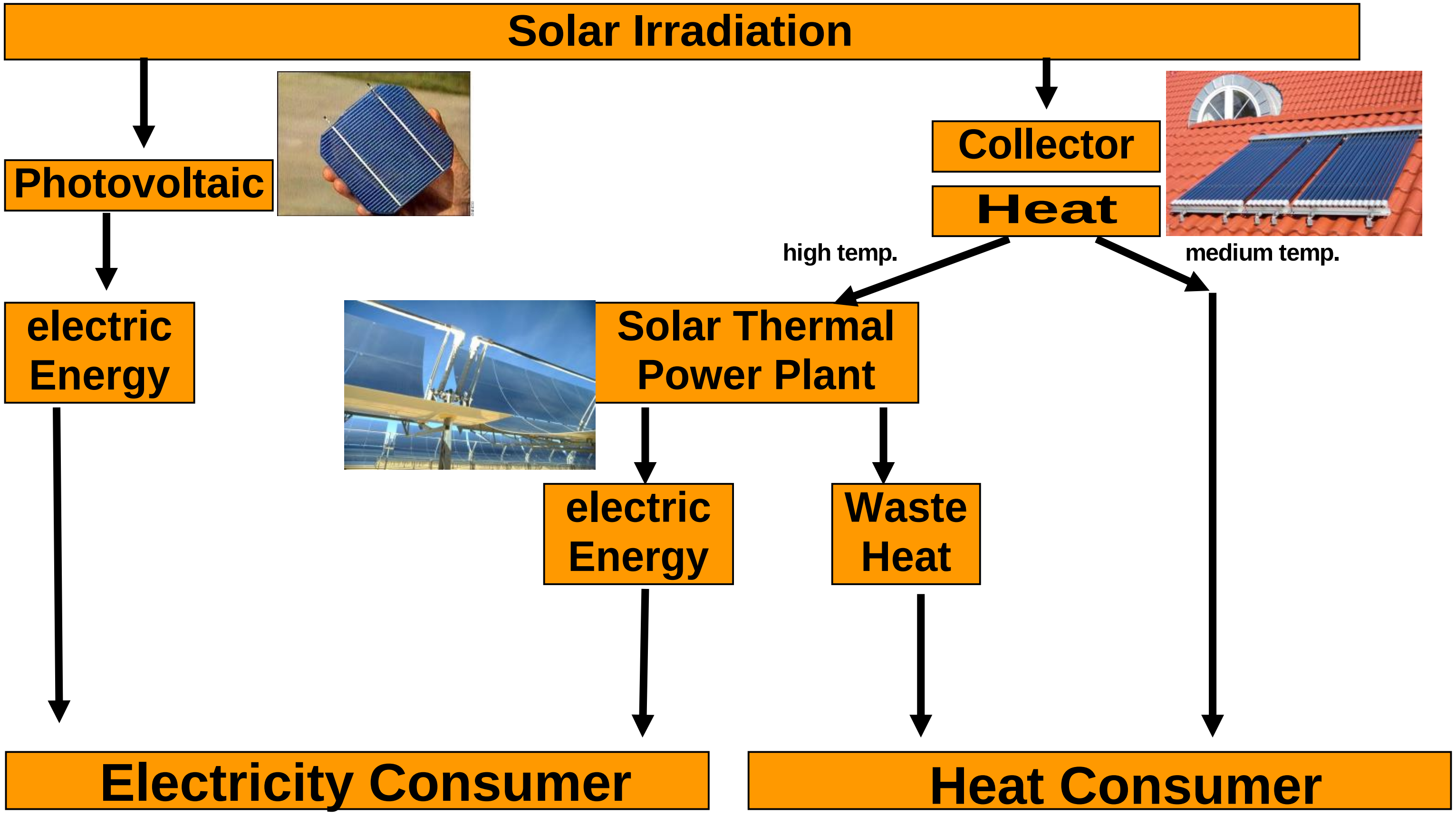

Solar Irradiation

Photovoltaic

electric Energy

Collector

Heat

high temp.

medium temp.

Solar Thermal Power Plant

electric Energy

Waste Heat

Electricity Consumer

Heat Consumer

Principle of Concentrated Solar Power, CSP

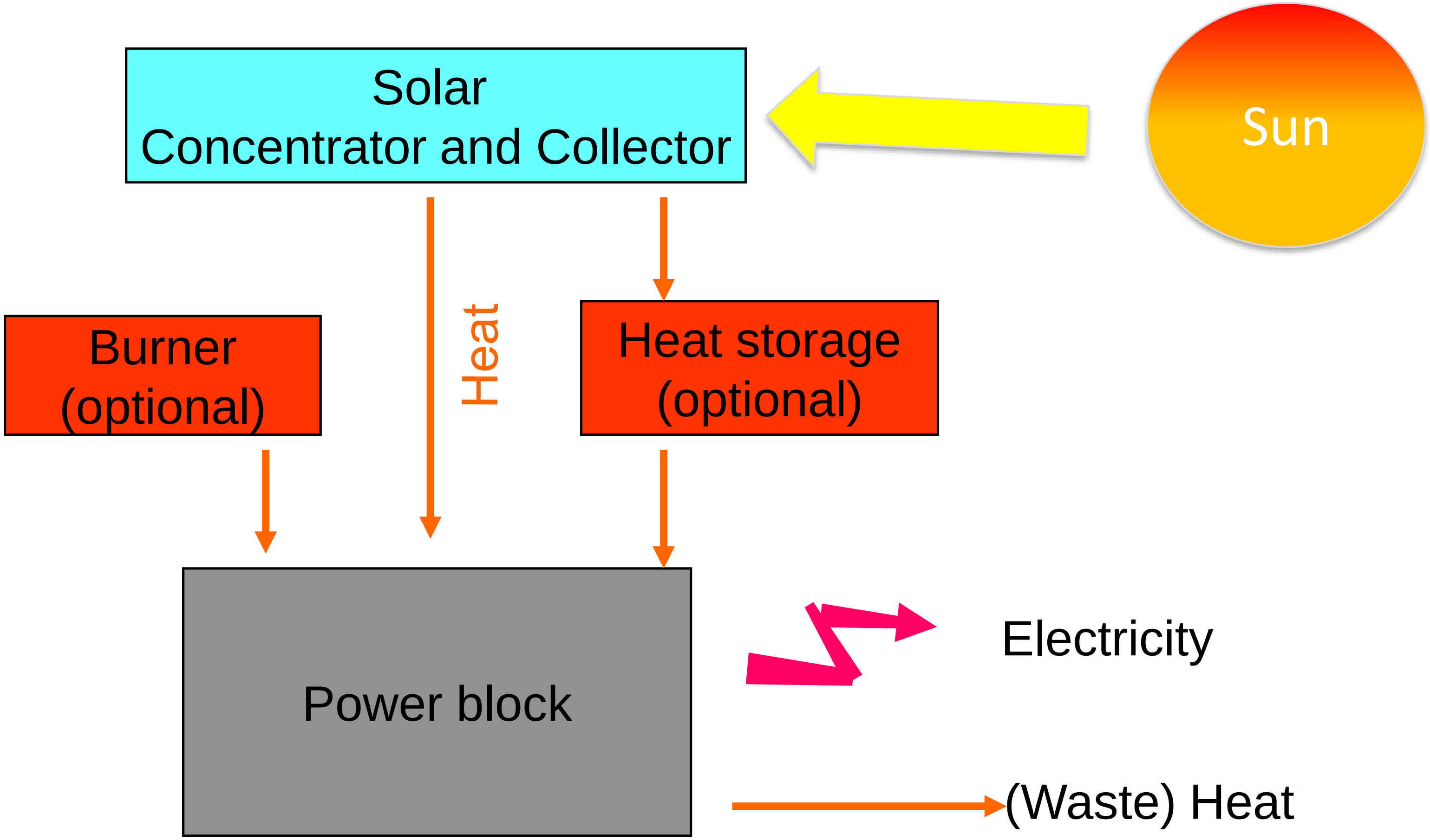
Solar
Concentrator and Collector

Sun

Heat

Burner
(optional)

Heat storage
(optional)

Power block

Electricity

(Waste) Heat

Types of CSP Power Plants

Trough

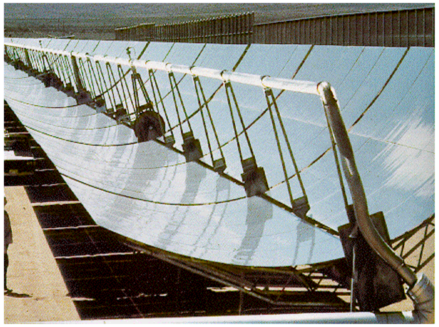

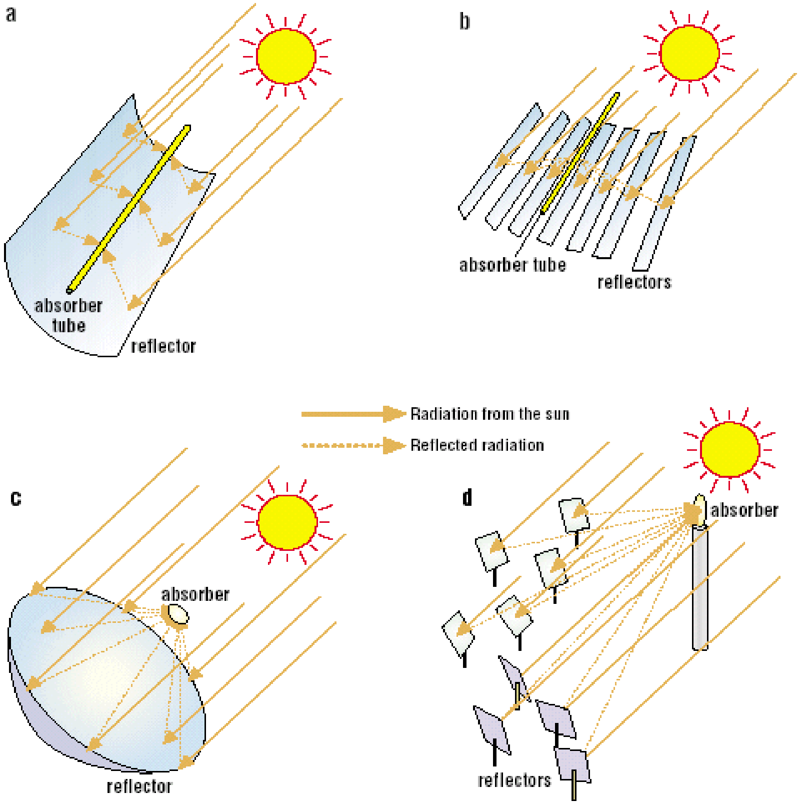

Linear Fresnel

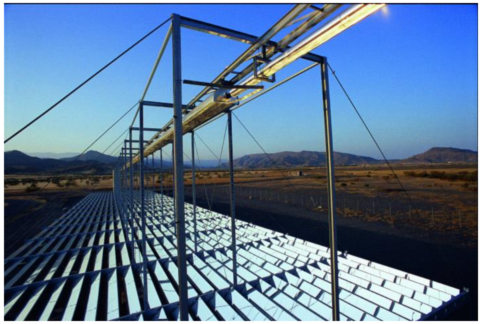

Dish

Tower

Types of CSP Power Plants Status of Application

1) Trough

- Most mature and most used CSP technology.
- Operational in 2014: 3,2 GW

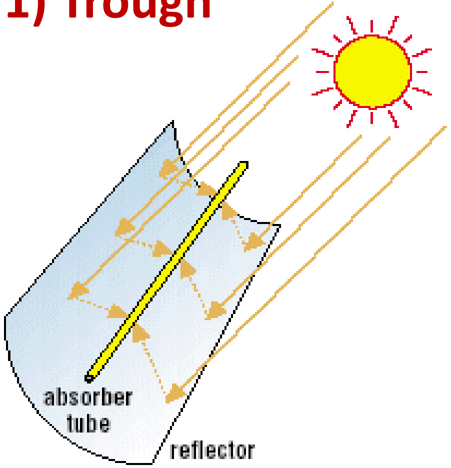

3) Linear Fresnel

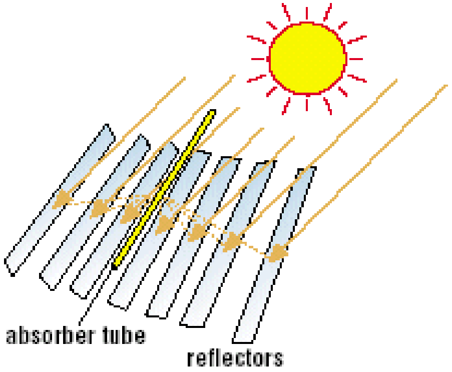

- Similar to trough
- Not yet accepted by market
- Operational in 2014: 36 MW

4) Dish

- Highest efficiency
- Difficult to integrate storage
- Expensive
- Future questionable
- Operational in 2014: < 1 MW

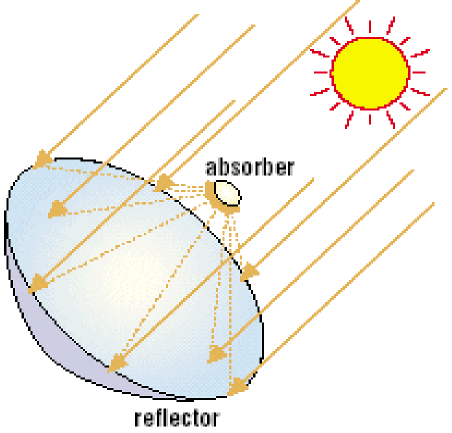

2) Tower

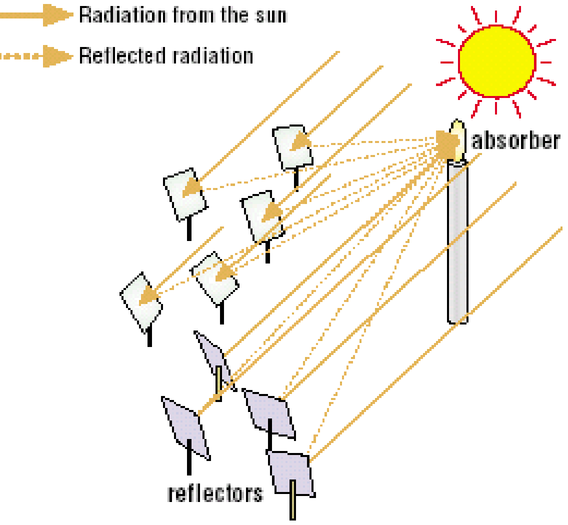

- 2nd in maturity and utilization
- Most promising CSP technology
- Operational in 2014: 0.44 GW

Systematic of Describing the Different CSP Technologies

1) Plant scheme

2) Heat Engine

3) Collector and collector field

4) Performance of the system

5) Status of application

6) Current developments

Parabolic Trough Solar Power Plants

Scheme of Parabolic Trough Solar Power Plant

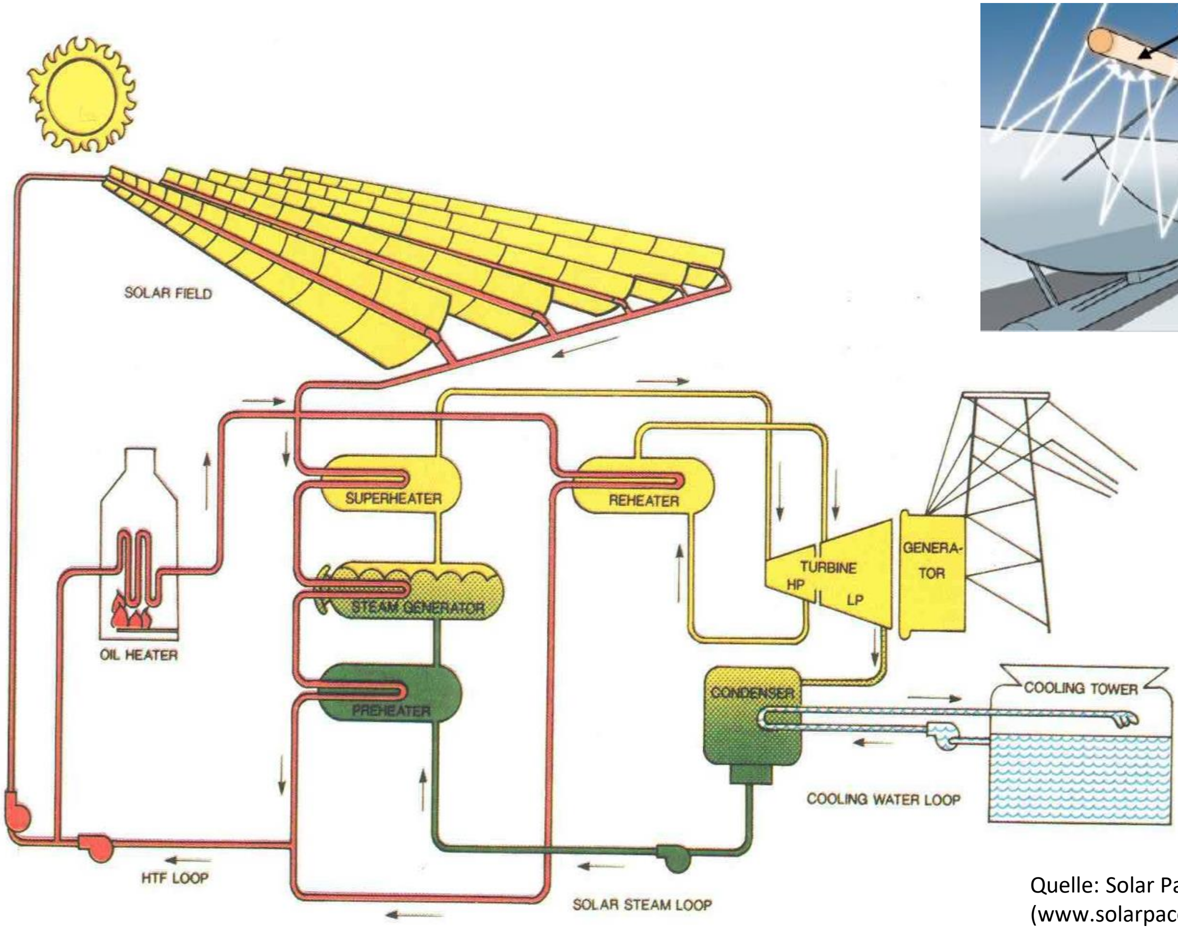

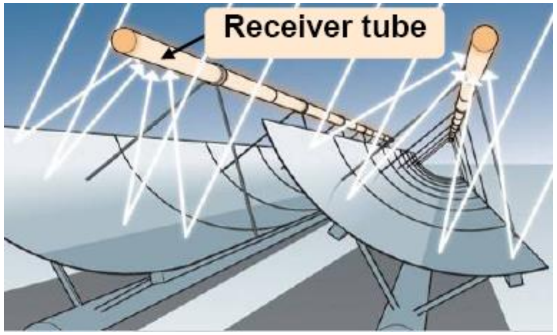

Quelle: Solar Paces
(www.solarpaces.org)

Possible Heat Engines

Possible are:

- Rankine Cycle with steam turbine or steam piston engine
- Stirling engine
- Gas turbine

So far used:

- Rankine Cycle with steam turbine

Reasons for not using the others:

- Stirling engine and steam engine are less suitable due to their small capacities (max. a few MW)
- Gas turbine is less suitable, because it requires very high temperatures which cannot be achieved with Trough Collectors

The Rankine Process, the Process used in Steam Turbine Power Plants

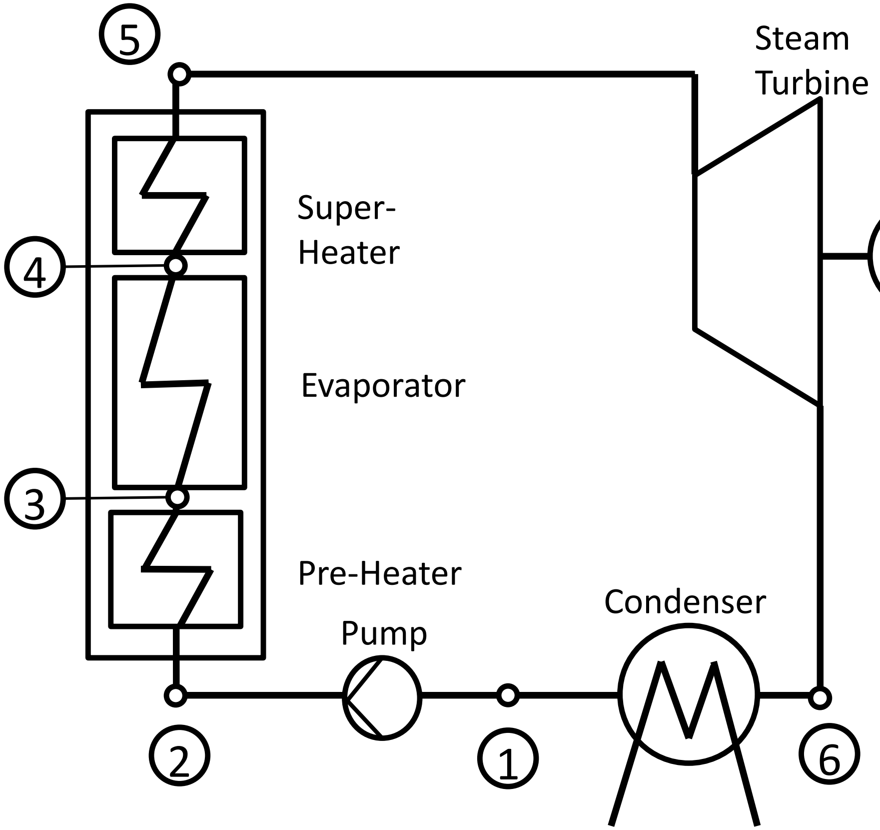

1→2 pressure increase in pump

2→3 pre heating

3→4 evaporation

4→5 super heating

5→6 expansion in turbine

6→1 condensing in condenser

The Rankine Process in h,s-Diagram

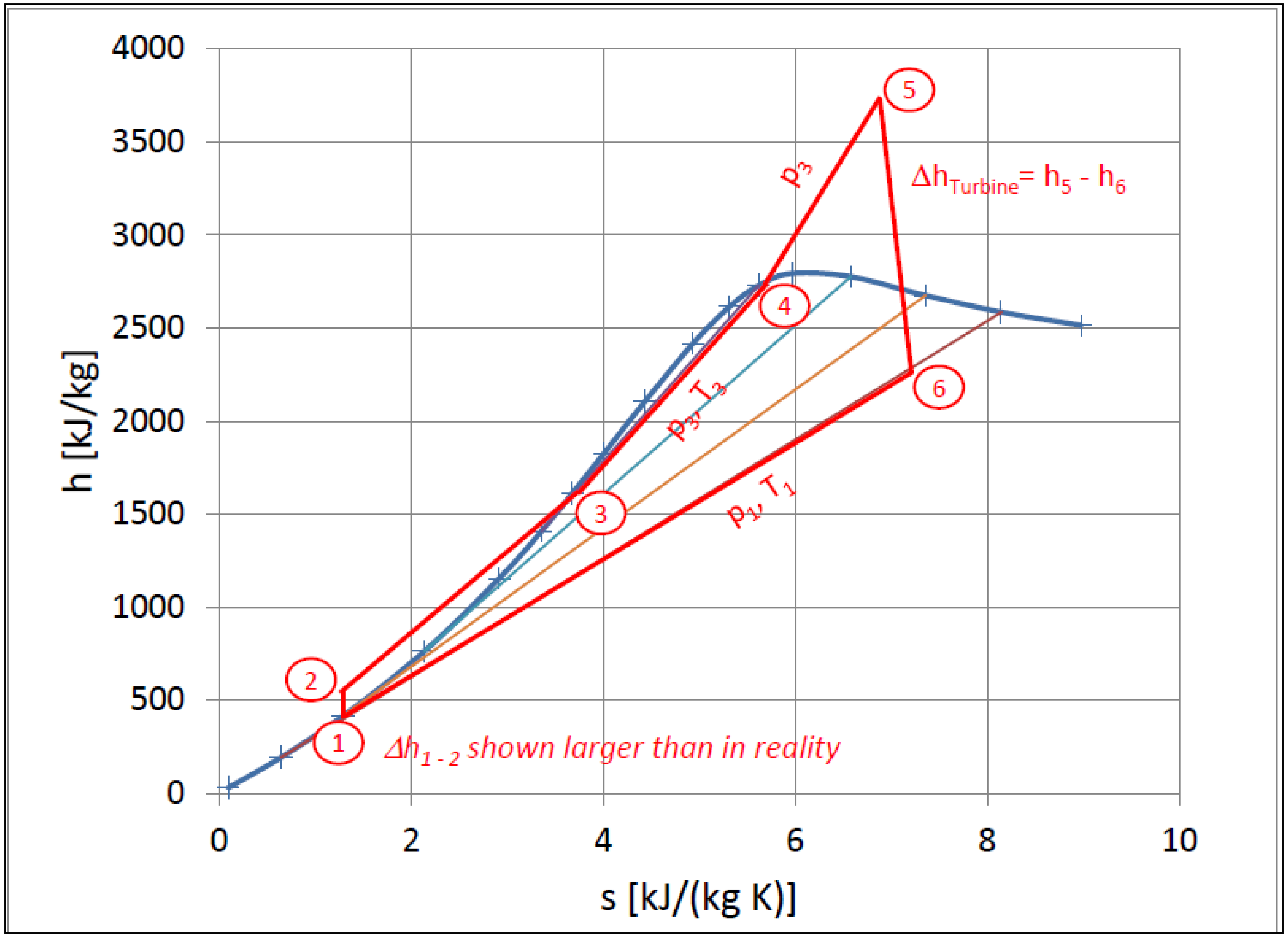

- 1→2 pump
- 2→3 pre heating
- 3→4 evaporation
- 4→5 super heating
- 5→6 turbine
- 6→1 condenser

Source: Prof. Dr.-Ing. O. Goebel

Depiction of the Expansion in the h,s-Diagram of Water and Steam

The start point of the expansion is defined by the temperature and pressure of the steam at the inlet of the turbine (point 5).

The end point is defined by the pressure in the condenser and the steam quality, x at the outlet of the turbine (point 6).

Determining the end point with a given inner efficiency of the turbine ($\eta_{\text{Turb\_inner}}$):

Initially we draw the expansion line isentropically downward, until we hit the isobar of the condenser pressure (isentropic expansion). Measuring the enthalpy difference of the isentropic expansion ($\Delta h_{\text{exp\_isentrop}}$). Then we follow the isobar to the right, until we have gained $\Delta h_{\text{exp\_isentrop}}$ * (1- $\eta_{\text{Turb\_inner}}$) on the enthalpy scale. There is the end point of the technical (real) expansion.

Example: p_{in} = 100 bar, T_{in} = 500°C, p_{Kond} = 0,1 bar, $\eta_{\text{Turb\_inner}}$ = 85%:

$\Delta h_{\text{exp\_isentrop}}$ = 3374 – 2060 = 1314 kJ / kg

$\Delta h_{\text{exp\_isentrop}}$ * 15% = 197 kJ / kg

$h_{\text{Kond\_real}}$ = 2060 + 197 = 2257 kJ / kg

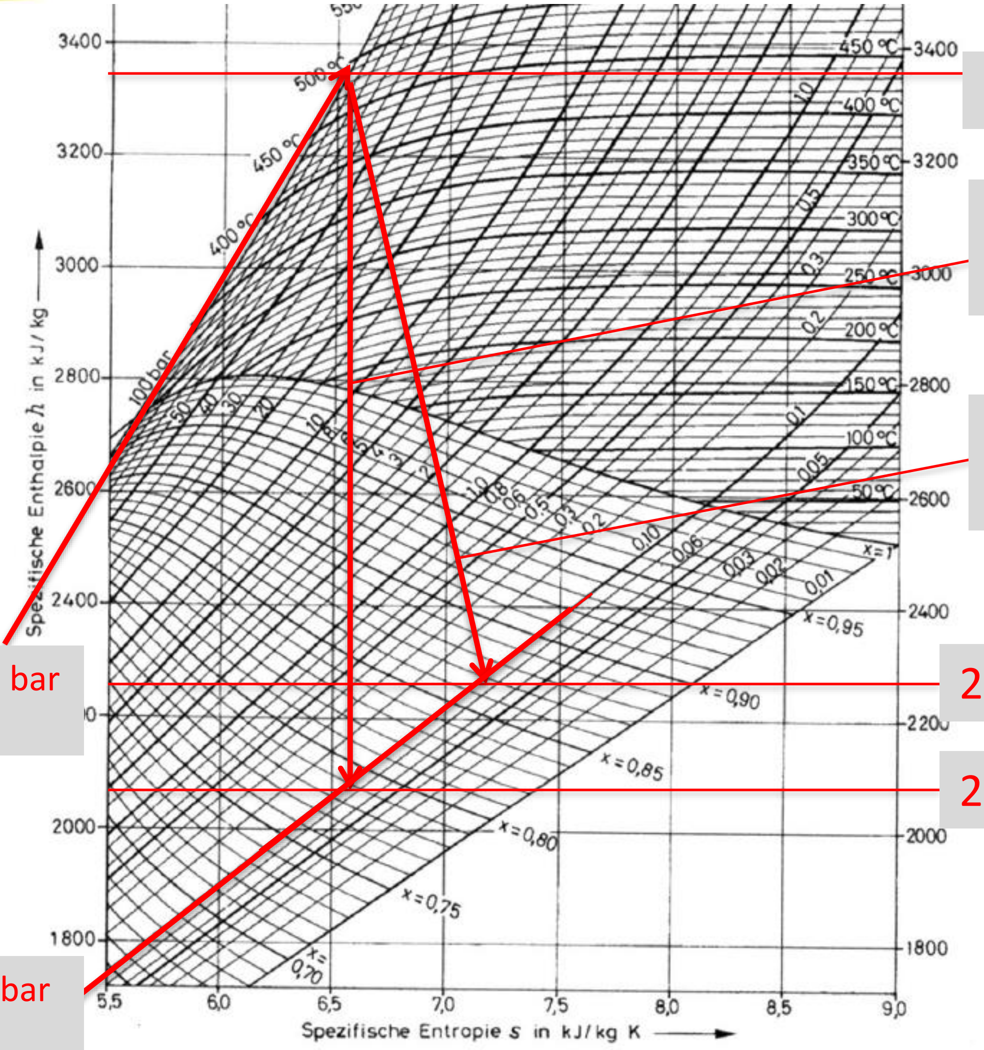

3374

isentropic expansion

technical expansion

2257

2060

100 bar line

0,1 bar line

The Problem of Low Super Heating at Parabolic Trough Solar Power Plants

The max. temperature of the HTF is limited to approx. 400°C. A typical steam temperature at the turbine inlet is 375°C.

A technical expansion would end at a steam wetness, x of 0.79. This is not acceptable for a steam turbine due to the amount of droplets entrained in the steam.

The smallest tolerable values of x are around 0.85.

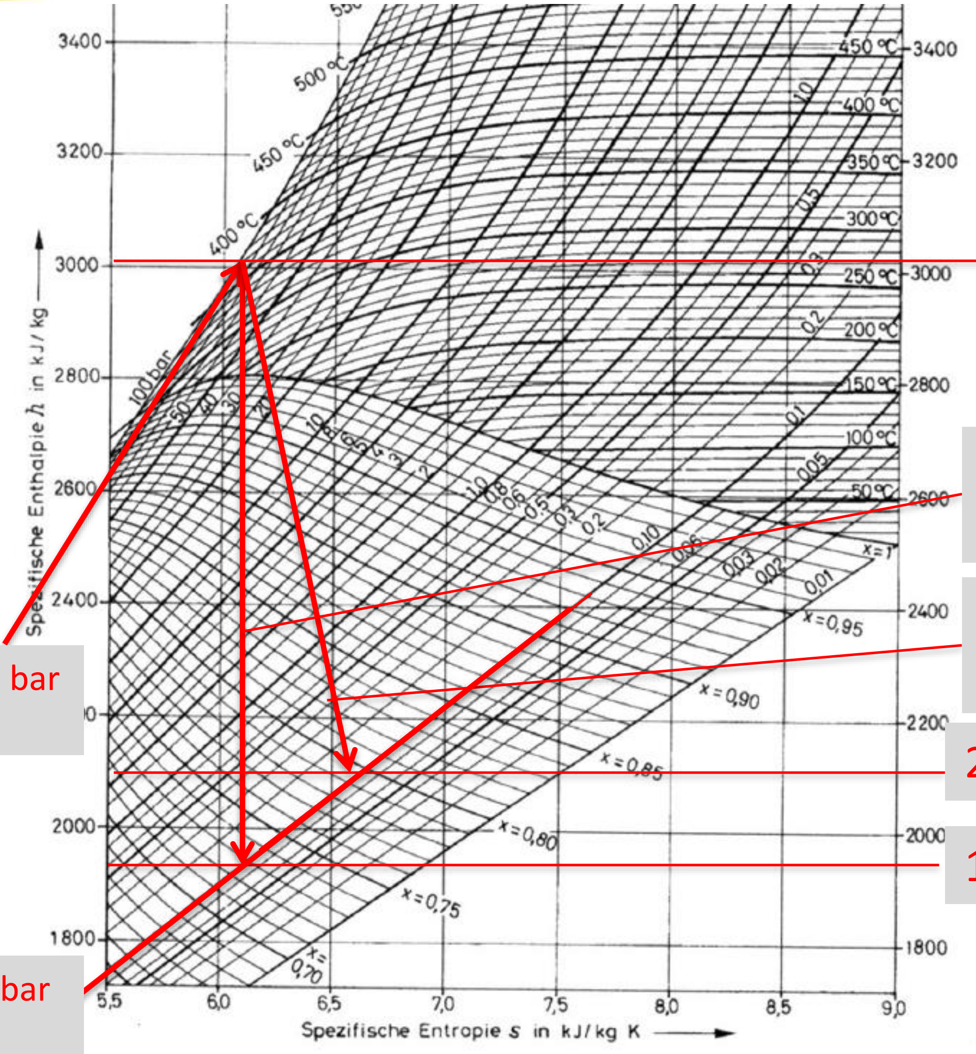

3020

isentropic expansion

technical expansion

2101

1939

100 bar line

0,1 bar line

The necessity of Reheating at Parabolic Trough Solar Power Plants

Solution: We introduce a re-heat at the point when the expansion line first hits the wet steam line. The steam is super heated again in the re-heater until it reaches again 375°C. But now at a pressure of only 20 to 30bar. Hence, the expansion path is shifted to the right in the h,s-Diagram, and the isobar of the condenser pressure is reached at an acceptable steam wetness of x=0,90.

Furthermore the efficiency of the process is increased. We do need additional heat for the re-heat, but we also do get more work out of the turbine. The gain in work is larger then the increase of heat demand.

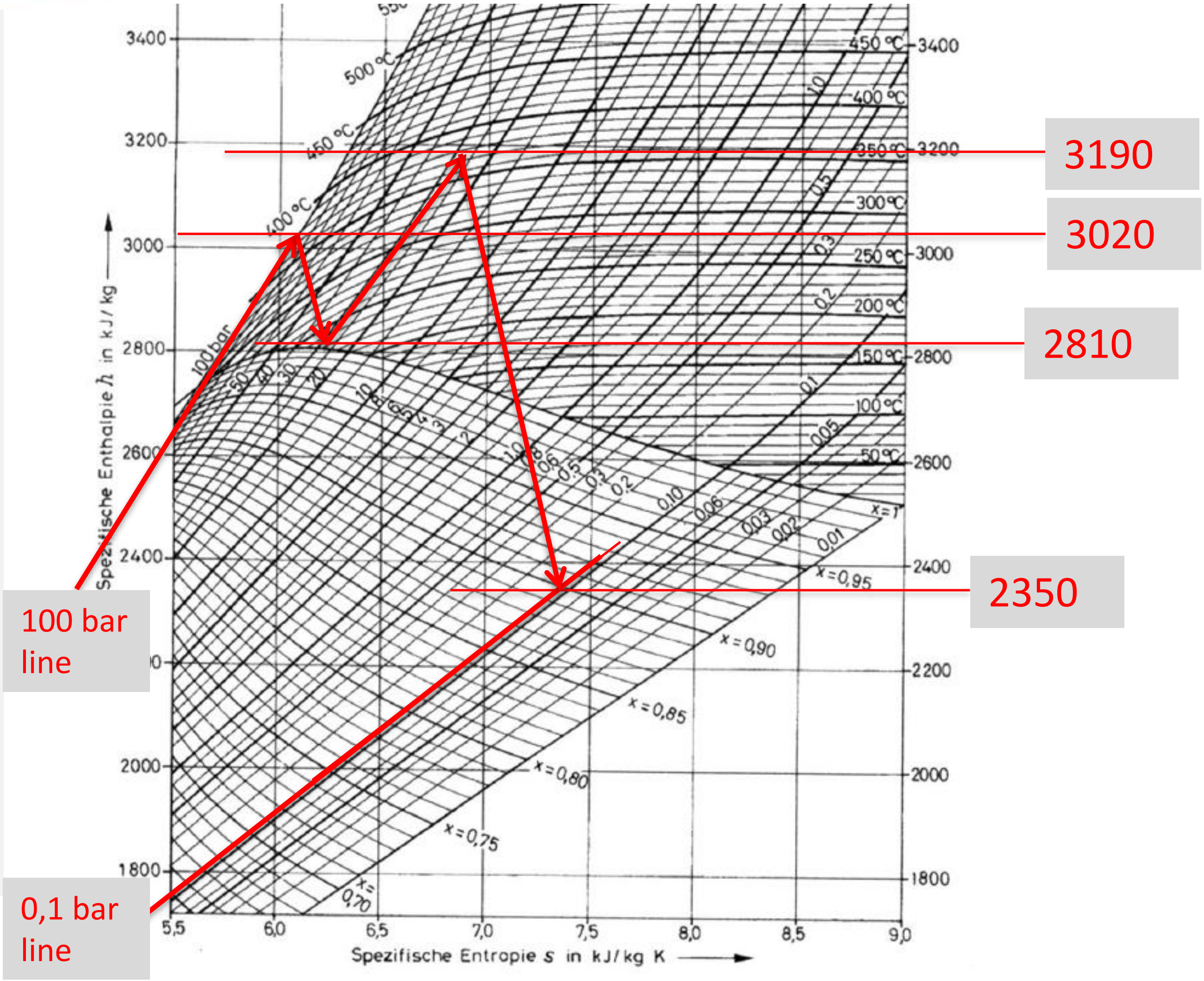

3190

3020

2810

2350

100 bar line

0,1 bar line

Multi Stage Feed Water Pre-Heating

- The scheme below shows the multi stage feed water pre heating in a Parabolic Trough Solar Power Plant without Re-Heat.
- The feed water has already a temperature of 220°C when it enters the solar pre-heater.
- The pre-heating is performed with steam extracted from the turbine.

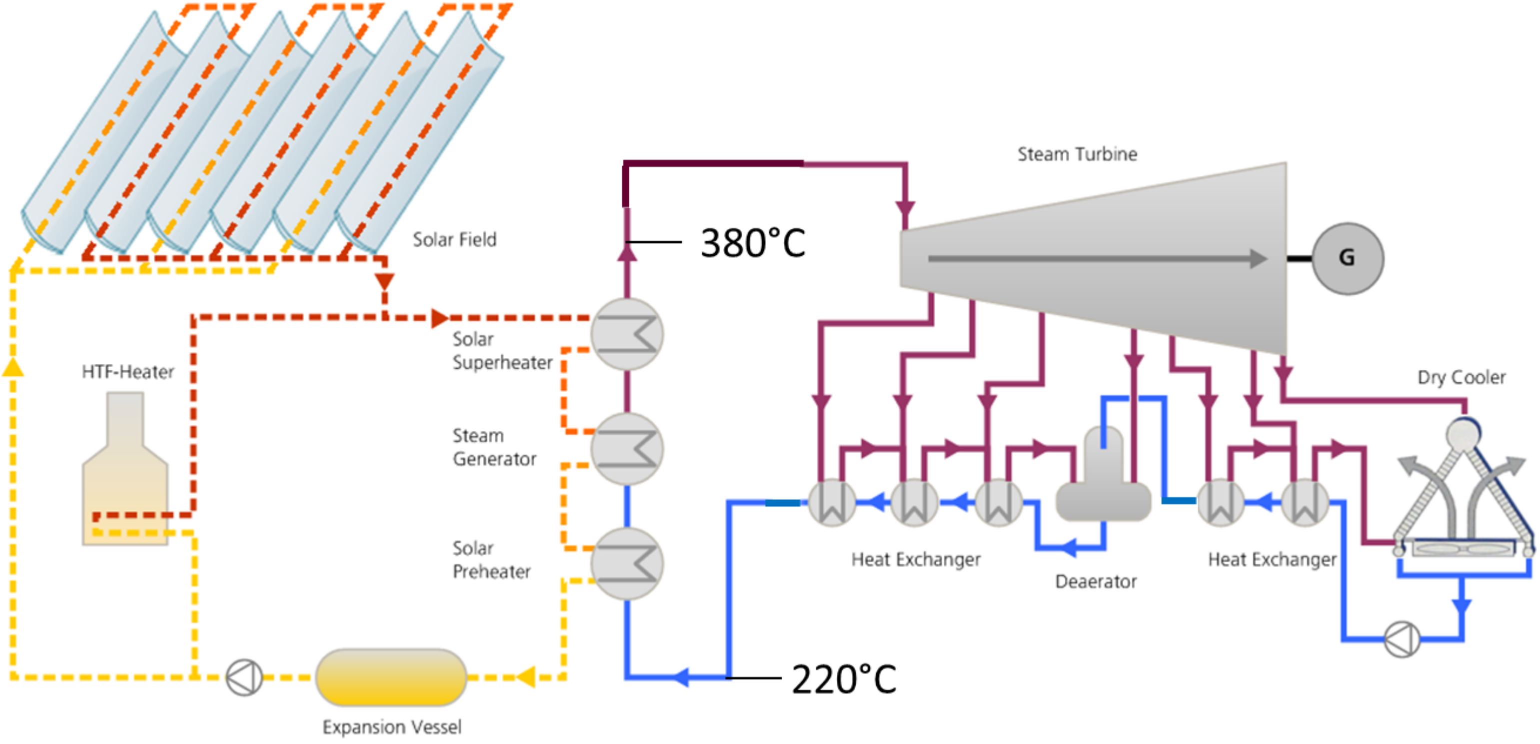

Multi Stage Feed Water Pre-Heating

Example Calculation:

How much temperature gain, $\Delta T_{feedwater}$ can be achieved for the feed water flow in the 2nd pre-heater with the following given data?

$$\dot{m}_{feedwater} = 103\frac{kg}{s}\,;\, \dot{m}_{extraction} = 4.8\frac{kg}{s}$$

$$h_{extr.,HX\ in} = 2600\frac{kJ}{kg}\,;\, h_{extr.,HX\ out} = 467\frac{kJ}{kg}$$

Solution:

Power provided by the extraction:

$$\dot{Q} = \dot{m}_{extraction} \cdot \Delta h = 10.238\ MW$$

Power received by the feed water flow (the same as above):

$$\dot{Q} = \dot{m}_{feedwater} \cdot c_p \cdot \Delta T$$

$$\Delta T_{feedwater} = \frac{\dot{Q}}{\dot{m}_{feedwater} \cdot c_p} = \frac{10238\ kJ/s}{103 kg/s \cdot 4.18 \frac{kJ}{kg\ K}} = \underline{\mathbf{23.78K}}$$

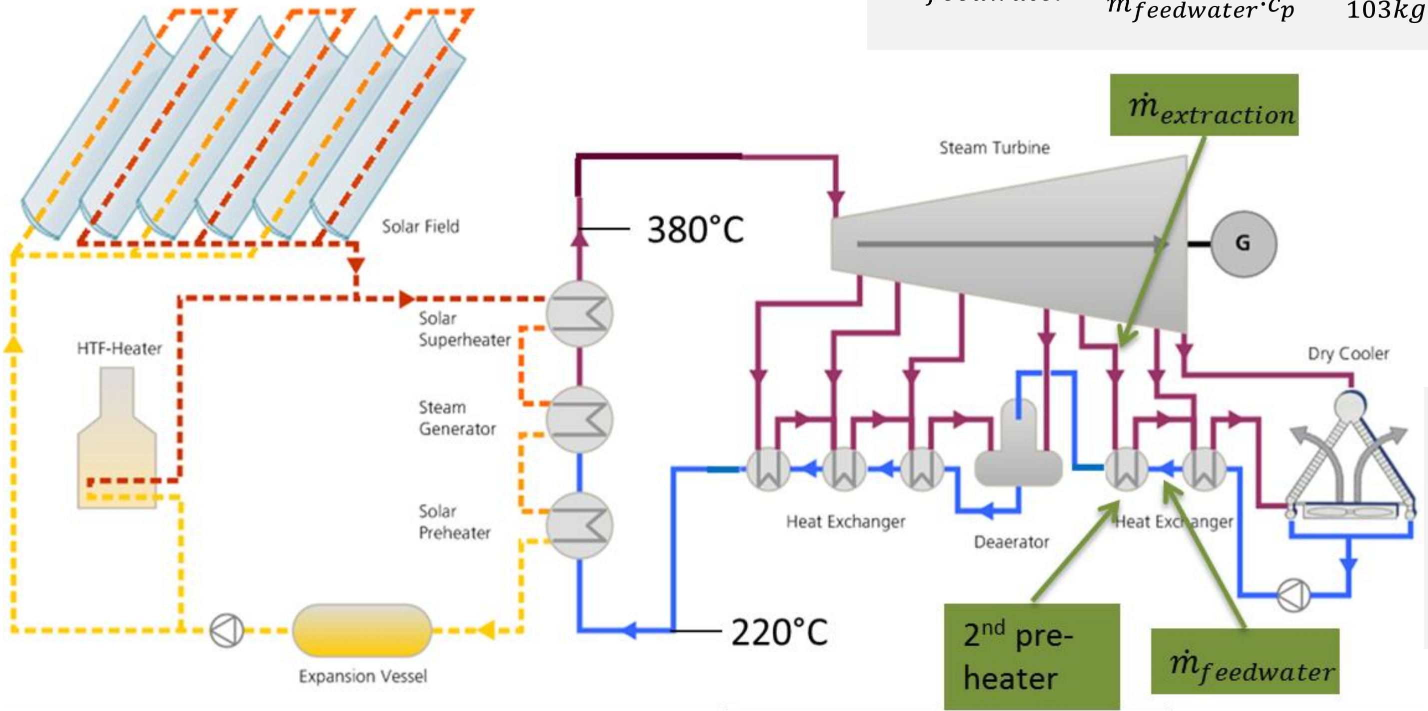

Lesson learned:

A rather small mass flow of extracted steam causes a rather big increase of feed water temperature.

Efficiency of Rankine Process

- The efficiency of a Rankine Process can be calculated by the following equation:
- $\eta = \frac{\Delta h_{6-5} - \Delta h_{2-1}}{\Delta h_{5-2}}$ *(Enthalpies, h as defined in the slide "Rankine Process in h,s-diagram")*
- In case of a re-heat: both expansion enthalpy differences are in the numerator and the enthalpy difference of the re-heat is added to the nominator:
- $\eta = \frac{\Delta h_{HP-turbine} + \Delta h_{LP-turbine} - \Delta h_{2-1}}{\Delta h_{steam\ generator} + \Delta h_{re-heat}}$
- In case feed water pre-heating is used, it is no longer possible to calculate the efficiency with enthalpy differences only. They need to be multiplied with the respective mass flows, because they are different at the different process steps.
- For a first estimate of the Rankine Cycle efficiency it can be calculated with the Carnot efficiency and the thermodynamic performance factor (tpf).
- $\eta_{Carnot} = \frac{T_{up} - T_{low}}{T_{up}}$ or $= 1 - \frac{T_{low}}{T_{up}}$ with all temperatures in [Kelvin]
- The thermodynamic performance factor (tpf) can be assumed with 0.75 for large scale plants and 0.70 for smaller plants.
- Example: $T_{up} = 400°C;\quad T_{low} = 30°C;\quad tpf = 0{,}72$ => $\eta_{Carnot} = \frac{370\ K}{673{,}15\ K}$ = 55%
- $\eta_{Rankine} = \eta_{Carnot} * tpf$ = 55% * 0,72 = 39.6%

h,s-Diagram for Water and Steam

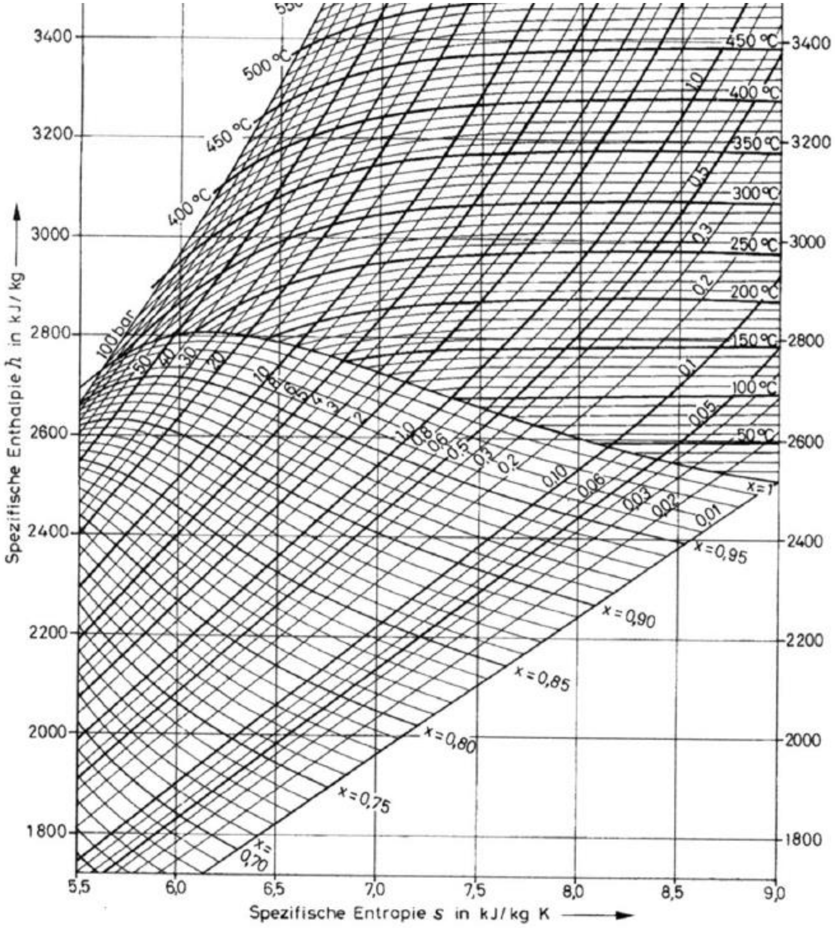

- The h,s-Diagram is especially useful for reading values in the area of super heated steam. Therefore mostly only this area is depicted in the diagram.
- In the area of liquid state water the values are difficult to depict in the diagram.
- Therefore mostly tables are used to describe the liquid state and the wet steam area.
- These table can be found on the following pages.
- The tables also show the values for super heated steam which is depicted in the diagram on the left.

Saturated Steam

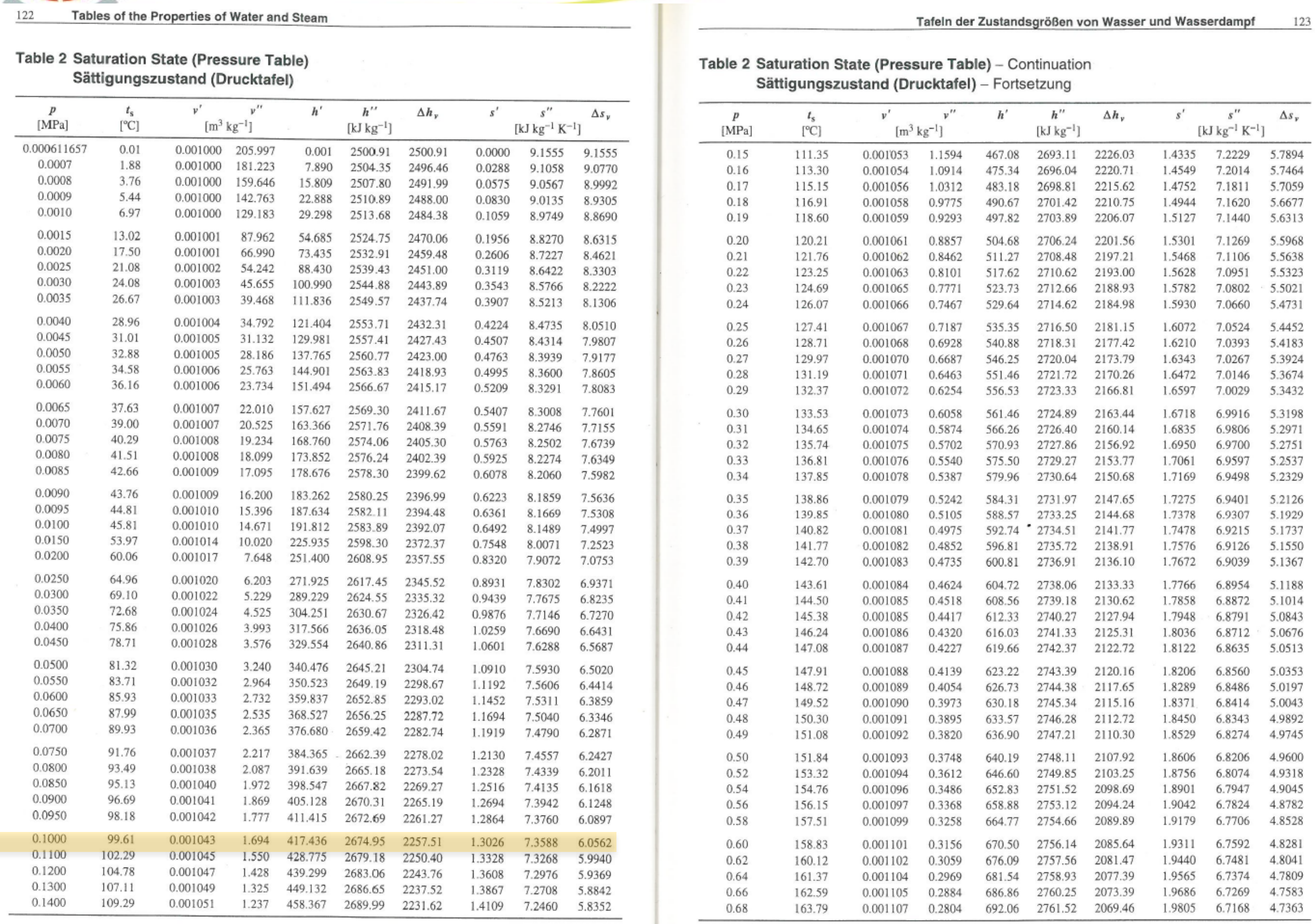

122 Tables of the Properties of Water and Steam

Table 2 Saturation State (Pressure Table)
Sättigungszustand (Drucktafel)

p [MPa]	t_s [°C]	v'	v''	h'	h''	Δh_v	s'	s''	Δs_v
		[m³ kg⁻¹]		[kJ kg⁻¹]			[kJ kg⁻¹ K⁻¹]		
0.000611657	0.01	0.001000	205.997	0.001	2500.91	2500.91	0.0000	9.1555	9.1555
0.0007	1.88	0.001000	181.223	7.890	2504.35	2496.46	0.0288	9.1058	9.0770
0.0008	3.76	0.001000	159.646	15.809	2507.80	2491.99	0.0575	9.0567	8.9992
0.0009	5.44	0.001000	142.763	22.888	2510.89	2488.00	0.0830	9.0135	8.9305
0.0010	6.97	0.001000	129.183	29.298	2513.68	2484.38	0.1059	8.9749	8.8690
0.0015	13.02	0.001001	87.962	54.685	2524.75	2470.06	0.1956	8.8270	8.6315
0.0020	17.50	0.001001	66.990	73.435	2532.91	2459.48	0.2606	8.7227	8.4621
0.0025	21.08	0.001002	54.242	88.430	2539.43	2451.00	0.3119	8.6422	8.3303
0.0030	24.08	0.001003	45.655	100.990	2544.88	2443.89	0.3543	8.5766	8.2222
0.0035	26.67	0.001003	39.468	111.836	2549.57	2437.74	0.3907	8.5213	8.1306
0.0040	28.96	0.001004	34.792	121.404	2553.71	2432.31	0.4224	8.4735	8.0510
0.0045	31.01	0.001005	31.132	129.981	2557.41	2427.43	0.4507	8.4314	7.9807
0.0050	32.88	0.001005	28.186	137.765	2560.77	2423.00	0.4763	8.3939	7.9177
0.0055	34.58	0.001006	25.763	144.901	2563.83	2418.93	0.4995	8.3600	7.8605
0.0060	36.16	0.001006	23.734	151.494	2566.67	2415.17	0.5209	8.3291	7.8083
0.0065	37.63	0.001007	22.010	157.627	2569.30	2411.67	0.5407	8.3008	7.7601
0.0070	39.00	0.001007	20.525	163.366	2571.76	2408.39	0.5591	8.2746	7.7155
0.0075	40.29	0.001008	19.234	168.760	2574.06	2405.30	0.5763	8.2502	7.6739
0.0080	41.51	0.001008	18.099	173.852	2576.24	2402.39	0.5925	8.2274	7.6349
0.0085	42.66	0.001009	17.095	178.676	2578.30	2399.62	0.6078	8.2060	7.5982
0.0090	43.76	0.001009	16.200	183.262	2580.25	2396.99	0.6223	8.1859	7.5636
0.0095	44.81	0.001010	15.396	187.634	2582.11	2394.48	0.6361	8.1669	7.5308
0.0100	45.81	0.001010	14.671	191.812	2583.89	2392.07	0.6492	8.1489	7.4997
0.0150	53.97	0.001014	10.020	225.935	2598.30	2372.37	0.7548	8.0071	7.2523
0.0200	60.06	0.001017	7.648	251.400	2608.95	2357.55	0.8320	7.9072	7.0753
0.0250	64.96	0.001020	6.203	271.925	2617.45	2345.52	0.8931	7.8302	6.9371
0.0300	69.10	0.001022	5.229	289.229	2624.55	2335.32	0.9439	7.7675	6.8235
0.0350	72.68	0.001024	4.525	304.251	2630.67	2326.42	0.9876	7.7146	6.7270
0.0400	75.86	0.001026	3.993	317.566	2636.05	2318.48	1.0259	7.6690	6.6431
0.0450	78.71	0.001028	3.576	329.554	2640.86	2311.31	1.0601	7.6288	6.5687
0.0500	81.32	0.001030	3.240	340.476	2645.21	2304.74	1.0910	7.5930	6.5020
0.0550	83.71	0.001032	2.964	350.523	2649.19	2298.67	1.1192	7.5606	6.4414
0.0600	85.93	0.001033	2.732	359.837	2652.85	2293.02	1.1452	7.5311	6.3859
0.0650	87.99	0.001035	2.535	368.527	2656.25	2287.72	1.1694	7.5040	6.3346
0.0700	89.93	0.001036	2.365	376.680	2659.42	2282.74	1.1919	7.4790	6.2871
0.0750	91.76	0.001037	2.217	384.365	2662.39	2278.02	1.2130	7.4557	6.2427
0.0800	93.49	0.001038	2.087	391.639	2665.18	2273.54	1.2328	7.4339	6.2011
0.0850	95.13	0.001040	1.972	398.547	2667.82	2269.27	1.2516	7.4135	6.1618
0.0900	96.69	0.001041	1.869	405.128	2670.31	2265.19	1.2694	7.3942	6.1248
0.0950	98.18	0.001042	1.777	411.415	2672.69	2261.27	1.2864	7.3760	6.0897
0.1000	99.61	0.001043	1.694	417.436	2674.95	2257.51	1.3026	7.3588	6.0562
0.1100	102.29	0.001045	1.550	428.775	2679.18	2250.40	1.3328	7.3268	5.9940
0.1200	104.78	0.001047	1.428	439.299	2683.06	2243.76	1.3608	7.2976	5.9369
0.1300	107.11	0.001049	1.325	449.132	2686.65	2237.52	1.3867	7.2708	5.8842
0.1400	109.29	0.001051	1.237	458.367	2689.99	2231.62	1.4109	7.2460	5.8352

1 bar

Tafeln der Zustandsgrößen von Wasser und Wasserdampf 123

Table 2 Saturation State (Pressure Table) – Continuation
Sättigungszustand (Drucktafel) – Fortsetzung

p [MPa]	t_s [°C]	v'	v''	h'	h''	Δh_v	s'	s''	Δs_v
		[m³ kg⁻¹]		[kJ kg⁻¹]			[kJ kg⁻¹ K⁻¹]		
0.15	111.35	0.001053	1.1594	467.08	2693.11	2226.03	1.4335	7.2229	5.7894
0.16	113.30	0.001054	1.0914	475.34	2696.04	2220.71	1.4549	7.2014	5.7464
0.17	115.15	0.001056	1.0312	483.18	2698.81	2215.62	1.4752	7.1811	5.7059
0.18	116.91	0.001058	0.9775	490.67	2701.42	2210.75	1.4944	7.1620	5.6677
0.19	118.60	0.001059	0.9293	497.82	2703.89	2206.07	1.5127	7.1440	5.6313
0.20	120.21	0.001061	0.8857	504.68	2706.24	2201.56	1.5301	7.1269	5.5968
0.21	121.76	0.001062	0.8462	511.27	2708.48	2197.21	1.5468	7.1106	5.5638
0.22	123.25	0.001063	0.8101	517.62	2710.62	2193.00	1.5628	7.0951	5.5323
0.23	124.69	0.001065	0.7771	523.73	2712.66	2188.93	1.5782	7.0802	5.5021
0.24	126.07	0.001066	0.7467	529.64	2714.62	2184.98	1.5930	7.0660	5.4731
0.25	127.41	0.001067	0.7187	535.35	2716.50	2181.15	1.6072	7.0524	5.4452
0.26	128.71	0.001068	0.6928	540.88	2718.31	2177.42	1.6210	7.0393	5.4183
0.27	129.97	0.001070	0.6687	546.25	2720.04	2173.79	1.6343	7.0267	5.3924
0.28	131.19	0.001071	0.6463	551.46	2721.72	2170.26	1.6472	7.0146	5.3674
0.29	132.37	0.001072	0.6254	556.53	2723.33	2166.81	1.6597	7.0029	5.3432
0.30	133.53	0.001073	0.6058	561.46	2724.89	2163.44	1.6718	6.9916	5.3198
0.31	134.65	0.001074	0.5874	566.26	2726.40	2160.14	1.6835	6.9806	5.2971
0.32	135.74	0.001075	0.5702	570.93	2727.86	2156.92	1.6950	6.9700	5.2751
0.33	136.81	0.001076	0.5540	575.50	2729.27	2153.77	1.7061	6.9597	5.2537
0.34	137.85	0.001078	0.5387	579.96	2730.64	2150.68	1.7169	6.9498	5.2329
0.35	138.86	0.001079	0.5242	584.31	2731.97	2147.65	1.7275	6.9401	5.2126
0.36	139.85	0.001080	0.5105	588.57	2733.25	2144.68	1.7378	6.9307	5.1929
0.37	140.82	0.001081	0.4975	592.74	2734.51	2141.77	1.7478	6.9215	5.1737
0.38	141.77	0.001082	0.4852	596.81	2735.72	2138.91	1.7576	6.9126	5.1550
0.39	142.70	0.001083	0.4735	600.81	2736.91	2136.10	1.7672	6.9039	5.1367
0.40	143.61	0.001084	0.4624	604.72	2738.06	2133.33	1.7766	6.8954	5.1188
0.41	144.50	0.001085	0.4518	608.56	2739.18	2130.62	1.7858	6.8872	5.1014
0.42	145.38	0.001085	0.4417	612.33	2740.27	2127.94	1.7948	6.8791	5.0843
0.43	146.24	0.001086	0.4320	616.03	2741.33	2125.31	1.8036	6.8712	5.0676
0.44	147.08	0.001087	0.4227	619.66	2742.37	2122.72	1.8122	6.8635	5.0513
0.45	147.91	0.001088	0.4139	623.22	2743.39	2120.16	1.8206	6.8560	5.0353
0.46	148.72	0.001089	0.4054	626.73	2744.38	2117.65	1.8289	6.8486	5.0197
0.47	149.52	0.001090	0.3973	630.18	2745.34	2115.16	1.8371	6.8414	5.0043
0.48	150.30	0.001091	0.3895	633.57	2746.28	2112.72	1.8450	6.8343	4.9892
0.49	151.08	0.001092	0.3820	636.90	2747.21	2110.30	1.8529	6.8274	4.9745
0.50	151.84	0.001093	0.3748	640.19	2748.11	2107.92	1.8606	6.8206	4.9600
0.52	153.32	0.001094	0.3612	646.60	2749.85	2103.25	1.8756	6.8074	4.9318
0.54	154.76	0.001096	0.3486	652.83	2751.52	2098.69	1.8901	6.7947	4.9045
0.56	156.15	0.001097	0.3368	658.88	2753.12	2094.24	1.9042	6.7824	4.8782
0.58	157.51	0.001099	0.3258	664.77	2754.66	2089.89	1.9179	6.7706	4.8528
0.60	158.83	0.001101	0.3156	670.50	2756.14	2085.64	1.9311	6.7592	4.8281
0.62	160.12	0.001102	0.3059	676.09	2757.56	2081.47	1.9440	6.7481	4.8041
0.64	161.37	0.001104	0.2969	681.54	2758.93	2077.39	1.9565	6.7374	4.7809
0.66	162.59	0.001105	0.2884	686.86	2760.25	2073.39	1.9686	6.7269	4.7583
0.68	163.79	0.001107	0.2804	692.06	2761.52	2069.46	1.9805	6.7168	4.7363

Quelle: Wagner, W.; Kruse, A. Properties of Water and Steam, Springer

Saturated Steam

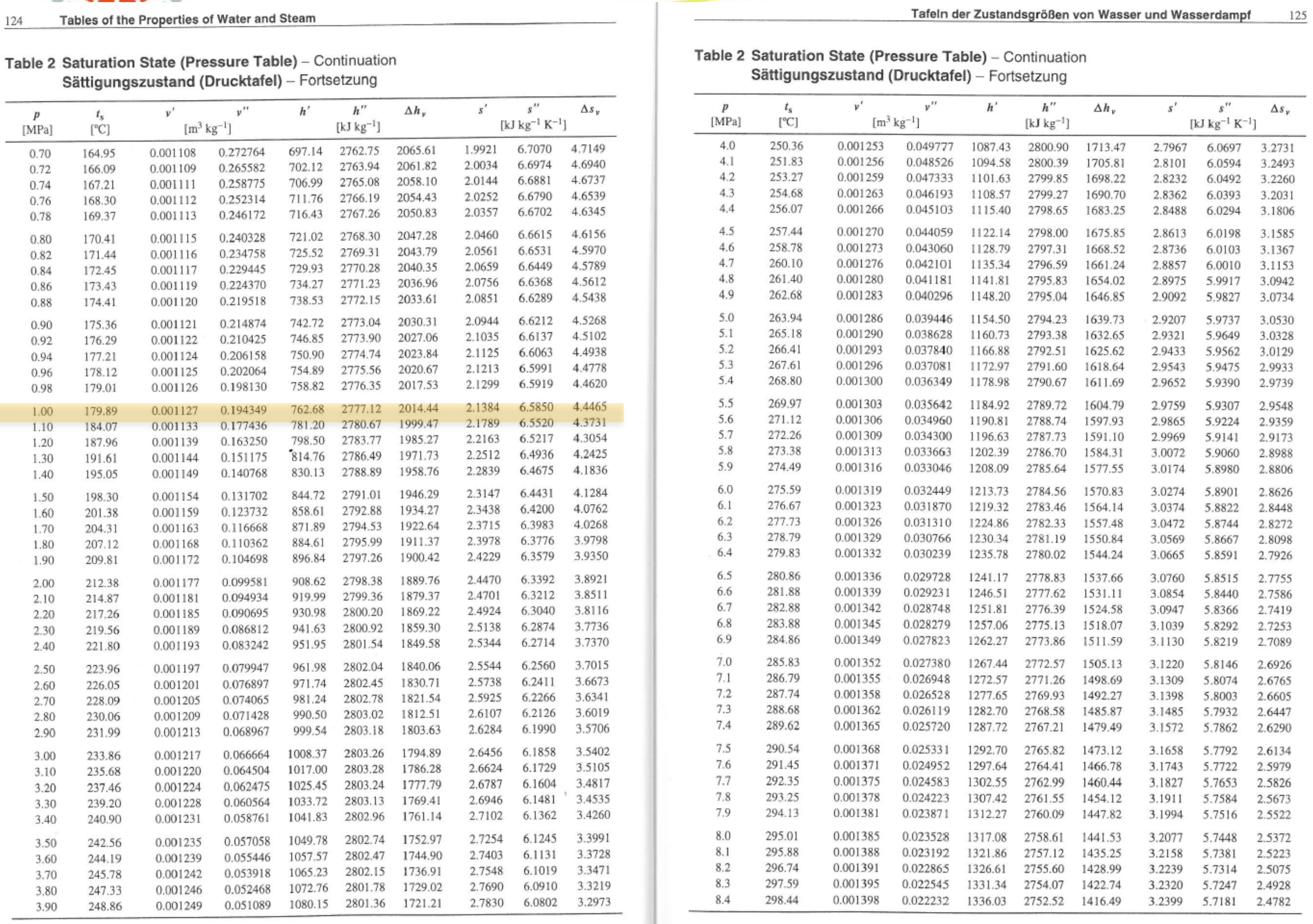

Table 2 Saturation State (Pressure Table) – Continuation
Sättigungszustand (Drucktafel) – Fortsetzung

10 bar

p	t_s	v'	v''	h'	h''	Δh_v	s'	s''	Δs_v
[MPa]	[°C]	$[\mathrm{m}^3\,\mathrm{kg}^{-1}]$		$[\mathrm{kJ\,kg}^{-1}]$			$[\mathrm{kJ\,kg}^{-1}\,\mathrm{K}^{-1}]$		
0.70	164.95	0.001108	0.272764	697.14	2762.75	2065.61	1.9921	6.7070	4.7149
0.72	166.09	0.001109	0.265582	702.12	2763.94	2061.82	2.0034	6.6974	4.6940
0.74	167.21	0.001111	0.258775	706.99	2765.08	2058.10	2.0144	6.6881	4.6737
0.76	168.30	0.001112	0.252314	711.76	2766.19	2054.43	2.0252	6.6790	4.6539
0.78	169.37	0.001113	0.246172	716.43	2767.26	2050.83	2.0357	6.6702	4.6345
0.80	170.41	0.001115	0.240328	721.02	2768.30	2047.28	2.0460	6.6615	4.6156
0.82	171.44	0.001116	0.234758	725.52	2769.31	2043.79	2.0561	6.6531	4.5970
0.84	172.45	0.001117	0.229445	729.93	2770.28	2040.35	2.0659	6.6449	4.5789
0.86	173.43	0.001119	0.224370	734.27	2771.23	2036.96	2.0756	6.6368	4.5612
0.88	174.41	0.001120	0.219518	738.53	2772.15	2033.61	2.0851	6.6289	4.5438
0.90	175.36	0.001121	0.214874	742.72	2773.04	2030.31	2.0944	6.6212	4.5268
0.92	176.29	0.001122	0.210425	746.85	2773.90	2027.06	2.1035	6.6137	4.5102
0.94	177.21	0.001124	0.206158	750.90	2774.74	2023.84	2.1125	6.6063	4.4938
0.96	178.12	0.001125	0.202064	754.89	2775.56	2020.67	2.1213	6.5991	4.4778
0.98	179.01	0.001126	0.198130	758.82	2776.35	2017.53	2.1299	6.5919	4.4620
1.00	179.89	0.001127	0.194349	762.68	2777.12	2014.44	2.1384	6.5850	4.4465
1.10	184.07	0.001133	0.177436	781.20	2780.67	1999.47	2.1789	6.5520	4.3731
1.20	187.96	0.001139	0.163250	798.50	2783.77	1985.27	2.2163	6.5217	4.3054
1.30	191.61	0.001144	0.151175	814.76	2786.49	1971.73	2.2512	6.4936	4.2425
1.40	195.05	0.001149	0.140768	830.13	2788.89	1958.76	2.2839	6.4675	4.1836
1.50	198.30	0.001154	0.131702	844.72	2791.01	1946.29	2.3147	6.4431	4.1284
1.60	201.38	0.001159	0.123732	858.61	2792.88	1934.27	2.3438	6.4200	4.0762
1.70	204.31	0.001163	0.116668	871.89	2794.53	1922.64	2.3715	6.3983	4.0268
1.80	207.12	0.001168	0.110362	884.61	2795.99	1911.37	2.3978	6.3776	3.9798
1.90	209.81	0.001172	0.104698	896.84	2797.26	1900.42	2.4229	6.3579	3.9350
2.00	212.38	0.001177	0.099581	908.62	2798.38	1889.76	2.4470	6.3392	3.8921
2.10	214.87	0.001181	0.094934	919.99	2799.36	1879.37	2.4701	6.3212	3.8511
2.20	217.26	0.001185	0.090695	930.98	2800.20	1869.22	2.4924	6.3040	3.8116
2.30	219.56	0.001189	0.086812	941.63	2800.92	1859.30	2.5138	6.2874	3.7736
2.40	221.80	0.001193	0.083242	951.95	2801.54	1849.58	2.5344	6.2714	3.7370
2.50	223.96	0.001197	0.079947	961.98	2802.04	1840.06	2.5544	6.2560	3.7015
2.60	226.05	0.001201	0.076897	971.74	2802.45	1830.71	2.5738	6.2411	3.6673
2.70	228.09	0.001205	0.074065	981.24	2802.78	1821.54	2.5925	6.2266	3.6341
2.80	230.06	0.001209	0.071428	990.50	2803.02	1812.51	2.6107	6.2126	3.6019
2.90	231.99	0.001213	0.068967	999.54	2803.18	1803.63	2.6284	6.1990	3.5706
3.00	233.86	0.001217	0.066664	1008.37	2803.26	1794.89	2.6456	6.1858	3.5402
3.10	235.68	0.001220	0.064504	1017.00	2803.28	1786.28	2.6624	6.1729	3.5105
3.20	237.46	0.001224	0.062475	1025.45	2803.24	1777.79	2.6787	6.1604	3.4817
3.30	239.20	0.001228	0.060564	1033.72	2803.13	1769.41	2.6946	6.1481	3.4535
3.40	240.90	0.001231	0.058761	1041.83	2802.96	1761.14	2.7102	6.1362	3.4260
3.50	242.56	0.001235	0.057058	1049.78	2802.74	1752.97	2.7254	6.1245	3.3991
3.60	244.19	0.001239	0.055446	1057.57	2802.47	1744.90	2.7403	6.1131	3.3728
3.70	245.78	0.001242	0.053918	1065.23	2802.15	1736.91	2.7548	6.1019	3.3471
3.80	247.33	0.001246	0.052468	1072.76	2801.78	1729.02	2.7690	6.0910	3.3219
3.90	248.86	0.001249	0.051089	1080.15	2801.36	1721.21	2.7830	6.0802	3.2973

Table 2 Saturation State (Pressure Table) – Continuation
Sättigungszustand (Drucktafel) – Fortsetzung

p	t_s	v'	v''	h'	h''	Δh_v	s'	s''	Δs_v
[MPa]	[°C]	$[\mathrm{m}^3\,\mathrm{kg}^{-1}]$		$[\mathrm{kJ\,kg}^{-1}]$			$[\mathrm{kJ\,kg}^{-1}\,\mathrm{K}^{-1}]$		
4.0	250.36	0.001253	0.049777	1087.43	2800.90	1713.47	2.7967	6.0697	3.2731
4.1	251.83	0.001256	0.048526	1094.58	2800.39	1705.81	2.8101	6.0594	3.2493
4.2	253.27	0.001259	0.047333	1101.63	2799.85	1698.22	2.8232	6.0492	3.2260
4.3	254.68	0.001263	0.046193	1108.57	2799.27	1690.70	2.8362	6.0393	3.2031
4.4	256.07	0.001266	0.045103	1115.40	2798.65	1683.25	2.8488	6.0294	3.1806
4.5	257.44	0.001270	0.044059	1122.14	2798.00	1675.85	2.8613	6.0198	3.1585
4.6	258.78	0.001273	0.043060	1128.79	2797.31	1668.52	2.8736	6.0103	3.1367
4.7	260.10	0.001276	0.042101	1135.34	2796.59	1661.24	2.8857	6.0010	3.1153
4.8	261.40	0.001280	0.041181	1141.81	2795.83	1654.02	2.8975	5.9917	3.0942
4.9	262.68	0.001283	0.040296	1148.20	2795.04	1646.85	2.9092	5.9827	3.0734
5.0	263.94	0.001286	0.039446	1154.50	2794.23	1639.73	2.9207	5.9737	3.0530
5.1	265.18	0.001290	0.038628	1160.73	2793.38	1632.65	2.9321	5.9649	3.0328
5.2	266.41	0.001293	0.037840	1166.88	2792.51	1625.62	2.9433	5.9562	3.0129
5.3	267.61	0.001296	0.037081	1172.97	2791.60	1618.64	2.9543	5.9475	2.9933
5.4	268.80	0.001300	0.036349	1178.98	2790.67	1611.69	2.9652	5.9390	2.9739
5.5	269.97	0.001303	0.035642	1184.92	2789.72	1604.79	2.9759	5.9307	2.9548
5.6	271.12	0.001306	0.034960	1190.81	2788.74	1597.93	2.9865	5.9224	2.9359
5.7	272.26	0.001309	0.034300	1196.63	2787.73	1591.10	2.9969	5.9141	2.9173
5.8	273.38	0.001313	0.033663	1202.39	2786.70	1584.31	3.0072	5.9060	2.8988
5.9	274.49	0.001316	0.033046	1208.09	2785.64	1577.55	3.0174	5.8980	2.8806
6.0	275.59	0.001319	0.032449	1213.73	2784.56	1570.83	3.0274	5.8901	2.8626
6.1	276.67	0.001323	0.031870	1219.32	2783.46	1564.14	3.0374	5.8822	2.8448
6.2	277.73	0.001326	0.031310	1224.86	2782.33	1557.48	3.0472	5.8744	2.8272
6.3	278.79	0.001329	0.030766	1230.34	2781.19	1550.84	3.0569	5.8667	2.8098
6.4	279.83	0.001332	0.030239	1235.78	2780.02	1544.24	3.0665	5.8591	2.7926
6.5	280.86	0.001336	0.029728	1241.17	2778.83	1537.66	3.0760	5.8515	2.7755
6.6	281.88	0.001339	0.029231	1246.51	2777.62	1531.11	3.0854	5.8440	2.7586
6.7	282.88	0.001342	0.028748	1251.81	2776.39	1524.58	3.0947	5.8366	2.7419
6.8	283.88	0.001345	0.028279	1257.06	2775.13	1518.07	3.1039	5.8292	2.7253
6.9	284.86	0.001349	0.027823	1262.27	2773.86	1511.59	3.1130	5.8219	2.7089
7.0	285.83	0.001352	0.027380	1267.44	2772.57	1505.13	3.1220	5.8146	2.6926
7.1	286.79	0.001355	0.026948	1272.57	2771.26	1498.69	3.1309	5.8074	2.6765
7.2	287.74	0.001358	0.026528	1277.65	2769.93	1492.27	3.1398	5.8003	2.6605
7.3	288.68	0.001362	0.026119	1282.70	2768.58	1485.87	3.1485	5.7932	2.6447
7.4	289.62	0.001365	0.025720	1287.72	2767.21	1479.49	3.1572	5.7862	2.6290
7.5	290.54	0.001368	0.025331	1292.70	2765.82	1473.12	3.1658	5.7792	2.6134
7.6	291.45	0.001371	0.024952	1297.64	2764.41	1466.78	3.1743	5.7722	2.5979
7.7	292.35	0.001375	0.024583	1302.55	2762.99	1460.44	3.1827	5.7653	2.5826
7.8	293.25	0.001378	0.024223	1307.42	2761.55	1454.12	3.1911	5.7584	2.5673
7.9	294.13	0.001381	0.023871	1312.27	2760.09	1447.82	3.1994	5.7516	2.5522
8.0	295.01	0.001385	0.023528	1317.08	2758.61	1441.53	3.2077	5.7448	2.5372
8.1	295.88	0.001388	0.023192	1321.86	2757.12	1435.25	3.2158	5.7381	2.5223
8.2	296.74	0.001391	0.022865	1326.61	2755.60	1428.99	3.2239	5.7314	2.5075
8.3	297.59	0.001395	0.022545	1331.34	2754.07	1422.74	3.2320	5.7247	2.4928
8.4	298.44	0.001398	0.022232	1336.03	2752.52	1416.49	3.2399	5.7181	2.4782

Quelle: Wagner, W.; Kruse, A. Properties of Water and Steam, Springer

Saturated Steam

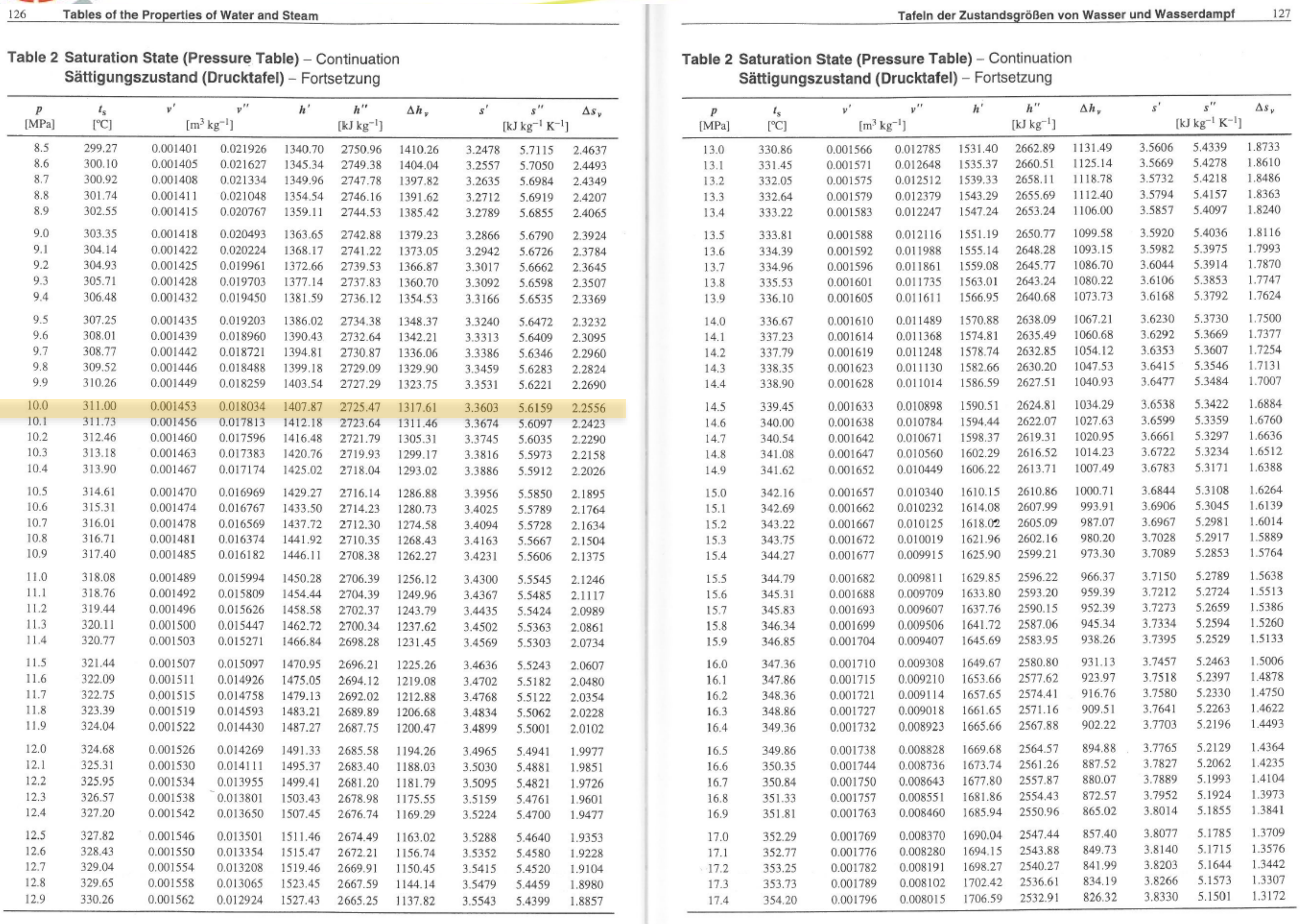

126 Tables of the Properties of Water and Steam

Table 2 Saturation State (Pressure Table) – Continuation
Sättigungszustand (Drucktafel) – Fortsetzung

100 bar

p	t_s	v'	v''	h'	h''	Δh_v	s'	s''	Δs_v
[MPa]	[°C]	$[\mathrm{m^3\,kg^{-1}}]$			$[\mathrm{kJ\,kg^{-1}}]$			$[\mathrm{kJ\,kg^{-1}\,K^{-1}}]$	
8.5	299.27	0.001401	0.021926	1340.70	2750.96	1410.26	3.2478	5.7115	2.4637
8.6	300.10	0.001405	0.021627	1345.34	2749.38	1404.04	3.2557	5.7050	2.4493
8.7	300.92	0.001408	0.021334	1349.96	2747.78	1397.82	3.2635	5.6984	2.4349
8.8	301.74	0.001411	0.021048	1354.54	2746.16	1391.62	3.2712	5.6919	2.4207
8.9	302.55	0.001415	0.020767	1359.11	2744.53	1385.42	3.2789	5.6855	2.4065
9.0	303.35	0.001418	0.020493	1363.65	2742.88	1379.23	3.2866	5.6790	2.3924
9.1	304.14	0.001422	0.020224	1368.17	2741.22	1373.05	3.2942	5.6726	2.3784
9.2	304.93	0.001425	0.019961	1372.66	2739.53	1366.87	3.3017	5.6662	2.3645
9.3	305.71	0.001428	0.019703	1377.14	2737.83	1360.70	3.3092	5.6598	2.3507
9.4	306.48	0.001432	0.019450	1381.59	2736.12	1354.53	3.3166	5.6535	2.3369
9.5	307.25	0.001435	0.019203	1386.02	2734.38	1348.37	3.3240	5.6472	2.3232
9.6	308.01	0.001439	0.018960	1390.43	2732.64	1342.21	3.3313	5.6409	2.3095
9.7	308.77	0.001442	0.018721	1394.81	2730.87	1336.06	3.3386	5.6346	2.2960
9.8	309.52	0.001446	0.018488	1399.18	2729.09	1329.90	3.3459	5.6283	2.2824
9.9	310.26	0.001449	0.018259	1403.54	2727.29	1323.75	3.3531	5.6221	2.2690
10.0	311.00	0.001453	0.018034	1407.87	2725.47	1317.61	3.3603	5.6159	2.2556
10.1	311.73	0.001456	0.017813	1412.18	2723.64	1311.46	3.3674	5.6097	2.2423
10.2	312.46	0.001460	0.017596	1416.48	2721.79	1305.31	3.3745	5.6035	2.2290
10.3	313.18	0.001463	0.017383	1420.76	2719.93	1299.17	3.3816	5.5973	2.2158
10.4	313.90	0.001467	0.017174	1425.02	2718.04	1293.02	3.3886	5.5912	2.2026
10.5	314.61	0.001470	0.016969	1429.27	2716.14	1286.88	3.3956	5.5850	2.1895
10.6	315.31	0.001474	0.016767	1433.50	2714.23	1280.73	3.4025	5.5789	2.1764
10.7	316.01	0.001478	0.016569	1437.72	2712.30	1274.58	3.4094	5.5728	2.1634
10.8	316.71	0.001481	0.016374	1441.92	2710.35	1268.43	3.4163	5.5667	2.1504
10.9	317.40	0.001485	0.016182	1446.11	2708.38	1262.27	3.4231	5.5606	2.1375
11.0	318.08	0.001489	0.015994	1450.28	2706.39	1256.12	3.4300	5.5545	2.1246
11.1	318.76	0.001492	0.015809	1454.44	2704.39	1249.96	3.4367	5.5485	2.1117
11.2	319.44	0.001496	0.015626	1458.58	2702.37	1243.79	3.4435	5.5424	2.0989
11.3	320.11	0.001500	0.015447	1462.72	2700.34	1237.62	3.4502	5.5363	2.0861
11.4	320.77	0.001503	0.015271	1466.84	2698.28	1231.45	3.4569	5.5303	2.0734
11.5	321.44	0.001507	0.015097	1470.95	2696.21	1225.26	3.4636	5.5243	2.0607
11.6	322.09	0.001511	0.014926	1475.05	2694.12	1219.08	3.4702	5.5182	2.0480
11.7	322.75	0.001515	0.014758	1479.13	2692.02	1212.88	3.4768	5.5122	2.0354
11.8	323.39	0.001519	0.014593	1483.21	2689.89	1206.68	3.4834	5.5062	2.0228
11.9	324.04	0.001522	0.014430	1487.27	2687.75	1200.47	3.4899	5.5001	2.0102
12.0	324.68	0.001526	0.014269	1491.33	2685.58	1194.26	3.4965	5.4941	1.9977
12.1	325.31	0.001530	0.014111	1495.37	2683.40	1188.03	3.5030	5.4881	1.9851
12.2	325.95	0.001534	0.013955	1499.41	2681.20	1181.79	3.5095	5.4821	1.9726
12.3	326.57	0.001538	0.013801	1503.43	2678.98	1175.55	3.5159	5.4761	1.9601
12.4	327.20	0.001542	0.013650	1507.45	2676.74	1169.29	3.5224	5.4700	1.9477
12.5	327.82	0.001546	0.013501	1511.46	2674.49	1163.02	3.5288	5.4640	1.9353
12.6	328.43	0.001550	0.013354	1515.47	2672.21	1156.74	3.5352	5.4580	1.9228
12.7	329.04	0.001554	0.013208	1519.46	2669.91	1150.45	3.5415	5.4520	1.9104
12.8	329.65	0.001558	0.013065	1523.45	2667.59	1144.14	3.5479	5.4459	1.8980
12.9	330.26	0.001562	0.012924	1527.43	2665.25	1137.82	3.5543	5.4399	1.8857

Tafeln der Zustandsgrößen von Wasser und Wasserdampf 127

Table 2 Saturation State (Pressure Table) – Continuation
Sättigungszustand (Drucktafel) – Fortsetzung

p	t_s	v'	v''	h'	h''	Δh_v	s'	s''	Δs_v
[MPa]	[°C]	$[\mathrm{m^3\,kg^{-1}}]$			$[\mathrm{kJ\,kg^{-1}}]$			$[\mathrm{kJ\,kg^{-1}\,K^{-1}}]$	
13.0	330.86	0.001566	0.012785	1531.40	2662.89	1131.49	3.5606	5.4339	1.8733
13.1	331.45	0.001571	0.012648	1535.37	2660.51	1125.14	3.5669	5.4278	1.8610
13.2	332.05	0.001575	0.012512	1539.33	2658.11	1118.78	3.5732	5.4218	1.8486
13.3	332.64	0.001579	0.012379	1543.29	2655.69	1112.40	3.5794	5.4157	1.8363
13.4	333.22	0.001583	0.012247	1547.24	2653.24	1106.00	3.5857	5.4097	1.8240
13.5	333.81	0.001588	0.012116	1551.19	2650.77	1099.58	3.5920	5.4036	1.8116
13.6	334.39	0.001592	0.011988	1555.14	2648.28	1093.15	3.5982	5.3975	1.7993
13.7	334.96	0.001596	0.011861	1559.08	2645.77	1086.70	3.6044	5.3914	1.7870
13.8	335.53	0.001601	0.011735	1563.01	2643.24	1080.22	3.6106	5.3853	1.7747
13.9	336.10	0.001605	0.011611	1566.95	2640.68	1073.73	3.6168	5.3792	1.7624
14.0	336.67	0.001610	0.011489	1570.88	2638.09	1067.21	3.6230	5.3730	1.7500
14.1	337.23	0.001614	0.011368	1574.81	2635.49	1060.68	3.6292	5.3669	1.7377
14.2	337.79	0.001619	0.011248	1578.74	2632.85	1054.12	3.6353	5.3607	1.7254
14.3	338.35	0.001623	0.011130	1582.66	2630.20	1047.53	3.6415	5.3546	1.7131
14.4	338.90	0.001628	0.011014	1586.59	2627.51	1040.93	3.6477	5.3484	1.7007
14.5	339.45	0.001633	0.010898	1590.51	2624.81	1034.29	3.6538	5.3422	1.6884
14.6	340.00	0.001638	0.010784	1594.44	2622.07	1027.63	3.6599	5.3359	1.6760
14.7	340.54	0.001642	0.010671	1598.37	2619.31	1020.95	3.6661	5.3297	1.6636
14.8	341.08	0.001647	0.010560	1602.29	2616.52	1014.23	3.6722	5.3234	1.6512
14.9	341.62	0.001652	0.010449	1606.22	2613.71	1007.49	3.6783	5.3171	1.6388
15.0	342.16	0.001657	0.010340	1610.15	2610.86	1000.71	3.6844	5.3108	1.6264
15.1	342.69	0.001662	0.010232	1614.08	2607.99	993.91	3.6906	5.3045	1.6139
15.2	343.22	0.001667	0.010125	1618.02	2605.09	987.07	3.6967	5.2981	1.6014
15.3	343.75	0.001672	0.010019	1621.96	2602.16	980.20	3.7028	5.2917	1.5889
15.4	344.27	0.001677	0.009915	1625.90	2599.21	973.30	3.7089	5.2853	1.5764
15.5	344.79	0.001682	0.009811	1629.85	2596.22	966.37	3.7150	5.2789	1.5638
15.6	345.31	0.001688	0.009709	1633.80	2593.20	959.39	3.7212	5.2724	1.5513
15.7	345.83	0.001693	0.009607	1637.76	2590.15	952.39	3.7273	5.2659	1.5386
15.8	346.34	0.001699	0.009506	1641.72	2587.06	945.34	3.7334	5.2594	1.5260
15.9	346.85	0.001704	0.009407	1645.69	2583.95	938.26	3.7395	5.2529	1.5133
16.0	347.36	0.001710	0.009308	1649.67	2580.80	931.13	3.7457	5.2463	1.5006
16.1	347.86	0.001715	0.009210	1653.66	2577.62	923.97	3.7518	5.2397	1.4878
16.2	348.36	0.001721	0.009114	1657.65	2574.41	916.76	3.7580	5.2330	1.4750
16.3	348.86	0.001727	0.009018	1661.65	2571.16	909.51	3.7641	5.2263	1.4622
16.4	349.36	0.001732	0.008923	1665.66	2567.88	902.22	3.7703	5.2196	1.4493
16.5	349.86	0.001738	0.008828	1669.68	2564.57	894.88	3.7765	5.2129	1.4364
16.6	350.35	0.001744	0.008736	1673.74	2561.26	887.52	3.7827	5.2062	1.4235
16.7	350.84	0.001750	0.008643	1677.80	2557.87	880.07	3.7889	5.1993	1.4104
16.8	351.33	0.001757	0.008551	1681.86	2554.43	872.57	3.7952	5.1924	1.3973
16.9	351.81	0.001763	0.008460	1685.94	2550.96	865.02	3.8014	5.1855	1.3841
17.0	352.29	0.001769	0.008370	1690.04	2547.44	857.40	3.8077	5.1785	1.3709
17.1	352.77	0.001776	0.008280	1694.15	2543.88	849.73	3.8140	5.1715	1.3576
17.2	353.25	0.001782	0.008191	1698.27	2540.27	841.99	3.8203	5.1644	1.3442
17.3	353.73	0.001789	0.008102	1702.42	2536.61	834.19	3.8266	5.1573	1.3307
17.4	354.20	0.001796	0.008015	1706.59	2532.91	826.32	3.8330	5.1501	1.3172

Quelle: Wagner, W.; Kruse, A. Properties of Water and Steam, Springer

Saturated Steam, Table & Diagram

density and enthalpy as a function of pressure

property.xls

p	ts	rho'	rho"	h'	h"	r
[bar]	[°C]	[kg/m³]	[kg/m³]	[kJ/kg]	[kJ/kg]	[kJ/kg]
0,1	45,817	989,82	0,068	191,83	2583,8	2392,0
0,2	60,073	983,13	0,131	251,46	2608,9	2357,4
0,3	69,114	978,25	0,191	289,30	2624,6	2335,3
0,5	81,339	970,96	0,309	340,54	2645,3	2304,8
0,7	89,956	965,36	0,423	376,75	2659,6	2282,9
0,9	96,713	960,73	0,535	405,20	2670,5	2265,3
1	99,632	958,66	0,590	417,51	2675,1	2257,6
2	120,241	942,96	1,129	504,80	2706,5	2201,7
3	133,555	931,84	1,651	561,61	2725,3	2163,7
4	143,643	922,91	2,162	604,91	2738,5	2133,6
5	151,866	915,31	2,668	640,38	2748,6	2108,2
6	158,863	908,61	3,168	670,71	2756,7	2086,0
8	170,444	897,05	4,160	721,23	2768,9	2047,7
10	179,916	887,15	5,144	762,88	2777,7	2014,8
15	198,327	866,69	7,592	844,85	2791,5	1946,7
20	212,417	849,85	10,041	908,69	2798,7	1890,0
25	223,989	835,19	12,508	961,97	2802,2	1840,2
30	233,892	822,00	15,000	1008,29	2803,3	1795,0
35	242,595	809,84	17,527	1049,63	2802,6	1753,0
40	250,392	798,49	20,092	1087,22	2800,6	1713,4
45	257,474	787,76	22,700	1121,89	2797,6	1675,7
50	263,977	777,52	25,355	1154,20	2793,7	1639,5
60	275,621	758,17	30,825	1213,34	2783,9	1570,6
70	285,864	739,91	36,534	1266,98	2771,8	1504,8
80	295,042	722,40	42,518	1316,57	2757,8	1441,2
90	303,379	705,37	48,817	1363,10	2742,0	1378,9
100	311,031	688,63	55,480	1407,28	2724,5	1317,2
120	324,709	655,35	70,120	1490,73	2684,5	1193,8
140	336,700	621,30	87,070	1570,40	2637,1	1066,7
160	347,394	584,80	107,410	1649,50	2580,3	930,8
180	357,038	543,50	133,250	1732,00	2509,7	777,7
200	365,800	491,20	170,250	1826,70	2413,6	586,9
210	369,881	454,50	199,190	1887,60	2342,8	455,2
215	371,848	427,90	221,500	1929,00	2290,7	361,7
220	373,767	370,00	274,000	2013,00	2177,0	164,0
220,55	373,976	322,00	322,000	2086,00	2086,0	0,0

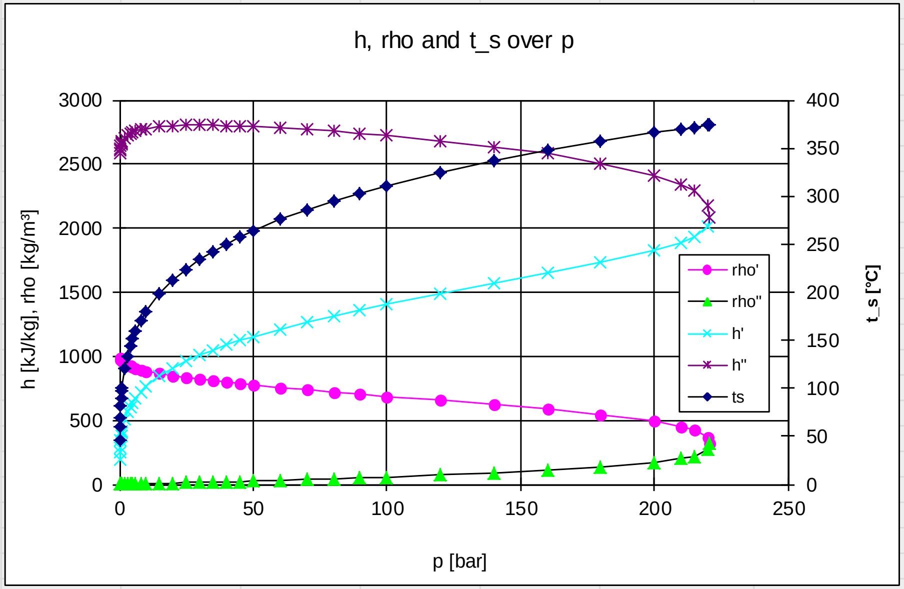

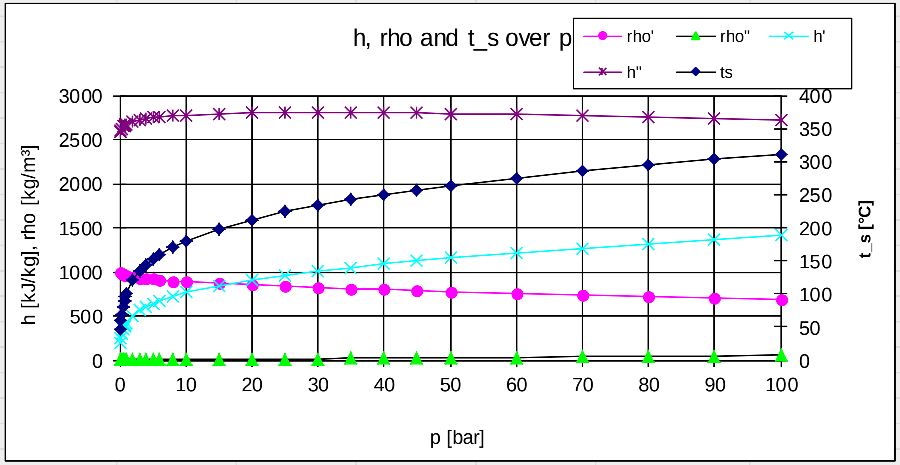

Table of Water & Steam: 0,1 bar

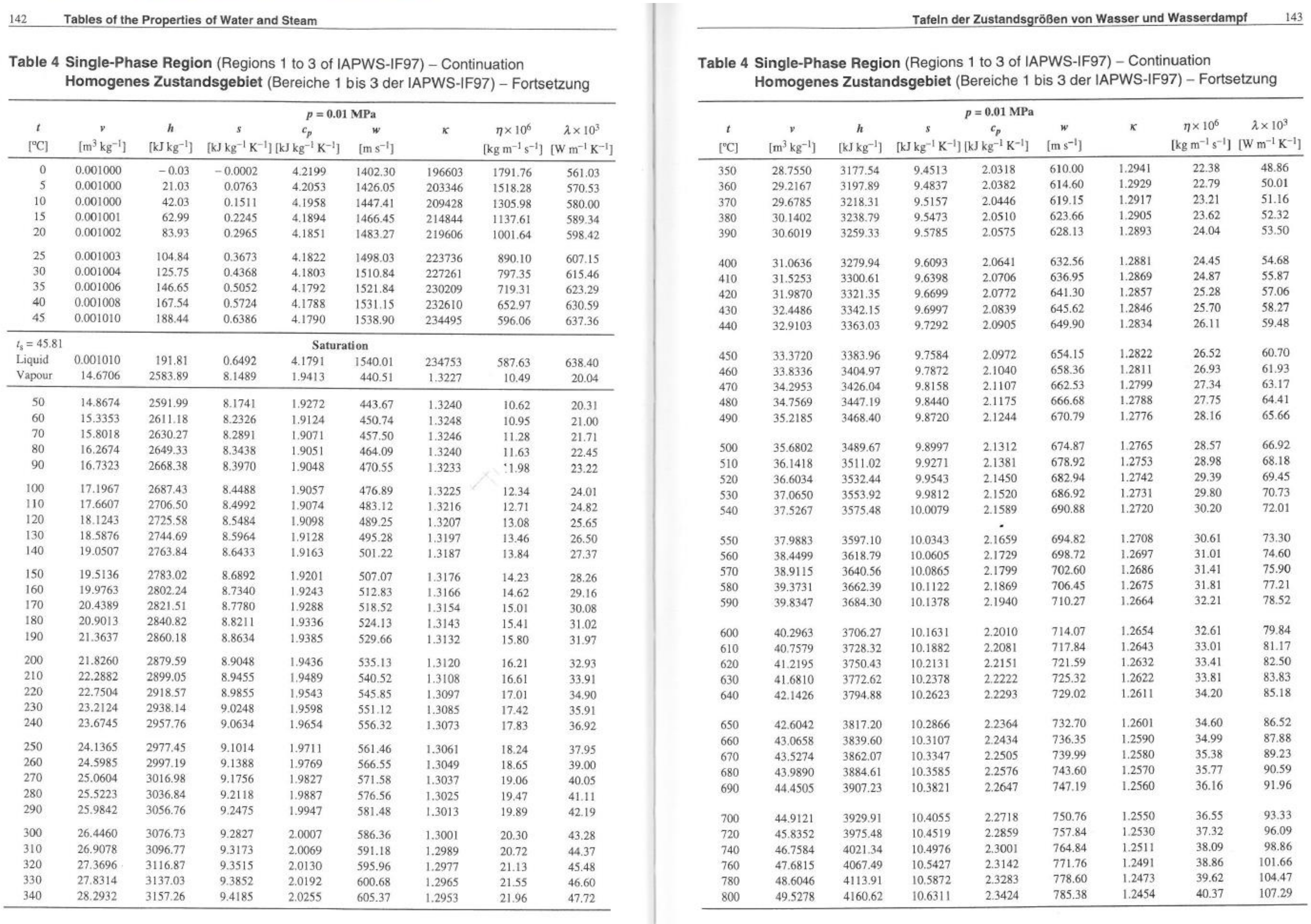

142 Tables of the Properties of Water and Steam

Table 4 Single-Phase Region (Regions 1 to 3 of IAPWS-IF97) – Continuation
Homogenes Zustandsgebiet (Bereiche 1 bis 3 der IAPWS-IF97) – Fortsetzung

$p = 0.01$ MPa

t [°C]	v [m³ kg⁻¹]	h [kJ kg⁻¹]	s [kJ kg⁻¹ K⁻¹]	c_p [kJ kg⁻¹ K⁻¹]	w [m s⁻¹]	κ	$\eta \times 10^6$ [kg m⁻¹ s⁻¹]	$\lambda \times 10^3$ [W m⁻¹ K⁻¹]
0	0.001000	−0.03	−0.0002	4.2199	1402.30	196603	1791.76	561.03
5	0.001000	21.03	0.0763	4.2053	1426.05	203346	1518.28	570.53
10	0.001000	42.03	0.1511	4.1958	1447.41	209428	1305.98	580.00
15	0.001001	62.99	0.2245	4.1894	1466.45	214844	1137.61	589.34
20	0.001002	83.93	0.2965	4.1851	1483.27	219606	1001.64	598.42
25	0.001003	104.84	0.3673	4.1822	1498.03	223736	890.10	607.15
30	0.001004	125.75	0.4368	4.1803	1510.84	227261	797.35	615.46
35	0.001006	146.65	0.5052	4.1792	1521.84	230209	719.31	623.29
40	0.001008	167.54	0.5724	4.1788	1531.15	232610	652.97	630.59
45	0.001010	188.44	0.6386	4.1790	1538.90	234495	596.06	637.36
$t_s = 45.81$				Saturation				
Liquid	0.001010	191.81	0.6492	4.1791	1540.01	234753	587.63	638.40
Vapour	14.6706	2583.89	8.1489	1.9413	440.51	1.3227	10.49	20.04
50	14.8674	2591.99	8.1741	1.9272	443.67	1.3240	10.62	20.31
60	15.3353	2611.18	8.2326	1.9124	450.74	1.3248	10.95	21.00
70	15.8018	2630.27	8.2891	1.9071	457.50	1.3246	11.28	21.71
80	16.2674	2649.33	8.3438	1.9051	464.09	1.3240	11.63	22.45
90	16.7323	2668.38	8.3970	1.9048	470.55	1.3233	11.98	23.22
100	17.1967	2687.43	8.4488	1.9057	476.89	1.3225	12.34	24.01
110	17.6607	2706.50	8.4992	1.9074	483.12	1.3216	12.71	24.82
120	18.1243	2725.58	8.5484	1.9098	489.25	1.3207	13.08	25.65
130	18.5876	2744.69	8.5964	1.9128	495.28	1.3197	13.46	26.50
140	19.0507	2763.84	8.6433	1.9163	501.22	1.3187	13.84	27.37
150	19.5136	2783.02	8.6892	1.9201	507.07	1.3176	14.23	28.26
160	19.9763	2802.24	8.7340	1.9243	512.83	1.3166	14.62	29.16
170	20.4389	2821.51	8.7780	1.9288	518.52	1.3154	15.01	30.08
180	20.9013	2840.82	8.8211	1.9336	524.13	1.3143	15.41	31.02
190	21.3637	2860.18	8.8634	1.9385	529.66	1.3132	15.80	31.97
200	21.8260	2879.59	8.9048	1.9436	535.13	1.3120	16.21	32.93
210	22.2882	2899.05	8.9455	1.9489	540.52	1.3108	16.61	33.91
220	22.7504	2918.57	8.9855	1.9543	545.85	1.3097	17.01	34.90
230	23.2124	2938.14	9.0248	1.9598	551.12	1.3085	17.42	35.91
240	23.6745	2957.76	9.0634	1.9654	556.32	1.3073	17.83	36.92
250	24.1365	2977.45	9.1014	1.9711	561.46	1.3061	18.24	37.95
260	24.5985	2997.19	9.1388	1.9769	566.55	1.3049	18.65	39.00
270	25.0604	3016.98	9.1756	1.9827	571.58	1.3037	19.06	40.05
280	25.5223	3036.84	9.2118	1.9887	576.56	1.3025	19.47	41.11
290	25.9842	3056.76	9.2475	1.9947	581.48	1.3013	19.89	42.19
300	26.4460	3076.73	9.2827	2.0007	586.36	1.3001	20.30	43.28
310	26.9078	3096.77	9.3173	2.0069	591.18	1.2989	20.72	44.37
320	27.3696	3116.87	9.3515	2.0130	595.96	1.2977	21.13	45.48
330	27.8314	3137.03	9.3852	2.0192	600.68	1.2965	21.55	46.60
340	28.2932	3157.26	9.4185	2.0255	605.37	1.2953	21.96	47.72

Tafeln der Zustandsgrößen von Wasser und Wasserdampf 143

Table 4 Single-Phase Region (Regions 1 to 3 of IAPWS-IF97) – Continuation
Homogenes Zustandsgebiet (Bereiche 1 bis 3 der IAPWS-IF97) – Fortsetzung

$p = 0.01$ MPa

t [°C]	v [m³ kg⁻¹]	h [kJ kg⁻¹]	s [kJ kg⁻¹ K⁻¹]	c_p [kJ kg⁻¹ K⁻¹]	w [m s⁻¹]	κ	$\eta \times 10^6$ [kg m⁻¹ s⁻¹]	$\lambda \times 10^3$ [W m⁻¹ K⁻¹]
350	28.7550	3177.54	9.4513	2.0318	610.00	1.2941	22.38	48.86
360	29.2167	3197.89	9.4837	2.0382	614.60	1.2929	22.79	50.01
370	29.6785	3218.31	9.5157	2.0446	619.15	1.2917	23.21	51.16
380	30.1402	3238.79	9.5473	2.0510	623.66	1.2905	23.62	52.32
390	30.6019	3259.33	9.5785	2.0575	628.13	1.2893	24.04	53.50
400	31.0636	3279.94	9.6093	2.0641	632.56	1.2881	24.45	54.68
410	31.5253	3300.61	9.6398	2.0706	636.95	1.2869	24.87	55.87
420	31.9870	3321.35	9.6699	2.0772	641.30	1.2857	25.28	57.06
430	32.4486	3342.15	9.6997	2.0839	645.62	1.2846	25.70	58.27
440	32.9103	3363.03	9.7292	2.0905	649.90	1.2834	26.11	59.48
450	33.3720	3383.96	9.7584	2.0972	654.15	1.2822	26.52	60.70
460	33.8336	3404.97	9.7872	2.1040	658.36	1.2811	26.93	61.93
470	34.2953	3426.04	9.8158	2.1107	662.53	1.2799	27.34	63.17
480	34.7569	3447.19	9.8440	2.1175	666.68	1.2788	27.75	64.41
490	35.2185	3468.40	9.8720	2.1244	670.79	1.2776	28.16	65.66
500	35.6802	3489.67	9.8997	2.1312	674.87	1.2765	28.57	66.92
510	36.1418	3511.02	9.9271	2.1381	678.92	1.2753	28.98	68.18
520	36.6034	3532.44	9.9543	2.1450	682.94	1.2742	29.39	69.45
530	37.0650	3553.92	9.9812	2.1520	686.92	1.2731	29.80	70.73
540	37.5267	3575.48	10.0079	2.1589	690.88	1.2720	30.20	72.01
550	37.9883	3597.10	10.0343	2.1659	694.82	1.2708	30.61	73.30
560	38.4499	3618.79	10.0605	2.1729	698.72	1.2697	31.01	74.60
570	38.9115	3640.56	10.0865	2.1799	702.60	1.2686	31.41	75.90
580	39.3731	3662.39	10.1122	2.1869	706.45	1.2675	31.81	77.21
590	39.8347	3684.30	10.1378	2.1940	710.27	1.2664	32.21	78.52
600	40.2963	3706.27	10.1631	2.2010	714.07	1.2654	32.61	79.84
610	40.7579	3728.32	10.1882	2.2081	717.84	1.2643	33.01	81.17
620	41.2195	3750.43	10.2131	2.2151	721.59	1.2632	33.41	82.50
630	41.6810	3772.62	10.2378	2.2222	725.32	1.2622	33.81	83.83
640	42.1426	3794.88	10.2623	2.2293	729.02	1.2611	34.20	85.18
650	42.6042	3817.20	10.2866	2.2364	732.70	1.2601	34.60	86.52
660	43.0658	3839.60	10.3107	2.2434	736.35	1.2590	34.99	87.88
670	43.5274	3862.07	10.3347	2.2505	739.99	1.2580	35.38	89.23
680	43.9890	3884.61	10.3585	2.2576	743.60	1.2570	35.77	90.59
690	44.4505	3907.23	10.3821	2.2647	747.19	1.2560	36.16	91.96
700	44.9121	3929.91	10.4055	2.2718	750.76	1.2550	36.55	93.33
720	45.8352	3975.48	10.4519	2.2859	757.84	1.2530	37.32	96.09
740	46.7584	4021.34	10.4976	2.3001	764.84	1.2511	38.09	98.86
760	47.6815	4067.49	10.5427	2.3142	771.76	1.2491	38.86	101.66
780	48.6046	4113.91	10.5872	2.3283	778.60	1.2473	39.62	104.47
800	49.5278	4160.62	10.6311	2.3424	785.38	1.2454	40.37	107.29

Quelle: Wagner, W.; Kruse, A. Properties of Water and Steam, Springer

Table of Water & Steam: 0,25 bar

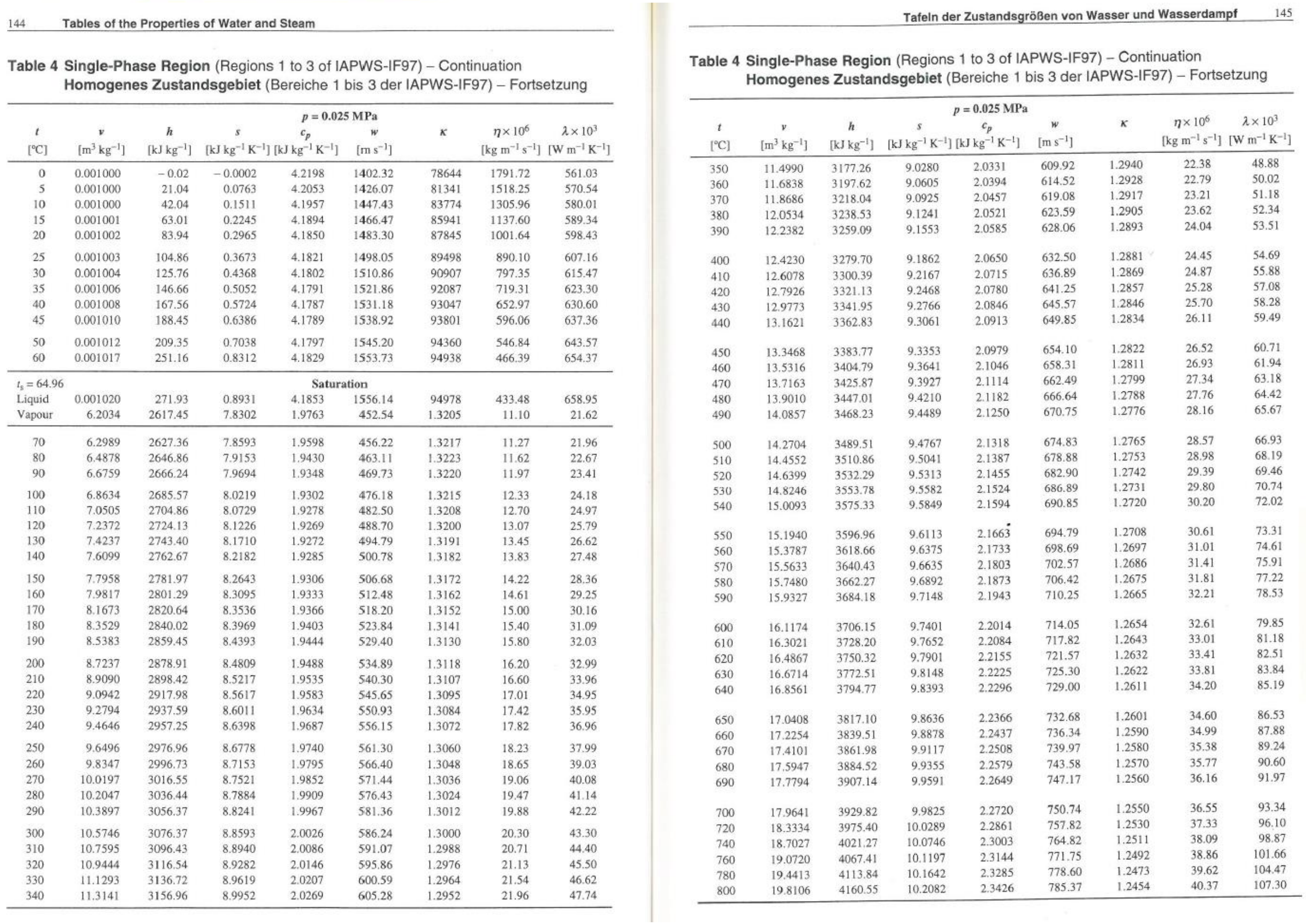

144 Tables of the Properties of Water and Steam

Table 4 Single-Phase Region (Regions 1 to 3 of IAPWS-IF97) – Continuation
Homogenes Zustandsgebiet (Bereiche 1 bis 3 der IAPWS-IF97) – Fortsetzung

				$p = 0.025$ MPa				
t [°C]	v [m^3 kg^{-1}]	h [kJ kg^{-1}]	s [kJ kg^{-1} K^{-1}]	c_p [kJ kg^{-1} K^{-1}]	w [m s^{-1}]	κ	$\eta \times 10^6$ [kg m^{-1} s^{-1}]	$\lambda \times 10^3$ [W m^{-1} K^{-1}]
0	0.001000	– 0.02	– 0.0002	4.2198	1402.32	78644	1791.72	561.03
5	0.001000	21.04	0.0763	4.2053	1426.07	81341	1518.25	570.54
10	0.001000	42.04	0.1511	4.1957	1447.43	83774	1305.96	580.01
15	0.001001	63.01	0.2245	4.1894	1466.47	85941	1137.60	589.34
20	0.001002	83.94	0.2965	4.1850	1483.30	87845	1001.64	598.43
25	0.001003	104.86	0.3673	4.1821	1498.05	89498	890.10	607.16
30	0.001004	125.76	0.4368	4.1802	1510.86	90907	797.35	615.47
35	0.001006	146.66	0.5052	4.1791	1521.86	92087	719.31	623.30
40	0.001008	167.56	0.5724	4.1787	1531.18	93047	652.97	630.60
45	0.001010	188.45	0.6386	4.1789	1538.92	93801	596.06	637.36
50	0.001012	209.35	0.7038	4.1797	1545.20	94360	546.84	643.57
60	0.001017	251.16	0.8312	4.1829	1553.73	94938	466.39	654.37
$t_s = 64.96$				Saturation				
Liquid	0.001020	271.93	0.8931	4.1853	1556.14	94978	433.48	658.95
Vapour	6.2034	2617.45	7.8302	1.9763	452.54	1.3205	11.10	21.62
70	6.2989	2627.36	7.8593	1.9598	456.22	1.3217	11.27	21.96
80	6.4878	2646.86	7.9153	1.9430	463.11	1.3223	11.62	22.67
90	6.6759	2666.24	7.9694	1.9348	469.73	1.3220	11.97	23.41
100	6.8634	2685.57	8.0219	1.9302	476.18	1.3215	12.33	24.18
110	7.0505	2704.86	8.0729	1.9278	482.50	1.3208	12.70	24.97
120	7.2372	2724.13	8.1226	1.9269	488.70	1.3200	13.07	25.79
130	7.4237	2743.40	8.1710	1.9272	494.79	1.3191	13.45	26.62
140	7.6099	2762.67	8.2182	1.9285	500.78	1.3182	13.83	27.48
150	7.7958	2781.97	8.2643	1.9306	506.68	1.3172	14.22	28.36
160	7.9817	2801.29	8.3095	1.9333	512.48	1.3162	14.61	29.25
170	8.1673	2820.64	8.3536	1.9366	518.20	1.3152	15.00	30.16
180	8.3529	2840.02	8.3969	1.9403	523.84	1.3141	15.40	31.09
190	8.5383	2859.45	8.4393	1.9444	529.40	1.3130	15.80	32.03
200	8.7237	2878.91	8.4809	1.9488	534.89	1.3118	16.20	32.99
210	8.9090	2898.42	8.5217	1.9535	540.30	1.3107	16.60	33.96
220	9.0942	2917.98	8.5617	1.9583	545.65	1.3095	17.01	34.95
230	9.2794	2937.59	8.6011	1.9634	550.93	1.3084	17.42	35.95
240	9.4646	2957.25	8.6398	1.9687	556.15	1.3072	17.82	36.96
250	9.6496	2976.96	8.6778	1.9740	561.30	1.3060	18.23	37.99
260	9.8347	2996.73	8.7153	1.9795	566.40	1.3048	18.65	39.03
270	10.0197	3016.55	8.7521	1.9852	571.44	1.3036	19.06	40.08
280	10.2047	3036.44	8.7884	1.9909	576.43	1.3024	19.47	41.14
290	10.3897	3056.37	8.8241	1.9967	581.36	1.3012	19.88	42.22
300	10.5746	3076.37	8.8593	2.0026	586.24	1.3000	20.30	43.30
310	10.7595	3096.43	8.8940	2.0086	591.07	1.2988	20.71	44.40
320	10.9444	3116.54	8.9282	2.0146	595.86	1.2976	21.13	45.50
330	11.1293	3136.72	8.9619	2.0207	600.59	1.2964	21.54	46.62
340	11.3141	3156.96	8.9952	2.0269	605.28	1.2952	21.96	47.74

Tafeln der Zustandsgrößen von Wasser und Wasserdampf 145

Table 4 Single-Phase Region (Regions 1 to 3 of IAPWS-IF97) – Continuation
Homogenes Zustandsgebiet (Bereiche 1 bis 3 der IAPWS-IF97) – Fortsetzung

				$p = 0.025$ MPa				
t [°C]	v [m^3 kg^{-1}]	h [kJ kg^{-1}]	s [kJ kg^{-1} K^{-1}]	c_p [kJ kg^{-1} K^{-1}]	w [m s^{-1}]	κ	$\eta \times 10^6$ [kg m^{-1} s^{-1}]	$\lambda \times 10^3$ [W m^{-1} K^{-1}]
350	11.4990	3177.26	9.0280	2.0331	609.92	1.2940	22.38	48.88
360	11.6838	3197.62	9.0605	2.0394	614.52	1.2928	22.79	50.02
370	11.8686	3218.04	9.0925	2.0457	619.08	1.2917	23.21	51.18
380	12.0534	3238.53	9.1241	2.0521	623.59	1.2905	23.62	52.34
390	12.2382	3259.09	9.1553	2.0585	628.06	1.2893	24.04	53.51
400	12.4230	3279.70	9.1862	2.0650	632.50	1.2881	24.45	54.69
410	12.6078	3300.39	9.2167	2.0715	636.89	1.2869	24.87	55.88
420	12.7926	3321.13	9.2468	2.0780	641.25	1.2857	25.28	57.08
430	12.9773	3341.95	9.2766	2.0846	645.57	1.2846	25.70	58.28
440	13.1621	3362.83	9.3061	2.0913	649.85	1.2834	26.11	59.49
450	13.3468	3383.77	9.3353	2.0979	654.10	1.2822	26.52	60.71
460	13.5316	3404.79	9.3641	2.1046	658.31	1.2811	26.93	61.94
470	13.7163	3425.87	9.3927	2.1114	662.49	1.2799	27.34	63.18
480	13.9010	3447.01	9.4210	2.1182	666.64	1.2788	27.76	64.42
490	14.0857	3468.23	9.4489	2.1250	670.75	1.2776	28.16	65.67
500	14.2704	3489.51	9.4767	2.1318	674.83	1.2765	28.57	66.93
510	14.4552	3510.86	9.5041	2.1387	678.88	1.2753	28.98	68.19
520	14.6399	3532.29	9.5313	2.1455	682.90	1.2742	29.39	69.46
530	14.8246	3553.78	9.5582	2.1524	686.89	1.2731	29.80	70.74
540	15.0093	3575.33	9.5849	2.1594	690.85	1.2720	30.20	72.02
550	15.1940	3596.96	9.6113	2.1663	694.79	1.2708	30.61	73.31
560	15.3787	3618.66	9.6375	2.1733	698.69	1.2697	31.01	74.61
570	15.5633	3640.43	9.6635	2.1803	702.57	1.2686	31.41	75.91
580	15.7480	3662.27	9.6892	2.1873	706.42	1.2675	31.81	77.22
590	15.9327	3684.18	9.7148	2.1943	710.25	1.2665	32.21	78.53
600	16.1174	3706.15	9.7401	2.2014	714.05	1.2654	32.61	79.85
610	16.3021	3728.20	9.7652	2.2084	717.82	1.2643	33.01	81.18
620	16.4867	3750.32	9.7901	2.2155	721.57	1.2632	33.41	82.51
630	16.6714	3772.51	9.8148	2.2225	725.30	1.2622	33.81	83.84
640	16.8561	3794.77	9.8393	2.2296	729.00	1.2611	34.20	85.19
650	17.0408	3817.10	9.8636	2.2366	732.68	1.2601	34.60	86.53
660	17.2254	3839.51	9.8878	2.2437	736.34	1.2590	34.99	87.88
670	17.4101	3861.98	9.9117	2.2508	739.97	1.2580	35.38	89.24
680	17.5947	3884.52	9.9355	2.2579	743.58	1.2570	35.77	90.60
690	17.7794	3907.14	9.9591	2.2649	747.17	1.2560	36.16	91.97
700	17.9641	3929.82	9.9825	2.2720	750.74	1.2550	36.55	93.34
720	18.3334	3975.40	10.0289	2.2861	757.82	1.2530	37.33	96.10
740	18.7027	4021.27	10.0746	2.3003	764.82	1.2511	38.09	98.87
760	19.0720	4067.41	10.1197	2.3144	771.75	1.2492	38.86	101.66
780	19.4413	4113.84	10.1642	2.3285	778.60	1.2473	39.62	104.47
800	19.8106	4160.55	10.2082	2.3426	785.37	1.2454	40.37	107.30

Quelle: Wagner, W.; Kruse, A. Properties of Water and Steam, Springer

Table of Water & Steam: 1 bar

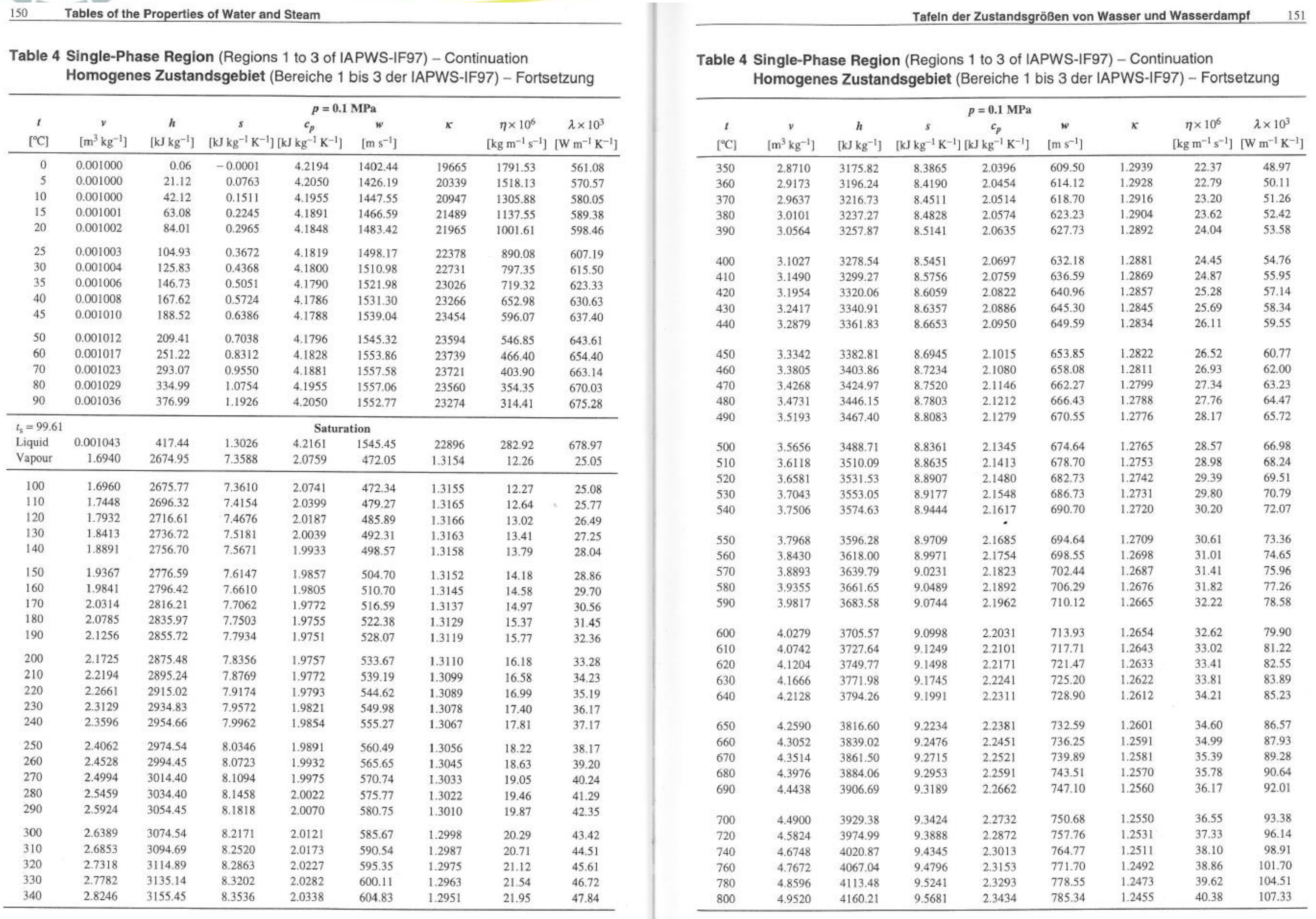

150 Tables of the Properties of Water and Steam

Table 4 Single-Phase Region (Regions 1 to 3 of IAPWS-IF97) – Continuation
Homogenes Zustandsgebiet (Bereiche 1 bis 3 der IAPWS-IF97) – Fortsetzung

$p = 0.1$ MPa

t [°C]	v [m³ kg⁻¹]	h [kJ kg⁻¹]	s [kJ kg⁻¹ K⁻¹]	c_p [kJ kg⁻¹ K⁻¹]	w [m s⁻¹]	κ	$\eta \times 10^6$ [kg m⁻¹ s⁻¹]	$\lambda \times 10^3$ [W m⁻¹ K⁻¹]
0	0.001000	0.06	−0.0001	4.2194	1402.44	19665	1791.53	561.08
5	0.001000	21.12	0.0763	4.2050	1426.19	20339	1518.13	570.57
10	0.001000	42.12	0.1511	4.1955	1447.55	20947	1305.88	580.05
15	0.001001	63.08	0.2245	4.1891	1466.59	21489	1137.55	589.38
20	0.001002	84.01	0.2965	4.1848	1483.42	21965	1001.61	598.46
25	0.001003	104.93	0.3672	4.1819	1498.17	22378	890.08	607.19
30	0.001004	125.83	0.4368	4.1800	1510.98	22731	797.35	615.50
35	0.001006	146.73	0.5051	4.1790	1521.98	23026	719.32	623.33
40	0.001008	167.62	0.5724	4.1786	1531.30	23266	652.98	630.63
45	0.001010	188.52	0.6386	4.1788	1539.04	23454	596.07	637.40
50	0.001012	209.41	0.7038	4.1796	1545.32	23594	546.85	643.61
60	0.001017	251.22	0.8312	4.1828	1553.86	23739	466.40	654.40
70	0.001023	293.07	0.9550	4.1881	1557.58	23721	403.90	663.14
80	0.001029	334.99	1.0754	4.1955	1557.06	23560	354.35	670.03
90	0.001036	376.99	1.1926	4.2050	1552.77	23274	314.41	675.28
$t_s = 99.61$				**Saturation**				
Liquid	0.001043	417.44	1.3026	4.2161	1545.45	22896	282.92	678.97
Vapour	1.6940	2674.95	7.3588	2.0759	472.05	1.3154	12.26	25.05
100	1.6960	2675.77	7.3610	2.0741	472.34	1.3155	12.27	25.08
110	1.7448	2696.32	7.4154	2.0399	479.27	1.3165	12.64	25.77
120	1.7932	2716.61	7.4676	2.0187	485.89	1.3166	13.02	26.49
130	1.8413	2736.72	7.5181	2.0039	492.31	1.3163	13.41	27.25
140	1.8891	2756.70	7.5671	1.9933	498.57	1.3158	13.79	28.04
150	1.9367	2776.59	7.6147	1.9857	504.70	1.3152	14.18	28.86
160	1.9841	2796.42	7.6610	1.9805	510.70	1.3145	14.58	29.70
170	2.0314	2816.21	7.7062	1.9772	516.59	1.3137	14.97	30.56
180	2.0785	2835.97	7.7503	1.9755	522.38	1.3129	15.37	31.45
190	2.1256	2855.72	7.7934	1.9751	528.07	1.3119	15.77	32.36
200	2.1725	2875.48	7.8356	1.9757	533.67	1.3110	16.18	33.28
210	2.2194	2895.24	7.8769	1.9772	539.19	1.3099	16.58	34.23
220	2.2661	2915.02	7.9174	1.9793	544.62	1.3089	16.99	35.19
230	2.3129	2934.83	7.9572	1.9821	549.98	1.3078	17.40	36.17
240	2.3596	2954.66	7.9962	1.9854	555.27	1.3067	17.81	37.17
250	2.4062	2974.54	8.0346	1.9891	560.49	1.3056	18.22	38.17
260	2.4528	2994.45	8.0723	1.9932	565.65	1.3045	18.63	39.20
270	2.4994	3014.40	8.1094	1.9975	570.74	1.3033	19.05	40.24
280	2.5459	3034.40	8.1458	2.0022	575.77	1.3022	19.46	41.29
290	2.5924	3054.45	8.1818	2.0070	580.75	1.3010	19.87	42.35
300	2.6389	3074.54	8.2171	2.0121	585.67	1.2998	20.29	43.42
310	2.6853	3094.69	8.2520	2.0173	590.54	1.2987	20.71	44.51
320	2.7318	3114.89	8.2863	2.0227	595.35	1.2975	21.12	45.61
330	2.7782	3135.14	8.3202	2.0282	600.11	1.2963	21.54	46.72
340	2.8246	3155.45	8.3536	2.0338	604.83	1.2951	21.95	47.84

Tafeln der Zustandsgrößen von Wasser und Wasserdampf 151

Table 4 Single-Phase Region (Regions 1 to 3 of IAPWS-IF97) – Continuation
Homogenes Zustandsgebiet (Bereiche 1 bis 3 der IAPWS-IF97) – Fortsetzung

$p = 0.1$ MPa

t [°C]	v [m³ kg⁻¹]	h [kJ kg⁻¹]	s [kJ kg⁻¹ K⁻¹]	c_p [kJ kg⁻¹ K⁻¹]	w [m s⁻¹]	κ	$\eta \times 10^6$ [kg m⁻¹ s⁻¹]	$\lambda \times 10^3$ [W m⁻¹ K⁻¹]
350	2.8710	3175.82	8.3865	2.0396	609.50	1.2939	22.37	48.97
360	2.9173	3196.24	8.4190	2.0454	614.12	1.2928	22.79	50.11
370	2.9637	3216.73	8.4511	2.0514	618.70	1.2916	23.20	51.26
380	3.0101	3237.27	8.4828	2.0574	623.23	1.2904	23.62	52.42
390	3.0564	3257.87	8.5141	2.0635	627.73	1.2892	24.04	53.58
400	3.1027	3278.54	8.5451	2.0697	632.18	1.2881	24.45	54.76
410	3.1490	3299.27	8.5756	2.0759	636.59	1.2869	24.87	55.95
420	3.1954	3320.06	8.6059	2.0822	640.96	1.2857	25.28	57.14
430	3.2417	3340.91	8.6357	2.0886	645.30	1.2845	25.69	58.34
440	3.2879	3361.83	8.6653	2.0950	649.59	1.2834	26.11	59.55
450	3.3342	3382.81	8.6945	2.1015	653.85	1.2822	26.52	60.77
460	3.3805	3403.86	8.7234	2.1080	658.08	1.2811	26.93	62.00
470	3.4268	3424.97	8.7520	2.1146	662.27	1.2799	27.34	63.23
480	3.4731	3446.15	8.7803	2.1212	666.43	1.2788	27.76	64.47
490	3.5193	3467.40	8.8083	2.1279	670.55	1.2776	28.17	65.72
500	3.5656	3488.71	8.8361	2.1345	674.64	1.2765	28.57	66.98
510	3.6118	3510.09	8.8635	2.1413	678.70	1.2753	28.98	68.24
520	3.6581	3531.53	8.8907	2.1480	682.73	1.2742	29.39	69.51
530	3.7043	3553.05	8.9177	2.1548	686.73	1.2731	29.80	70.79
540	3.7506	3574.63	8.9444	2.1617	690.70	1.2720	30.20	72.07
550	3.7968	3596.28	8.9709	2.1685	694.64	1.2709	30.61	73.36
560	3.8430	3618.00	8.9971	2.1754	698.55	1.2698	31.01	74.65
570	3.8893	3639.79	9.0231	2.1823	702.44	1.2687	31.41	75.96
580	3.9355	3661.65	9.0489	2.1892	706.29	1.2676	31.82	77.26
590	3.9817	3683.58	9.0744	2.1962	710.12	1.2665	32.22	78.58
600	4.0279	3705.57	9.0998	2.2031	713.93	1.2654	32.62	79.90
610	4.0742	3727.64	9.1249	2.2101	717.71	1.2643	33.02	81.22
620	4.1204	3749.77	9.1498	2.2171	721.47	1.2633	33.41	82.55
630	4.1666	3771.98	9.1745	2.2241	725.20	1.2622	33.81	83.89
640	4.2128	3794.26	9.1991	2.2311	728.90	1.2612	34.21	85.23
650	4.2590	3816.60	9.2234	2.2381	732.59	1.2601	34.60	86.57
660	4.3052	3839.02	9.2476	2.2451	736.25	1.2591	34.99	87.93
670	4.3514	3861.50	9.2715	2.2521	739.89	1.2581	35.39	89.28
680	4.3976	3884.06	9.2953	2.2591	743.51	1.2570	35.78	90.64
690	4.4438	3906.69	9.3189	2.2662	747.10	1.2560	36.17	92.01
700	4.4900	3929.38	9.3424	2.2732	750.68	1.2550	36.55	93.38
720	4.5824	3974.99	9.3888	2.2872	757.76	1.2531	37.33	96.14
740	4.6748	4020.87	9.4345	2.3013	764.77	1.2511	38.10	98.91
760	4.7672	4067.04	9.4796	2.3153	771.70	1.2492	38.86	101.70
780	4.8596	4113.48	9.5241	2.3293	778.55	1.2473	39.62	104.51
800	4.9520	4160.21	9.5681	2.3434	785.34	1.2455	40.38	107.33

Quelle: Wagner, W.; Kruse, A. Properties of Water and Steam, Springer

Table of Water & Steam: 20 bar

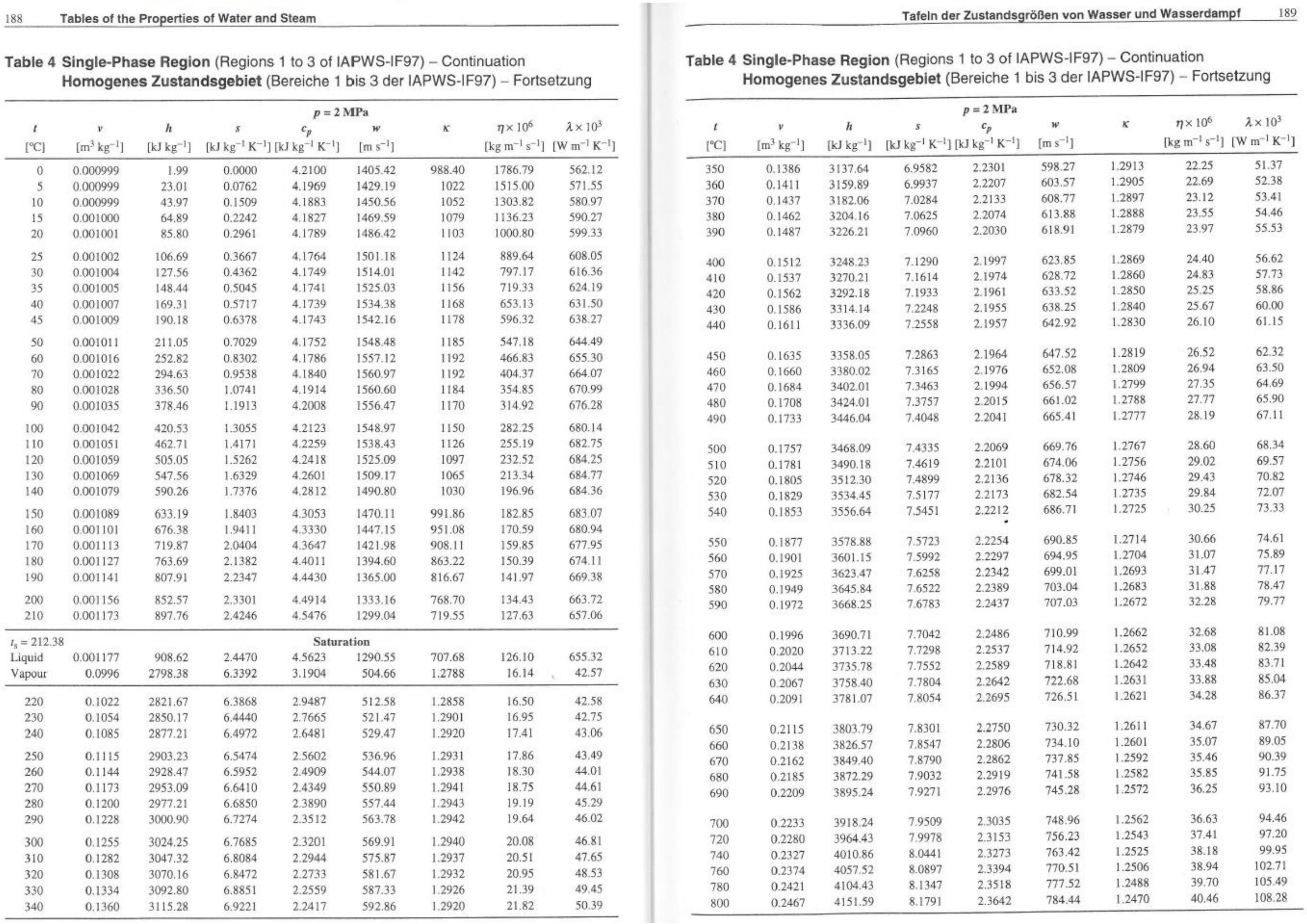

188 Tables of the Properties of Water and Steam

Table 4 Single-Phase Region (Regions 1 to 3 of IAPWS-IF97) – Continuation
Homogenes Zustandsgebiet (Bereiche 1 bis 3 der IAPWS-IF97) – Fortsetzung

$p = 2$ MPa

t [°C]	v [m³ kg⁻¹]	h [kJ kg⁻¹]	s [kJ kg⁻¹ K⁻¹]	c_p [kJ kg⁻¹ K⁻¹]	w [m s⁻¹]	κ	$\eta \times 10^6$ [kg m⁻¹ s⁻¹]	$\lambda \times 10^3$ [W m⁻¹ K⁻¹]
0	0.000999	1.99	0.0000	4.2100	1405.42	988.40	1786.79	562.12
5	0.000999	23.01	0.0762	4.1969	1429.19	1022	1515.00	571.55
10	0.000999	43.97	0.1509	4.1883	1450.56	1052	1303.82	580.97
15	0.001000	64.89	0.2242	4.1827	1469.59	1079	1136.23	590.27
20	0.001001	85.80	0.2961	4.1789	1486.42	1103	1000.80	599.33
25	0.001002	106.69	0.3667	4.1764	1501.18	1124	889.64	608.05
30	0.001004	127.56	0.4362	4.1749	1514.01	1142	797.17	616.36
35	0.001005	148.44	0.5045	4.1741	1525.03	1156	719.33	624.19
40	0.001007	169.31	0.5717	4.1739	1534.38	1168	653.13	631.50
45	0.001009	190.18	0.6378	4.1743	1542.16	1178	596.32	638.27
50	0.001011	211.05	0.7029	4.1752	1548.48	1185	547.18	644.49
60	0.001016	252.82	0.8302	4.1786	1557.12	1192	466.83	655.30
70	0.001022	294.63	0.9538	4.1840	1560.97	1192	404.37	664.07
80	0.001028	336.50	1.0741	4.1914	1560.60	1184	354.85	670.99
90	0.001035	378.46	1.1913	4.2008	1556.47	1170	314.92	676.28
100	0.001042	420.53	1.3055	4.2123	1548.97	1150	282.25	680.14
110	0.001051	462.71	1.4171	4.2259	1538.43	1126	255.19	682.75
120	0.001059	505.05	1.5262	4.2418	1525.09	1097	232.52	684.25
130	0.001069	547.56	1.6329	4.2601	1509.17	1065	213.34	684.77
140	0.001079	590.26	1.7376	4.2812	1490.80	1030	196.96	684.36
150	0.001089	633.19	1.8403	4.3053	1470.11	991.86	182.85	683.07
160	0.001101	676.38	1.9411	4.3330	1447.15	951.08	170.59	680.94
170	0.001113	719.87	2.0404	4.3647	1421.98	908.11	159.85	677.95
180	0.001127	763.69	2.1382	4.4011	1394.60	863.22	150.39	674.11
190	0.001141	807.91	2.2347	4.4430	1365.00	816.67	141.97	669.38
200	0.001156	852.57	2.3301	4.4914	1333.16	768.70	134.43	663.72
210	0.001173	897.76	2.4246	4.5476	1299.04	719.55	127.63	657.06
t_s = 212.38				**Saturation**				
Liquid	0.001177	908.62	2.4470	4.5623	1290.55	707.68	126.10	655.32
Vapour	0.0996	2798.38	6.3392	3.1904	504.66	1.2788	16.14	42.57
220	0.1022	2821.67	6.3868	2.9487	512.58	1.2858	16.50	42.58
230	0.1054	2850.17	6.4440	2.7665	521.47	1.2901	16.95	42.75
240	0.1085	2877.21	6.4972	2.6481	529.47	1.2920	17.41	43.06
250	0.1115	2903.23	6.5474	2.5602	536.96	1.2931	17.86	43.49
260	0.1144	2928.47	6.5952	2.4909	544.07	1.2938	18.30	44.01
270	0.1173	2953.09	6.6410	2.4349	550.89	1.2941	18.75	44.61
280	0.1200	2977.21	6.6850	2.3890	557.44	1.2943	19.19	45.29
290	0.1228	3000.90	6.7274	2.3512	563.78	1.2942	19.64	46.02
300	0.1255	3024.25	6.7685	2.3201	569.91	1.2940	20.08	46.81
310	0.1282	3047.32	6.8084	2.2944	575.87	1.2937	20.51	47.65
320	0.1308	3070.16	6.8472	2.2733	581.67	1.2932	20.95	48.53
330	0.1334	3092.80	6.8851	2.2559	587.33	1.2926	21.39	49.45
340	0.1360	3115.28	6.9221	2.2417	592.86	1.2920	21.82	50.39

Tafeln der Zustandsgrößen von Wasser und Wasserdampf 189

Table 4 Single-Phase Region (Regions 1 to 3 of IAPWS-IF97) – Continuation
Homogenes Zustandsgebiet (Bereiche 1 bis 3 der IAPWS-IF97) – Fortsetzung

$p = 2$ MPa

t [°C]	v [m³ kg⁻¹]	h [kJ kg⁻¹]	s [kJ kg⁻¹ K⁻¹]	c_p [kJ kg⁻¹ K⁻¹]	w [m s⁻¹]	κ	$\eta \times 10^6$ [kg m⁻¹ s⁻¹]	$\lambda \times 10^3$ [W m⁻¹ K⁻¹]
350	0.1386	3137.64	6.9582	2.2301	598.27	1.2913	22.25	51.37
360	0.1411	3159.89	6.9937	2.2207	603.57	1.2905	22.69	52.38
370	0.1437	3182.06	7.0284	2.2133	608.77	1.2897	23.12	53.41
380	0.1462	3204.16	7.0625	2.2074	613.88	1.2888	23.55	54.46
390	0.1487	3226.21	7.0960	2.2030	618.91	1.2879	23.97	55.53
400	0.1512	3248.23	7.1290	2.1997	623.85	1.2869	24.40	56.62
410	0.1537	3270.21	7.1614	2.1974	628.72	1.2860	24.83	57.73
420	0.1562	3292.18	7.1933	2.1961	633.52	1.2850	25.25	58.86
430	0.1586	3314.14	7.2248	2.1955	638.25	1.2840	25.67	60.00
440	0.1611	3336.09	7.2558	2.1957	642.92	1.2830	26.10	61.15
450	0.1635	3358.05	7.2863	2.1964	647.52	1.2819	26.52	62.32
460	0.1660	3380.02	7.3165	2.1976	652.08	1.2809	26.94	63.50
470	0.1684	3402.01	7.3463	2.1994	656.57	1.2799	27.35	64.69
480	0.1708	3424.01	7.3757	2.2015	661.02	1.2788	27.77	65.90
490	0.1733	3446.04	7.4048	2.2041	665.41	1.2777	28.19	67.11
500	0.1757	3468.09	7.4335	2.2069	669.76	1.2767	28.60	68.34
510	0.1781	3490.18	7.4619	2.2101	674.06	1.2756	29.02	69.57
520	0.1805	3512.30	7.4899	2.2136	678.32	1.2746	29.43	70.82
530	0.1829	3534.45	7.5177	2.2173	682.54	1.2735	29.84	72.07
540	0.1853	3556.64	7.5451	2.2212	686.71	1.2725	30.25	73.33
550	0.1877	3578.88	7.5723	2.2254	690.85	1.2714	30.66	74.61
560	0.1901	3601.15	7.5992	2.2297	694.95	1.2704	31.07	75.89
570	0.1925	3623.47	7.6258	2.2342	699.01	1.2693	31.47	77.17
580	0.1949	3645.84	7.6522	2.2389	703.04	1.2683	31.88	78.47
590	0.1972	3668.25	7.6783	2.2437	707.03	1.2672	32.28	79.77
600	0.1996	3690.71	7.7042	2.2486	710.99	1.2662	32.68	81.08
610	0.2020	3713.22	7.7298	2.2537	714.92	1.2652	33.08	82.39
620	0.2044	3735.78	7.7552	2.2589	718.81	1.2642	33.48	83.71
630	0.2067	3758.40	7.7804	2.2642	722.68	1.2631	33.88	85.04
640	0.2091	3781.07	7.8054	2.2695	726.51	1.2621	34.28	86.37
650	0.2115	3803.79	7.8301	2.2750	730.32	1.2611	34.67	87.70
660	0.2138	3826.57	7.8547	2.2806	734.10	1.2601	35.07	89.05
670	0.2162	3849.40	7.8790	2.2862	737.85	1.2592	35.46	90.39
680	0.2185	3872.29	7.9032	2.2919	741.58	1.2582	35.85	91.75
690	0.2209	3895.24	7.9271	2.2976	745.28	1.2572	36.25	93.10
700	0.2233	3918.24	7.9509	2.3035	748.96	1.2562	36.63	94.46
720	0.2280	3964.43	7.9978	2.3153	756.23	1.2543	37.41	97.20
740	0.2327	4010.86	8.0441	2.3273	763.42	1.2525	38.18	99.95
760	0.2374	4057.52	8.0897	2.3394	770.51	1.2506	38.94	102.71
780	0.2421	4104.43	8.1347	2.3518	777.52	1.2488	39.70	105.49
800	0.2467	4151.59	8.1791	2.3642	784.44	1.2470	40.46	108.28

Quelle: Wagner, W.; Kruse, A. Properties of Water and Steam, Springer

Table of Water & Steam: 100 bar

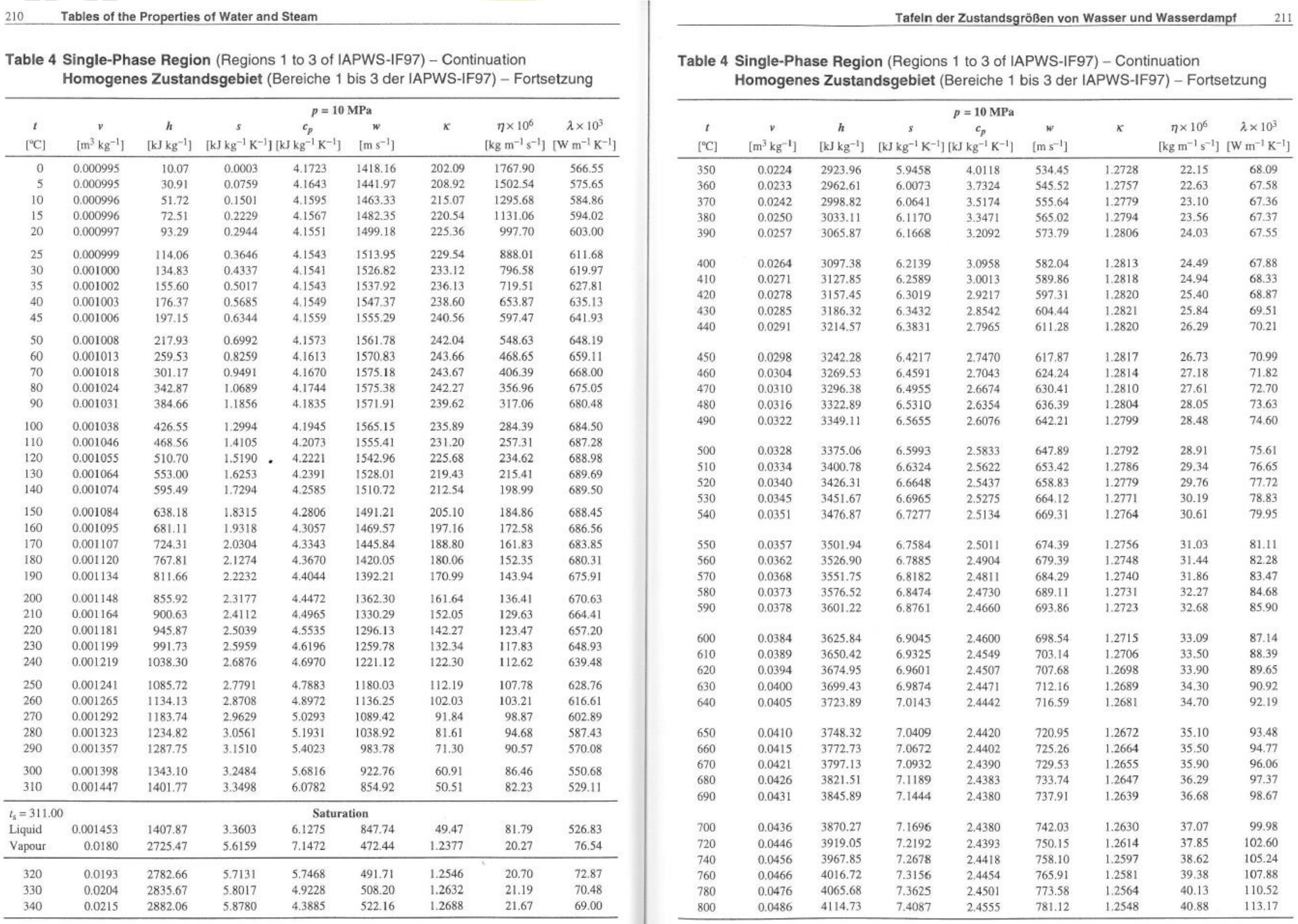

210 Tables of the Properties of Water and Steam

Table 4 Single-Phase Region (Regions 1 to 3 of IAPWS-IF97) – Continuation
Homogenes Zustandsgebiet (Bereiche 1 bis 3 der IAPWS-IF97) – Fortsetzung

				$p = 10$ MPa				
t [°C]	v [m^3 kg^{-1}]	h [kJ kg^{-1}]	s [kJ kg^{-1} K^{-1}]	c_p [kJ kg^{-1} K^{-1}]	w [m s^{-1}]	κ	$\eta \times 10^6$ [kg m^{-1} s^{-1}]	$\lambda \times 10^3$ [W m^{-1} K^{-1}]
0	0.000995	10.07	0.0003	4.1723	1418.16	202.09	1767.90	566.55
5	0.000995	30.91	0.0759	4.1643	1441.97	208.92	1502.54	575.65
10	0.000996	51.72	0.1501	4.1595	1463.33	215.07	1295.68	584.86
15	0.000996	72.51	0.2229	4.1567	1482.35	220.54	1131.06	594.02
20	0.000997	93.29	0.2944	4.1551	1499.18	225.36	997.70	603.00
25	0.000999	114.06	0.3646	4.1543	1513.95	229.54	888.01	611.68
30	0.001000	134.83	0.4337	4.1541	1526.82	233.12	796.58	619.97
35	0.001002	155.60	0.5017	4.1543	1537.92	236.13	719.51	627.81
40	0.001003	176.37	0.5685	4.1549	1547.37	238.60	653.87	635.13
45	0.001006	197.15	0.6344	4.1559	1555.29	240.56	597.47	641.93
50	0.001008	217.93	0.6992	4.1573	1561.78	242.04	548.63	648.19
60	0.001013	259.53	0.8259	4.1613	1570.83	243.66	468.65	659.11
70	0.001018	301.17	0.9491	4.1670	1575.18	243.67	406.39	668.00
80	0.001024	342.87	1.0689	4.1744	1575.38	242.27	356.96	675.05
90	0.001031	384.66	1.1856	4.1835	1571.91	239.62	317.06	680.48
100	0.001038	426.55	1.2994	4.1945	1565.15	235.89	284.39	684.50
110	0.001046	468.56	1.4105	4.2073	1555.41	231.20	257.31	687.28
120	0.001055	510.70	1.5190	4.2221	1542.96	225.68	234.62	688.98
130	0.001064	553.00	1.6253	4.2391	1528.01	219.43	215.41	689.69
140	0.001074	595.49	1.7294	4.2585	1510.72	212.54	198.99	689.50
150	0.001084	638.18	1.8315	4.2806	1491.21	205.10	184.86	688.45
160	0.001095	681.11	1.9318	4.3057	1469.57	197.16	172.58	686.56
170	0.001107	724.31	2.0304	4.3343	1445.84	188.80	161.83	683.85
180	0.001120	767.81	2.1274	4.3670	1420.05	180.06	152.35	680.31
190	0.001134	811.66	2.2232	4.4044	1392.21	170.99	143.94	675.91
200	0.001148	855.92	2.3177	4.4472	1362.30	161.64	136.41	670.63
210	0.001164	900.63	2.4112	4.4965	1330.29	152.05	129.63	664.41
220	0.001181	945.87	2.5039	4.5535	1296.13	142.27	123.47	657.20
230	0.001199	991.73	2.5959	4.6196	1259.78	132.34	117.83	648.93
240	0.001219	1038.30	2.6876	4.6970	1221.12	122.30	112.62	639.48
250	0.001241	1085.72	2.7791	4.7883	1180.03	112.19	107.78	628.76
260	0.001265	1134.13	2.8708	4.8972	1136.25	102.03	103.21	616.61
270	0.001292	1183.74	2.9629	5.0293	1089.42	91.84	98.87	602.89
280	0.001323	1234.82	3.0561	5.1931	1038.92	81.61	94.68	587.43
290	0.001357	1287.75	3.1510	5.4023	983.78	71.30	90.57	570.08
300	0.001398	1343.10	3.2484	5.6816	922.76	60.91	86.46	550.68
310	0.001447	1401.77	3.3498	6.0782	854.92	50.51	82.23	529.11
$t_s = 311.00$				**Saturation**				
Liquid	0.001453	1407.87	3.3603	6.1275	847.74	49.47	81.79	526.83
Vapour	0.0180	2725.47	5.6159	7.1472	472.44	1.2377	20.27	76.54
320	0.0193	2782.66	5.7131	5.7468	491.71	1.2546	20.70	72.87
330	0.0204	2835.67	5.8017	4.9228	508.20	1.2632	21.19	70.48
340	0.0215	2882.06	5.8780	4.3885	522.16	1.2688	21.67	69.00

Tafeln der Zustandsgrößen von Wasser und Wasserdampf 211

Table 4 Single-Phase Region (Regions 1 to 3 of IAPWS-IF97) – Continuation
Homogenes Zustandsgebiet (Bereiche 1 bis 3 der IAPWS-IF97) – Fortsetzung

				$p = 10$ MPa				
t [°C]	v [m^3 kg^{-1}]	h [kJ kg^{-1}]	s [kJ kg^{-1} K^{-1}]	c_p [kJ kg^{-1} K^{-1}]	w [m s^{-1}]	κ	$\eta \times 10^6$ [kg m^{-1} s^{-1}]	$\lambda \times 10^3$ [W m^{-1} K^{-1}]
350	0.0224	2923.96	5.9458	4.0118	534.45	1.2728	22.15	68.09
360	0.0233	2962.61	6.0073	3.7324	545.52	1.2757	22.63	67.58
370	0.0242	2998.82	6.0641	3.5174	555.64	1.2779	23.10	67.36
380	0.0250	3033.11	6.1170	3.3471	565.02	1.2794	23.56	67.37
390	0.0257	3065.87	6.1668	3.2092	573.79	1.2806	24.03	67.55
400	0.0264	3097.38	6.2139	3.0958	582.04	1.2813	24.49	67.88
410	0.0271	3127.85	6.2589	3.0013	589.86	1.2818	24.94	68.33
420	0.0278	3157.45	6.3019	2.9217	597.31	1.2820	25.40	68.87
430	0.0285	3186.32	6.3432	2.8542	604.44	1.2821	25.84	69.51
440	0.0291	3214.57	6.3831	2.7965	611.28	1.2820	26.29	70.21
450	0.0298	3242.28	6.4217	2.7470	617.87	1.2817	26.73	70.99
460	0.0304	3269.53	6.4591	2.7043	624.24	1.2814	27.18	71.82
470	0.0310	3296.38	6.4955	2.6674	630.41	1.2810	27.61	72.70
480	0.0316	3322.89	6.5310	2.6354	636.39	1.2804	28.05	73.63
490	0.0322	3349.11	6.5655	2.6076	642.21	1.2799	28.48	74.60
500	0.0328	3375.06	6.5993	2.5833	647.89	1.2792	28.91	75.61
510	0.0334	3400.78	6.6324	2.5622	653.42	1.2786	29.34	76.65
520	0.0340	3426.31	6.6648	2.5437	658.83	1.2779	29.76	77.72
530	0.0345	3451.67	6.6965	2.5275	664.12	1.2771	30.19	78.83
540	0.0351	3476.87	6.7277	2.5134	669.31	1.2764	30.61	79.95
550	0.0357	3501.94	6.7584	2.5011	674.39	1.2756	31.03	81.11
560	0.0362	3526.90	6.7885	2.4904	679.39	1.2748	31.44	82.28
570	0.0368	3551.75	6.8182	2.4811	684.29	1.2740	31.86	83.47
580	0.0373	3576.52	6.8474	2.4730	689.11	1.2731	32.27	84.68
590	0.0378	3601.22	6.8761	2.4660	693.86	1.2723	32.68	85.90
600	0.0384	3625.84	6.9045	2.4600	698.54	1.2715	33.09	87.14
610	0.0389	3650.42	6.9325	2.4549	703.14	1.2706	33.50	88.39
620	0.0394	3674.95	6.9601	2.4507	707.68	1.2698	33.90	89.65
630	0.0400	3699.43	6.9874	2.4471	712.16	1.2689	34.30	90.92
640	0.0405	3723.89	7.0143	2.4442	716.59	1.2681	34.70	92.19
650	0.0410	3748.32	7.0409	2.4420	720.95	1.2672	35.10	93.48
660	0.0415	3772.73	7.0672	2.4402	725.26	1.2664	35.50	94.77
670	0.0421	3797.13	7.0932	2.4390	729.53	1.2655	35.90	96.06
680	0.0426	3821.51	7.1189	2.4383	733.74	1.2647	36.29	97.37
690	0.0431	3845.89	7.1444	2.4380	737.91	1.2639	36.68	98.67
700	0.0436	3870.27	7.1696	2.4380	742.03	1.2630	37.07	99.98
720	0.0446	3919.05	7.2192	2.4393	750.15	1.2614	37.85	102.60
740	0.0456	3967.85	7.2678	2.4418	758.10	1.2597	38.62	105.24
760	0.0466	4016.72	7.3156	2.4454	765.91	1.2581	39.38	107.88
780	0.0476	4065.68	7.3625	2.4501	773.58	1.2564	40.13	110.52
800	0.0486	4114.73	7.4087	2.4555	781.12	1.2548	40.88	113.17

Quelle: Wagner, W.; Kruse, A. Properties of Water and Steam, Springer

The Three Main Components of a Parabolic Trough Collector

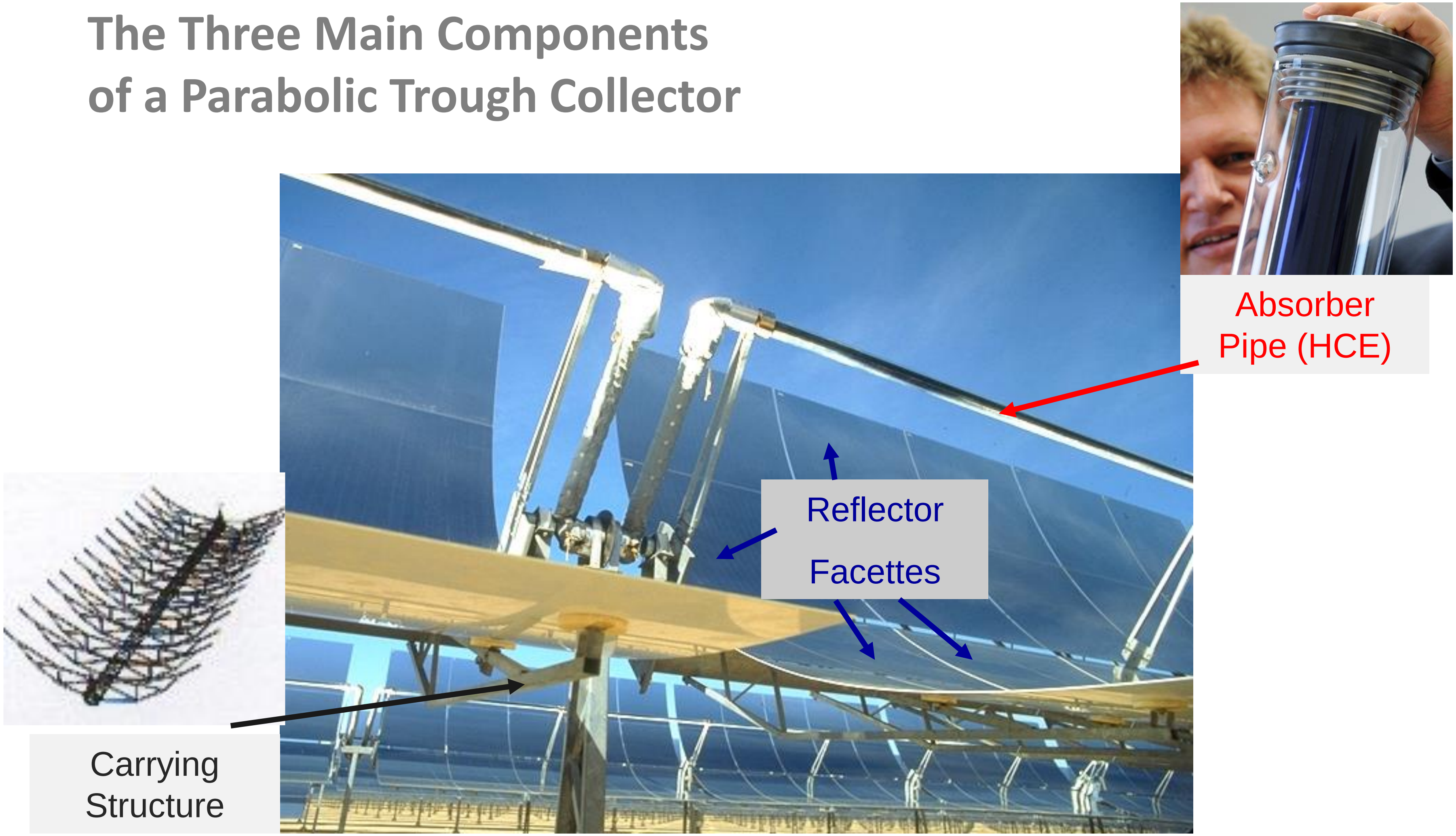

Absorber Pipe (HCE)

Reflector Facettes

Carrying Structure

Parabolic Trough Solar Collectors

- A trough shaped reflector focusses the light onto a focal line.
- A pipe which absorbs the concentrated light, the absorber pipe is located in this line.
- A heat transfer fluid, HTF, flowing through the pipe is heated up.

Collector Manufacturers:

- For a long time the Collectors LS2 and LS3 of the israeli company LUZ were the market leaders.
- Eurotrough, EU/D/ES
- SENER, ES
- Abengoa, ES
- Solargeneix, USA

- The company LUZ who supplied collectors to the trough plants in California in the 1980ies established a kind of standard for trough mirrors and the belonging absorber tubes with their "LS 3 Collector" :
- The collectors on the market today mainly differ regarding the carrying structure.

- Data of **LS3-compatible** Collectors:

– Reflector Aperture:	5,76 m
– Length of one collector unit:	100 m or 150 m
– Outer diameter of absorber pipe:	70 mm
– Concentration factor:	80

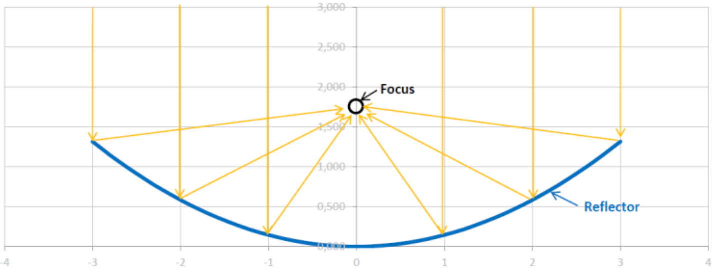

Collector Designs (not exhaustive)

SOLEL, Israel
Eurotrough, Europe
SENER, Spain

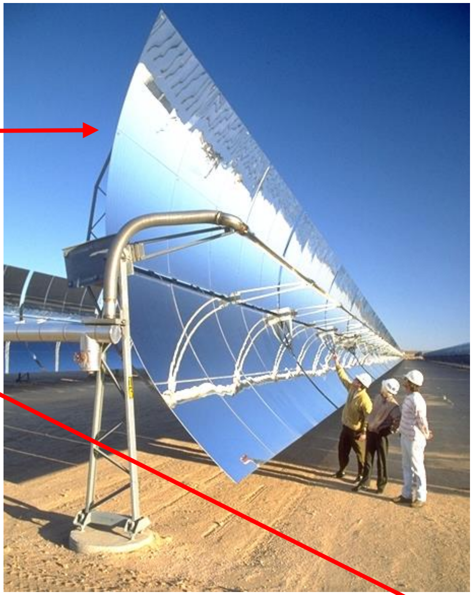

* **Eurotrough** is a development supported by the EU. From this some derivates developed by the participating companies have resulted. (e.g. „ASTRO“ from Abengoa, Spain.

The Parabolic Trough Solar Power Plants SEGS I to IV, which have been build between 1986 and 1991 in California, all were equipped with collectors of the company LUZ. LUZ built the carrying structure and the absorber pipes. The reflectors came from the company Flabeg, Germany. Until the renaissance of CSP in 2007 there were only these mirrors and pipes. Since 2008 there are several suppliers of carrying structures and mirrors. For absorber pipes there are so far only 2 serious suppliers, Schott Solar CSP GmbH, Germany and Solel, Israel (sucessor of LUZ). First Chinese suppliers occurred in 2012.

Parabolic Trough Solar Collectors

Schematic of „LS3 Collector “

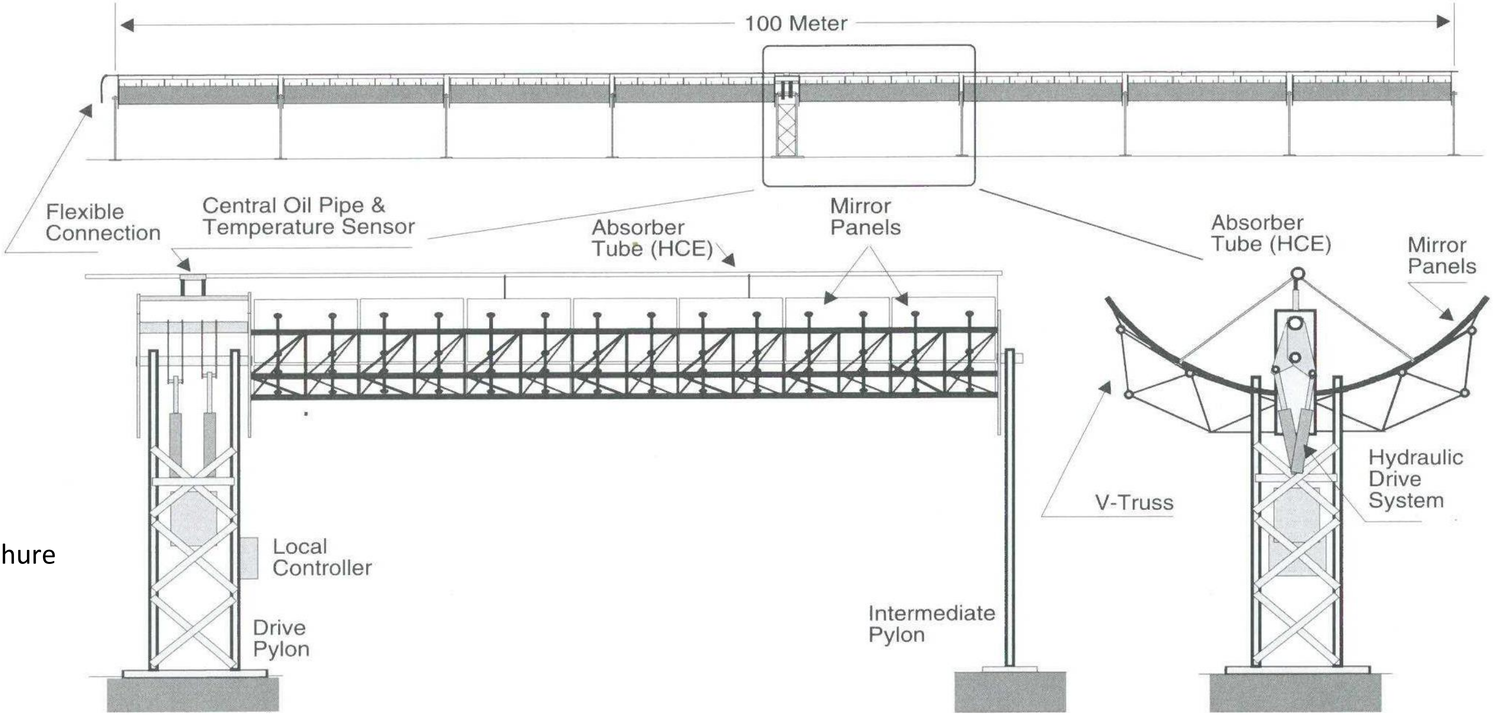

Source: Solar Millenium AG Company brochure 2001

The shown LS3 Collector (company Solel, previously LUZ) consists of 8 modules of approx. 12 m length each. Between two modules is one pylon. The central pylon is the so called drive pylon, where the tracking drive is located. One module has 28 mirror facets (4 rows of 7 facets each) and 3 absorber pipes of 4 m each. Up to today (2014) most commercially available collectors have these dimensions. Some collectors nowadays have 12 instead of 8 modules. The total collector is often called **„SCA“ (Solar Collector Assembly)** .

The Absorber Pipe

The absorber pipe consists of a steel pipe in which the heat transfer fluid, HTF is flowing, as well as the glass covering pipe. Between the glass and the steel pipe is a vacuum for avoiding convective heat loss. The connection between glass and steel pipe is realized by a bellow pipe in order to absorb the different heat expansion characteristics of glass and steel. A vacuum tight soldering connects the bellow with both pipes.

Schematic of a Absorber Pipe

Emission coefficient, $\varepsilon = 14\%$; absorption coefficient, $\alpha = 95\%$

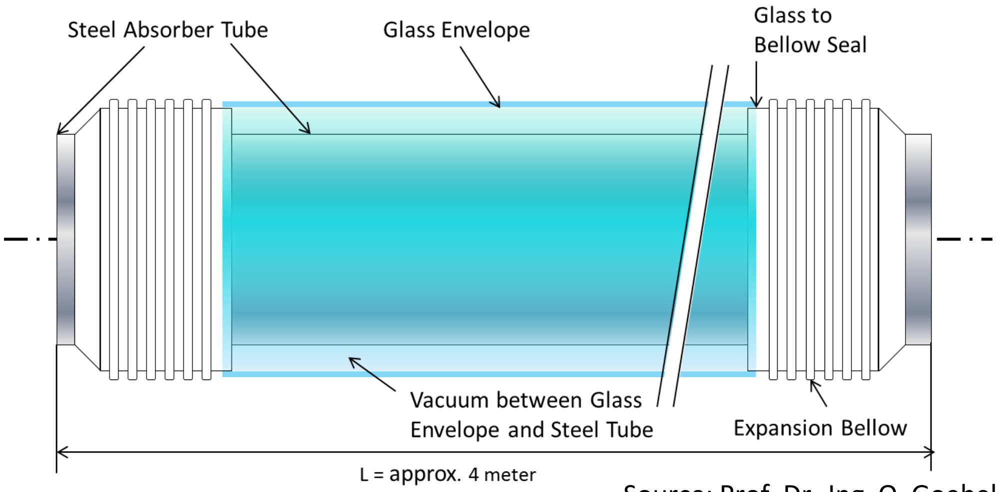

Source: Prof. Dr.-Ing. O. Goebel

The steel pipe is covered with a selective coating which absorbs the sun light pretty well, while the infrared emission coefficient is low.
The glass pipe is covered with an anti reflective coating which minimizes the reflective losses when the light comes in at high inclination angles.

Schematic of a Parabolic Trough Solar Collector Field

10 MW_{el} ==> 120 Collectors

8 Collectors per loop ==> 15 loops

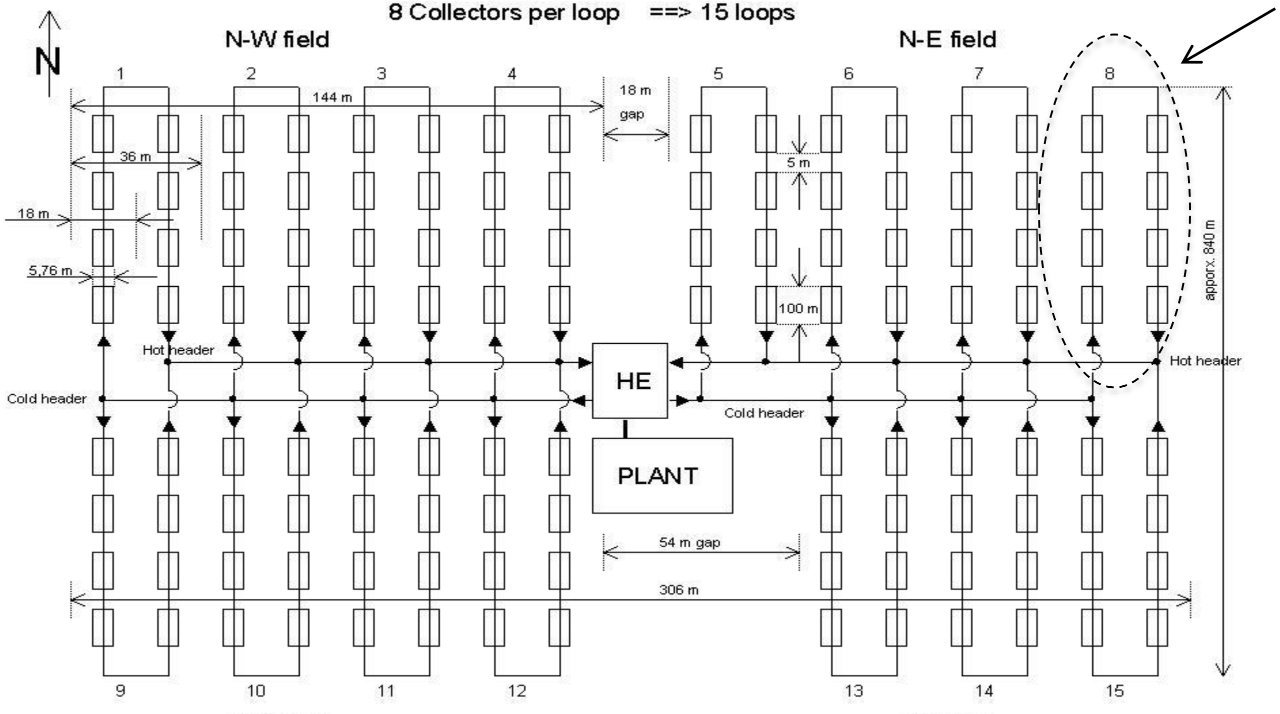

Collector loop

A_{net} = 306 m x 840 m = 257.040 m^2
A_{gross} = 326 m x 860 m = 280.360 m^2

HE = heat exchanger

Source: Prof. Dr.-Ing. O. Goebel

The scheme shows a collector field of a 10 MW_{el} power plant. The collectors have a length of 100 m and a width of 5.76 m (LS 3 compatible dimensions). Every 8 collectors form one loop. Each loop receives cold HTF from the cold header and delivers warm HTF to the hot header.

Schematic of Parabolic Trough Collector Field, Large Capacity

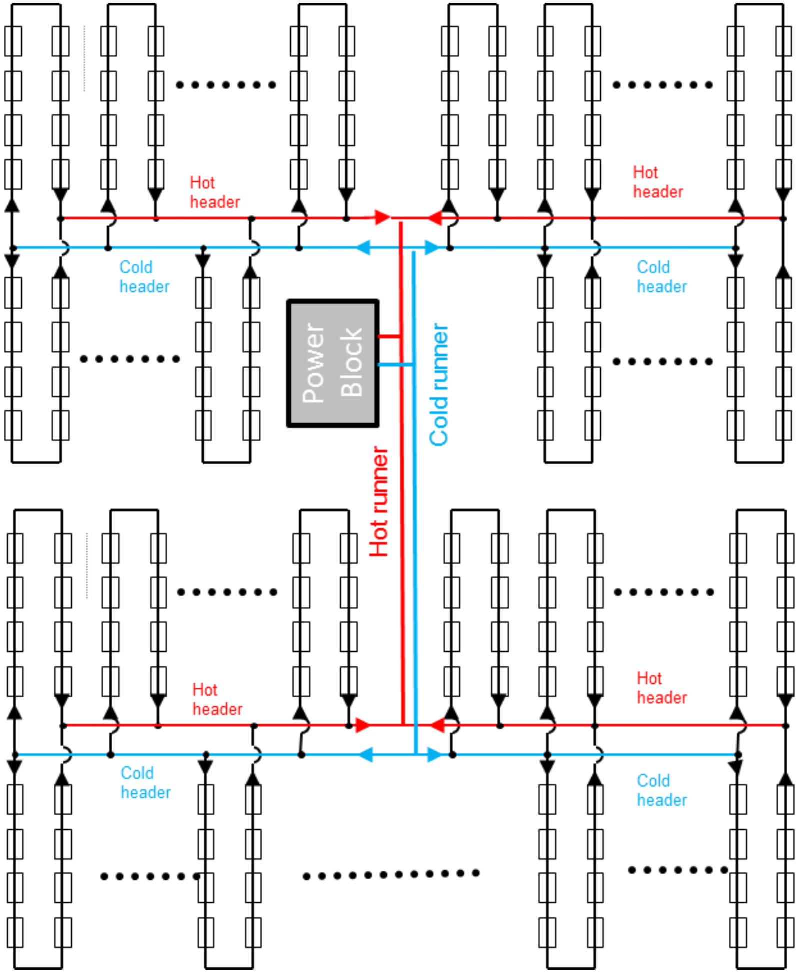

Source: Prof. Dr.-Ing. O. Goebel

- The HTF exit temperature at each loop is controlled by variation of the HTF mass flow in each loop.
- With today's HTF the maximum HTF temperature should be kept below 393°C.

Parabolic Trough Solar Collectors: Tracking and Efficiency

- The collectors are usually oriented in north-south direction. That means: The collector “looks” to the East in the morning and to the West in the evening.

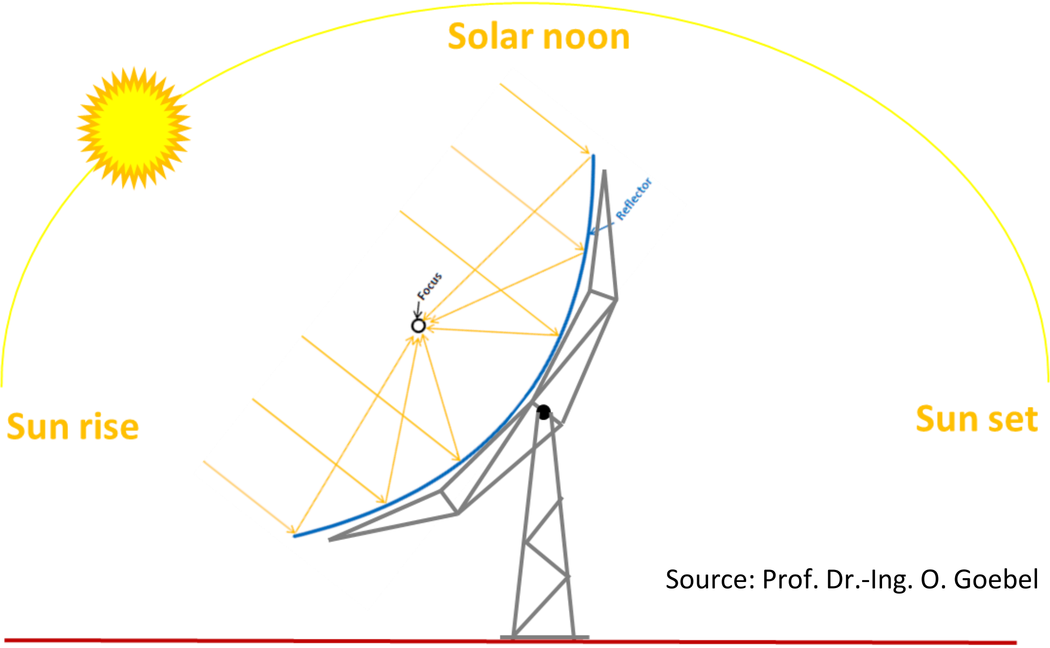

Source: Prof. Dr.-Ing. O. Goebel

Question: into which geographic direction looks the observer of this collector?

- The collector efficiency consists of an optical and a thermal component.

Parabolic Trough Solar Collectors: Efficiency

Data for describing the optical efficiency, example LS3:

	Input Data:	
Shading of the mirror by pipe holders and beam bending by glass pipe.	Shading (1 %):	99,0%
Area of absorber pipe shaded by bellows	shading by bellows (5%):	95,0%
Cosine factor for considering inclined insolation (is assumed with 100% in design point)	Cosine factor:	100,0%
Reflectivity of mirror*	Reflection:	92,0%
The part of the reflected light which hits the absorber pipe	Intercept:	95,0%
Absorption coefficient of the selective coating on the absorber pipe.	Absorption:	95,0%
	Eta optical (product of above data):	78,09%

* Reflectivity of clean mirror is approx. 94%. Mirror is washed when reflectivity falls below 90%. Avg. value = 92%

Parabolic Trough Solar Collectors: Efficiency

Total efficiency of LS 3 Collector as function of temperature and DII: $eta_{total} = eta_{optical} * eta_{thermal}$

Total efficiency of LS 3 collector

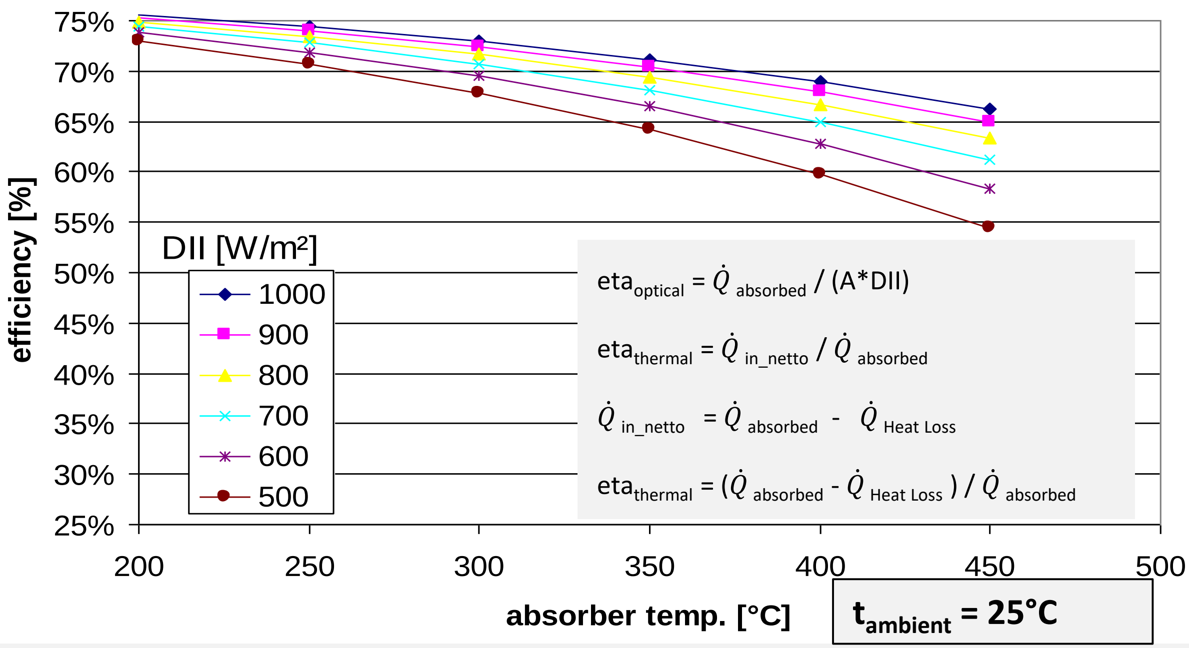

$eta_{optical} = \dot{Q}_{absorbed} / (A*DII)$

$eta_{thermal} = \dot{Q}_{in\_netto} / \dot{Q}_{absorbed}$

$\dot{Q}_{in\_netto} = \dot{Q}_{absorbed} - \dot{Q}_{Heat\ Loss}$

$eta_{thermal} = (\dot{Q}_{absorbed} - \dot{Q}_{Heat\ Loss}) / \dot{Q}_{absorbed}$

$t_{ambient}$ = 25°C

DII = Direct Incident Irradiation, the direct irradiation, perpendicular to the collector aperture.

- The thermal efficiency is reduced at high absorber temperatures, because thermal losses increase with high temperatures.
- At low DII the fraction of the heat losses is larger than at high DII. Therefore the thermal efficiency is lower at low DII values (for a given temperature).

Solar Field:
Heat Transfer Fluid (HTF) Circuit

- In the absorber tubes the HTF is heated by the concentrated sunlight
- The HTF temperature must not reach 400°C (cracking!)
- The HTF mass flow in the collector loops is controlled such that the final temperature always stays below 393°C
- The HTF transfers the collected heat to the water/steam circuit in a heat exchanger.
- The two-circuit system (Primary = HTF, Secondary = Water/Steam) had been selected in order to achieve a one phase flow in the absorber tubes. A two phase flow (liquid and gas phase) can cause problems, as will be shown in the Chapter “Developments”, when we shall discuss solar direct steam generation.

Performance Calculation of Total Plant System

The Performance of the plant is calculated / simulated by the following steps:

1. Thermal power of one collector as a function of DNI, position of sun and ambient temperature
2. Thermal power of entire solar field
3. Electrical power of steam turbine generator as a function of power block efficiency
4. Subtracting internal power demand of the plant
5. Doing the above mentioned steps for every hour of the year

=> Simulation of the annual energy yield

Solar Position Diagram of Madinat Zayed, UAE: 53.7° E, 23.57° N

First Step:
Calculating the sun‘s position for each hour of the year.

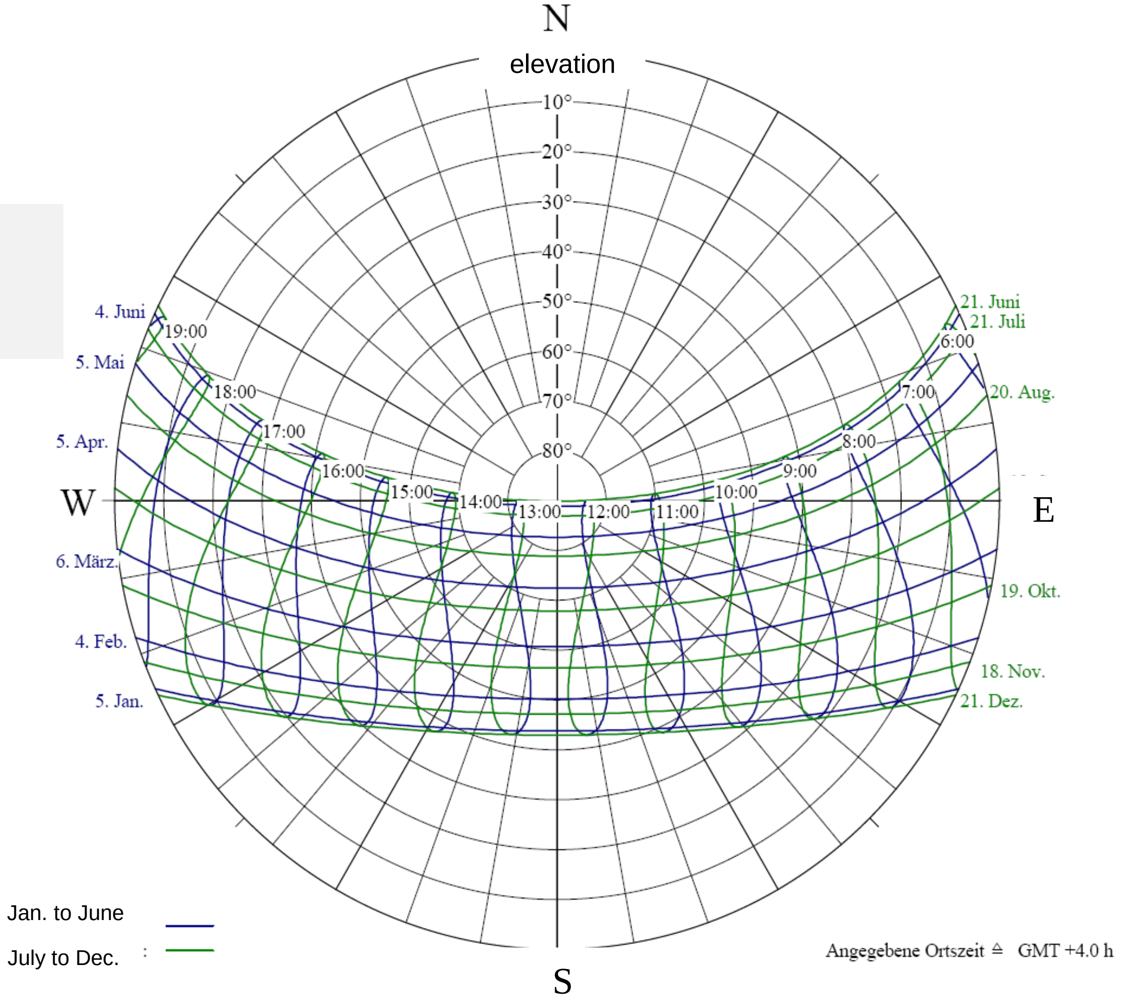

The Difference between Direct Normal Irradiation (DNI) and Direct Incident Irradiation (DII)

Next step:
Calculation of the incident angle (angle between the direction normal to aperture plane and the actual beam direction). It can be calculated from the sun's position.

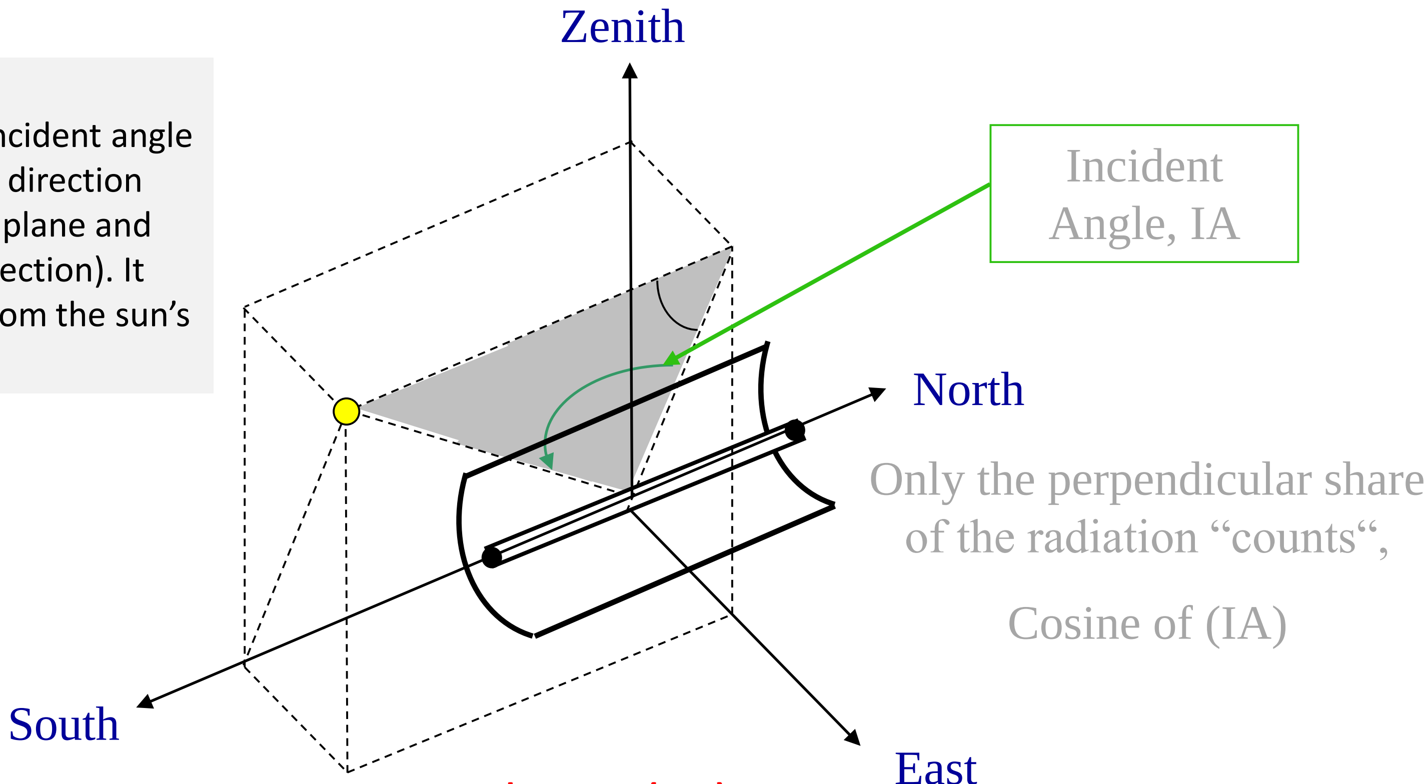

Only the perpendicular share of the radiation "counts",

Cosine of (IA)

$$DII = DNI * \cos(IA)$$

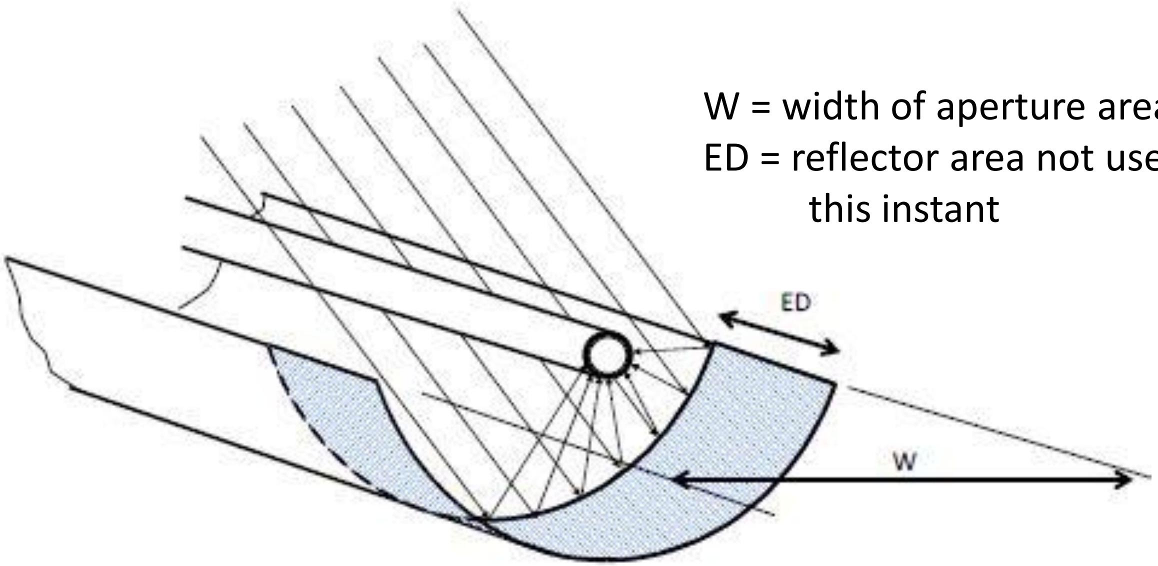

W = width of aperture area
ED = reflector area not used at this instant

Picture helping to define the incidence angle of solar radiation onto the aperture plane of a parabolic trough

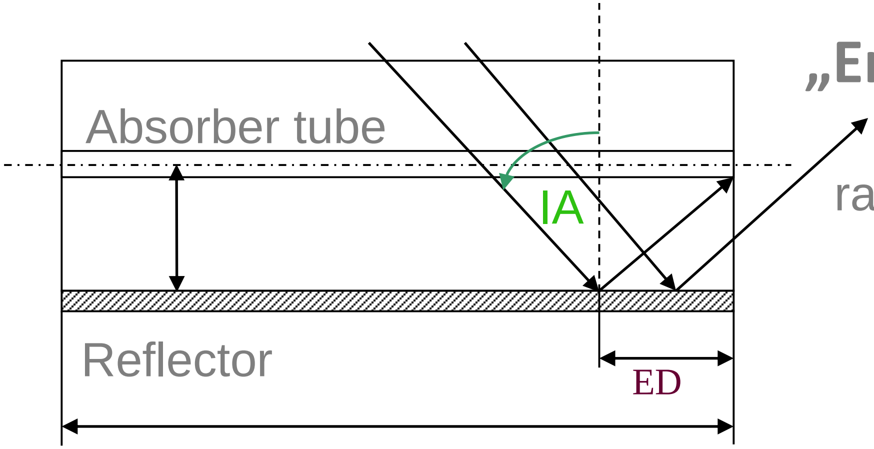

„End Losses“

Reflected radiation does not hit the tube

The Difference between Direct Normal Irradiation (DNI) and Direct Incident Irradiation (DII)

- DII = DNI * cos (IA)
- The DII calculated as shown above is the part of the Direct Irradiation which is theoretically usable by the collector.
- In reality DII = DNI * IAM is the usable part of the Direct Irradiation for the collector.
- IAM is the „Incident Angle Modifier“. IAM is obtained by measurements when the collector received light at different Incident Angles (IA).
- IAM is especially for large IA‘s smaller than cos (IA).
- **Important:** Due to the most of the time non perpendicular IA of the received DNI the collector efficiency is significantly lower in annual average, compared to the design efficiency, defined at DNI = 1000 W/m² and IA = zero.

Incident Angle Modifyer (IAM)

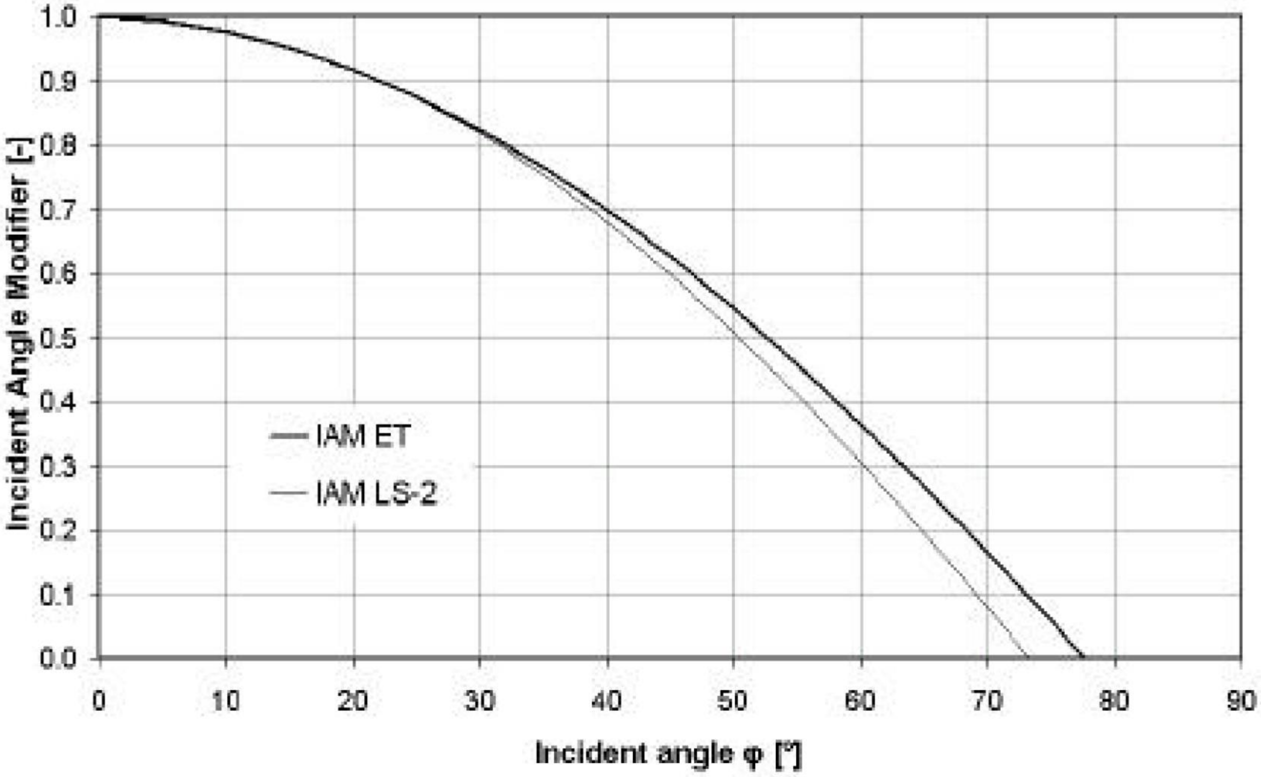

(φ = IA)

The Incident Angle Modifyer takes into account the cosine effect and other real collector loss mechanisms, such as „end losses“ and reduced Reflection at large IA’s.
ET = Eurotrough, LS 2 = Collector in early Californian Plants

Performance of a Collector (SCA) as Function of Sun's Position and DNI (slide 1 / 2)

Site: Yazd, Iran, 32° North, March 21st

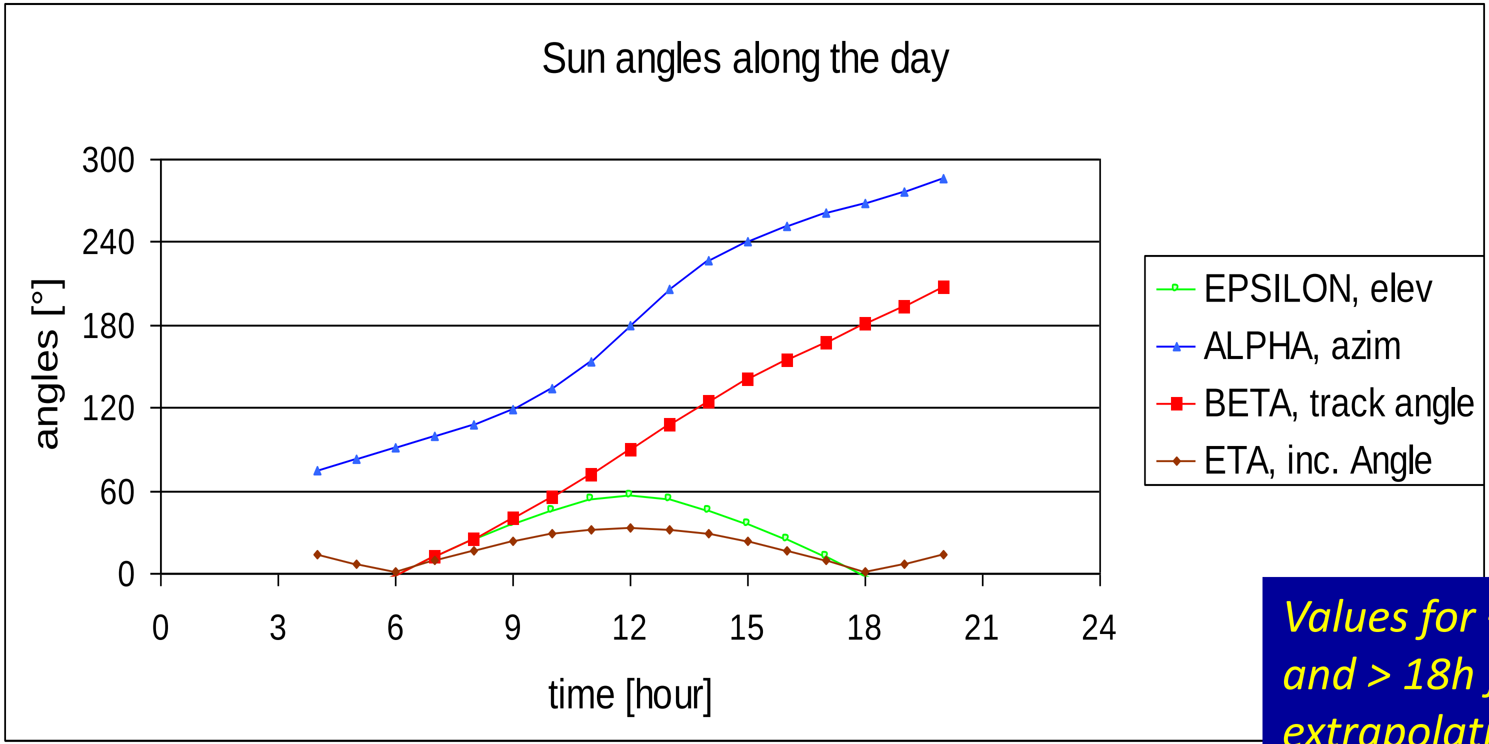

Values for < 6h and > 18h from extrapolation

Performance of a Collector (SCA) as Function of Sun‘s Position and DNI (slide 2 / 2)

Site: Yazd, Iran, 32° North, March 21st

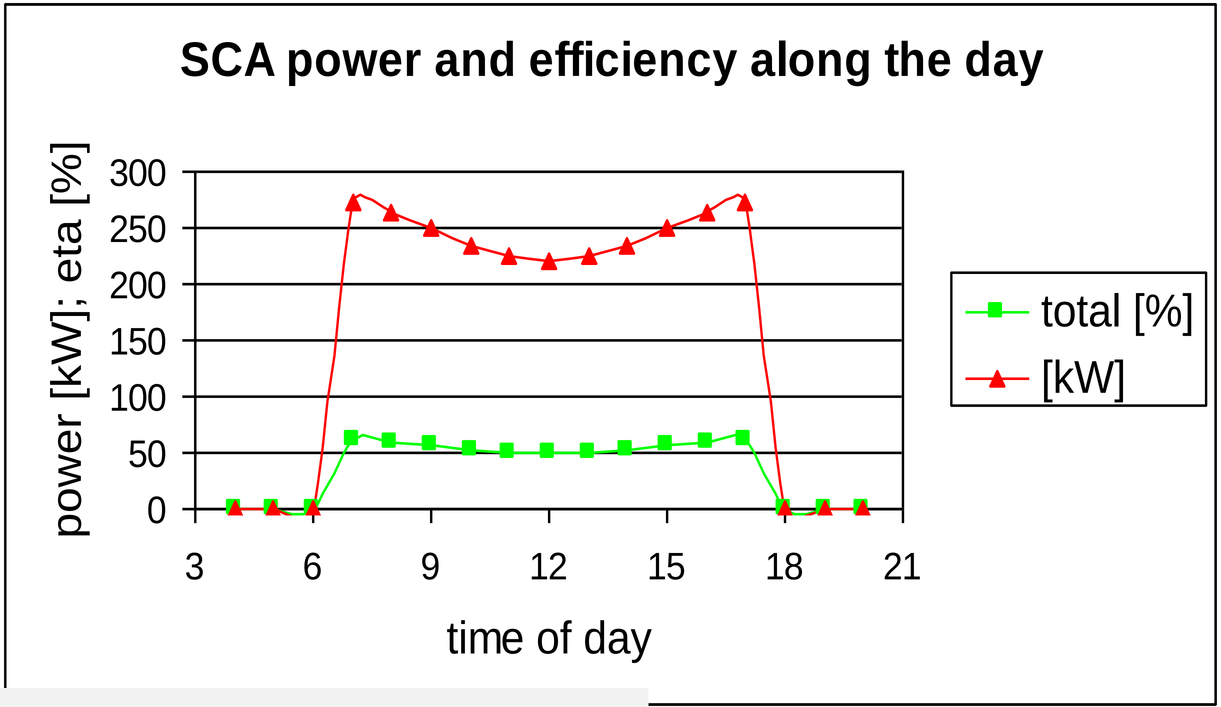

Next Step:
Calculation of collector efficiency at DNI = 1000 as a function of the sun‘s position. Collector efficiency is low at large IA‘s. Especially in winter IA is larger at noon than in the morning or evening (see solar position diagram).

$t_{absorber}$ = 340°C *(average from 290 and 390)*
$t_{ambient}$ = 20°C

Collector efficiency at Madinat Zayed (UAE, 23° North) at DNI always = 1000 W/m²

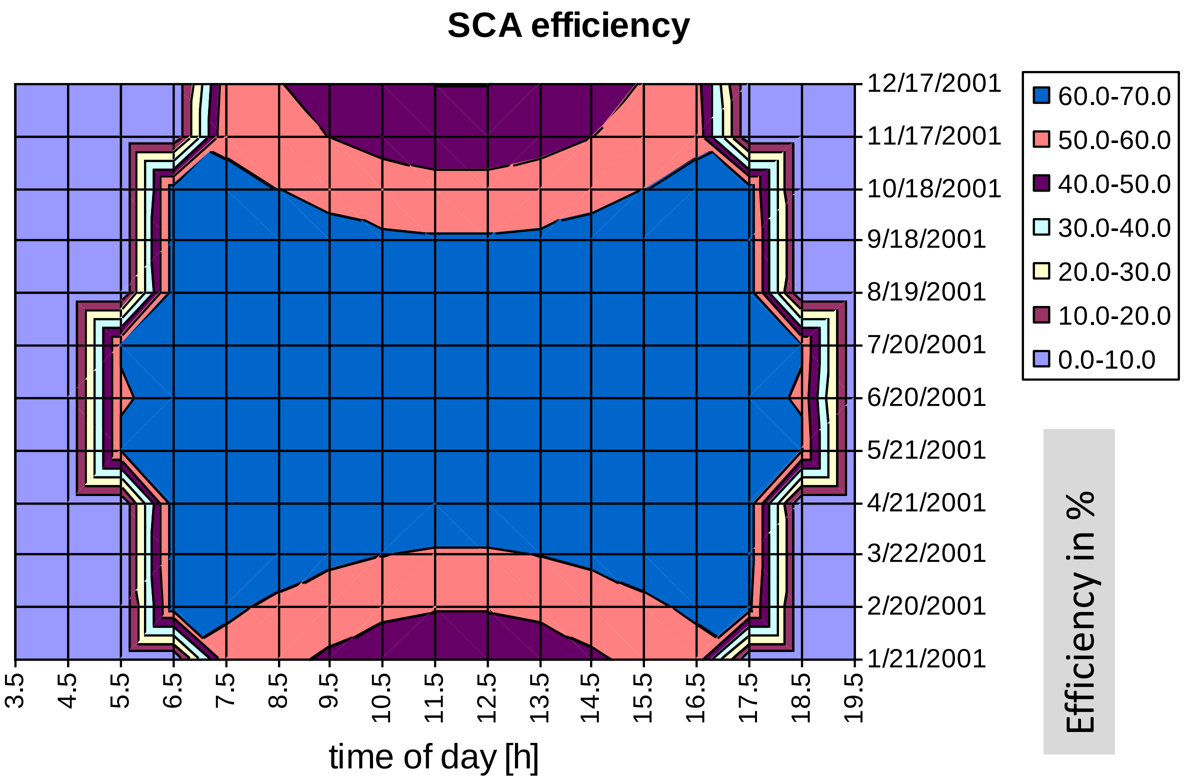

Efficiency in %

This diagram type is often used to display parameters over the day of the year and the time of the day.

Here we see that the collector efficiency reduction due to large IA's takes place mainly in winter close to noon.

Collector efficiency at Madinat Zayed (UAE, 23° North) at DNI always = 1000 W/m² (3 D diagram)

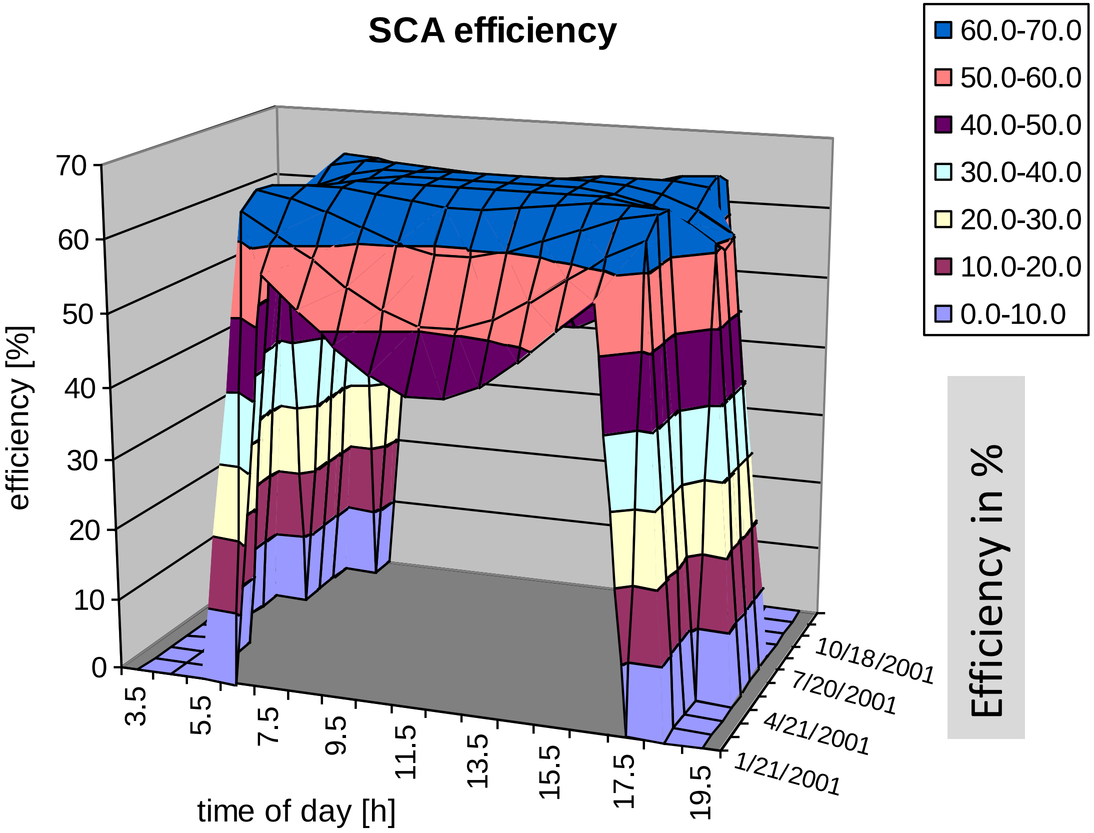

Efficiency in %

The same picture as before, just displayed as 3D.

Measured DNI at Madinat Zayed (UAE, 23° North) (Satellite Data)

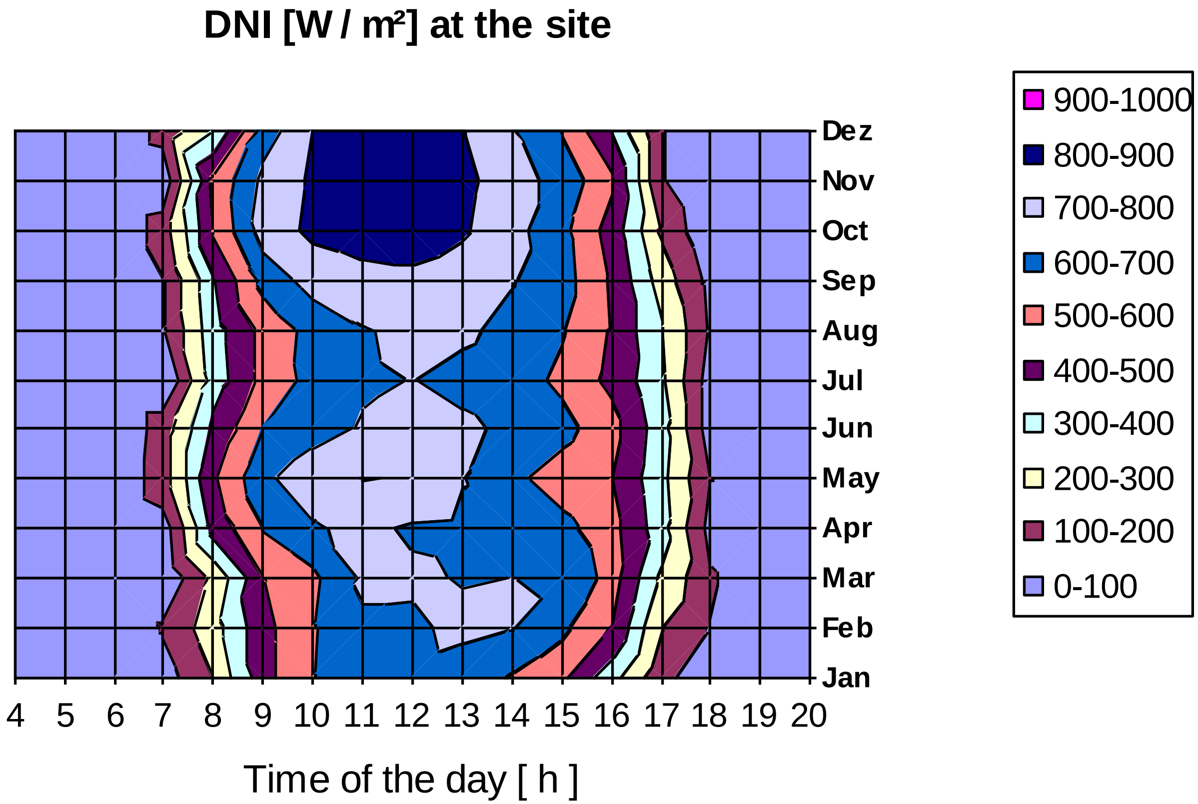

Next Step:
Considering the DNI at the project site.

Parabolic Trough Solar Collector at Madinat Zayed: Efficiency (at real DNI) as Function of Day and Time

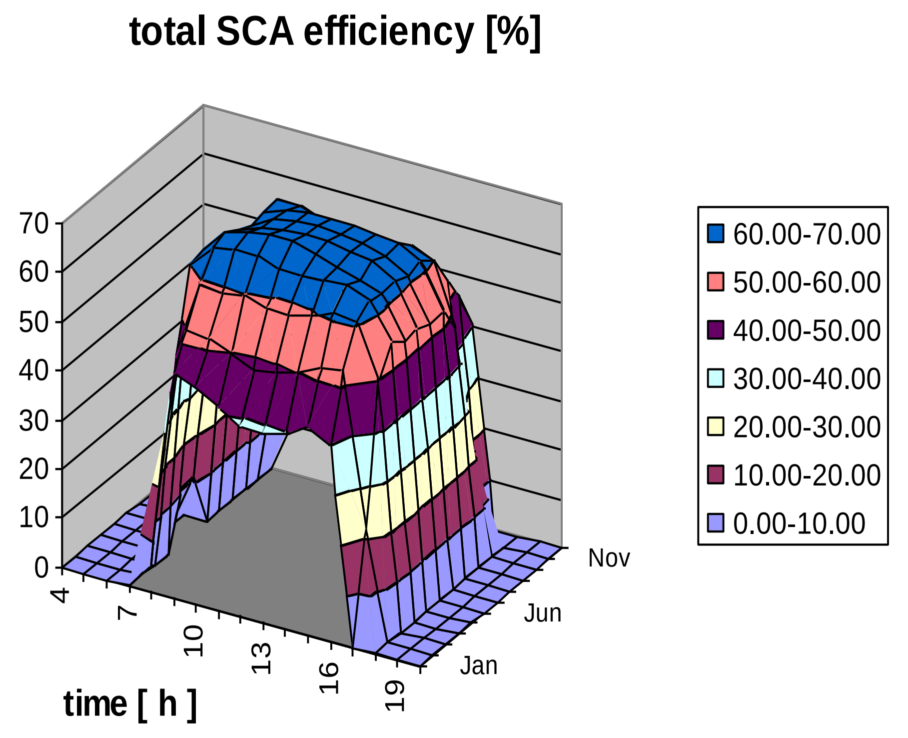

Due to the fact, that DNI in reality is mostly below 1000 W/m² (1000 W/m² case shown on the previous slide), the real collector efficiency is much lower than on the previous slide.

Parabolic Trough Solar Collector at Madinat Zayed: Thermal Output as Function of Day and Time

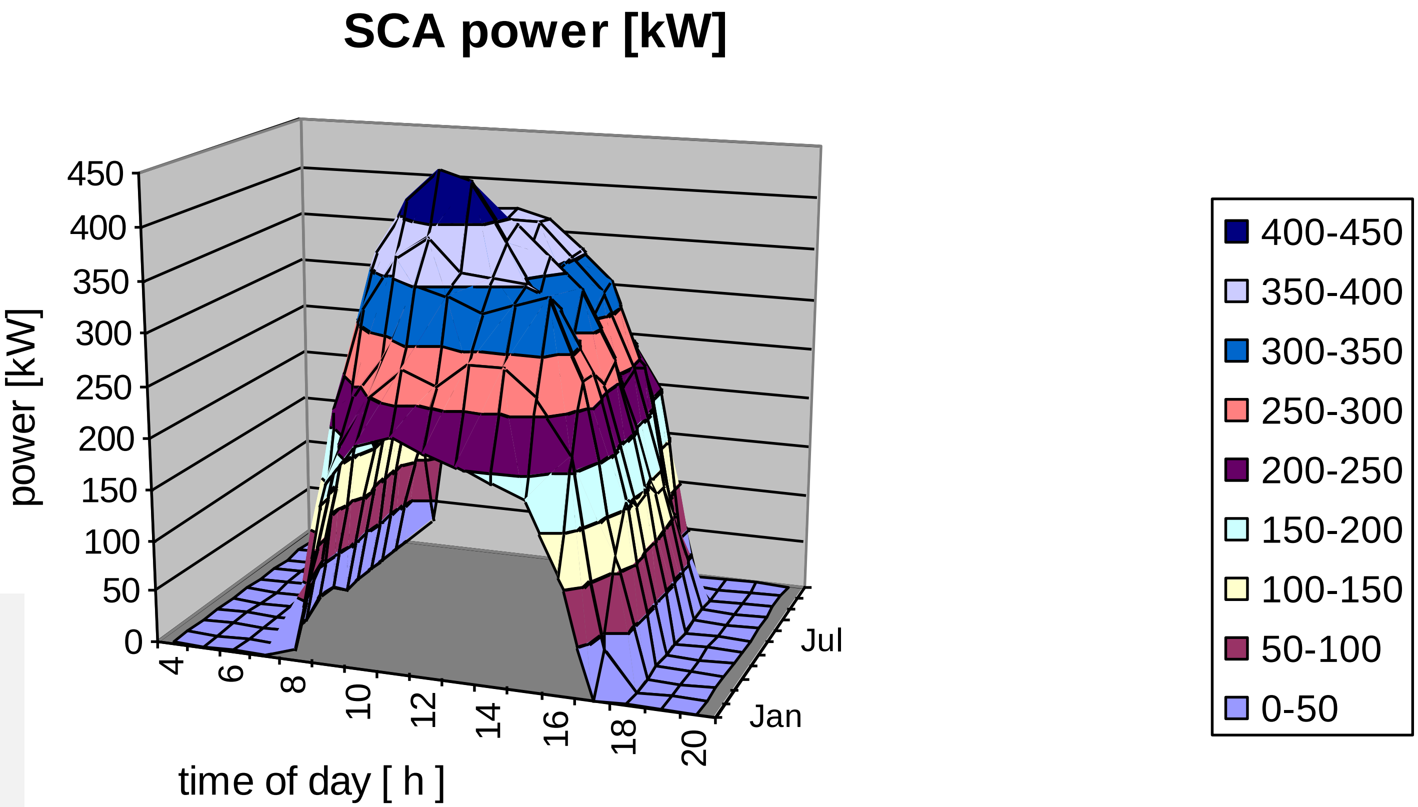

Next Step:
Calculation of SCA thermal power with:
$\dot{Q}_{Collector} = A_{Collector} * DNI * eta_{Collector}$

(with $A_{collector} = 817.5 m^2$)

Parabolic Trough Solar Collector: Power of the entire Collector Field without Shading and Thermal Inertia

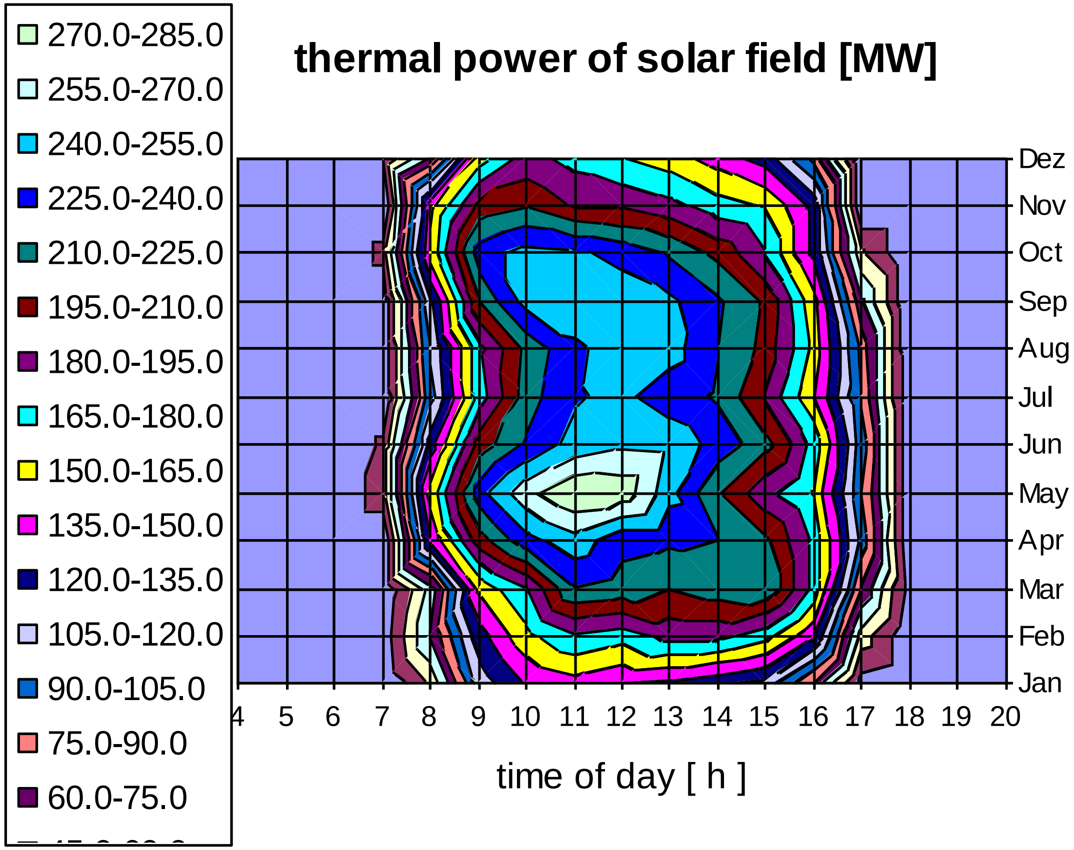

Next Step:
Calculation of thermal power of entire collector field with n collectors:

$$\dot{Q}_{Collectorfield} = \dot{Q}_{Collector} * n_{Collector}$$

Parabolic Trough Solar Collector: Shading by Neighbor Collectors

Next Step:
Considering shading effects of collectors in the morning and evening.

Site: Madinat Zayed, UAE

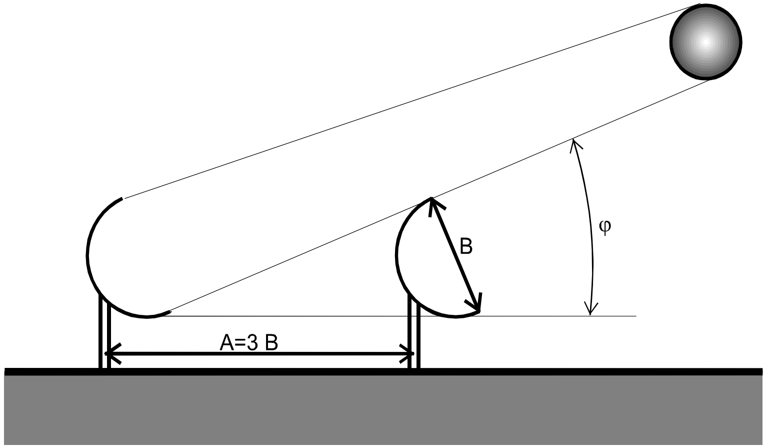

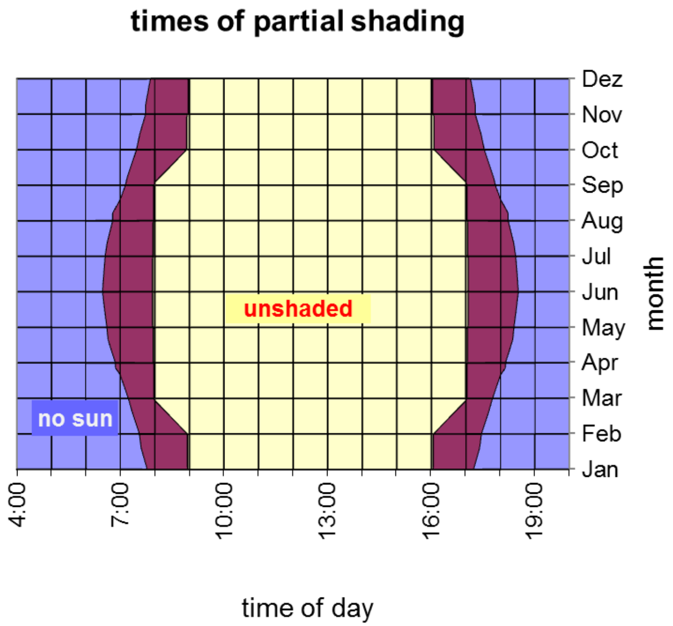

Parabolic Trough Solar Collector: Power of the entire Collector Field **with** Shading and Thermal Inertia

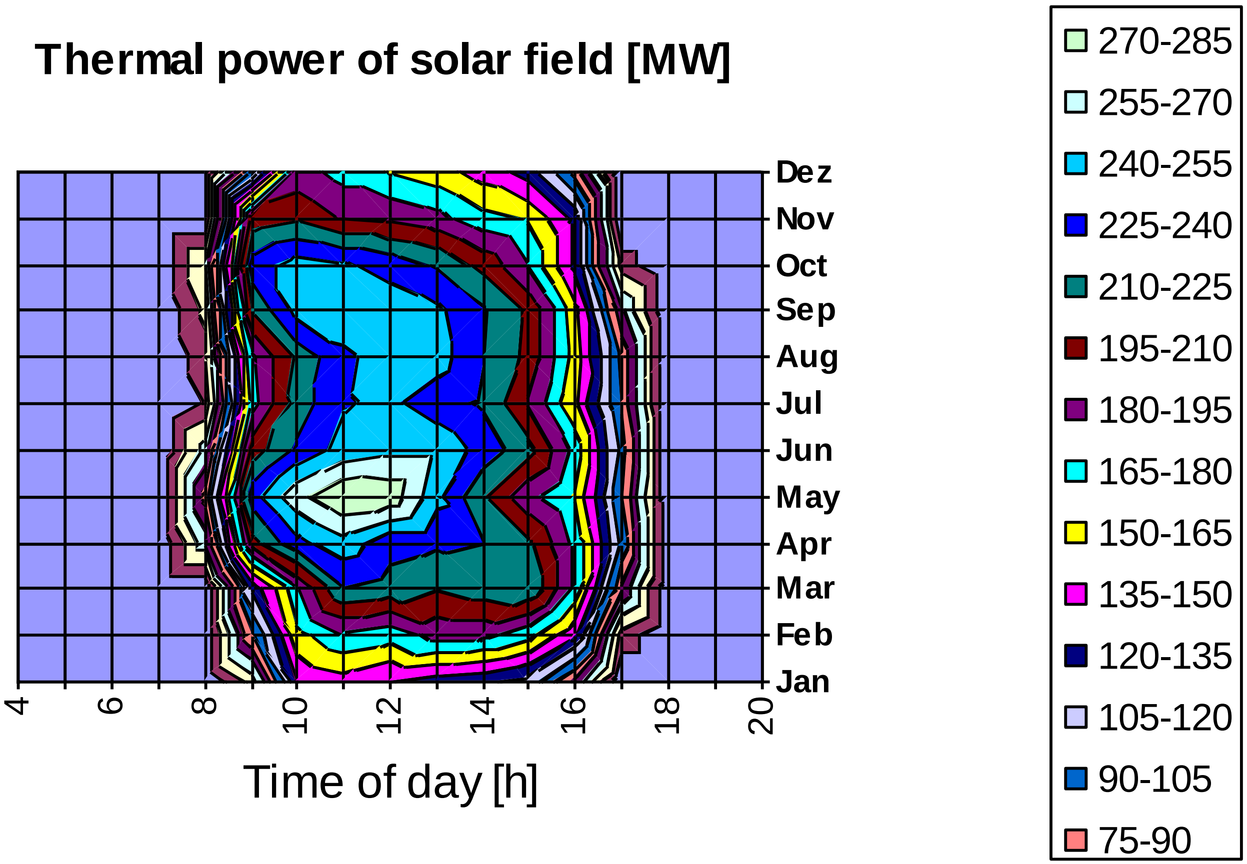

In this diagram the shading effects and the thermal inertia of the solar field are considered.
It can be seen that heat production starts later than in the previous diagram.

Parabolic Trough Solar Power Plant, “Shams 1” in Madinat Zayed (UAE) with Booster Heater

This diagram shows the location of the booster heater after the solar steam generator for the further super-heating of the steam before its entry to the turbine.

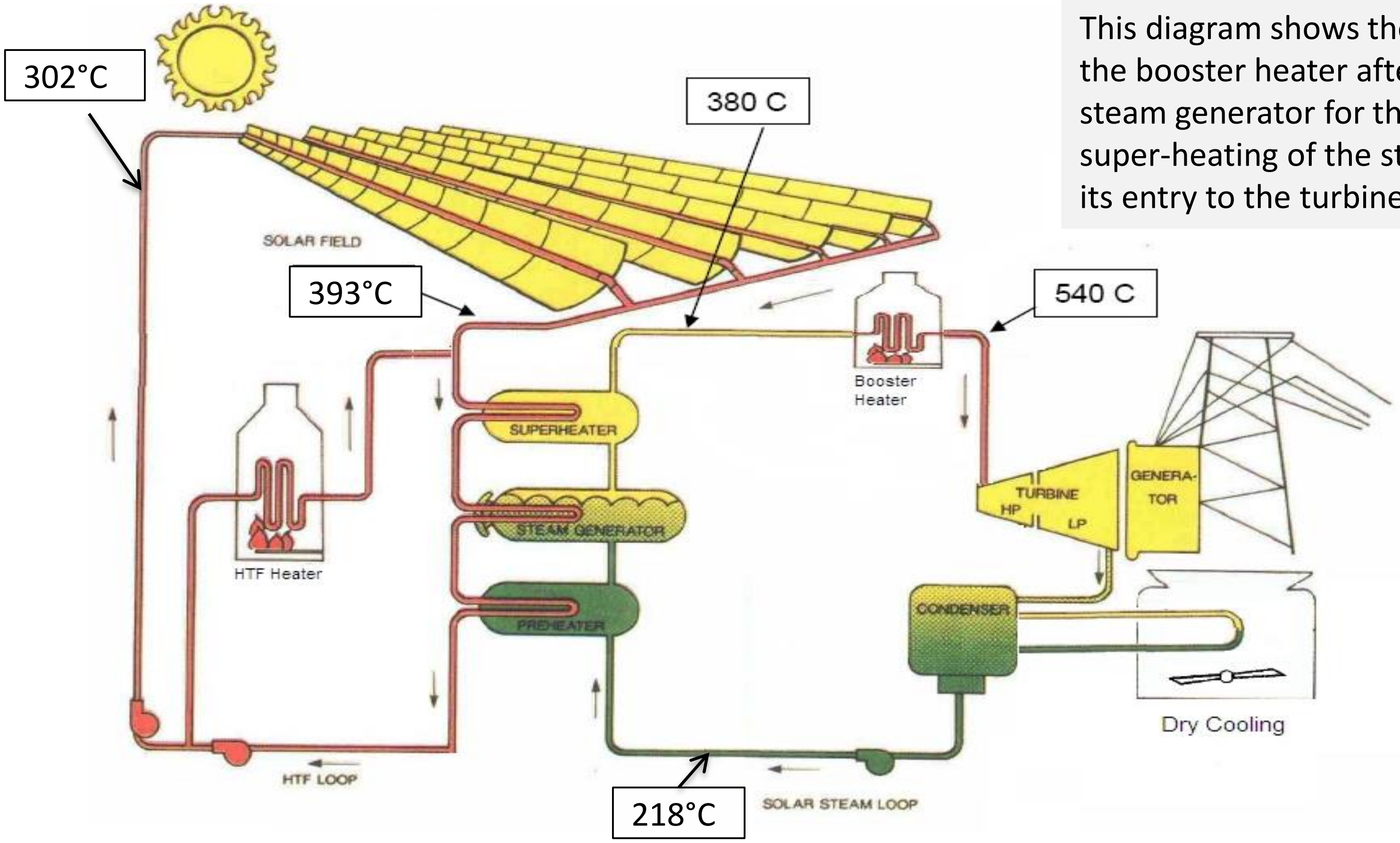

Thermal Power of the Solar Field including 18% from “Boost Burner”

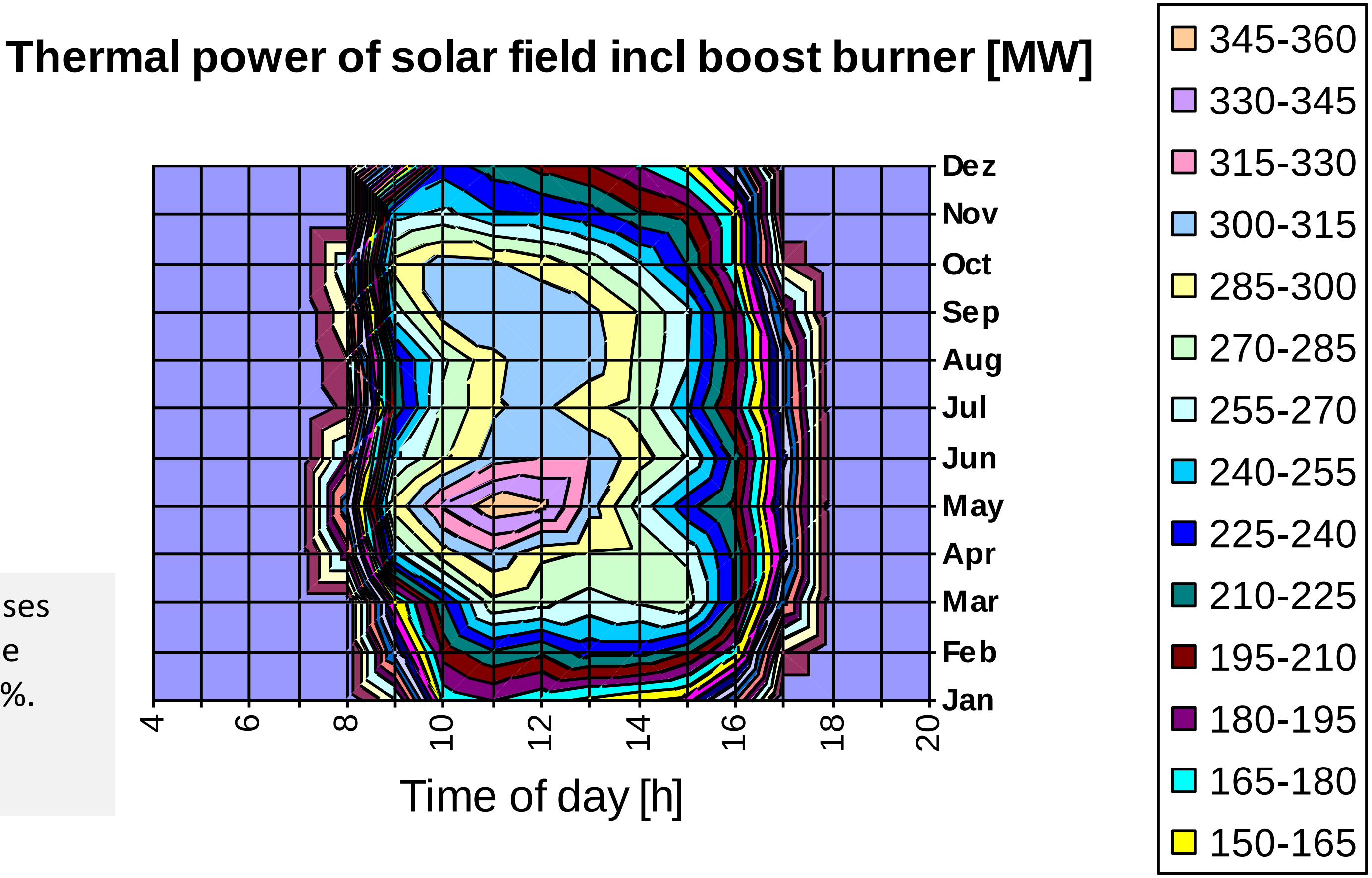

The Boost Burner increases the thermal power of the solar field by approx. 22%. (Compared to previous diagram)

Power Block (Rankine Cycle): Efficiency at Part Load

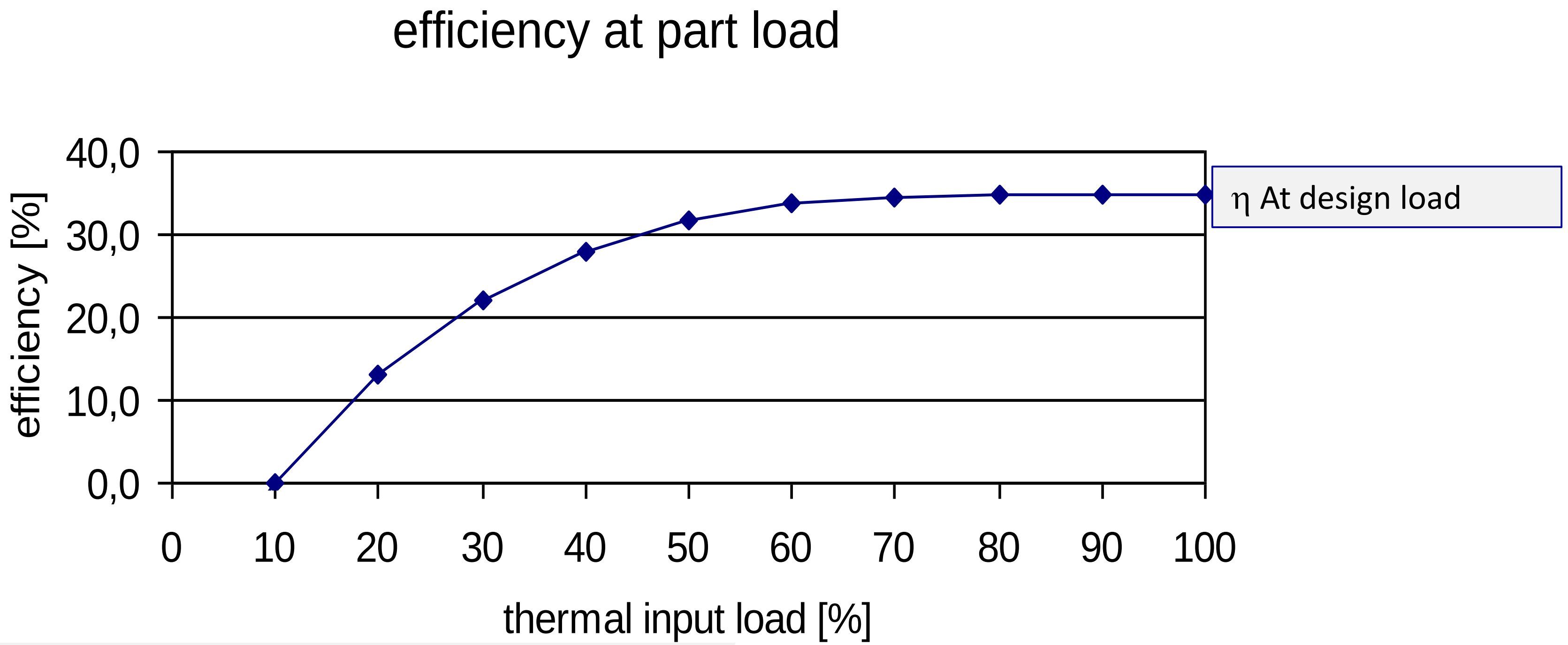

Next Step:
Calculation of turbine efficiency as a function of load factor. This is necessary, because the turbine often runs at part load.

PROJETO Energia Heliotérmica

Electrical Gross Output (theoretical, without considering steam turbine limit)

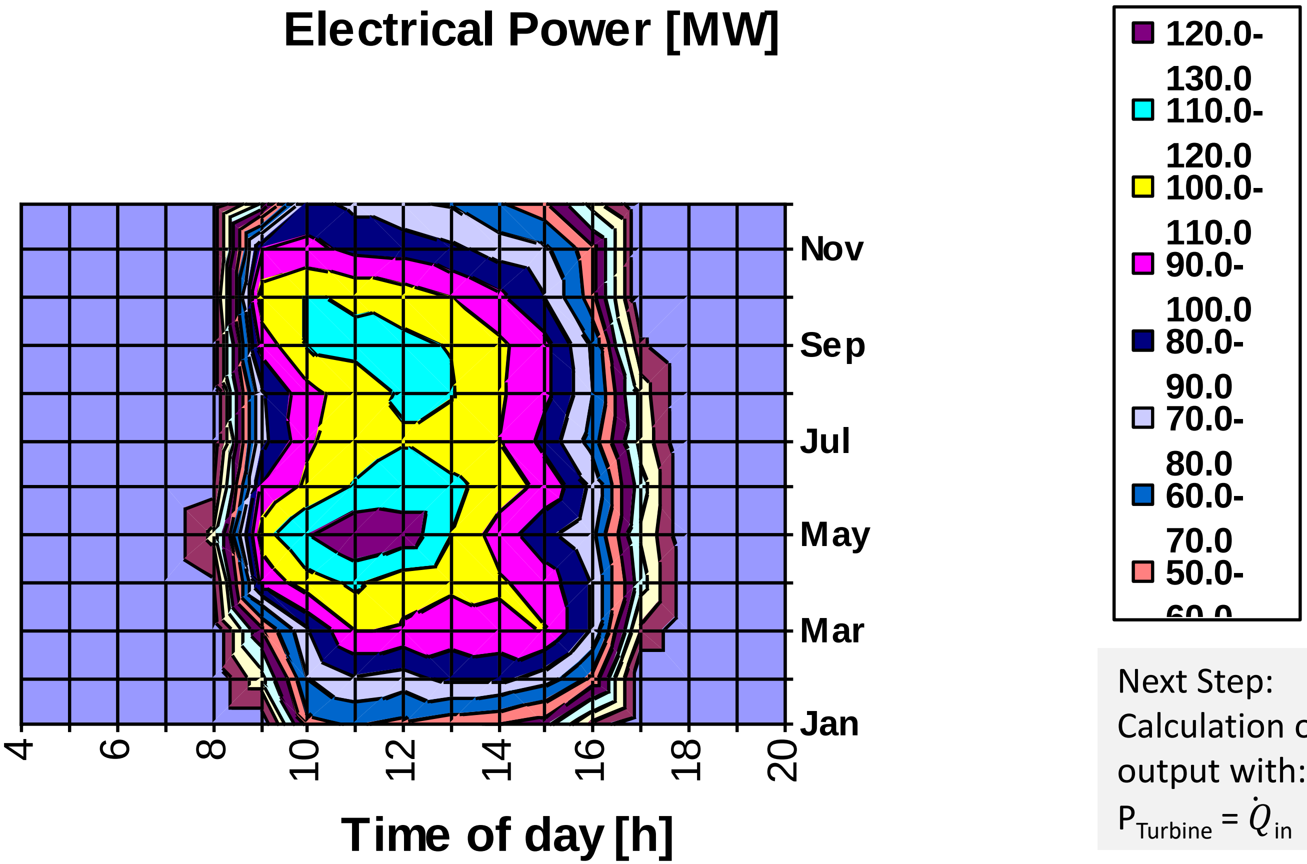

Next Step:
Calculation of electric power output with:
$P_{Turbine} = \dot{Q}_{in} * \eta_{Turbine}$

Capped Peak Thermal Power (by Defocussing Collectors)

There are several hours per year when the solar field generates more power than the steam turbine can swallow. In these periods some collectors have to be defocussed. Solar fields are usually designed to reach their nominal output at DNI values of 750 to 850 W/m².

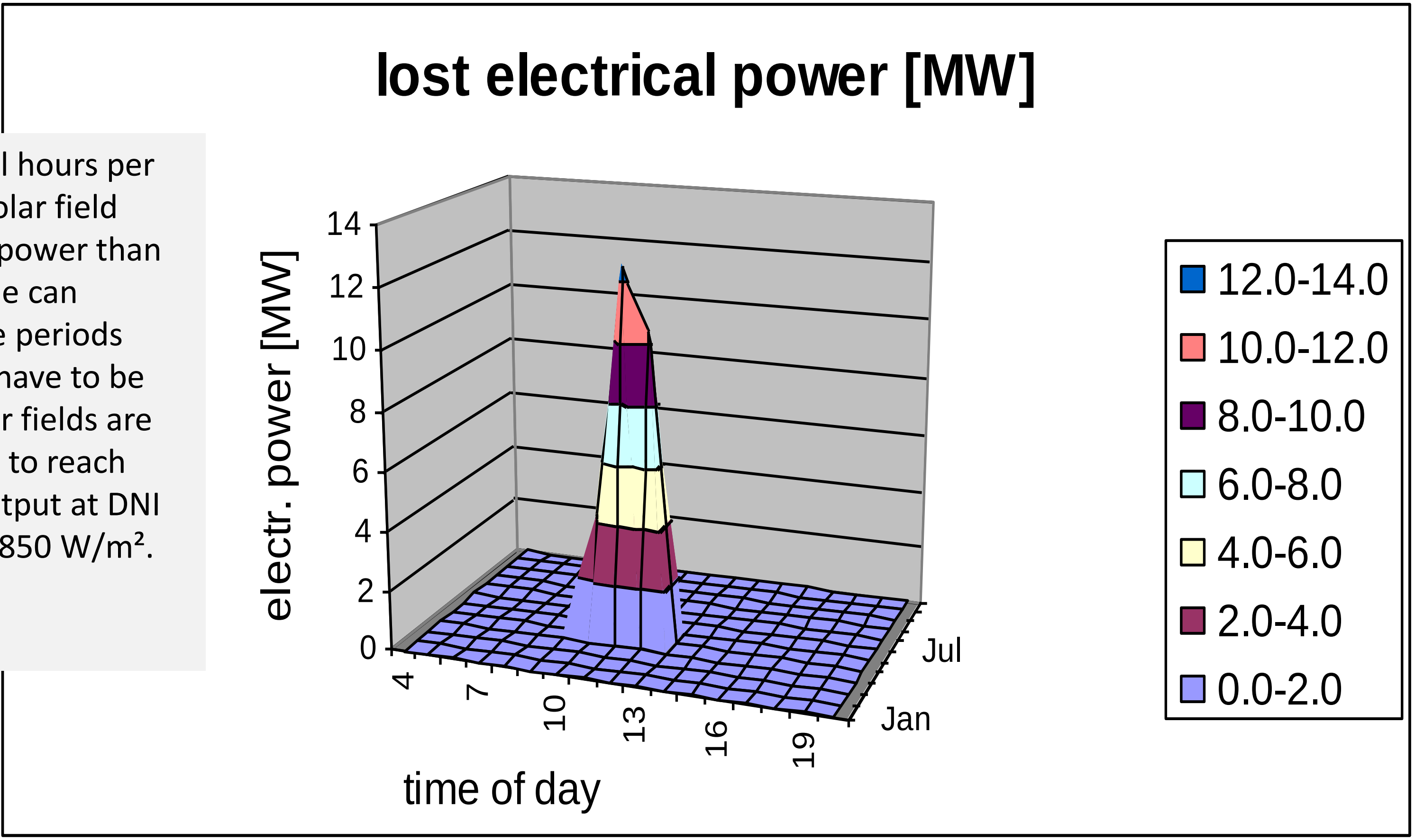

Electric Power, Gross, Capped

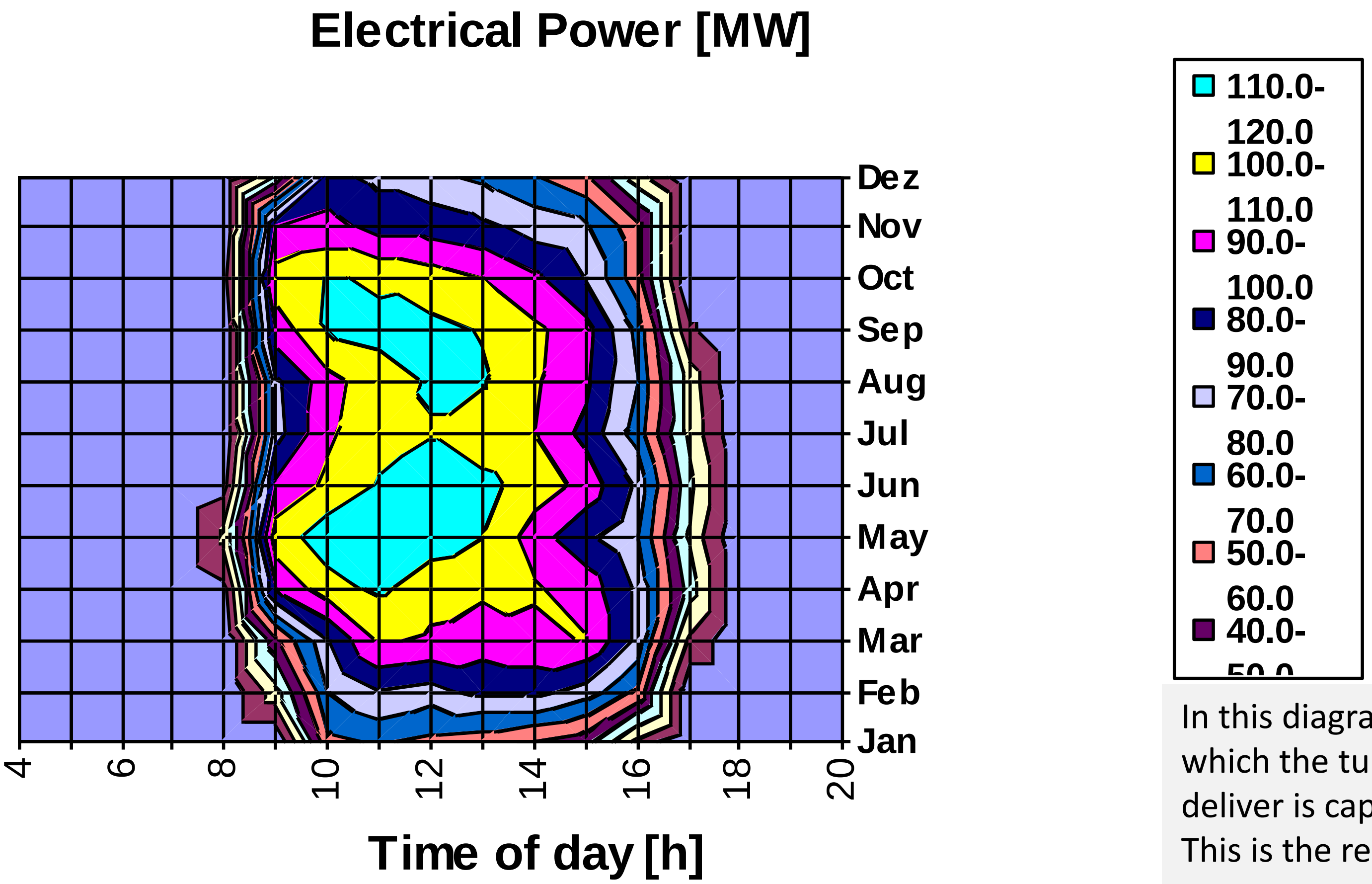

In this diagram the power peak which the turbine cannot deliver is capped.
This is the realistic gross electric power output of the plant.

Electric Power Output, net (after Deduction of 13% Internal Power Consumption)

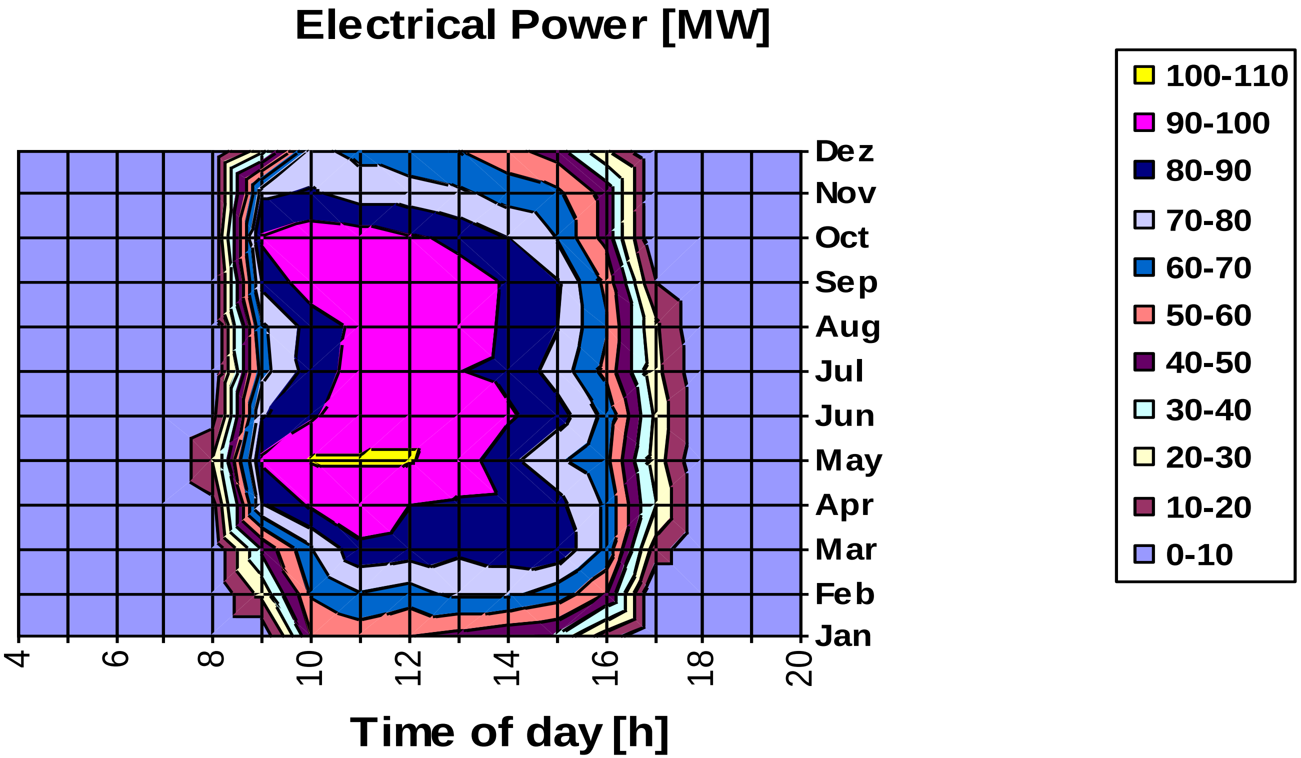

In this diagram we see the net power output of the plant. In comparison to the previous diagram, the internal power consumption of the plant has been deducted.

Main internal consumers are:

• Boiler feed water pump, • HTF pump, • cooling water pump, • cooling tower fan (see slide "scheme of PT solar power plant")

Electric Power Output, net (after Deduction of 13% Internal Power Consumption) (3D)

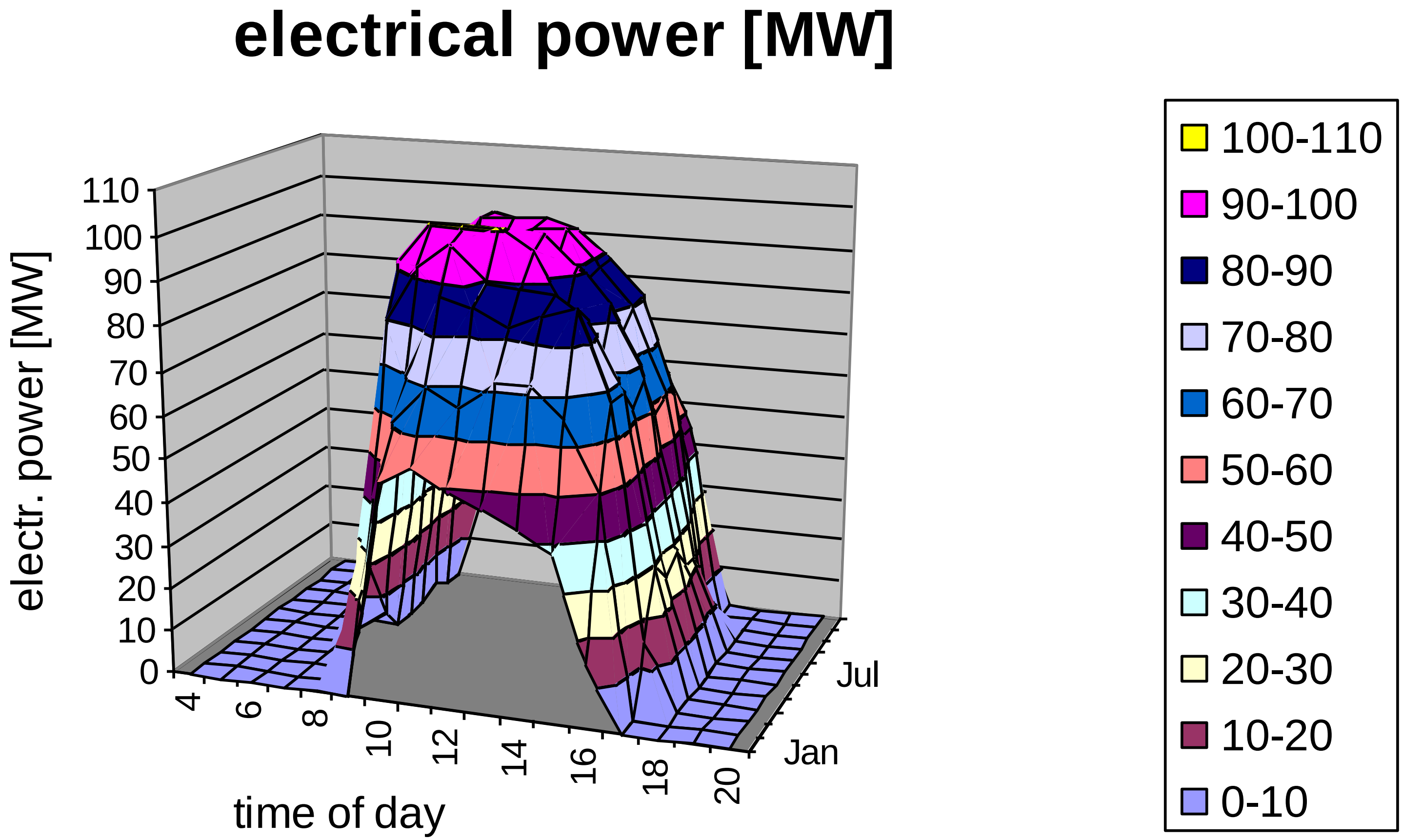

Parabolic Trough Solar Power Plant: Electric Output per Month

Site: Madinat Zayed, UAE, 23° North

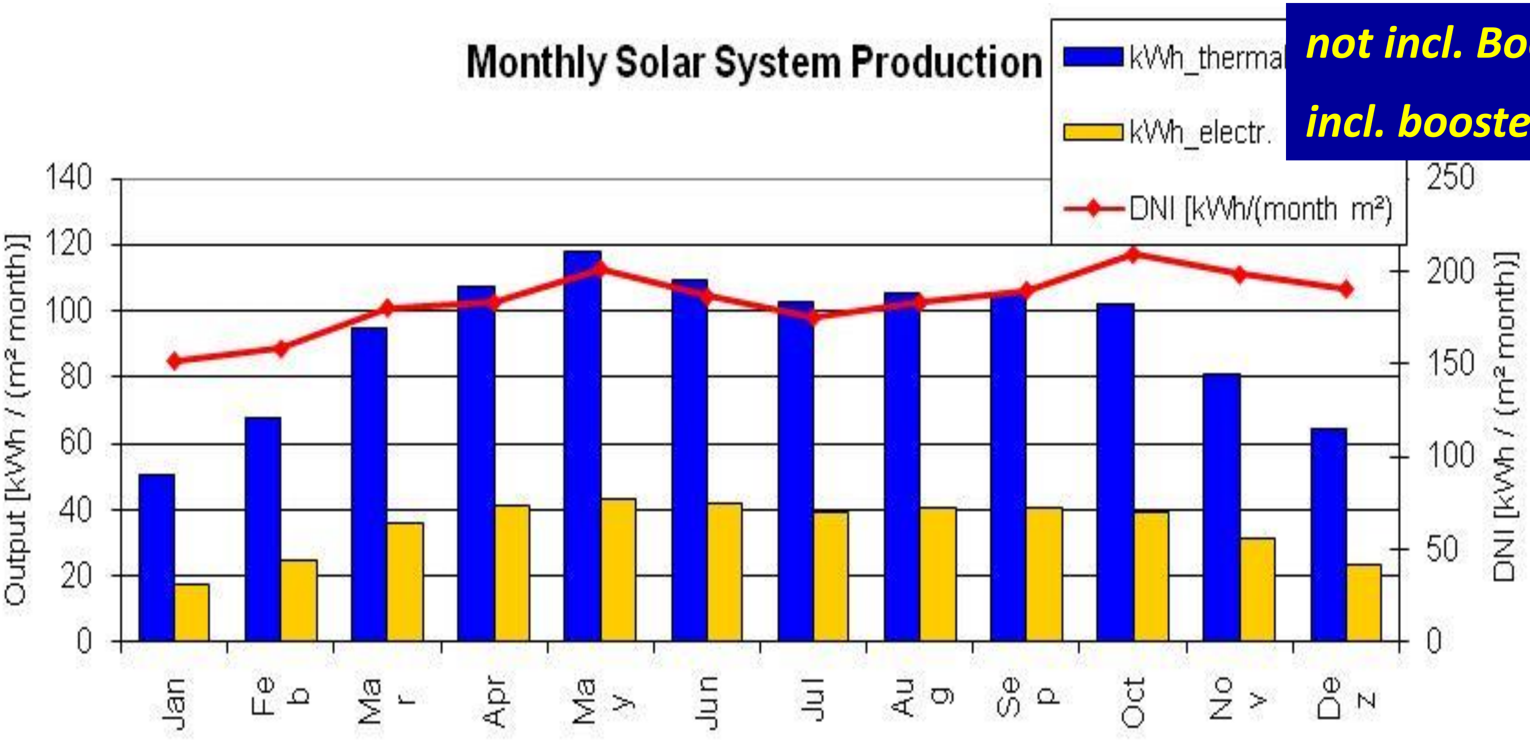

not incl. Booster

incl. booster

Power Generation Profile

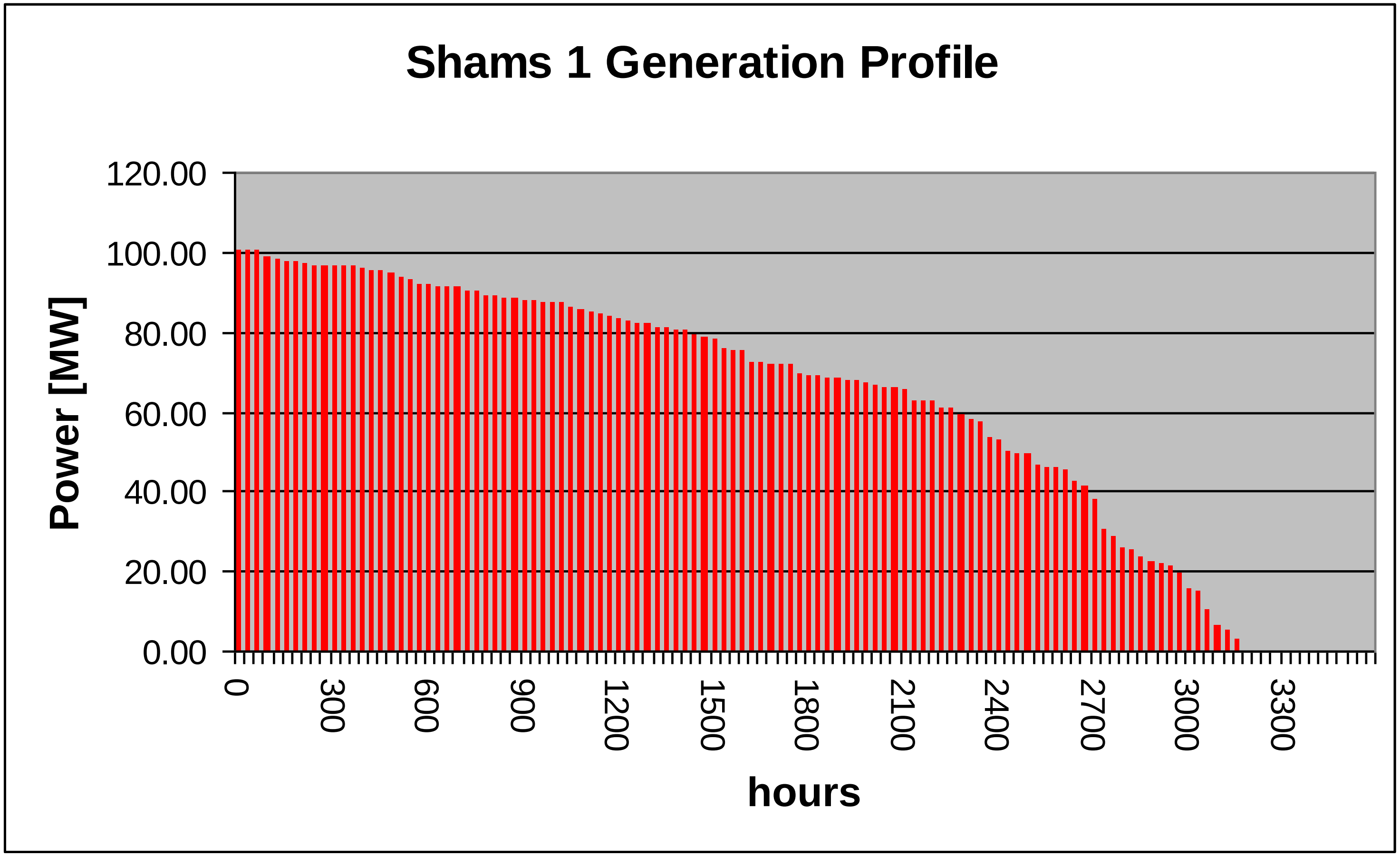

Annual Full Load Hours, FLH [kWh/kW/a] or [h/a]

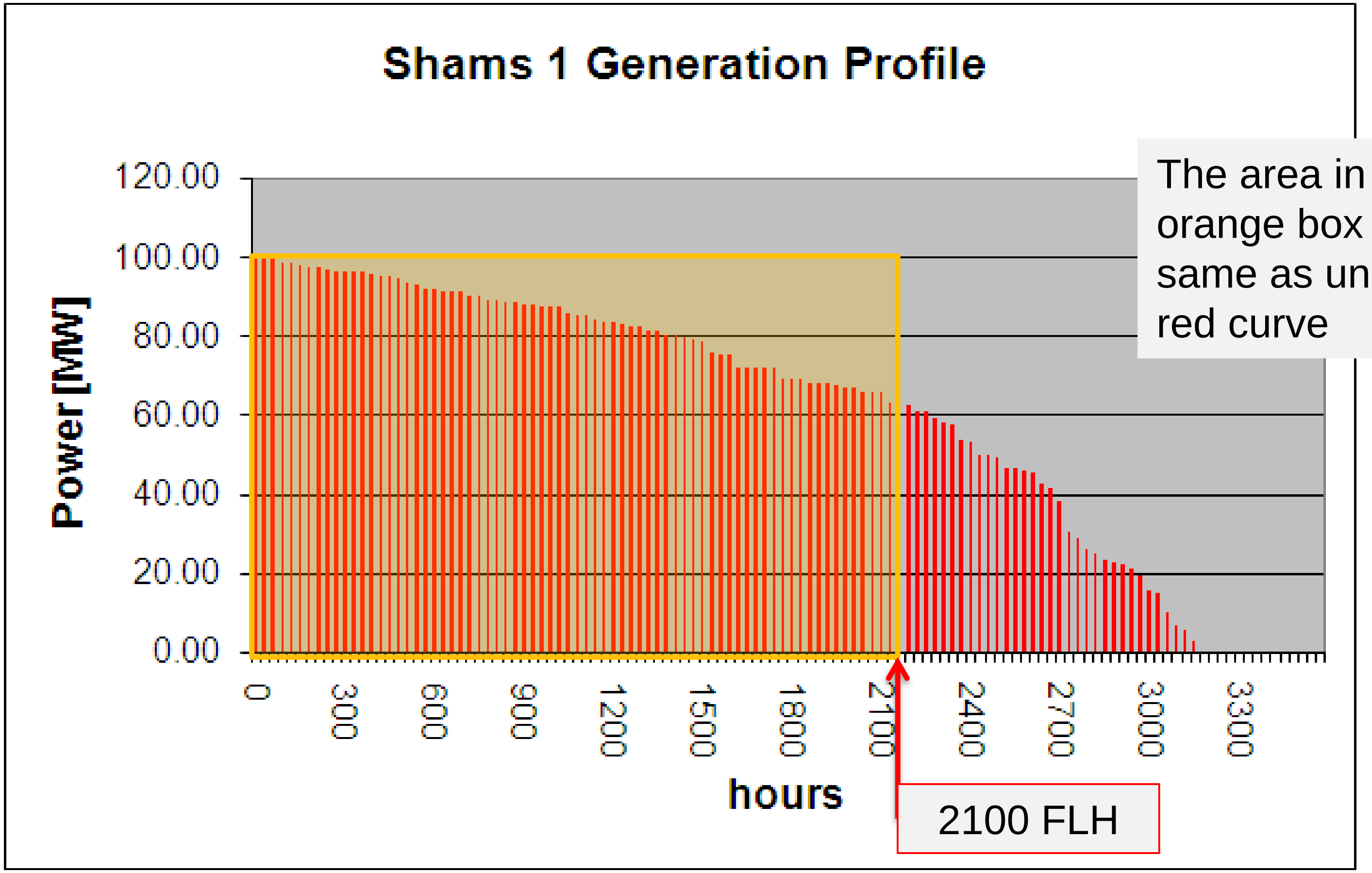

The area in the orange box is the same as under the red curve

2100 FLH

CSP Simulation Tools

There are two pretty good simulation tools available free of charge:

1) SAM, System Advisor Model of NREL (National Renewable Energy Laboratory, USA)

- Can be downloaded from NREL website

https://sam.nrel.gov/

2) Greenius of DLR (German Aerospace Agency):

- Can be downloaded from DLR website

http://freegreenius.dlr.de/

Parabolic Trough Solar Power Plants, Status of Application

Parabolic Trough Solar Power Plants in California

SEGS = Solar Electric Generating System

Technical Data:

- 354 MW_{el} installed capacity
- Commercial Operation since 1985
- More than 10,000 GWh of Electricity produced (up to year 2003)
- Guaranteed Capacity due to fossil burner back-up
- More than 2000 hours of rated capacity per year in solar mode

Economical Data:

- 2800 $ per kW installed capacity (1991 $ value)
- Electricity generation cost < 12 cents / kWh

(Valid for last 2 of the 9 plants; cost after tax-reduction)

Parabolic Trough Solar Power Plants, Status of Application

Table 1 Data of the SEGS parabolic trough solar power plants in California

Power of the block	14 MW	30 MW	80 MW
Number of blocks	1	6	2
Encoding	SEGS I	SEGS II - VII	SEGS VIII und IX
Location	Dagget	Dagget a. Kramer Jct.	Harper Lake
Start of operation	1985	1986 - 1989	1990 and 1991
Collector width	2.50 m	5.00 and 5.76 m	5.76 m
Max. fluid temperature	307°C	350°C und 390°C	390°C
Annual efficiency	9.3 %	10.7 - 12.4 %	13.8 %
Investment costs ($ value of 1991)	$4490\ \$/\mathrm{kW}_{el}$	$3200 - 3870\ \$/\mathrm{kW}_{el}$	$2890\ \$/\mathrm{kW}_{el}$

Parabolic Trough Solar Power Plants, Status of Application

- The SEGS plants in California have been the only commercially operating CSP plants between 1991 and 2007. They are the best analyzed and evaluated CSP plants of the world. They were subjects of many studies and R&D programs in the 1990ies.
- The SEGS Plants in California are IPP‘s (Independent Power Producers) who are commercially operating.
- The SEGS Plants deliver peak power at peak tariff time
- The PPA was first negotiated in the Mid Eighties, when the oil price peaked.
- The tariff was 14 US cent / kWh in the first 10 years term and 12 US cent / kWh in the second term (25% gas firing permitted)

Parabolic Trough Solar Power Plants,
Status of Application

- In 2007 the 64 MW Trough Plant „Nevada Solar One“ went on line
- Approx. 2200 MW of CSP plants have been commissioned in Spain between 2008 and 2014 (all in 50 MW units or smaller, limited by the feed in law). Mostly Parabolic Trough, only 51 MW Solar Tower and 30 MW linear Fresnel)
- 3 plants went into operation in Africa in 2011:
  - Algeria: ISCCS* with 30 MW solar share
  - Morocco: ISCCS* with 30 MW solar share
  - Egypt: ISCCS* with 20 MW solar share
- ISCCS = Integrated Solar Combined Cycle (Details: see Chapter „Developments“)
- Shams I, 100 MW Trough Plant went on line in UAE in 2013
- In USA approx. 900 MW of CSP Trough Plants have been commissioned from 2012 to 2014.

Parabolic Trough Solar Power Plants, Plants in Operation

MW	Name	Country	Location	Coordinates	Technology type	Notes and references
392	Ivanpah Solar Power Facility	USA	San Bernardino County, California	35°34′N 115°28′W	solar power tower	Completed in February 13, 2014[1][2][3]
354	Solar Energy Generating Systems (SEGS)	USA	Mojave Desert, California	35°01′54″N 117°20′53″W	parabolic trough	Collection of 9 units[4][5][6][7][8][9][10][11][12]
280	Mojave Solar Project	USA	Barstow, California	35°00′40″N 117°19′30″W	parabolic trough	Completed December 2014. Gross capacity of 280 MW corresponds to net capacity of 250 MW[13][14][15]
280	Solana Generating Station	USA	Gila Bend, Arizona	32°55′N 112°58′W	parabolic trough	Completed in October 2013, with 6h thermal energy storage[16][17]
250	Genesis Solar Energy Project	USA	Blythe, California	33°38′37.68″N 114°59′16.8″W	parabolic trough	Online April 24, 2014[18][19]
200	Solaben Solar Power Station [20]	Spain	Logrosán	39°13′29″N 5°23′26″W	parabolic trough	Solaben 3 completed June 2012[21] Solaben 2 completed October 2012[21] Solaben 1 and 6 completed September 2013[22]
150	Solnova Solar Power Station	Spain	Sanlúcar la Mayor	37°25′00″N 06°17′20″W	parabolic trough	Solnova 1 completed May 2010 Solnova 3 completed May 2010 Solnova 4 completed August 2010[23][24][25][26][27]
150	Andasol solar power station	Spain	Guadix	37°13′42.70″N 3°4′6.73″W	parabolic trough	Completed: Andasol 1 (2008), Andasol 2 (2009), Andasol 3 (2011). Each equipped with a 7.5-hour thermal energy storage.[28][29]
150	Extresol Solar Power Station	Spain	Torre de Miguel Sesmero	38°39′N 6°44′W	parabolic trough	Completed: Extresol 1 and 2 (2010), Extresol 3 (2012). Each equipped with a 7.5-hour thermal energy storage.[21][30][31]
100	Palma del Rio Solar Power Station	Spain	Palma del Río	37°38′N 5°15′W	parabolic trough	Palma del Rio 2 completed December 2010[21] Palma del Rio 1 completed July 2011[21]
100	Manchasol Power Station	Spain	Alcázar de San Juan	39°11′N 3°18′W	parabolic trough	Manchasol 1 and 2 completed in 2011, each with 7.5h heat storage[21]
100	Valle Solar Power Station	Spain	San José del Valle	36°39′N 5°50′W	parabolic trough	Completed December 2011, with 7.5h heat storage[21][32]
3650.8	**Overall operational capacity**					

Parabolic Trough Solar Power Plants, Plants in Operation

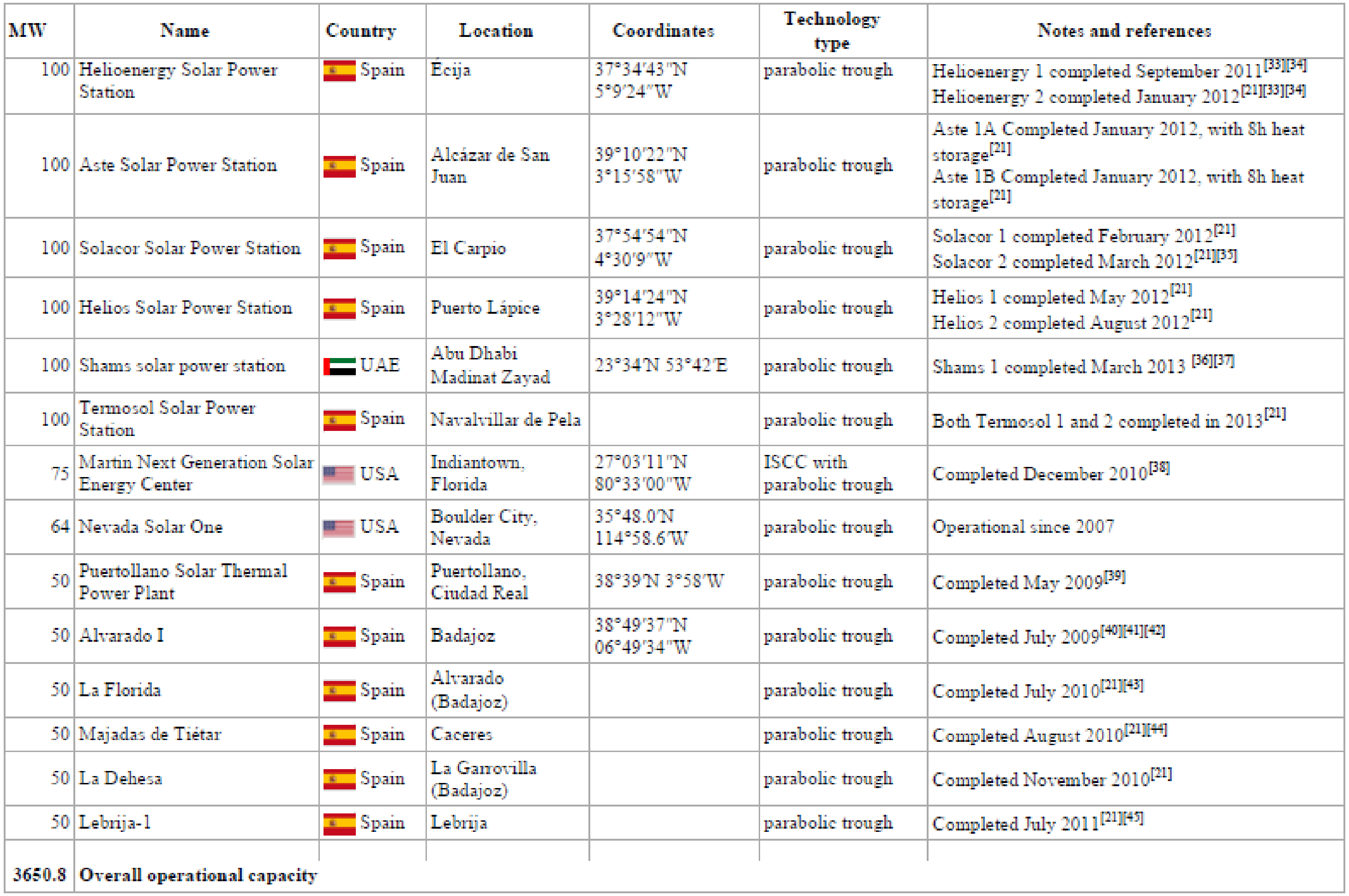

MW	Name	Country	Location	Coordinates	Technology type	Notes and references
100	Helioenergy Solar Power Station	Spain	Écija	37°34′43″N 5°9′24″W	parabolic trough	Helioenergy 1 completed September 2011[33][34] Helioenergy 2 completed January 2012[21][33][34]
100	Aste Solar Power Station	Spain	Alcázar de San Juan	39°10′22″N 3°15′58″W	parabolic trough	Aste 1A Completed January 2012, with 8h heat storage[21] Aste 1B Completed January 2012, with 8h heat storage[21]
100	Solacor Solar Power Station	Spain	El Carpio	37°54′54″N 4°30′9″W	parabolic trough	Solacor 1 completed February 2012[21] Solacor 2 completed March 2012[21][35]
100	Helios Solar Power Station	Spain	Puerto Lápice	39°14′24″N 3°28′12″W	parabolic trough	Helios 1 completed May 2012[21] Helios 2 completed August 2012[21]
100	Shams solar power station	UAE	Abu Dhabi Madinat Zayad	23°34′N 53°42′E	parabolic trough	Shams 1 completed March 2013 [36][37]
100	Termosol Solar Power Station	Spain	Navalvillar de Pela		parabolic trough	Both Termosol 1 and 2 completed in 2013[21]
75	Martin Next Generation Solar Energy Center	USA	Indiantown, Florida	27°03′11″N 80°33′00″W	ISCC with parabolic trough	Completed December 2010[38]
64	Nevada Solar One	USA	Boulder City, Nevada	35°48.0′N 114°58.6′W	parabolic trough	Operational since 2007
50	Puertollano Solar Thermal Power Plant	Spain	Puertollano, Ciudad Real	38°39′N 3°58′W	parabolic trough	Completed May 2009[39]
50	Alvarado I	Spain	Badajoz	38°49′37″N 06°49′34″W	parabolic trough	Completed July 2009[40][41][42]
50	La Florida	Spain	Alvarado (Badajoz)		parabolic trough	Completed July 2010[21][43]
50	Majadas de Tiétar	Spain	Caceres		parabolic trough	Completed August 2010[21][44]
50	La Dehesa	Spain	La Garrovilla (Badajoz)		parabolic trough	Completed November 2010[21]
50	Lebrija-1	Spain	Lebrija		parabolic trough	Completed July 2011[21][45]
3650.8	**Overall operational capacity**					

Parabolic Trough Solar Power Plants, Plants in Operation

MW	Name	Country	Location	Coordinates	Technology type	Notes and references
50	Astexol 2	Spain	Badajoz		parabolic trough	Completed November 2011, with 7.5h thermal energy storage[21][46]
50	Morón	Spain	Morón de la Frontera		parabolic trough	Completed May 2012[21]
50	La Africana	Spain	Posada		parabolic trough	Completed July 2012, with 7.5h thermal energy storag[21]
50	Guzman	Spain	Palma del Río		parabolic trough	Completed July 2012[21]
50	Olivenza 1	Spain	Olivenza		parabolic trough	Completed July 2012[21]
50	Orellana	Spain	Orellana la Vieja		parabolic trough	Completed August 2012[21]
50	Godawari Green Energy Limited	India	Nokh	27°36′01″N 72°13′25″E	parabolic trough	2013[47][48][49]
50	Enerstar Villena Power Plant	Spain	Villena		parabolic trough	Completed 2013[21][50]
31.4	Puerto Errado	Spain	Murcia	38°16′42″N 01°36′01″W	fresnel reflector	Puerto Errado 1 completed April 2009[21][51] Puerto Errado 2 completed February 2012[21][52]
25	Hassi R'Mel integrated solar combined cycle power station	Algeria	Hassi R'mel	33°07′29″N 03°21′07″E	ISCC with parabolic trough	Completed June 2011[53][54]
22.5	Termosolar Borges	Spain	Borges Blanques		parabolic trough biomass hybrid	Completed December 2012[21]
20	PS20 solar power tower	Spain	Seville	37°26′38″N 06°15′34″W	solar power tower	Completed April 2009
20	Kuraymat Plant	Egypt	Kuraymat		ISCC with parabolic trough	Completed December 2010[54][55][56]
20	Ain Beni Mathar Integrated Thermo Solar Combined Cycle Power Plant	Morocco	Ain Bni Mathar		ISCC with parabolic trough	Completed 2011 [57][58][59]
19.9	Gemasolar	Spain	Fuentes de Andalucia (Seville)	37°33′38.17″N 05°19′53.61″W	solar power tower	Completed May 2011[60] With 15h heat storage[21]
17		Iran	Yazd			Dedicated May 2011[61]
3650.8	**Overall operational capacity**					

Parabolic Trough Solar Power Plants, Plants in Operation

MW	Name	Country	Location	Coordinates	Technology type	Notes and references
	Yazd integrated solar combined cycle power station			31°57′5″N 54°5′30″E	ISCC with parabolic trough	
11	PS10 solar power tower	Spain	Seville	37°26′36.42″N 06°15′14.28″W	solar power tower	World's first commercial solar tower in 2007
10	Delingha Solar Power Plant	China	Delingha		solar power tower	Phase 1 of project completed in July 2013,[62] total 50 MW planned[63][64]
5	Greenway CSP Mersin Solar Tower Plant	Turkey	Mersin		solar power tower	Turkey's first CSP solar tower plant[65]
5	Kimberlina Solar Thermal Energy Plant	USA	Bakersfield, California	35°34′06″N 119°12′06″W	fresnel reflector	AREVA Solar, formerly Ausra demonstration plant [66]
5	Sierra SunTower	USA	Lancaster, California	34°46′0.0″N 118°8′0.0″W	solar power tower	Completed August 2009[67][68][69]
5	Archimede solar power plant	Italy	Syracuse, Sicily	37°8′0″N 15°12′58″E	ISCC with parabolic trough	Completed July 2010. Equipped with heat storage. [70][71]
5	Thai Solar Energy (TSE) 1	Thailand	Huaykrachao		parabolic trough	Completed November 2011[72]
9	Liddell Power Station Solar Steam Generator	Australia	New South Wales	32°22′26″S 150°58′40″E	ISCC with fresnel reflector	Electrical equivalent steam boost for coal station[73] [74]
2.5	Acme Solar Thermal Tower	India			solar power tower	Completed 2012[75]
2	Keahole Solar Power	USA	Hawaii	19°42′54″N 156°2′7″W	parabolic trough	[76][77]
1.5	Jülich Solar Tower	Germany	Jülich	50°54′54″N 06°23′16″E	solar power tower	Completed December 2008[78]
1.5	Beijing Badaling Solar Tower	China	Beijing	40°22′55″N 115°56′15″E	solar power tower	Completed August 2012[79][80]
1	Feranova CSP Plant	Turkey	Aydin, Turkey		fresnel reflector	Completed December 2012
1	Saguaro Solar Power Station	USA	Red Rock, Arizona		parabolic trough	[81]
1	Yanqing Solar Power Station	China	Yanqing County		solar power tower	Completed August 2010[82]
3650.8	**Overall operational capacity**					

Parabolic Trough Solar Power Plants, Plants under Construction (in 2015)

MW	Name	Country	Location	Co-ordinates	Expected completion	Technology	Notes
160	Ouarzazate solar power station	Morocco	Ouarzazate		2015	parabolic trough	with 3h heat storage[84]
121	Ashalim power station 1	Israel	Negev desert	30°58′N 34°42′E	2017	solar power tower	[85][86][87]
110	Crescent Dunes Solar Energy Project	USA	Nye County, Nevada	38°14′N 117°22′W	2013/14	solar power tower	with 10h heat storage[88]
100	KaXu Solar One	South Africa	Pofadder, Northern Cape		2014	parabolic trough	with 2.5h heat storage[89][90]
100	El Reboso 2+3	Spain	El Puebla del Rio (Seville)		2015	parabolic trough	[91][92]
100	Dhursar	India			2014	fresnel reflector	[93][94]
100	Diwakar	India	Askandra		2014	parabolic trough	with 3h heat storage[95]
100	KVK Energy Solar Project	India	Askandra		2014	parabolic trough	with 4h heat storage[96]
50	Arenales PS	Spain	Moron de la Frontera (Seville)		2013	parabolic trough	[21][46][97]
50	Casablanca	Spain	Casablanca		2013	parabolic trough	[21]
50	Erdos Solar Power Plant	China	Hanggin Banner		2013	parabolic trough	[98]
50	Khi Solar One	South Africa	Upington		2014	power tower	with 2h heat storage[89][90]
50	Megha Solar Plant	India	Anantapur		2013	parabolic trough	[99]
50	Bokpoort	South Africa	Groblershoop		2015	parabolic trough	with 9h heat storage[100][101]
44	Kogan Creek Solar Boost	Australia	Chinchilla		2015	fresnel reflector	[102]
27.5	Jinshawan	China	China			solar updraft tower	Operations underway at 200 kW.[103]
25	Gujarat Solar One	India	Kutch		2013	parabolic trough	with 9h heat storage[104]

Parabolic Trough Solar Power Plants, Plants under Construction (in 2015)

MW	Name	Country	Location	Co-ordinates	Expected completion	Technology	Notes
				23°22.233′N 70°41.988′E			
17	Stillwater	USA	Nevada		2014	parabolic trough	[105]
12	Alba Nova 1	France	Corsica		July, 2015	fresnel reflector	First utility-scale solar thermal plant in France[106][107]
5	Sundt Power Plant	USA	Arizona		2014	fresnel reflector	[108]
3	Airlight Energy Ait Baha Plant	Morocco	Ait Baha		2013	parabolic trough	with 12h heat storage[109]
1.5	Tooele Army Depot	USA	Tooele		2013	dish	[110]
1.4	THEMIS Solar Power Tower	France	Pyrénées-Orientales	42°30′5″N 1°58′27″E		solar power tower	Hybrid solar/gas power plant[111]
1	e-Cube 1	China	Hainan		2013	Modular Heliostat	First Modular Heliostat solar thermal plant in the world[112]
1	Renovalia	Spain	Albacete			dish	[21]

Parabolic Trough Solar Power Plants, Picture Gallery

Kramer Junction,
California,
5 x 30 MW Plants

Parabolic Trough Solar Power Plants, Picture Gallery

Harper Lake,
California,
2 x 80 MW Plants

Parabolic Trough Solar Power Plants, Picture Gallery

Kramer Junction, California, 5 x 30 MW Plants

Parabolic Trough Solar Power Plants, Picture Gallery

Kramer Junction, California, 5 x 30 MW Plants

Parabolic Trough Solar Power Plants, Picture Gallery

Kramer Junction, California,

5 x 30 MW Plants

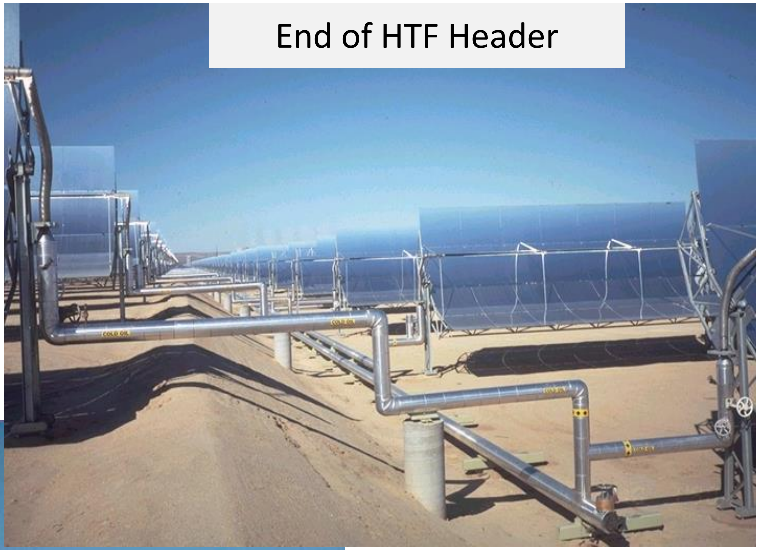

End of HTF Header

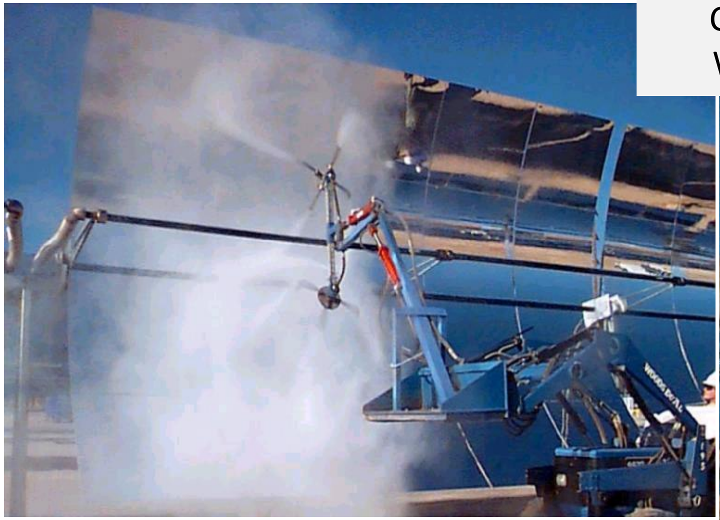

Collector Washing

Parabolic Trough Solar Power Plants, Picture Gallery

Collector Washing Truck of company “Laitu” in Spain.

source: laitusolar.com

Parabolic Trough Solar Power Plants, Picture Gallery

Andasol 1 near Guadix, Andalusia (Construction July 2008)

Excellent soil conditions for foundation placement at the site of the "Andasol" plants in Guadix, Spain.

Scheme of Shams 1 Plant

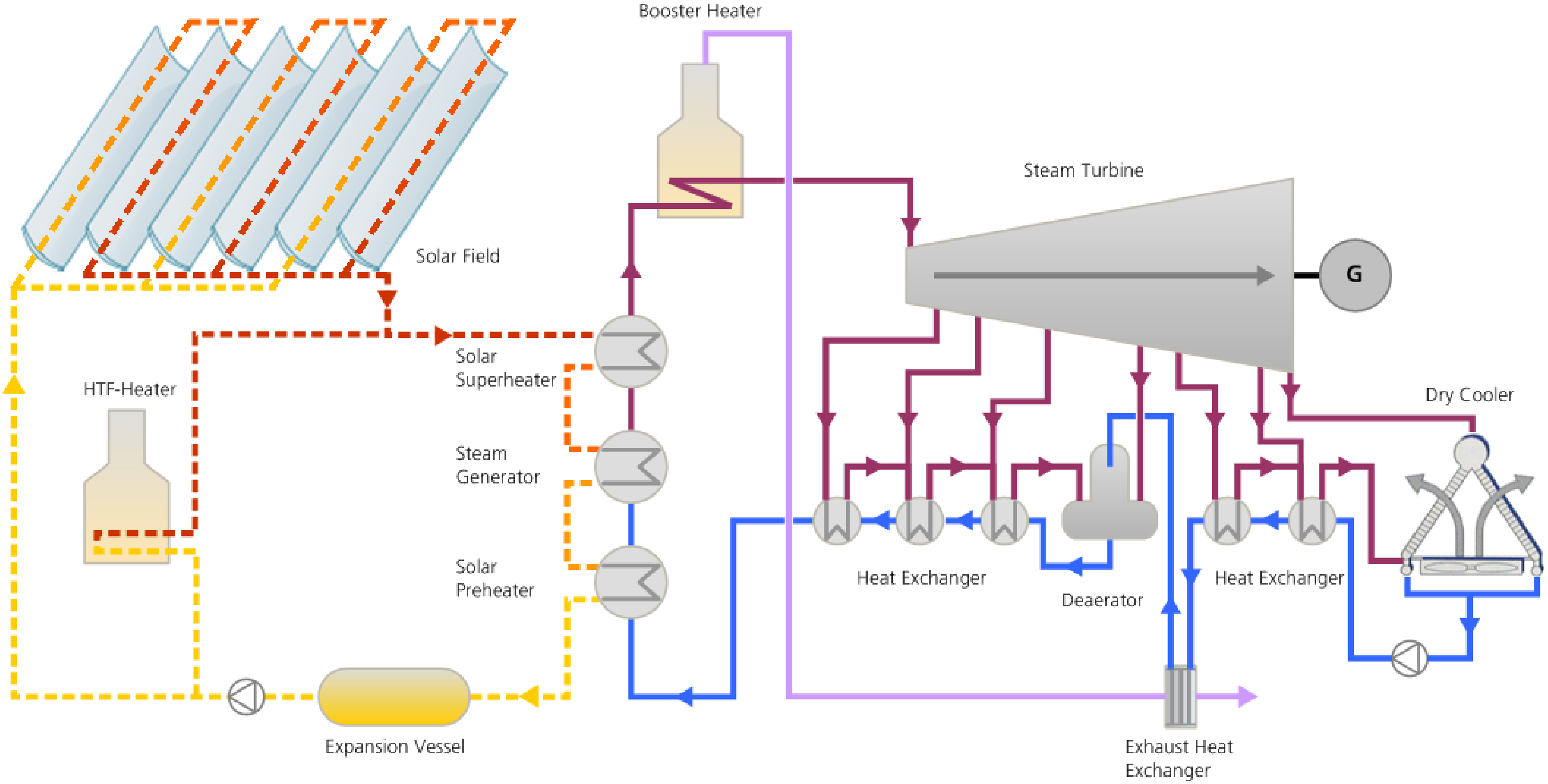

Shams 1 Location, UAE: 53.7o E, 23.57o N

Shams One
Plant Location

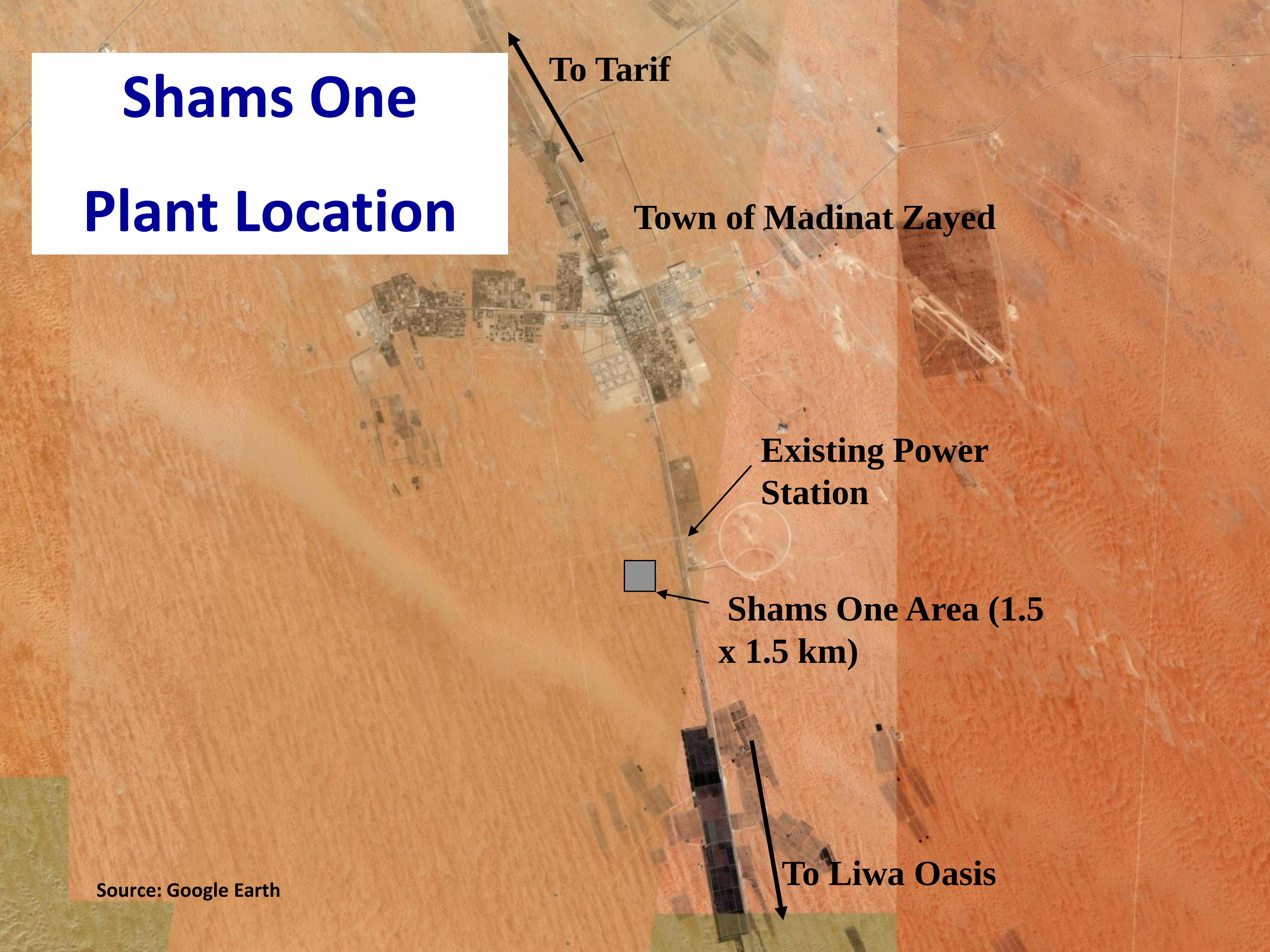

Source: Google Earth

Shams 1 Plant Layout

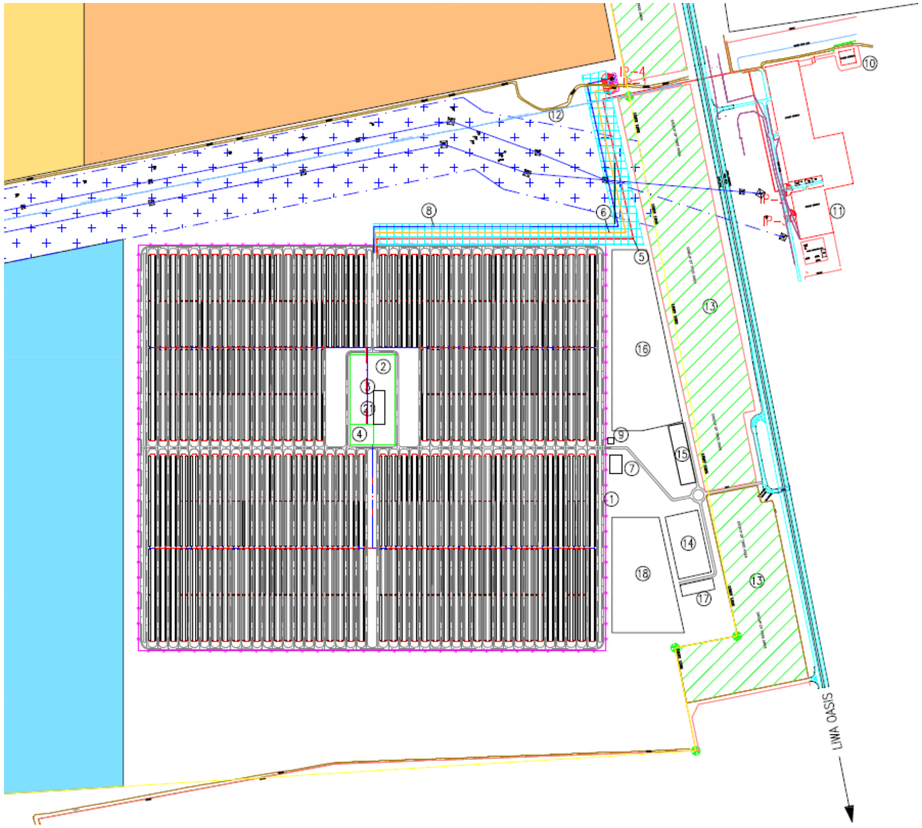

Legend:

🟧 Shams 2 site

🟧 Shams 3 site

🟦 Research & Demonstration areas

▨ OHL Corridor

- 192 loops
- 4 collectors per loop
- 817.5 m^2 aperture per collector
- 627 840 m^2 total aperture area

The first Bulldozers start working

Small Beginnings

Good Old Work Horses

Making Temporary Roads

Bite into the Dunes

Clearing 250 Hectares

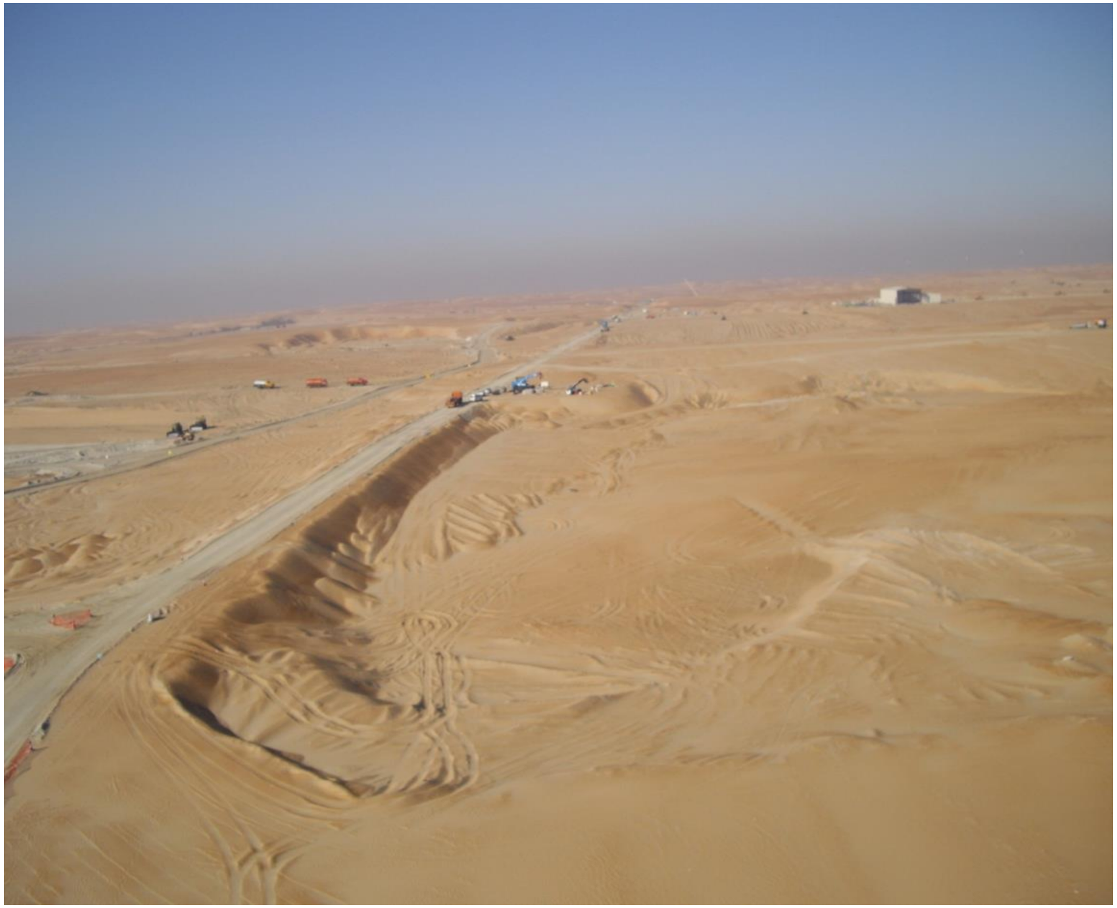

Building the Wind Breaker Wall

The First Collector in Place

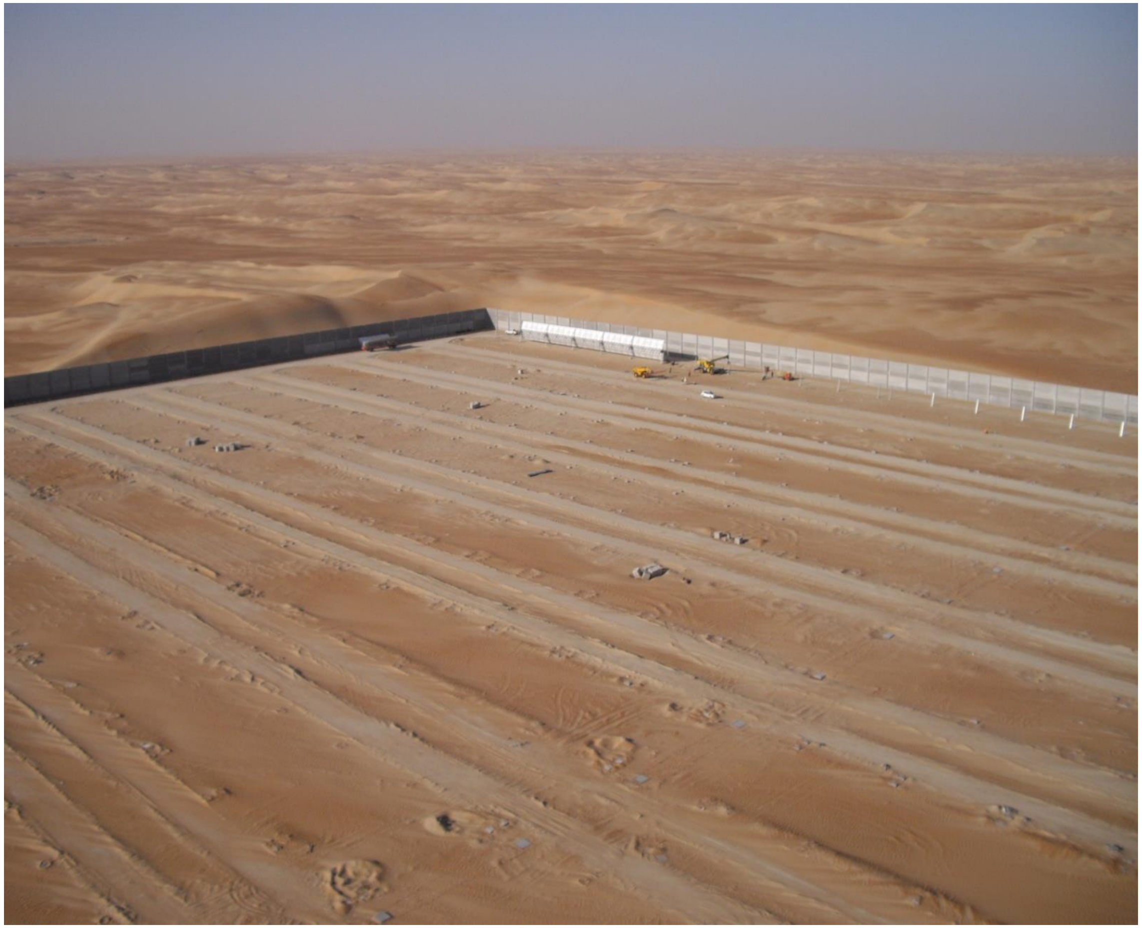

Solar Field in April 2011

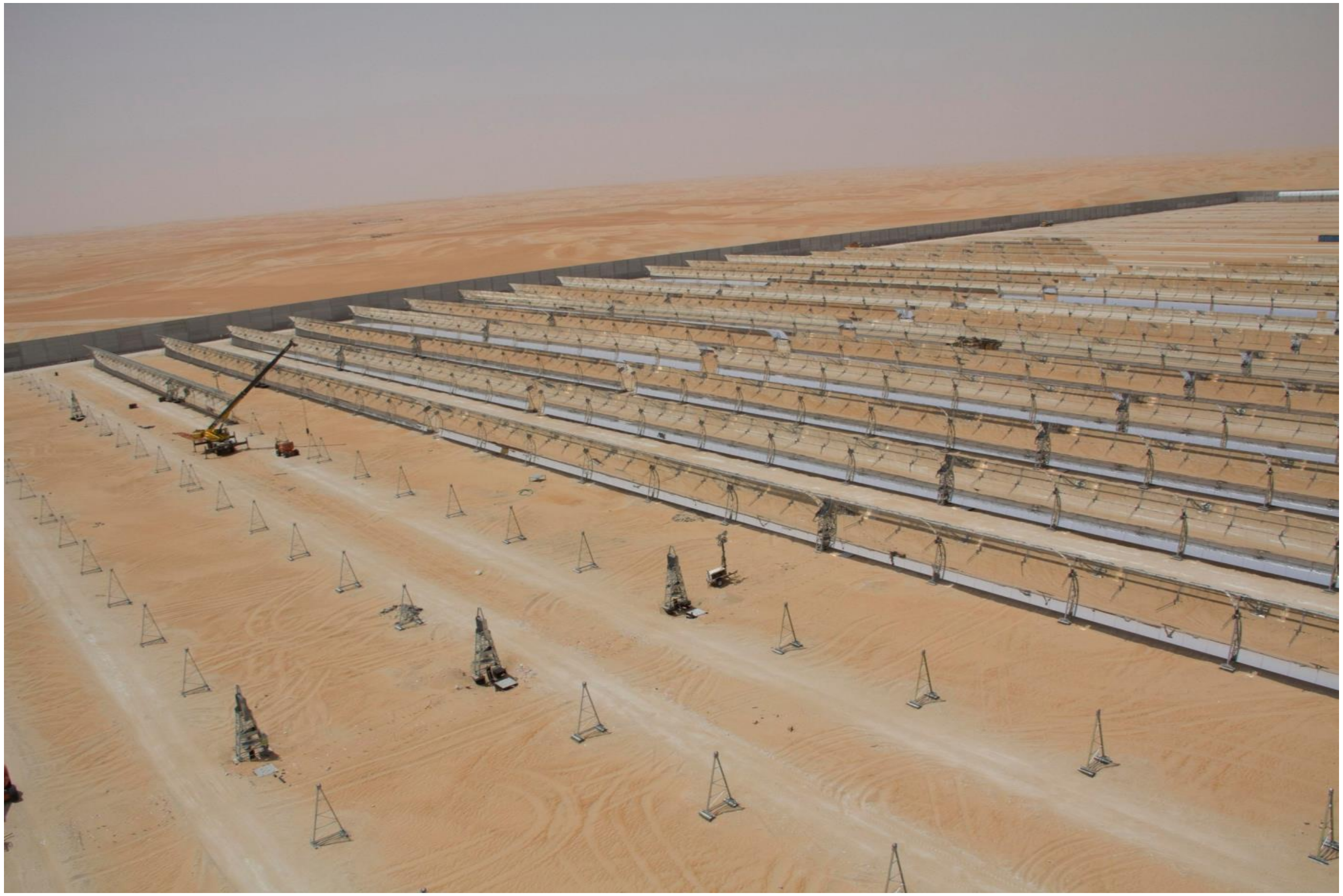

The End of a Long Journey: Mirror Panels from Germany

Steam Turbine & Generator in Place

Steam Turbine in Place (05/2011)

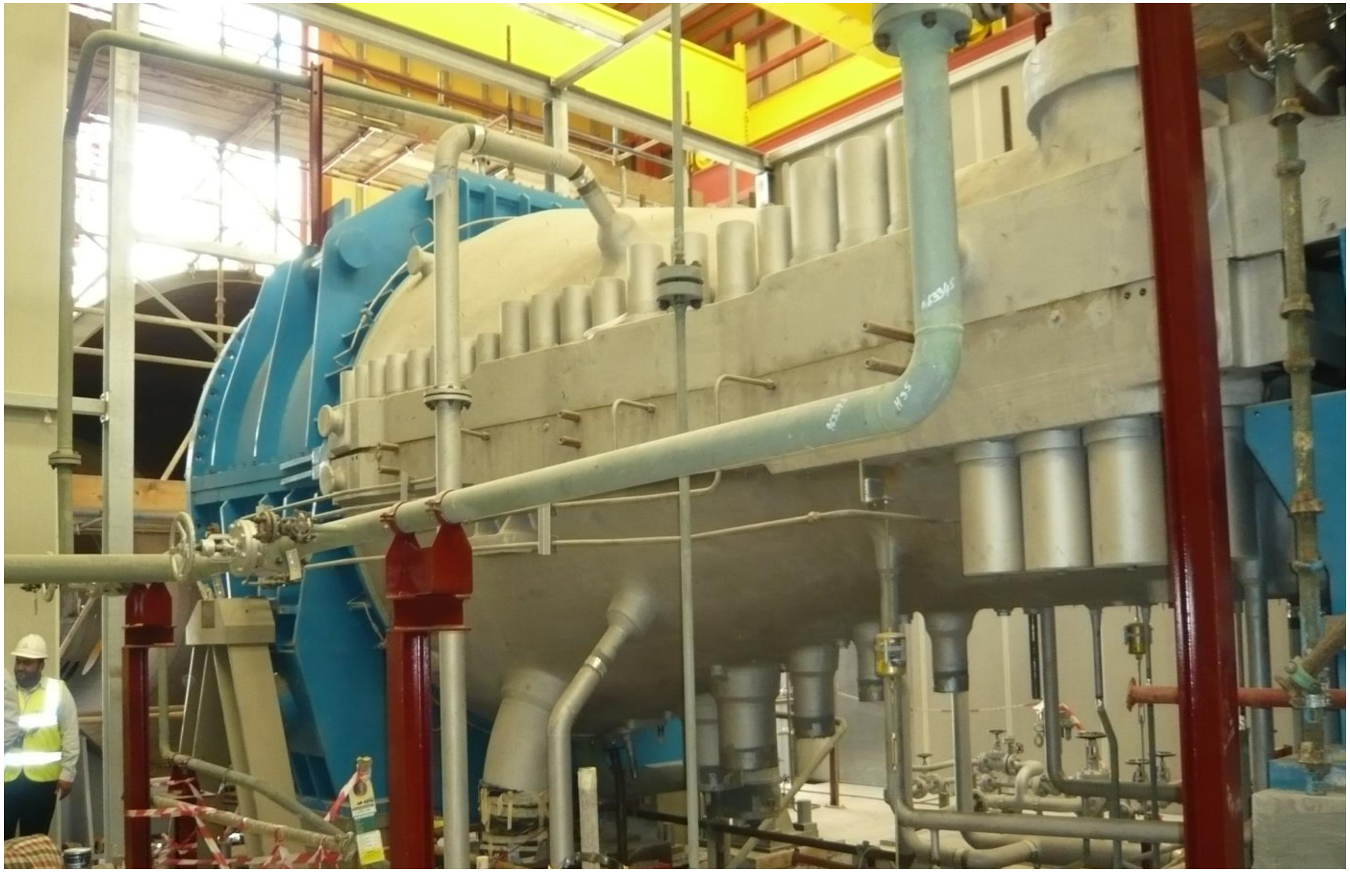

All Collectors installed (01/2012)

Parabolic Trough Solar Power Plants, Developments

1. Hybridization with Combined Cycle Concept = Integrated Solar Combined Cycle System, ISCCS

2. Direct Steam Generation in the Absorber Pipes (DSG)

3. Thermal Energy Storage, TES

Parabolic Trough Solar Power Plants:
Integrated Solar Combined Cycle System, ISCCS

The Problem of low efficiency when running a regular Parabolic Trough Plant on gas

- Due to the low efficiency of a simple Rankine Cycle (compared to a Combined Cycle) a Parabolic Trough Plant with simple hybridisation would consume more gas over the year than a CC plant if operated more than 6000 hour per year.
- Therefore with this kind of hybridisation fuels shall be used which cannot be used in CC plants (e.g. coal, heavy fuel oil or biomass).

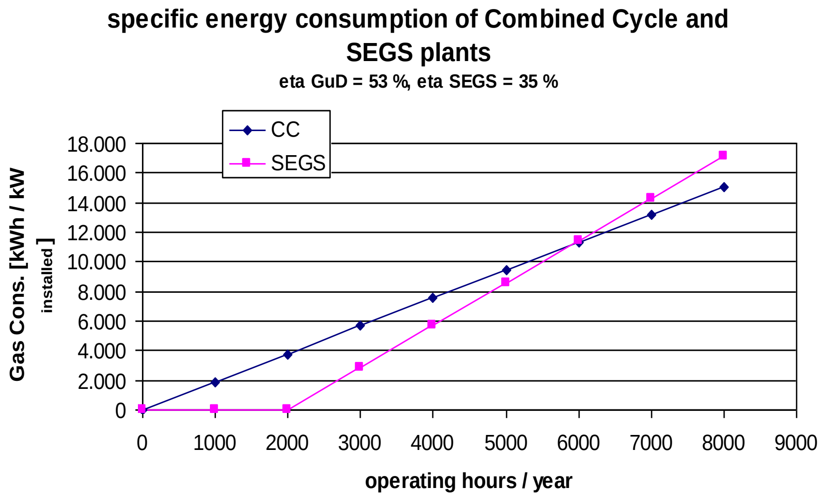

CC = Combined Cycle plant
SEGS = Parabolic Trough CSP plant

Parabolic Trough Solar Power Plants: Integrated Solar Combined Cycle System, ISCCS

- A ISCCS is a CC power plant where the Steam Turbine (ST) is fed with up to 50% of solar steam during sunshine hours. At night time it works like a regular CC plant (with ST in part load).
- Advantage: High Efficiency in fossil mode
- Power distribution in a regular CC plant: GT / ST = 2 / 1
- At ISCCS at daytime: 1 / 1 or better: 2 / (1+1)
- Solar peak share approx. 25 %
- Solar share of annual production: approx. 6-7 %
- Plants operating in: Morocco, Algeria and Egypt

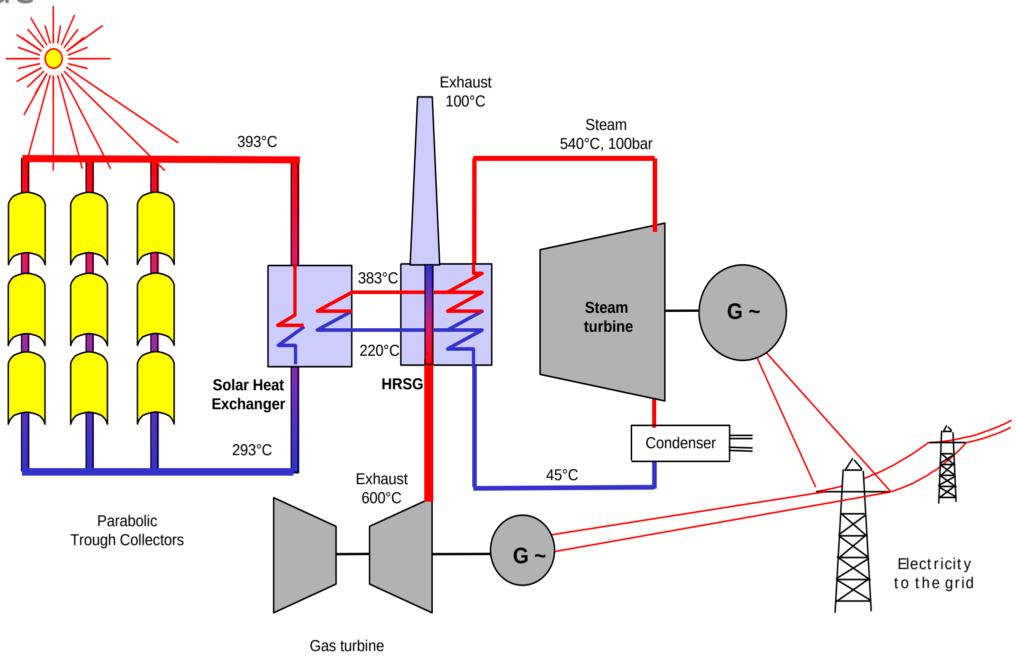

Parabolic Trough Solar Power Plants:
Integrated Solar Combined Cycle System, ISCCS

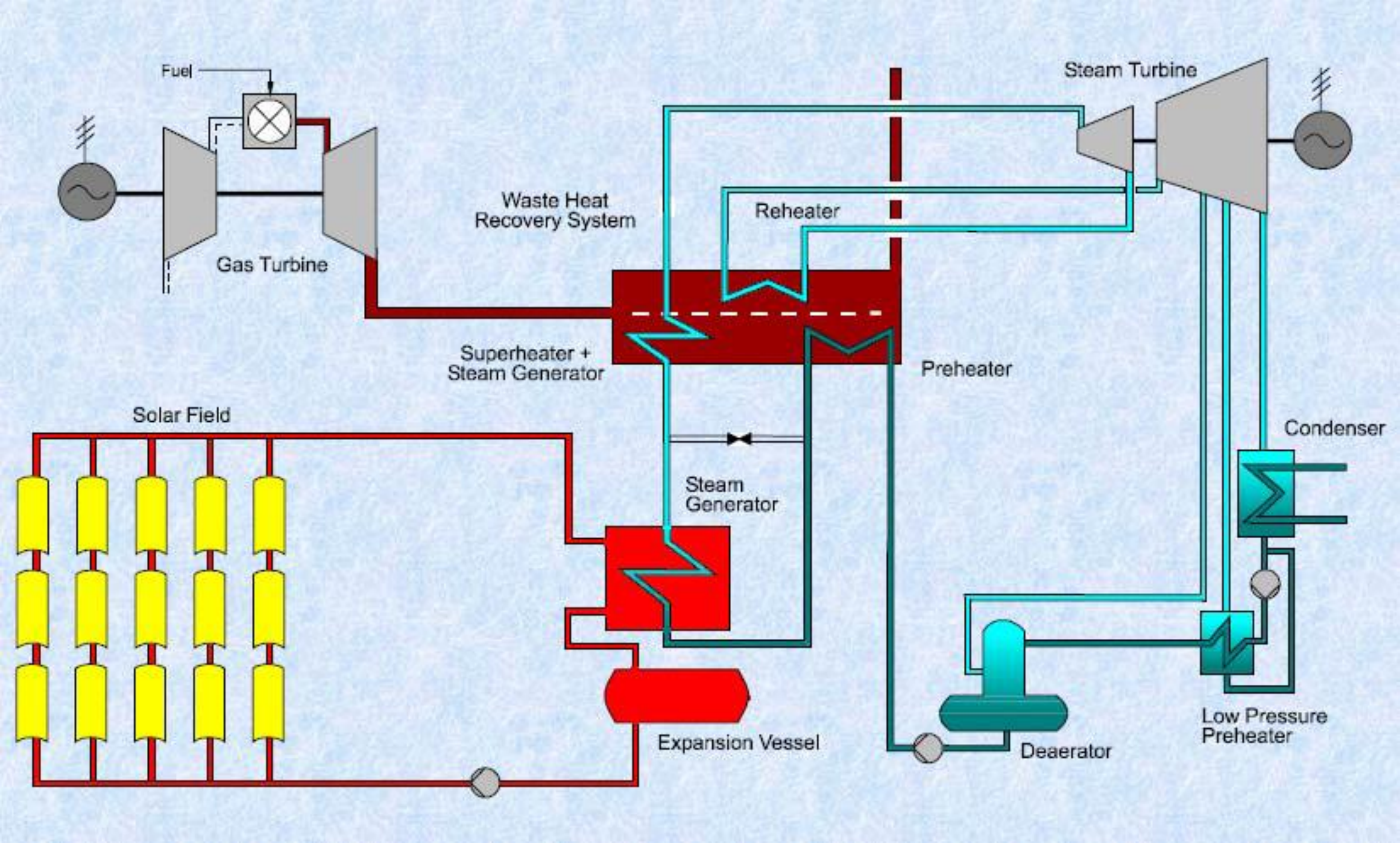

(Source: Bruce Kelly, Ulf Herrmann, Mary Jane Hale: OptimizationStudies for Integrated Solar Combined Cycle Systems; ASME Forum2001)

Parabolic Trough Solar Power Plants:
Integrated Solar Combined Cycle System, ISCCS

ISCC Location	CC (MW)	Solar (MW)
Ain Beni Mathar (Morocco)	228	20
Kurajmat (Egypt)	127	29
Hassi R'Mel (Algeria)	140	35
Martin County (USA)	3617	75
Archimede, Sicily (Italy)	760	5

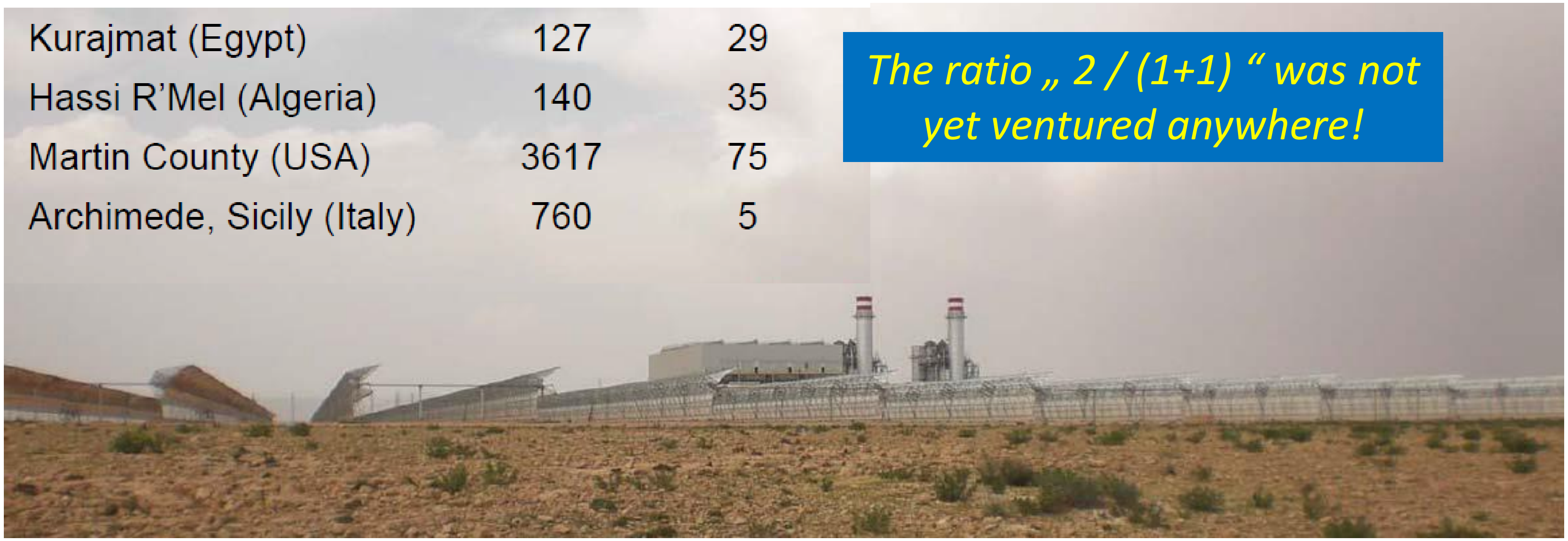

The ratio „ 2 / (1+1) " was not yet ventured anywhere!

Foto: ISCCS Ain Beni Mathar, Morocco

Parabolic Trough Solar Power Plants:
Integrated Solar Combined Cycle System, ISCCS

specific energy consumption of C C, ISCC and SEGS plant

eta C C = 53 %, eta ISCCS = 52 %, eta SEGS = 35 %

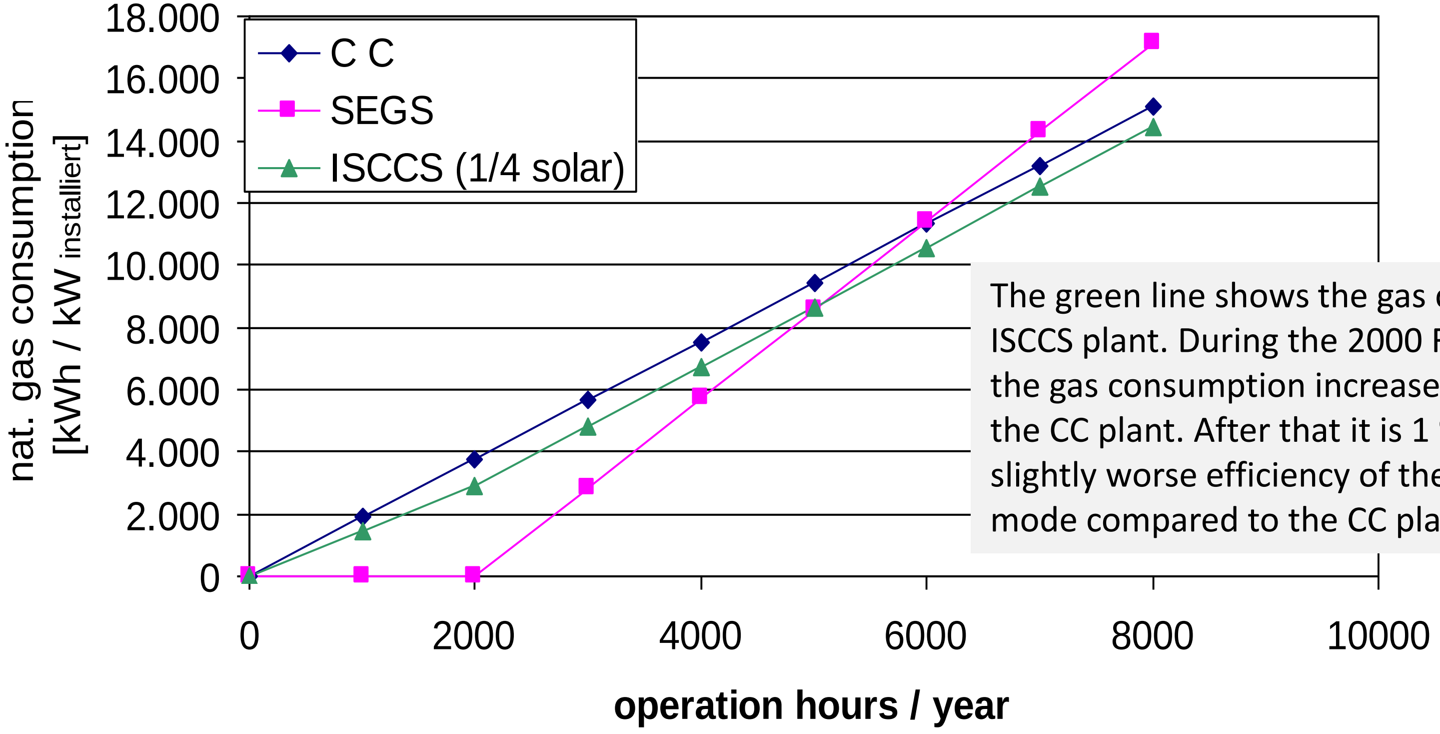

The green line shows the gas consumption of an ISCCS plant. During the 2000 FLH of the solar field the gas consumption increases ¼ slower than for the CC plant. After that it is 1 % steeper due to the slightly worse efficiency of the ISCCS in gas only mode compared to the CC plant.

Parabolic Trough Solar Power Plants, Direct Steam Generation, DSG

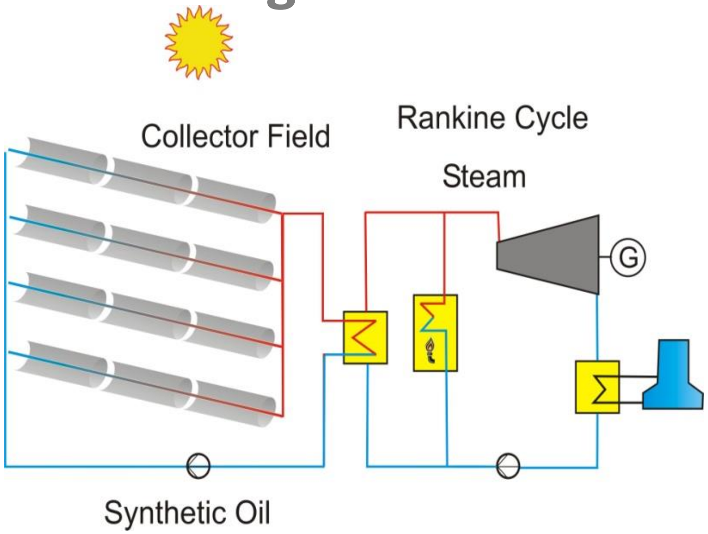

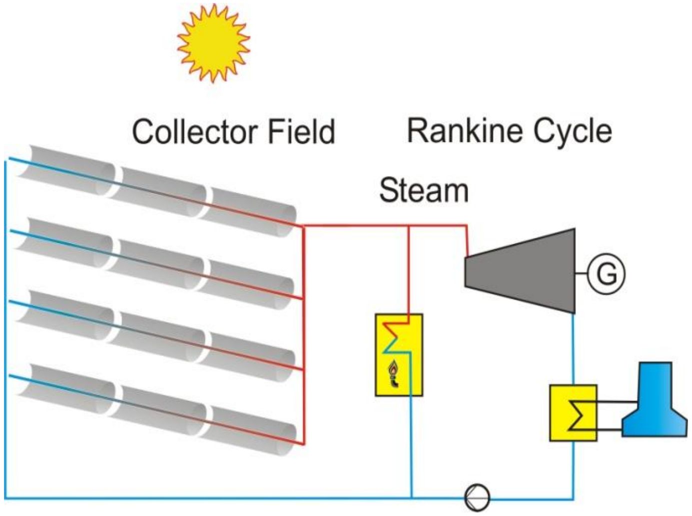

Direct Solar Steam (DSG) will lead to:

- No more HFT needed
- No more HTF / Water Heat exchanger
- No more temperature limit of HTF (400°C) => higher efficiency
- Less parasitic power consumption
- Expected overall reduction in LEC: approx. 18 %

Parabolic Trough Solar Power Plants, Direct Steam Generation, DSG

- The 2 circuit system with a thermal oil in the primary circuit has been chosen in order to avoid 2-phase flow in the horizontal absorber tubes.
- With evaporation on horizontal tubes of large diameters (70 mm (outer)) a stratified flow was anticipated (water at the bottom, steam at the top).
- This would lead to azimuthally uneven temperature distribution.
- Comparison: The evaporator tubes in conventional steam generators are smaller (approx. 25 mm) and are vertical or inclined.

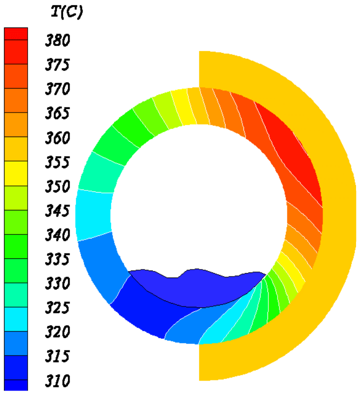

Parabolic Trough Solar Power Plants, Direct Steam Generation, DSG

R&D projects regarding DSG and key results

- **1993 - 1995: “GUDE” Real scale tests at electrically heated absorber tubes at the SIEMENS boiler test rig, results:**
  - Stratified flow can be avoided by proper selection of flow parameters (pressure and mass flow)
- **1996 - 2001: “DISS” Experiments in a real collector loop of 500 m length at the Plataforma Solar de Almeria (PSA), Spain, results:**
  - DSG works, the best concept is the Recirculation Concept.
  - Further experiments for investigating control algorithms and start up and shut down procedures have been completed successfully
  - However, before financing a project with new technology, banks want to see operating reference plants.
- **DSG Pilot project of 3 MW is in planning in Spain**

Parabolic Trough Solar Power Plants, Direct Steam Generation, DSG

The three DSG concepts:

1. The "Once Through Concept", steam quality from 0 to 100%

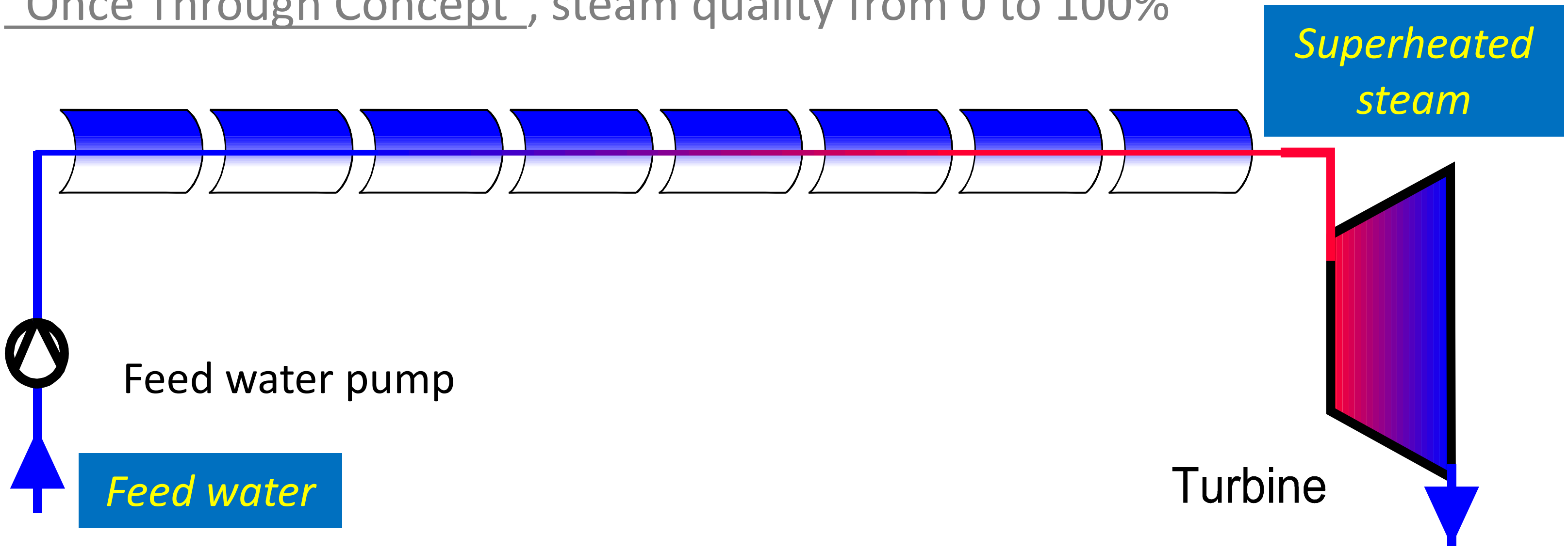

Superheated steam

Feed water pump

Feed water

Turbine

Parabolic Trough Solar Power Plants, Direct Steam Generation, DSG

The three DSG concepts:

2. The “Injection Concept”, only high steam qualities

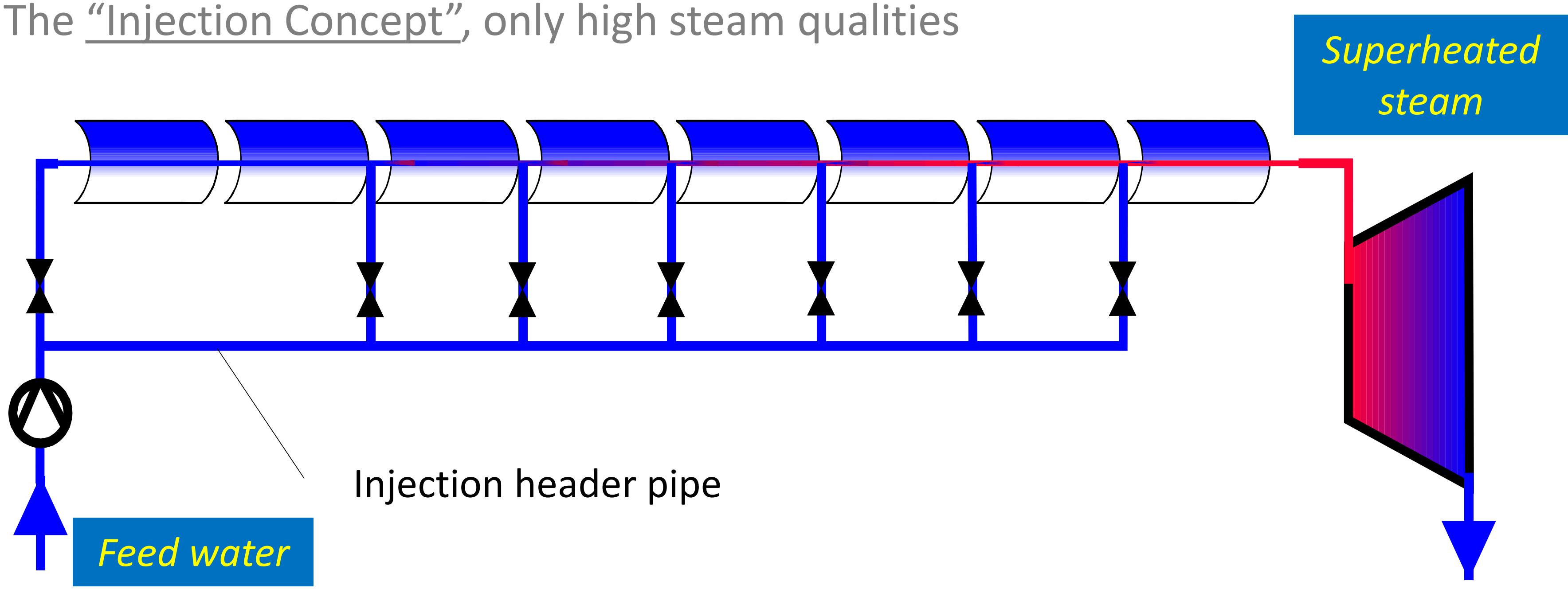

Parabolic Trough Solar Power Plants, Direct Steam Generation, DSG

The three DSG concepts:

3. The "Recirculation Concept", only low steam qualities (<70%) before separator

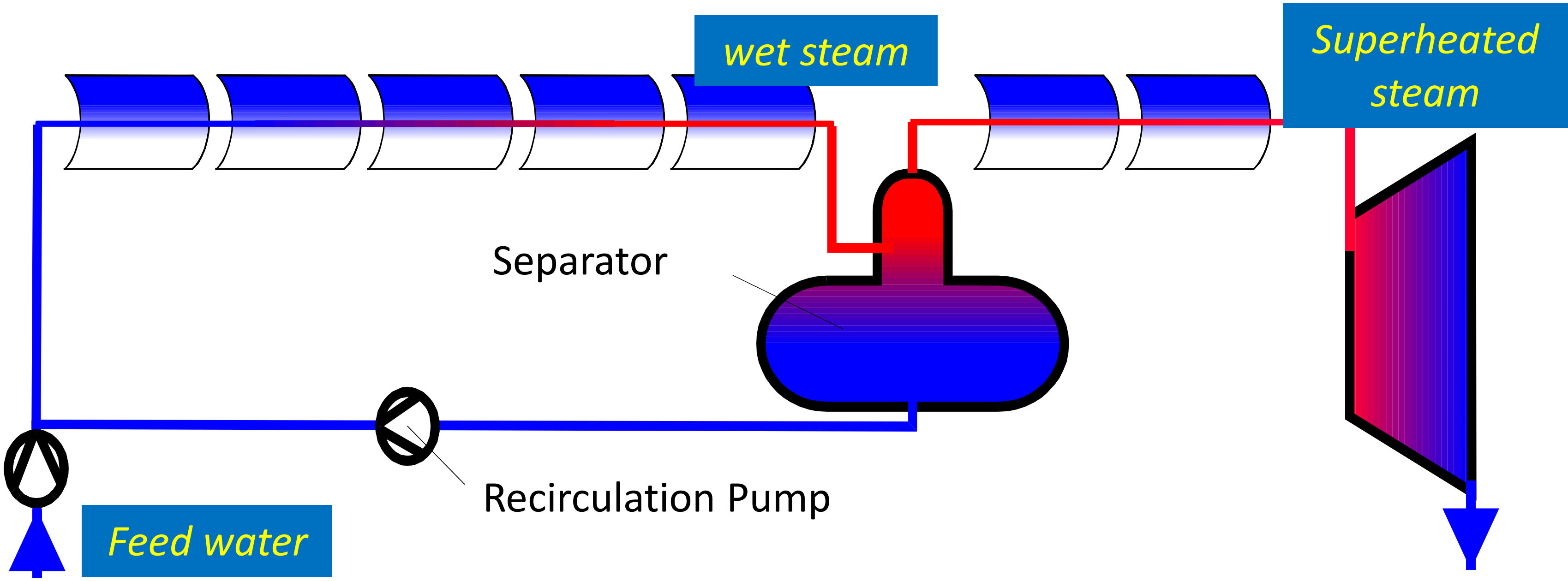

Parabolic Trough Solar Power Plants, Direct Steam Generation, DSG

DSG, Flow Patterns at the "Once Trough Concept" at 30 and 100 bar

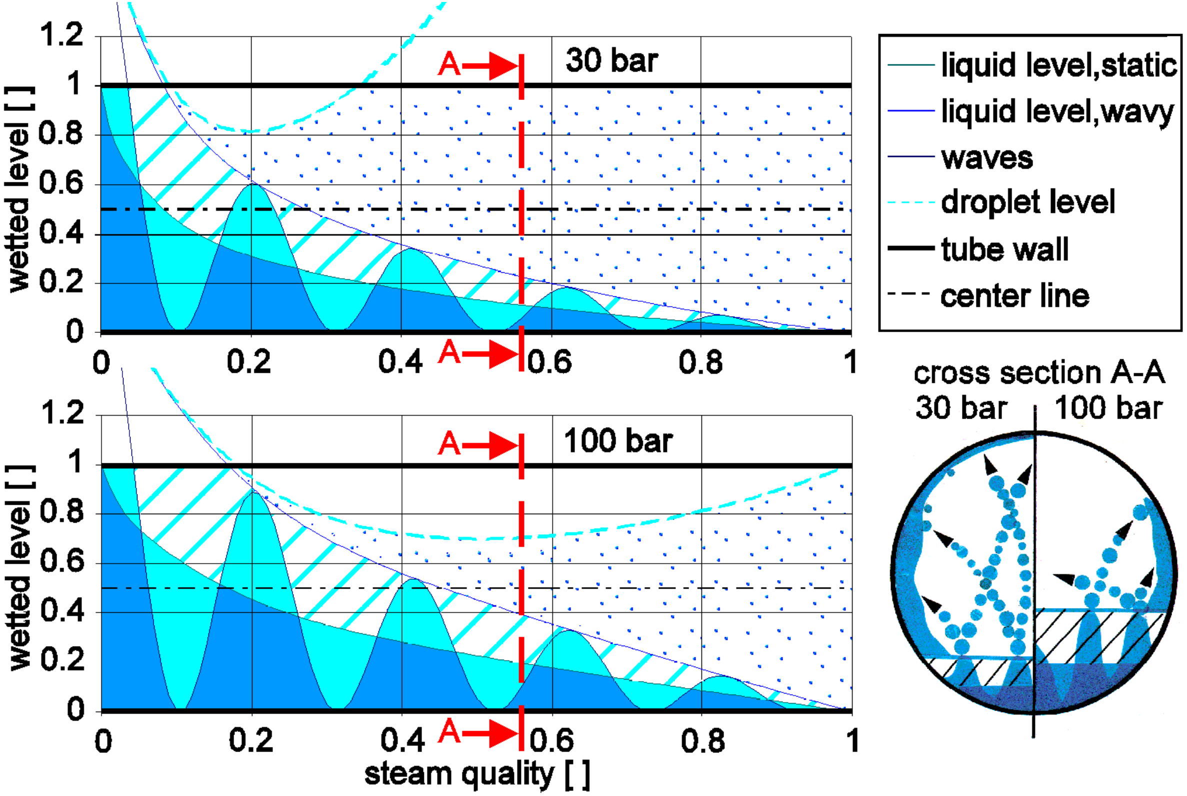

At 100 bar: wetting not sufficient! ➔ *Larger mass flow necessary.*

Parabolic Trough Solar Power Plants, Direct Steam Generation, DSG

Erection of the “DISS” Test Loop at the PSA in 1999

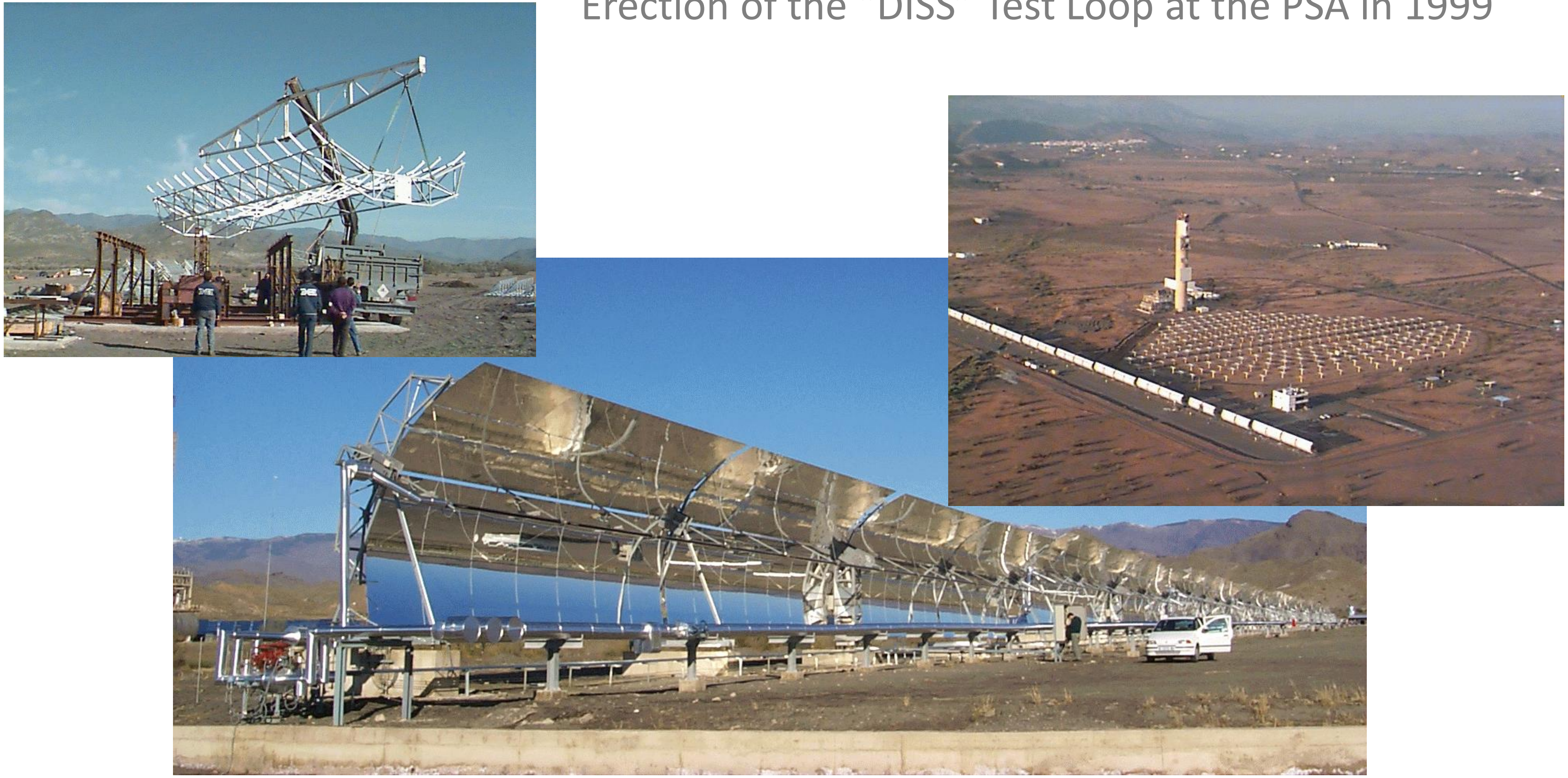

Parabolic Trough Solar Power Plants, Thermal Energy Storage, TES

Thermal Energy Storage:

- Operation after sun-set
- Buffering out cloud passages
- More flexibility in operation (operation at peak tariff time)
- Additional investment for TES
- Longer run time of the plant
- TES as shown on the right (direct storage of HTF) has been realised in the plant SEGS I

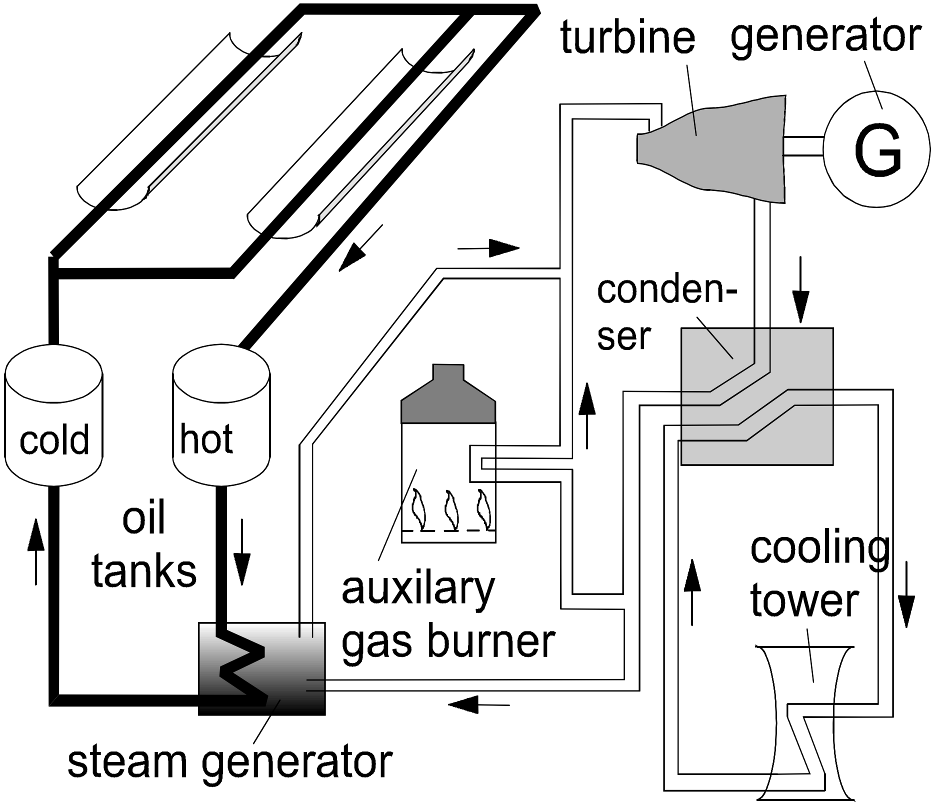

Parabolic Trough Solar Power Plants, Thermal Energy Storage, TES

Thermal Storage, technical Options:

- Direct storing of the Heat Transfer Fluid, HTF (used at SEGS I)
- Block of Concrete (DLR experiments at the PSA successfully completed)
- Molten Salt Storage Tanks (hot and cold) with heat exchanger to the HTF loop (so far most used technology)

Parabolic Trough Solar Power Plants, Thermal Energy Storage, TES

- When using a TES the solar field must be oversized (“Solar Multiple”) in order to have spare energy for charging the storage.
- The optimum relation between solar multiple and storage capacity needs to be derived by detailed simulation.
  - A TES which is big enough to store a full sunny day in June is too big, because it will never be fully charged during the rest of the year.
  - With a too small TES thermal energy often needs to be discharged (by de-focussing collectors).
  - Further relevant factors:
    - Tariff structure (when are the peak tariff times)
    - Cost of solar field capacity [$/MW] and cost of storage capacity [$/MWh]
    - Weather data (DNI)

Parabolic Trough Solar Power Plants with TES

Concrete Block Storage

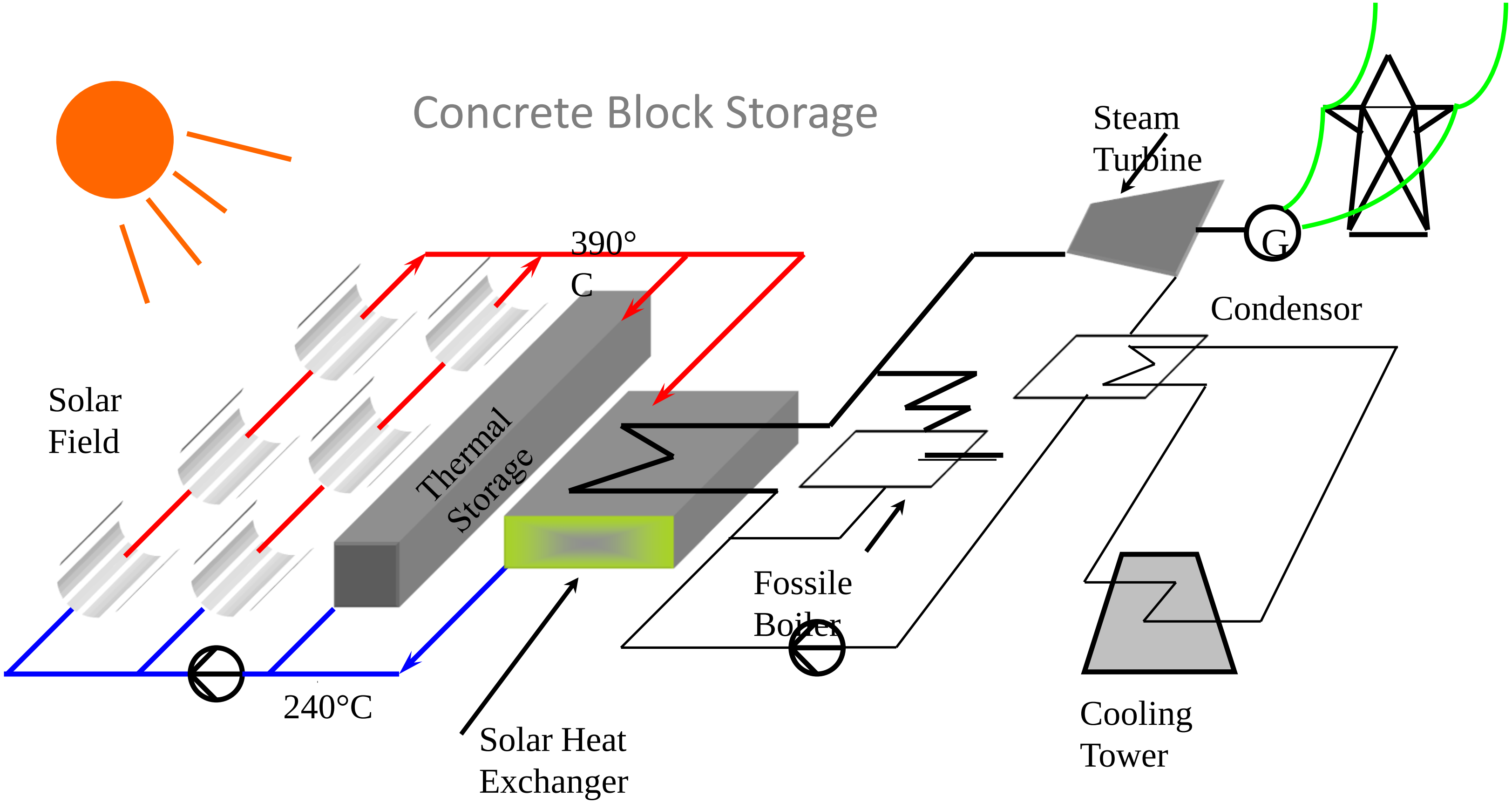

Parabolic Trough Solar Power Plants with TES

Molten Salt Storage

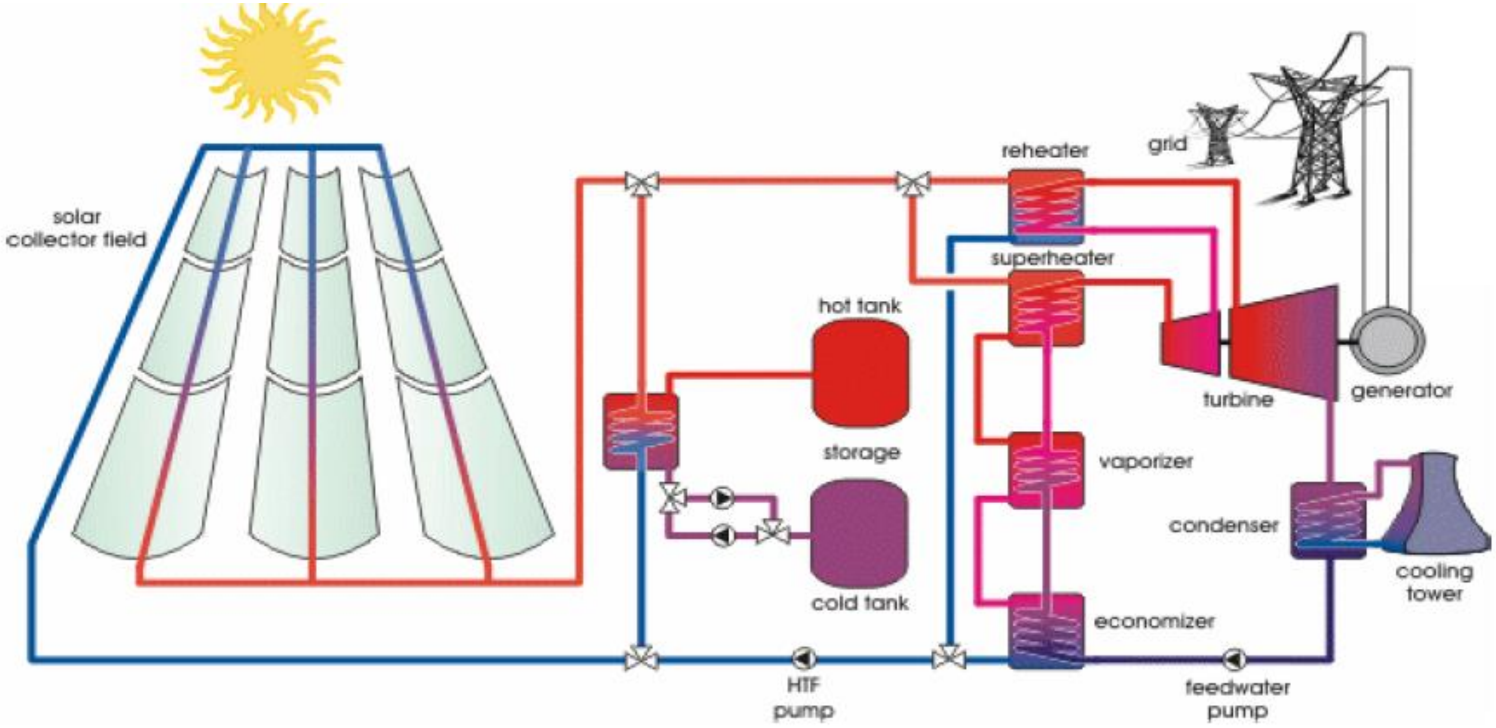

Parabolic Trough Solar Power Plants with TES

Concrete Block

DLR, ITT, W.-D. Steinmann et. al.

©DLR

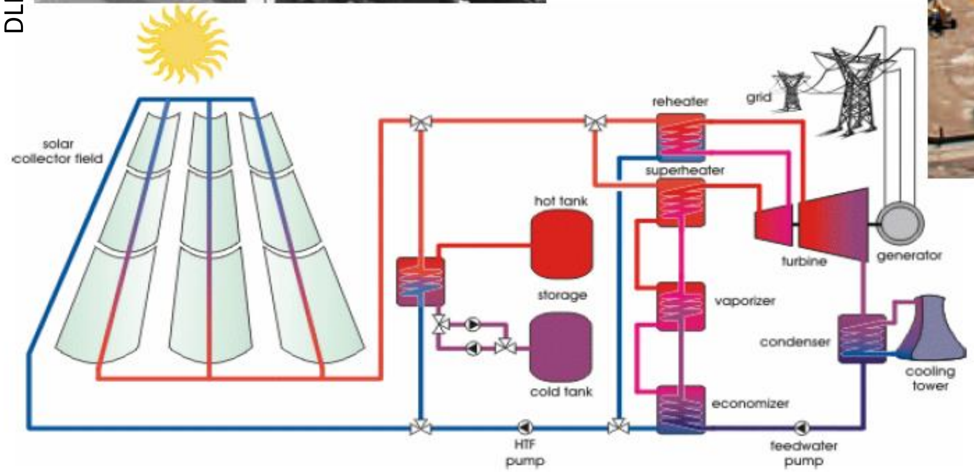

Molten Salt Tank

©SolarMillenium

Parabolic Trough Solar Power Plants with TES

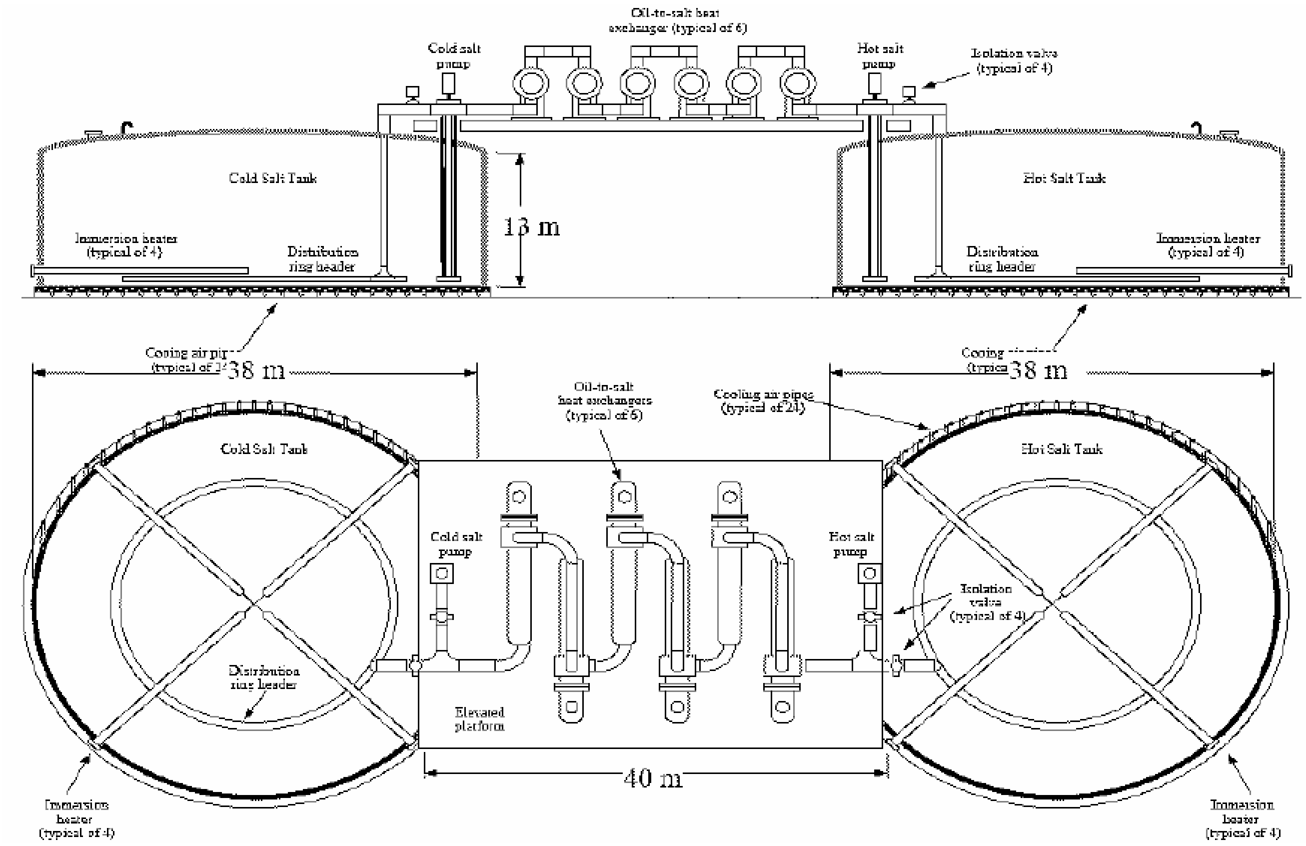

©SolarMillenium

Parabolic Trough Solar Power Plants with **TES**

TES of the plant Andasol 1

- Type: 2-Tank Molten Salt Storage
- Fluid: Nitrate salt mixture
  (60% NaNO3 and 40% KNO3)
- Melting Point: 223°C
- Storage Capacity: 1,010 MWh
  (~7.5 hrs full load operation)
- Storage Tank Size: 14 m height 37 m diameter
- Salt Mass: 27,500 tons
- Flow Rate: 953 kg/s
- Cold Tank Temperature: 292° C
- Hot Tank Temperature: 386°C

Parabolic Trough Solar Power Plants with TES:

Fictive Example: Matching 600 MW-demand-peaks at Abu Dhabi with 600 MW PTC plants with TES for ≈ 6 FLH

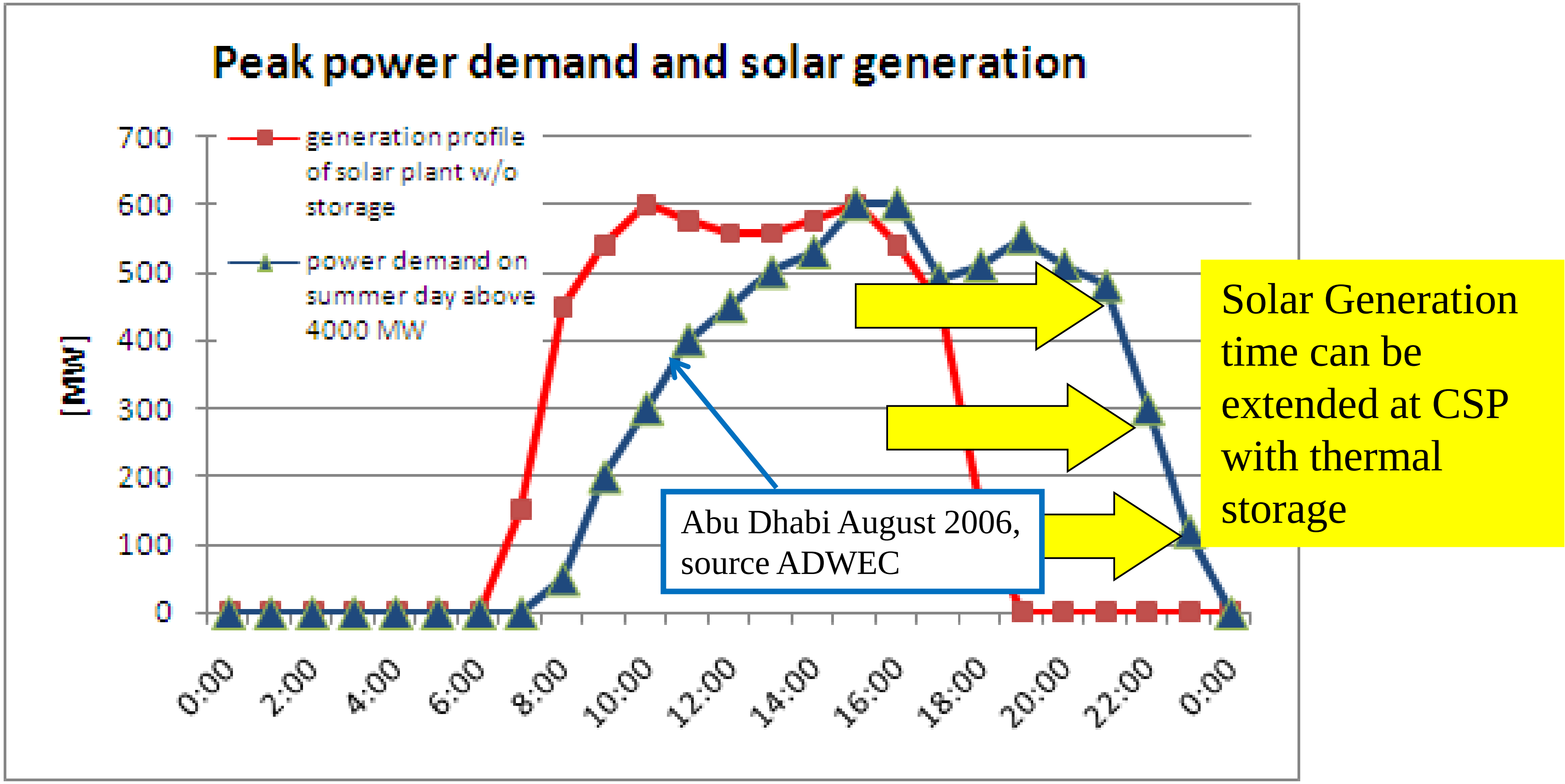

Abu Dhabi August 2006, source ADWEC

Solar Generation time can be extended at CSP with thermal storage

Parabolic Trough Solar Power Plants with TES

Charging diagram of a TES. Data:

Power requested from 08:00 to 22:00

$P = 30\ MW_{el}$

solar multiple = 1.75

$Q_{TES} = 600\ MWh$

=> *TES for ≈ 6 FLH*

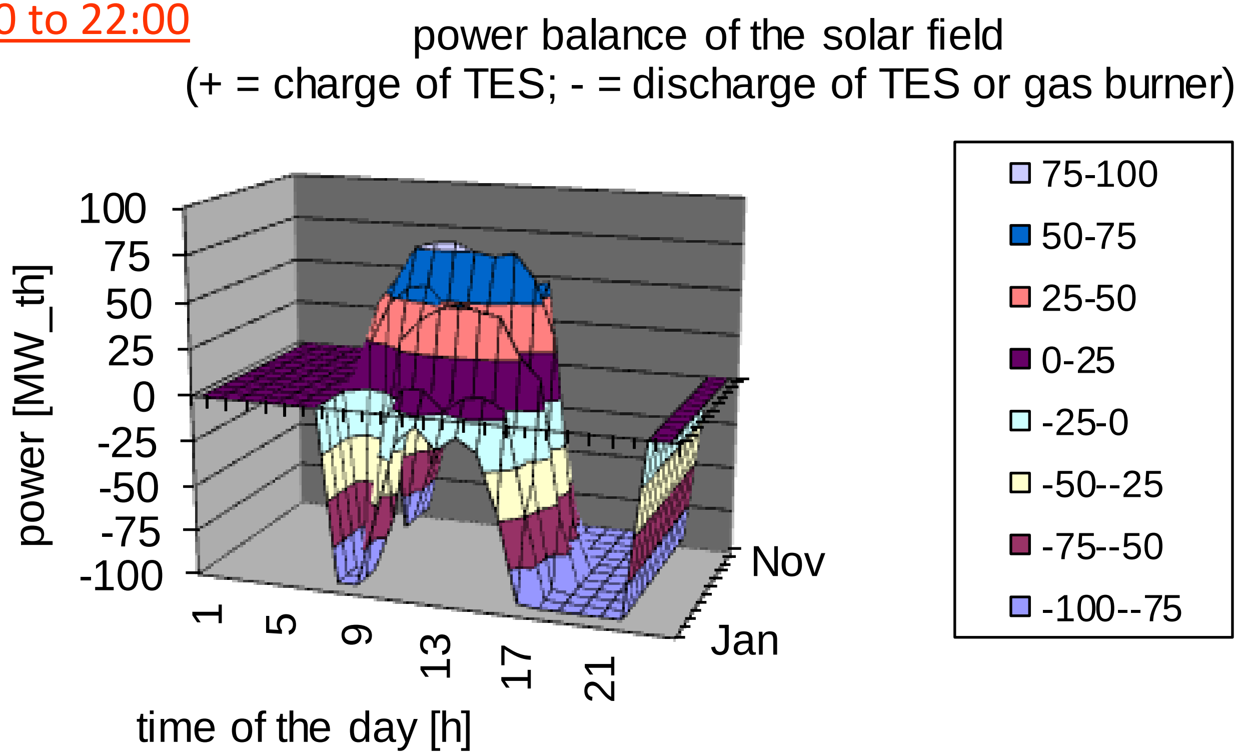

power balance of the solar field
(+ = charge of TES; - = discharge of TES or gas burner)

Parabolic Trough Solar Power Plants with TES

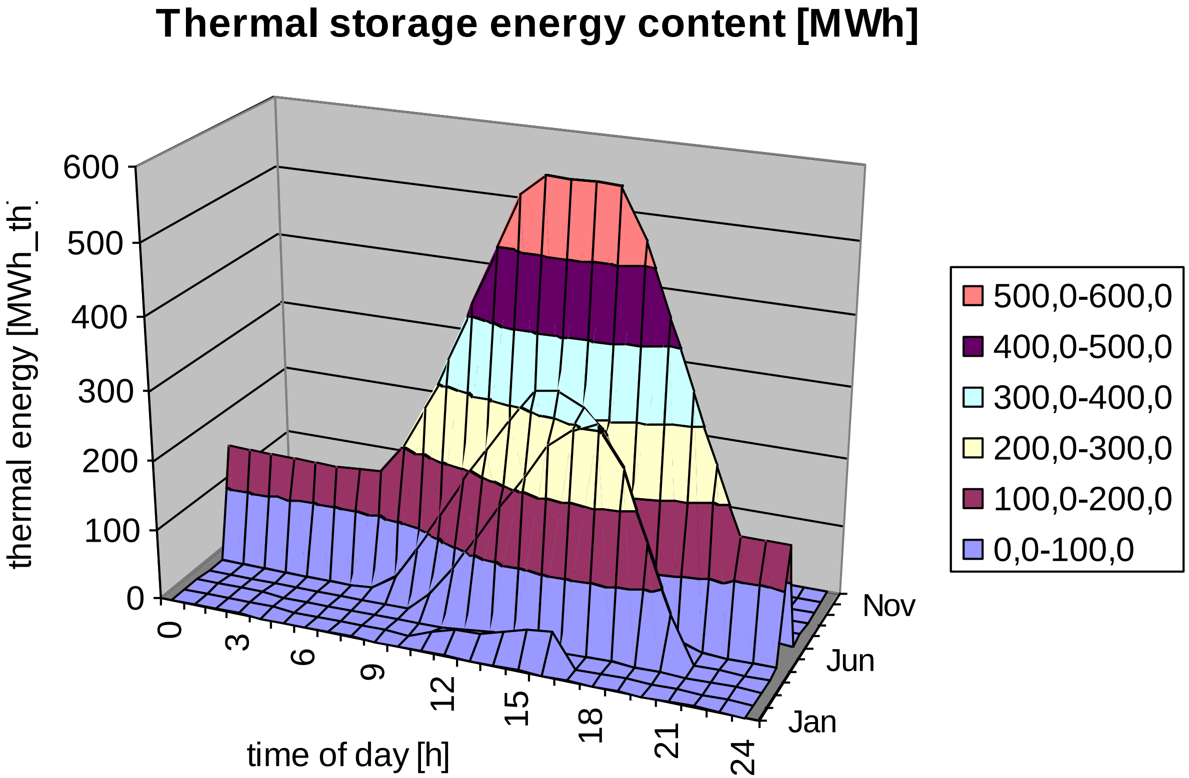

Parabolic Trough Solar Power Plants with **TES**

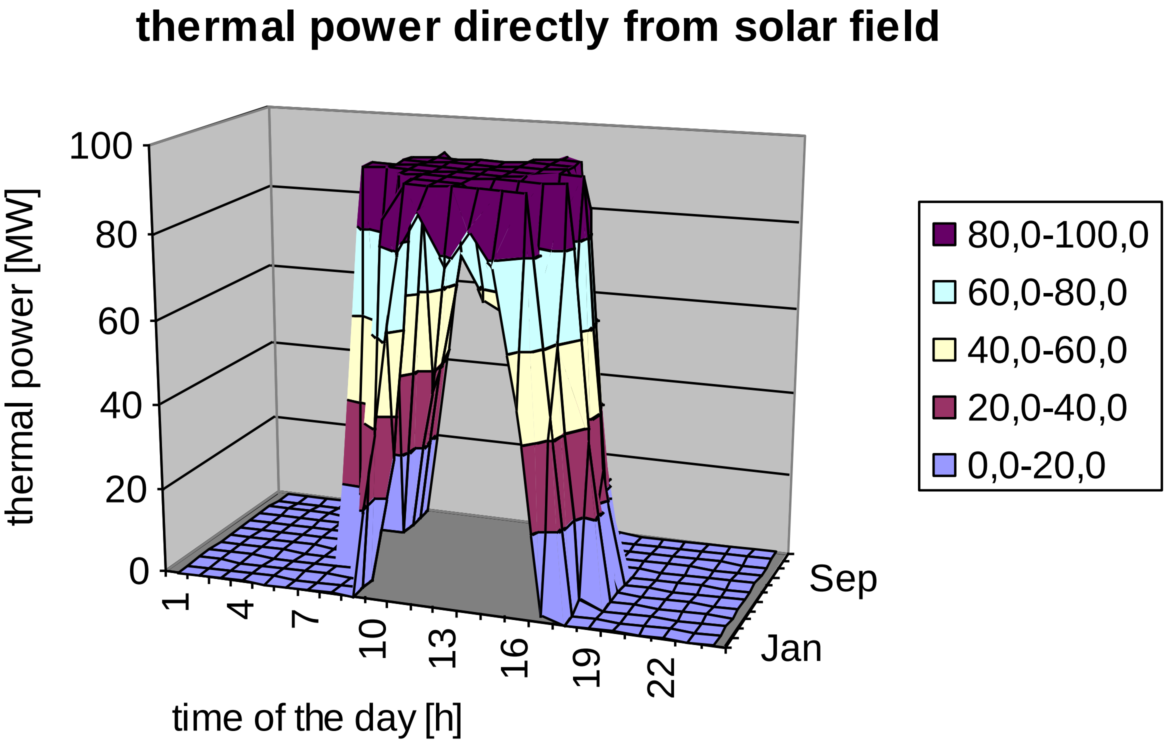

Parabolic Trough Solar Power Plants with TES

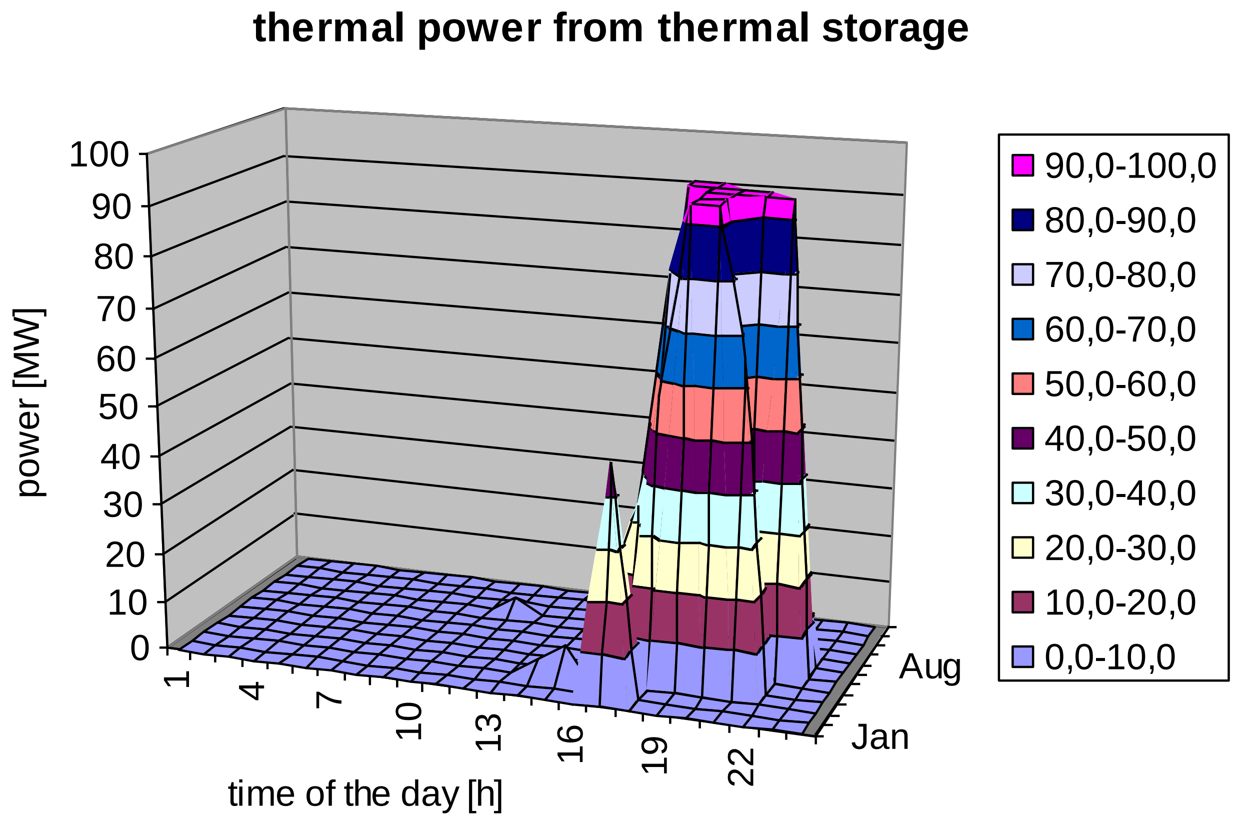

Parabolic Trough Solar Power Plants with TES

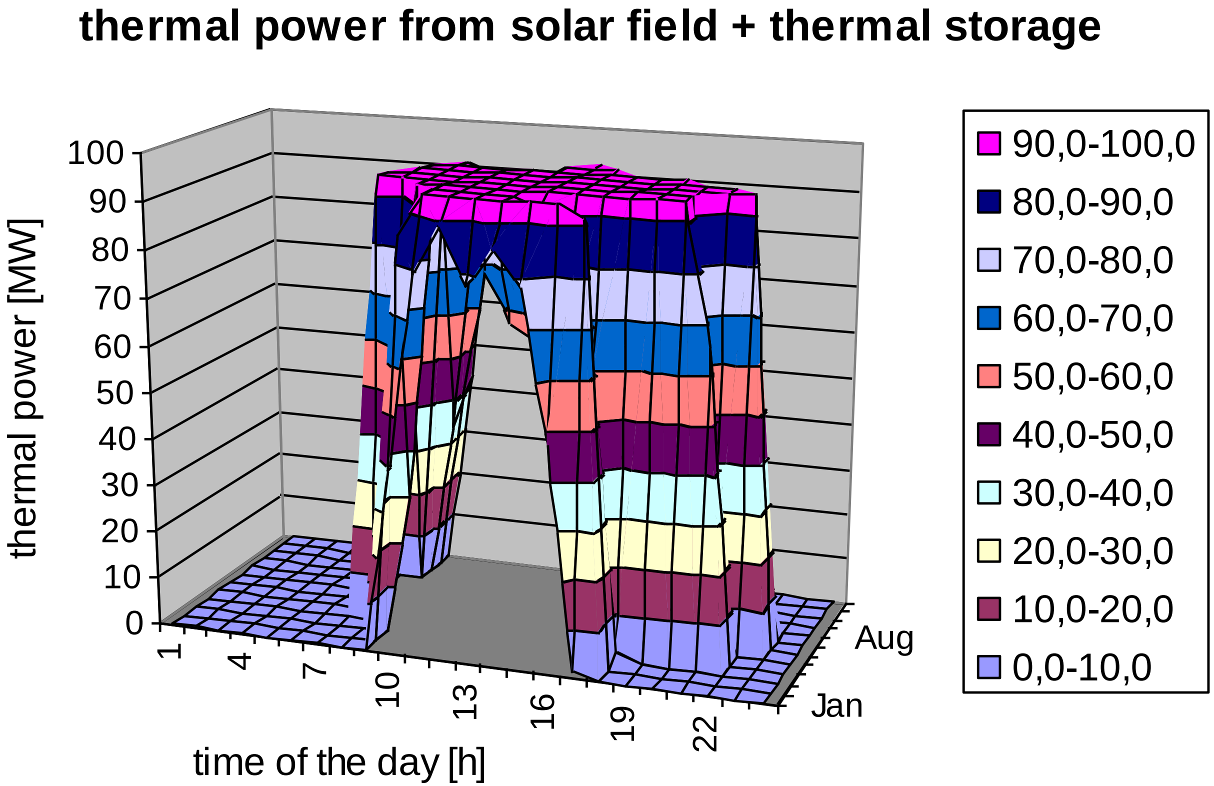

Parabolic Trough Solar Power Plants with TES

Not all the energy required by the grid (as shown in the first slide of the TES-series) could be delivered by the solar field and storage. The remaining difference is supplied by a gas fired burner.

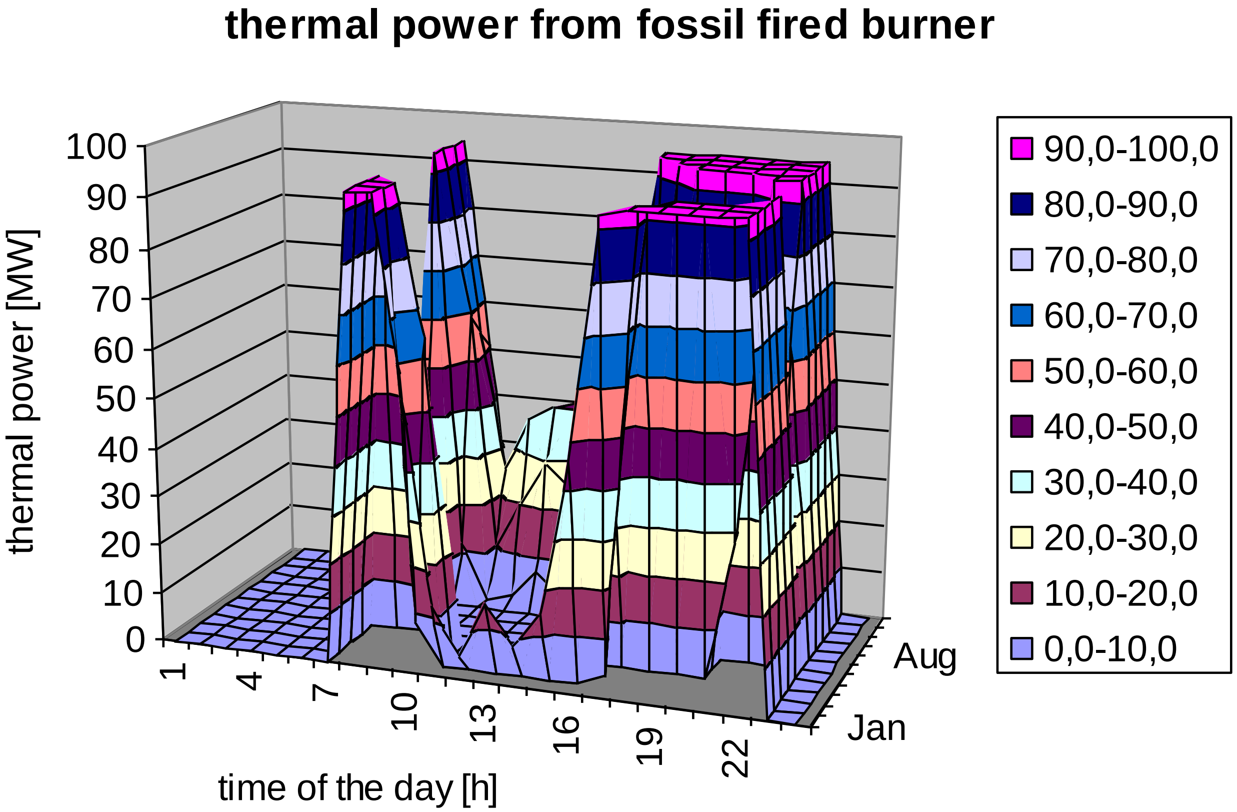

Parabolic Trough Solar Power Plants with TES

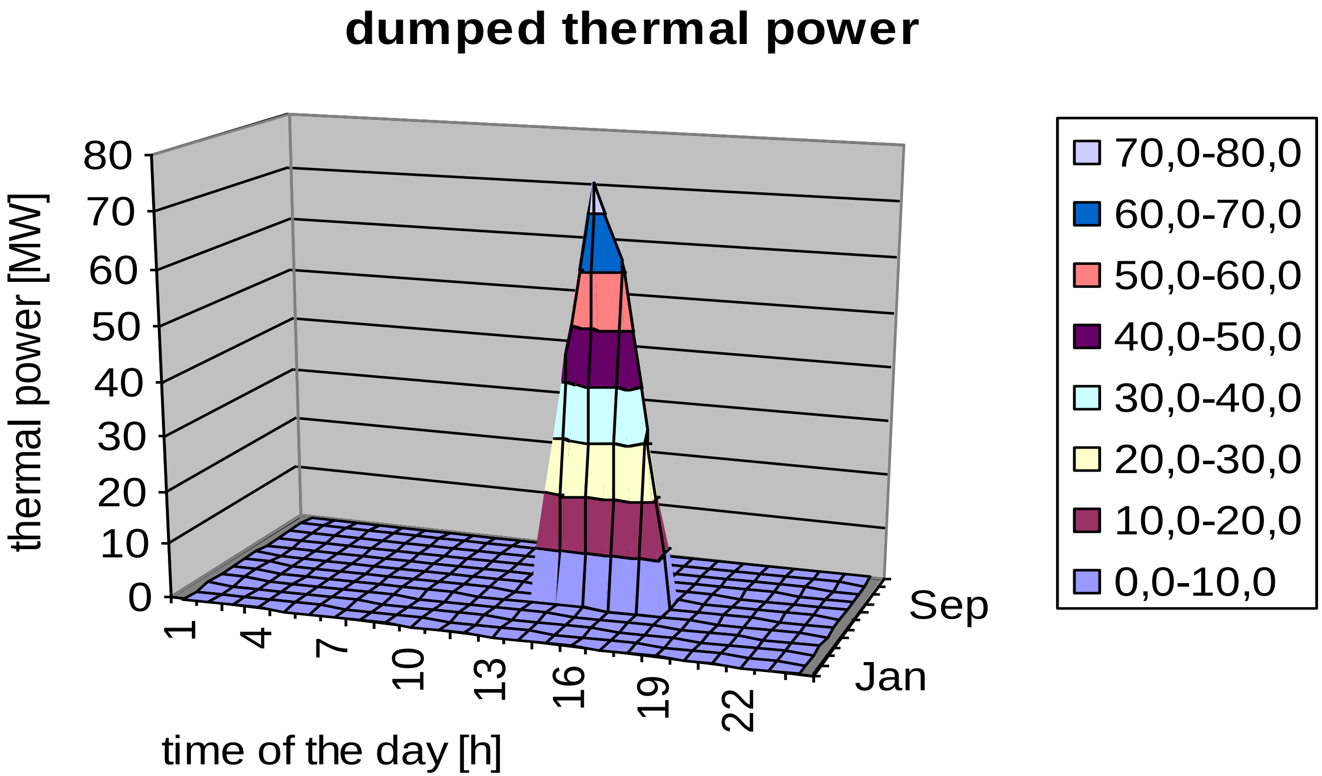

Load Curve in Abu Dhabi (red Line) Distribution of Load between Base-, Mid- and Peak Load Plants

100% = 5 GW in yr 2006.

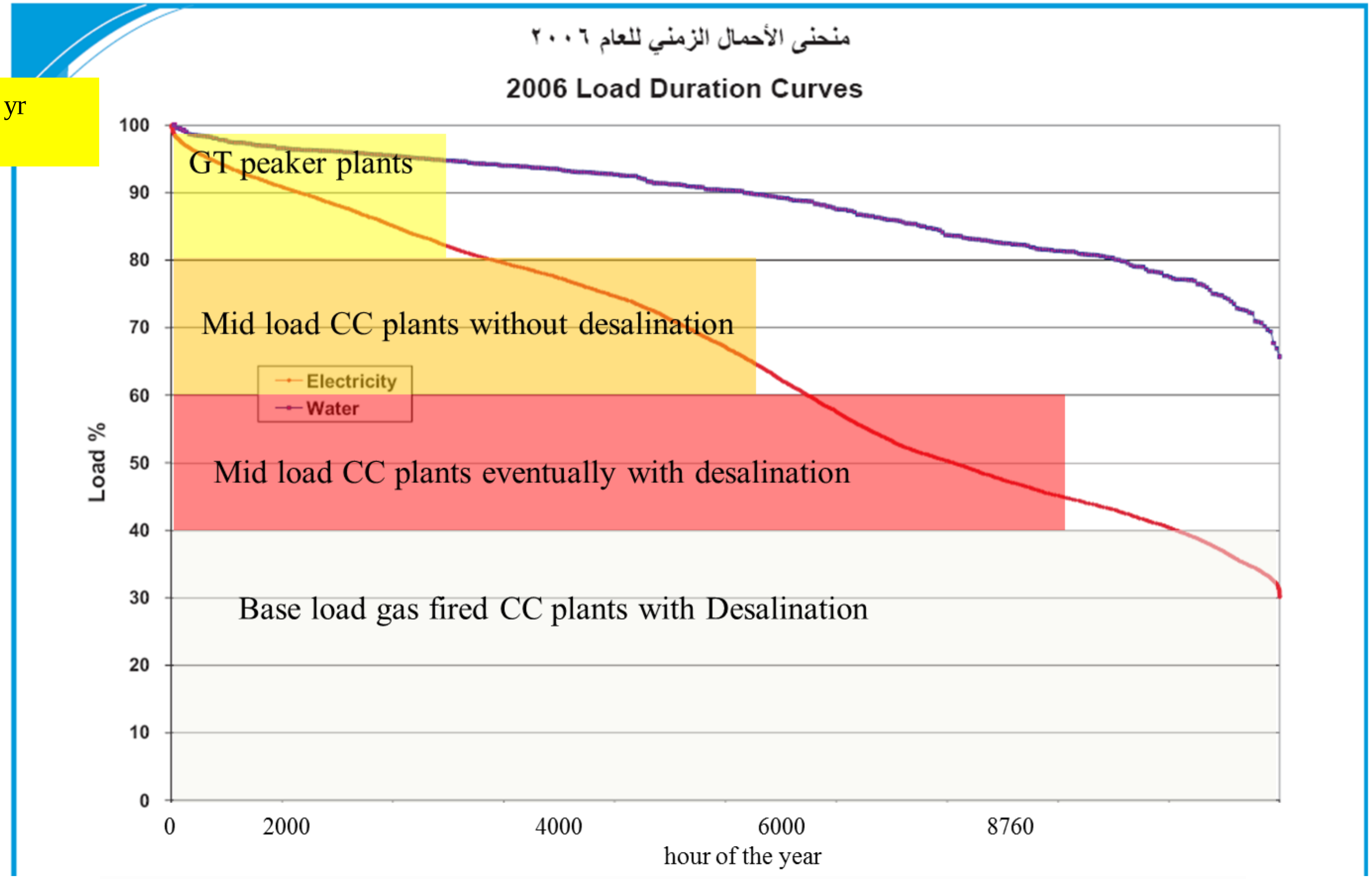

Possible Market Penetration with CSP Plants in 2030

100% = 20 GW in yr 2020
That means that 50% are equivalent to 10 GW capacity

SM = Solar Multiple = oversize factor of solar field in comparison to a plant without thermal storage

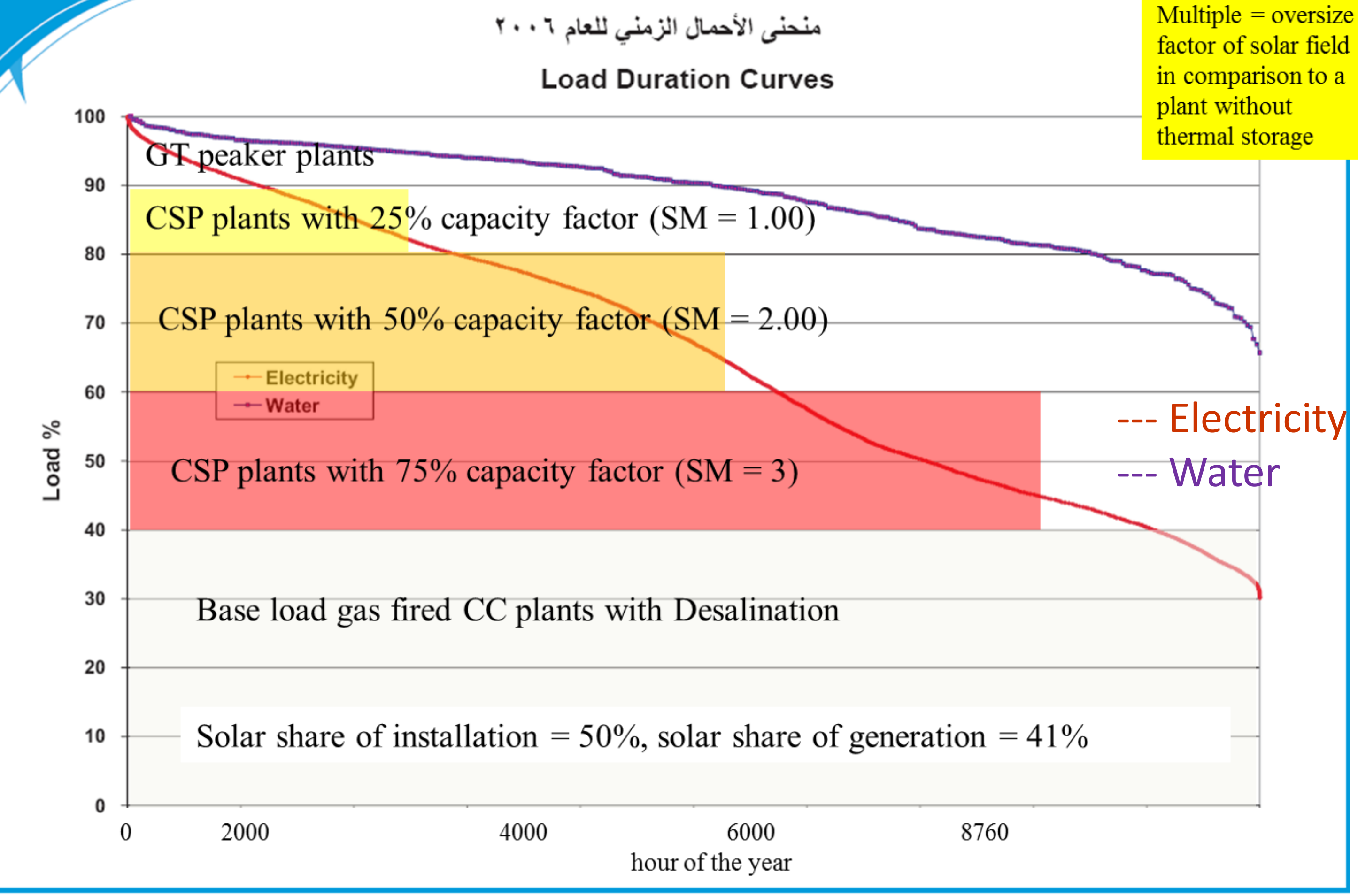

Max. possible PV Market Penetration

With PV: The mid load plants, which would be fully replaced by CSP plants need to be maintained by the utility, because the PV plants can only run when the sun shines, and do not replace capacity. Therefore the utility will only pay the saved fuel and variable O&M cost.

100% = 20 GW in yr 2020 .

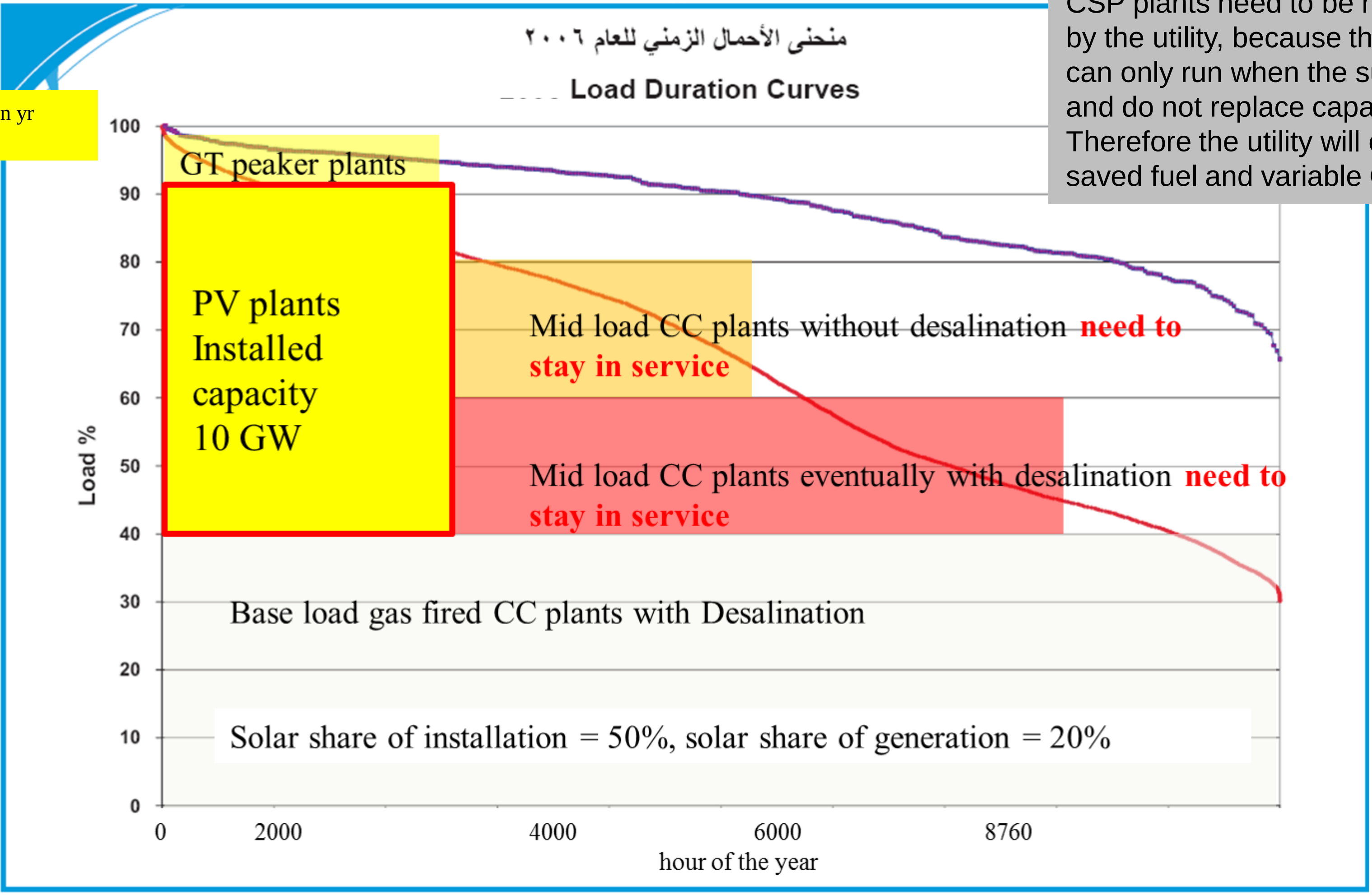

Cost of Thermal Storage at CSP

- Both CSP plants generate 200 million kWh per year
- Both plants cost 500 million $

without TES

100 MW x 2000 h / a

with TES

50 MW x 4000 h / a

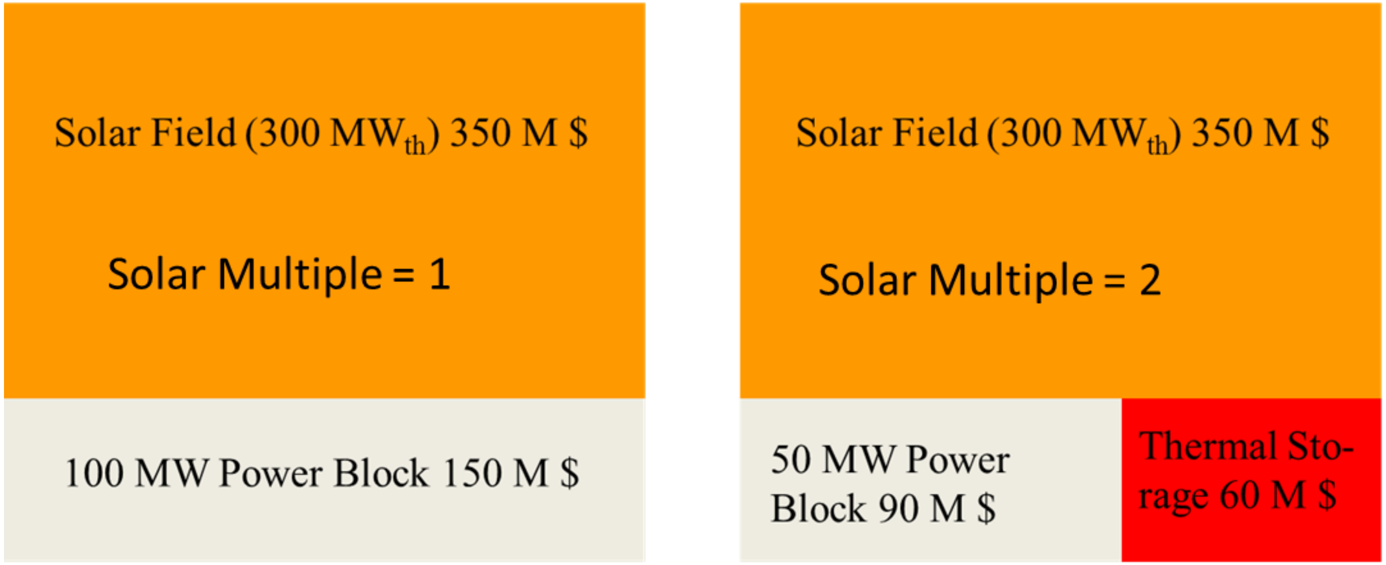

Solar Field (300 MW$_{th}$) 350 M $

Solar Multiple = 1

100 MW Power Block 150 M $

Solar Field (300 MW$_{th}$) 350 M $

Solar Multiple = 2

50 MW Power Block 90 M $

Thermal Storage 60 M $

- The despatchability is obtained without extra cost

Parabolic Trough Solar Power Plants, Thermal Energy Storage, TES

Advantages:

- Operation after sun set possible
- Riding through cloud passages
- More flexibility in operation (catching of peak tariff times and dispatchability)
- Smaller power block at same solar field size

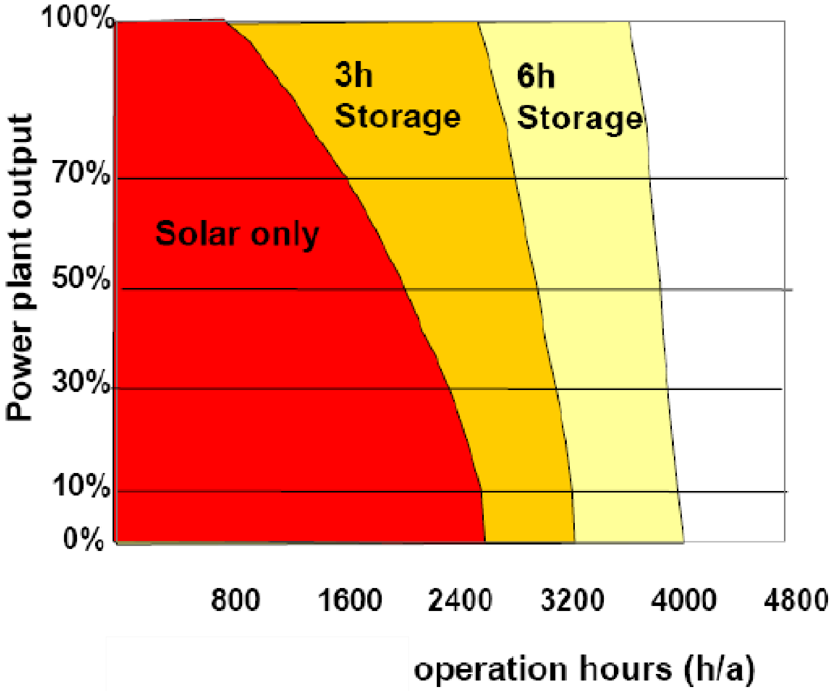

©DLR

Disadvantage:

- Additional cost of the storage itself

Linear Fresnel Collector CSP Plants

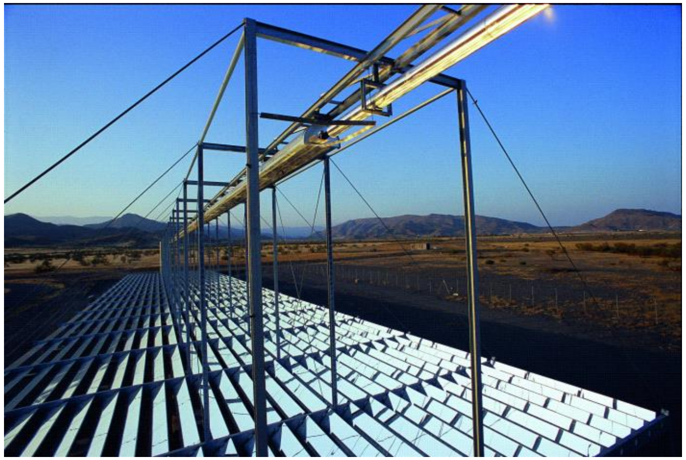

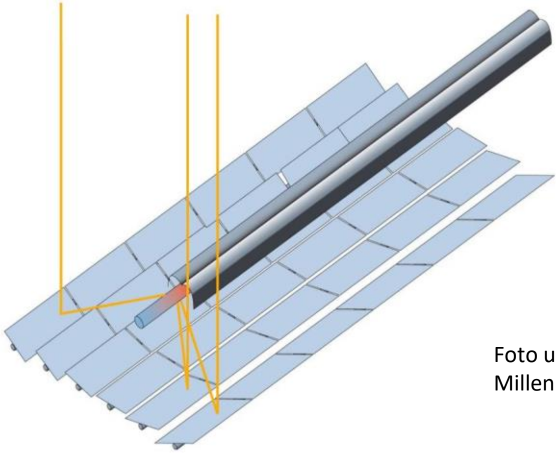

Foto und Grafik: Solar Millenium AG

- The youngest CSP technology. Currently (2014) in operation: 31 MW (Spain)
- Similar to trough, similar efficiency, less land demand due to dense mirror packing, but less FLH due to more shading in the morning and evening.
- Potentially cheaper than trough (according to studies, not yet proven in reality)

Solar Tower Plants

Solar Tower Power Plants (Power Tower)

Plant Principle

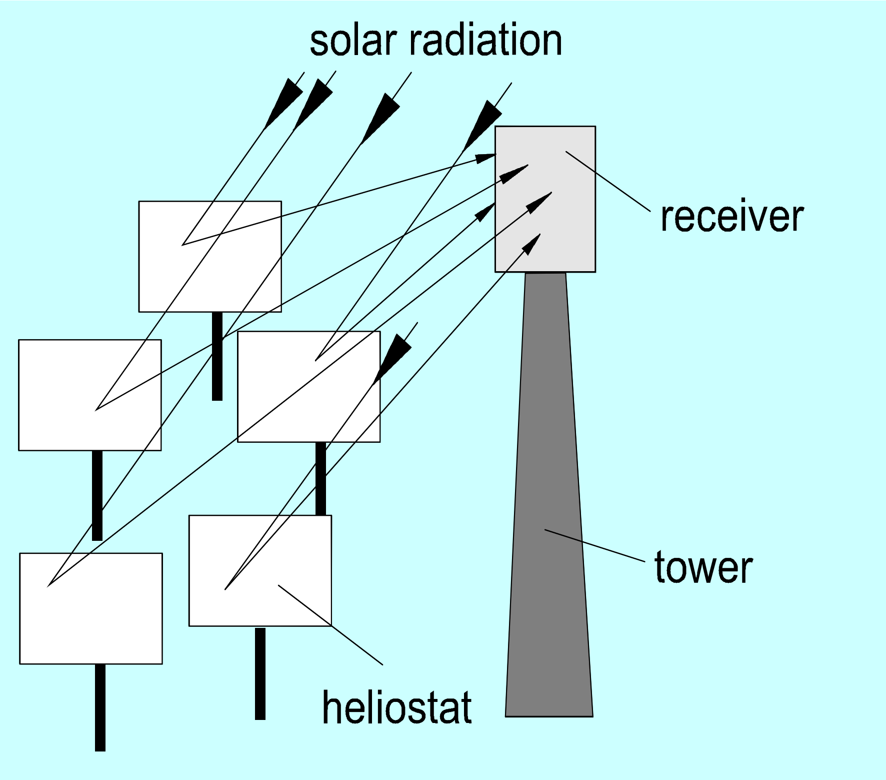

“Solar One” in California 1990

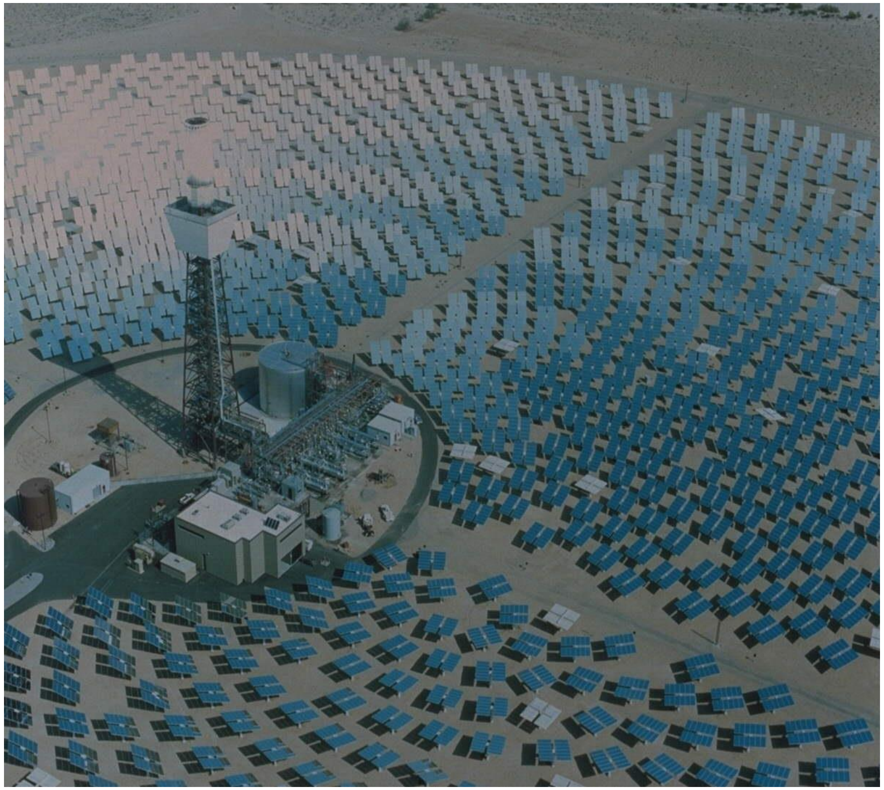

Solar Tower Power Plants, Possible Heat Engines

Possible:

- Rankine Cycle with steam turbine or steam engine
- Stirling engine
- Gas turbine

Used so far:

- Rankine Cycle with steam turbine and steam piston engine
- Gas turbine

- Stirling engine and steam piston engine are less suitable due to small capacity (max. a few MW)

Solar Tower Power Plants, Heliostat Field

- The mirrors which are located around the tower are called Heliostats, because they focus the light statically onto the receiver at the top of the tower.
- Heliostats have a two-axis tracking mechanism
- The tracking control works either with a sun sensor in each heliostat or with a sun algorithm and a central computer
- Heliostats are not flat, they are also slightly curved in order to achieve a small spot of concentrated light (curvature dependent on distance from tower)

Heliostat Field, Loss Mechanisms

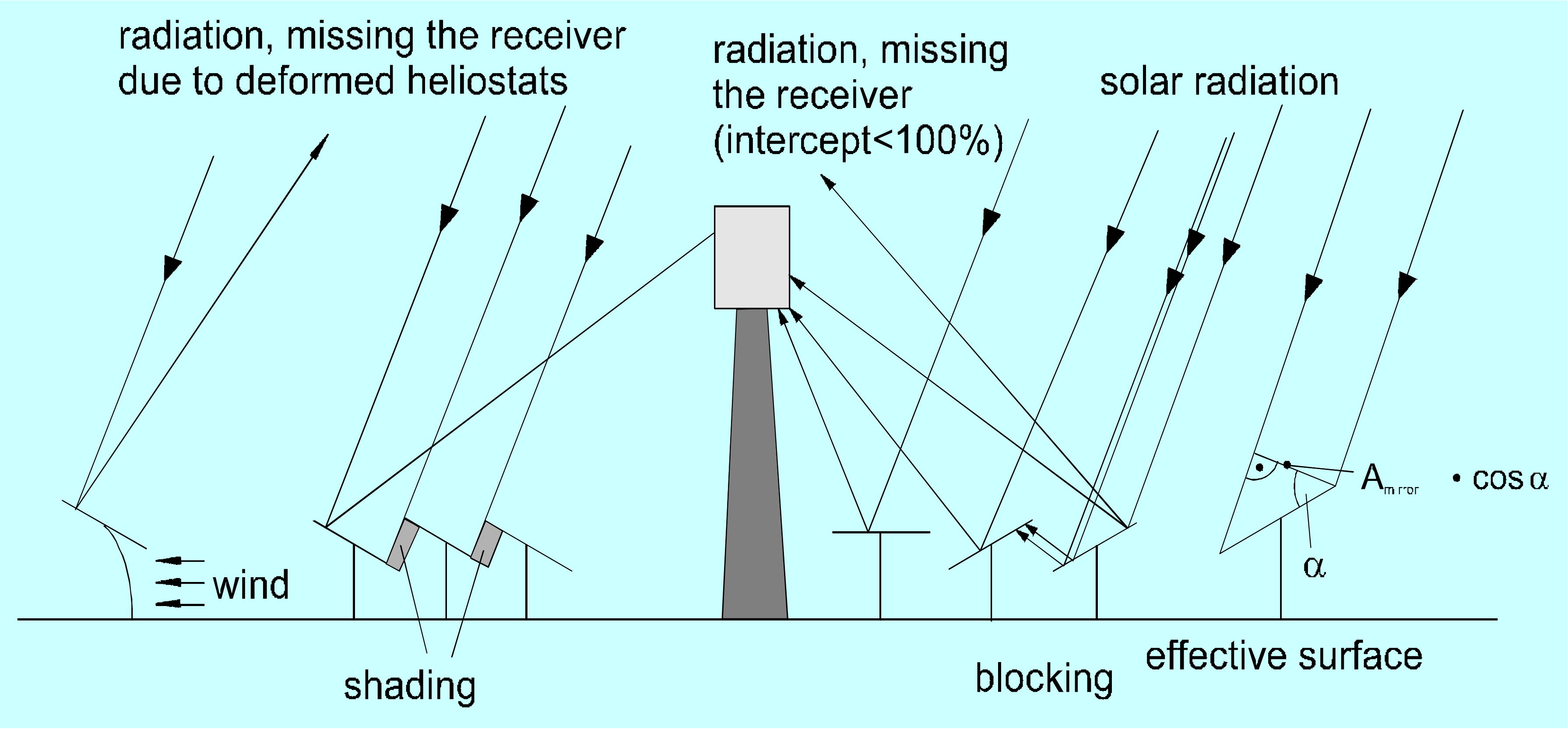

Heliostat Field, Design Considerations

- When the sun is in zenith, a dense packing of Heliostats would be efficient.
- At low elevation angles of sun (winter or in the morning or evening) shading is significantly higher with dense packing.
- The optimum positioning of Heliostats needs to be found with professional simulation tools.
- Heliostats far from the tower are sensitive against smallest disturbances
- Heliostats far from the tower generate larger light spot (beam opening angle = 1/100) *(see slide "Sun's diameter and distance from earth").* If the focal spot becomes larger than the receiver, a certain share of the reflected energy is lost.
- The light reflected by Heliostats far from the tower has a longer path through the atmosphere. That causes more losses due to dust in the air, called beam attenuation.
- The last 3 bullet points limit the useful size of a heliostat field

Solar Tower Power Plants, Heliostat Field

- Near to equator: surrounding field
- Far from equator (and/or small capacity): one sided field (on the North side at the northern hemisphere and vice versa)

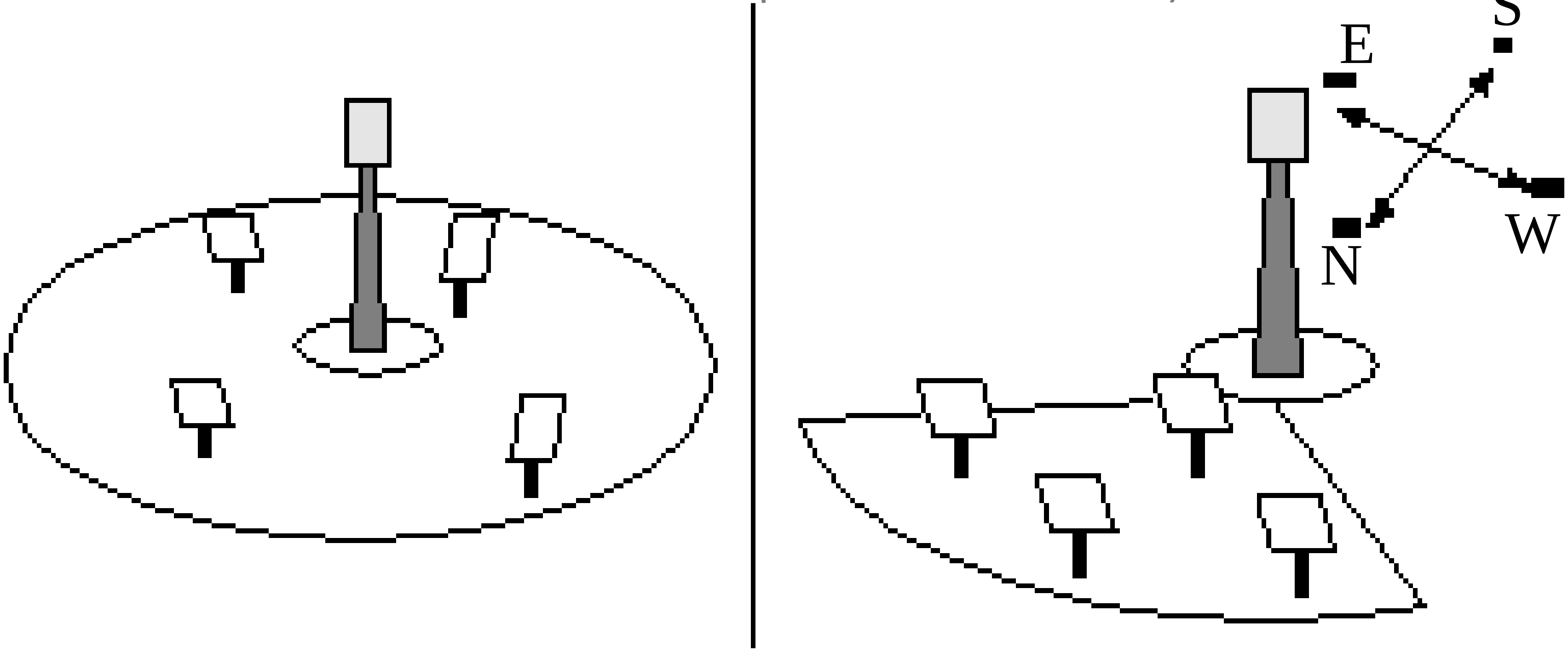

Heliostat Field, Cosine Effect

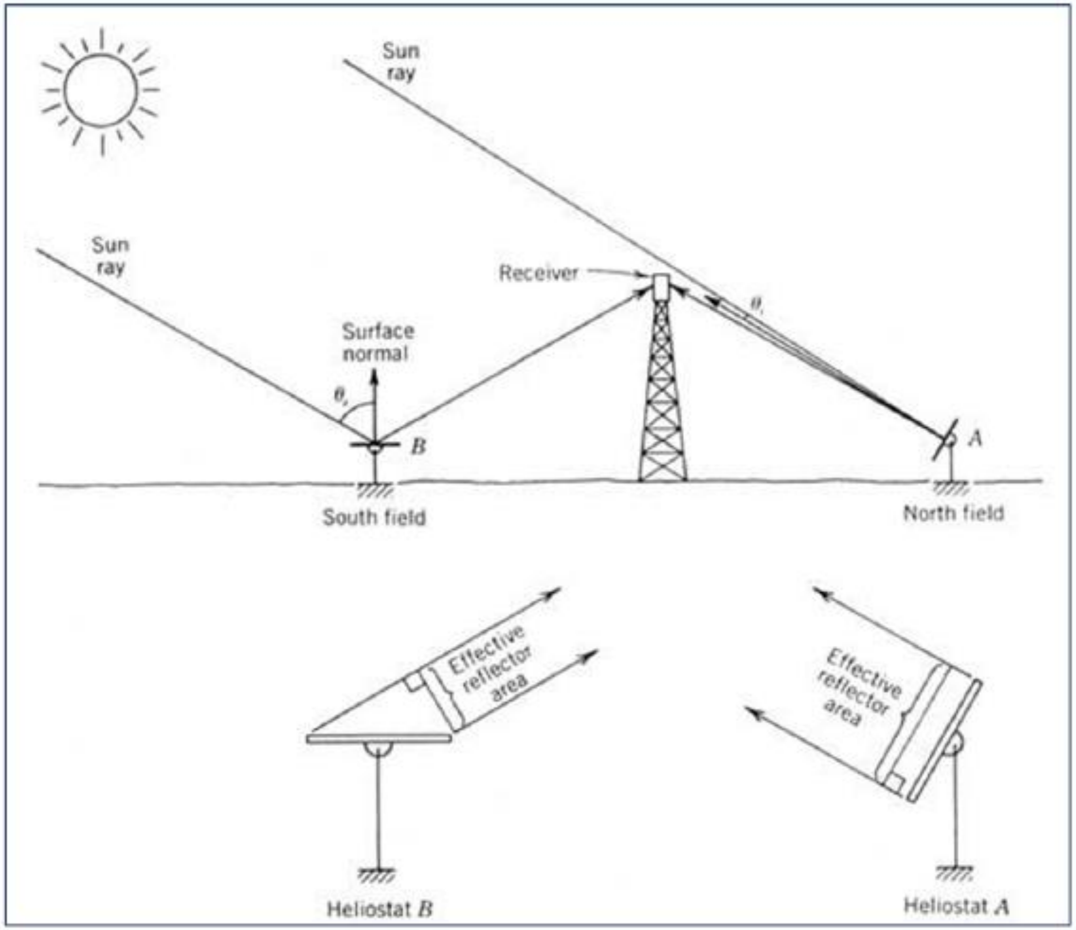

Heliostat, Tracking

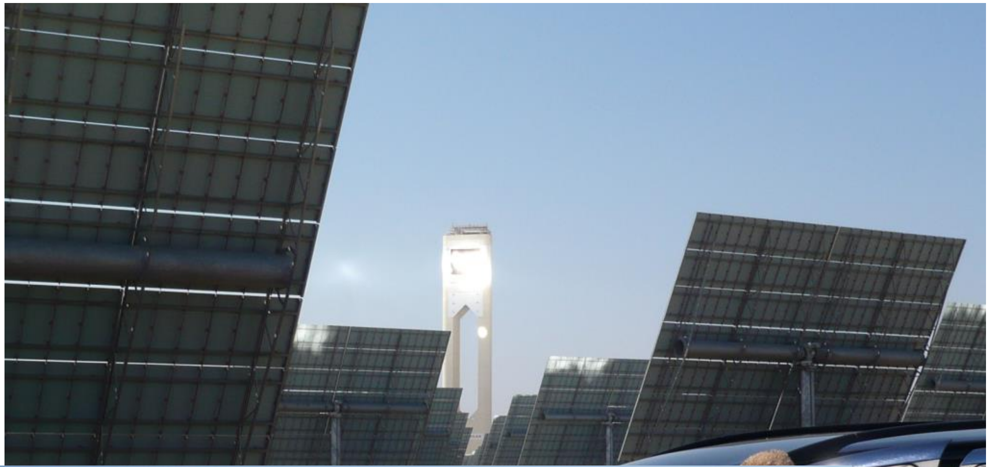

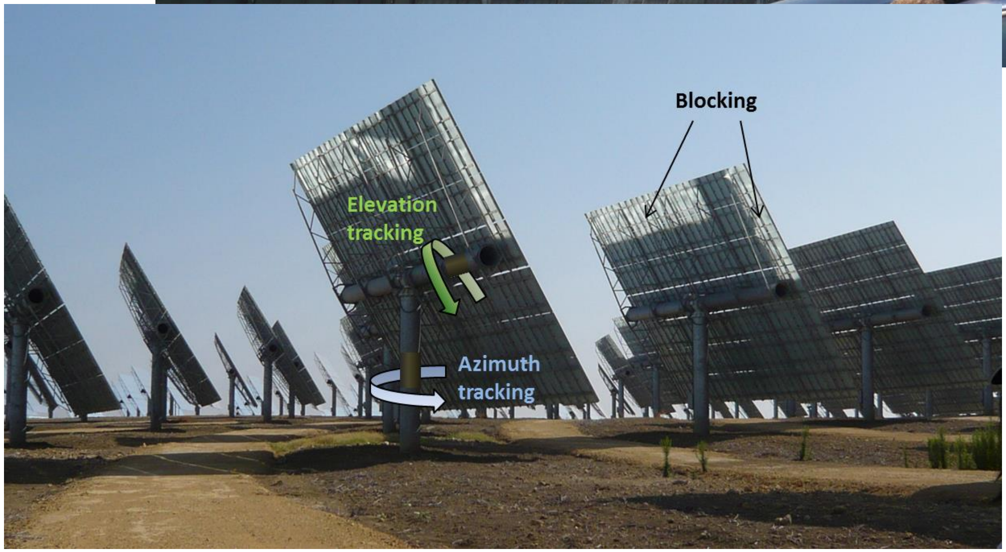

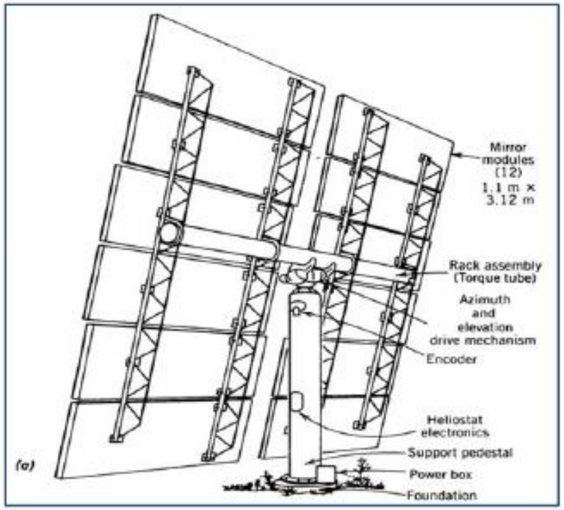

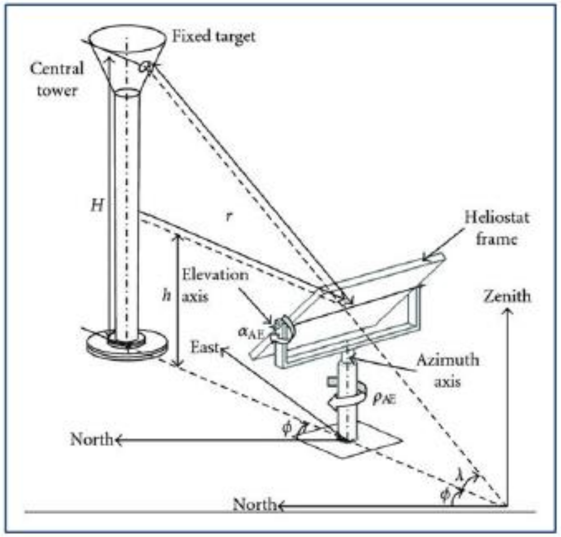

Heliostat Field, Example: „Gemasolar“
19.9 MW_{el}, 5500 kWh/kW/a

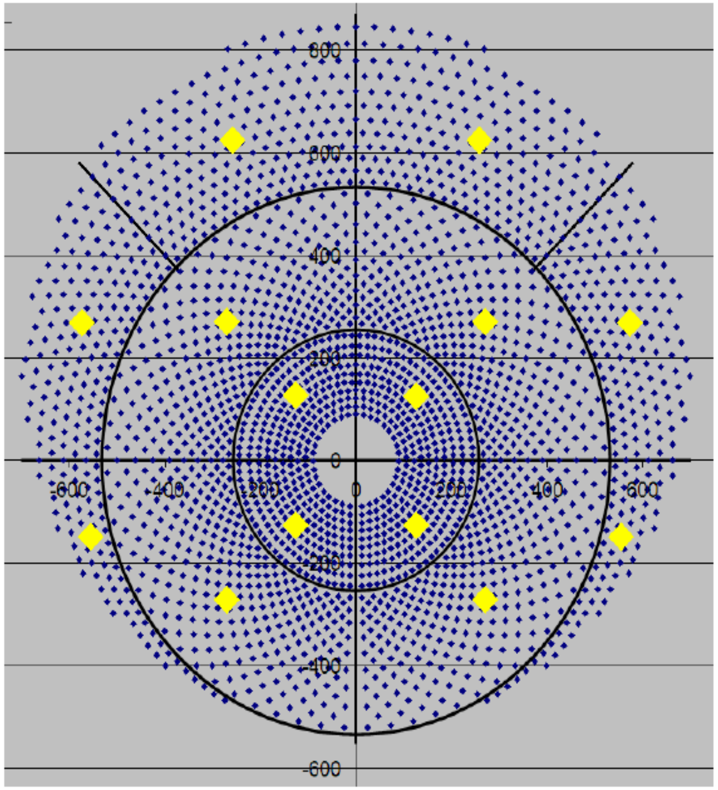

Figure 3-2: Distribution of heliostats and their "representatives" over the solar field around the receiver tower (scales in m)

Example: „PS 10“
11 Mw_{el}, no storage

Receiver Types: Open or Cavity

Cavity Receiver

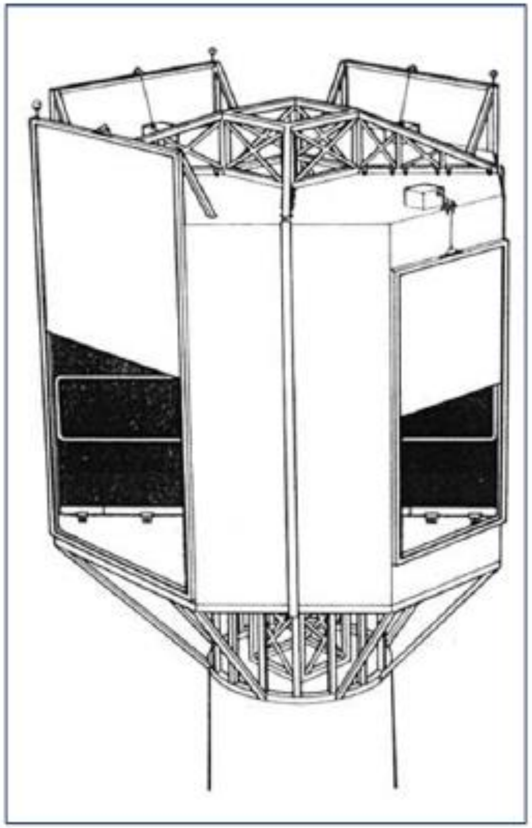

Open Receiver

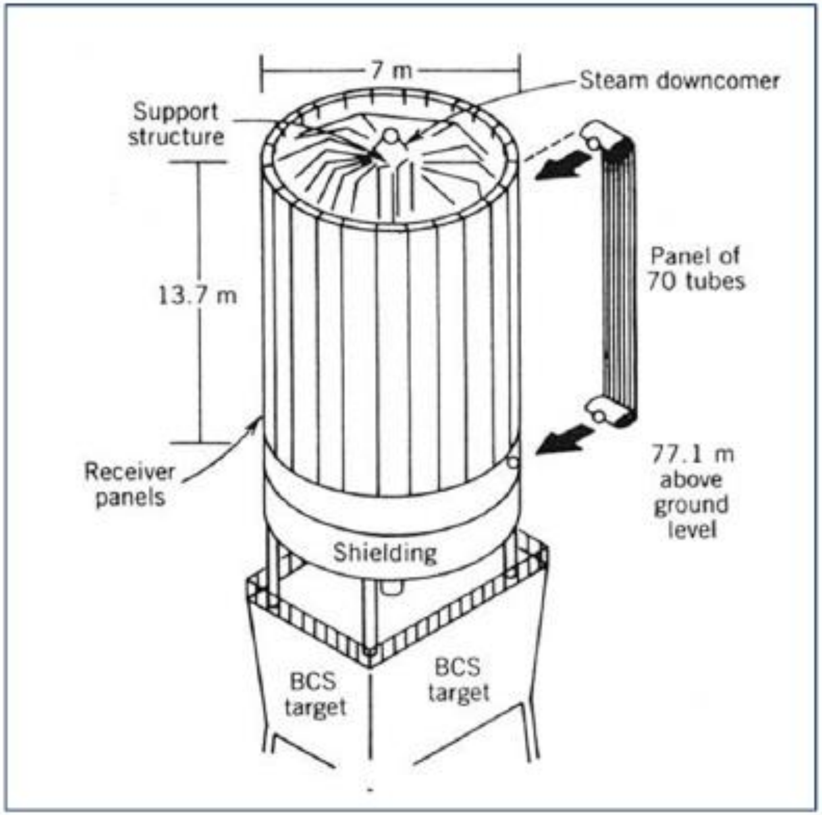

Source: NREL

Power Tower: The most simple System: Direct Steam Generation in Receiver

Scheme of “PS 10” Solar Tower (11 MW), Seville, Spain
and of “Ivanpah” Solar Tower (392 MW), USA

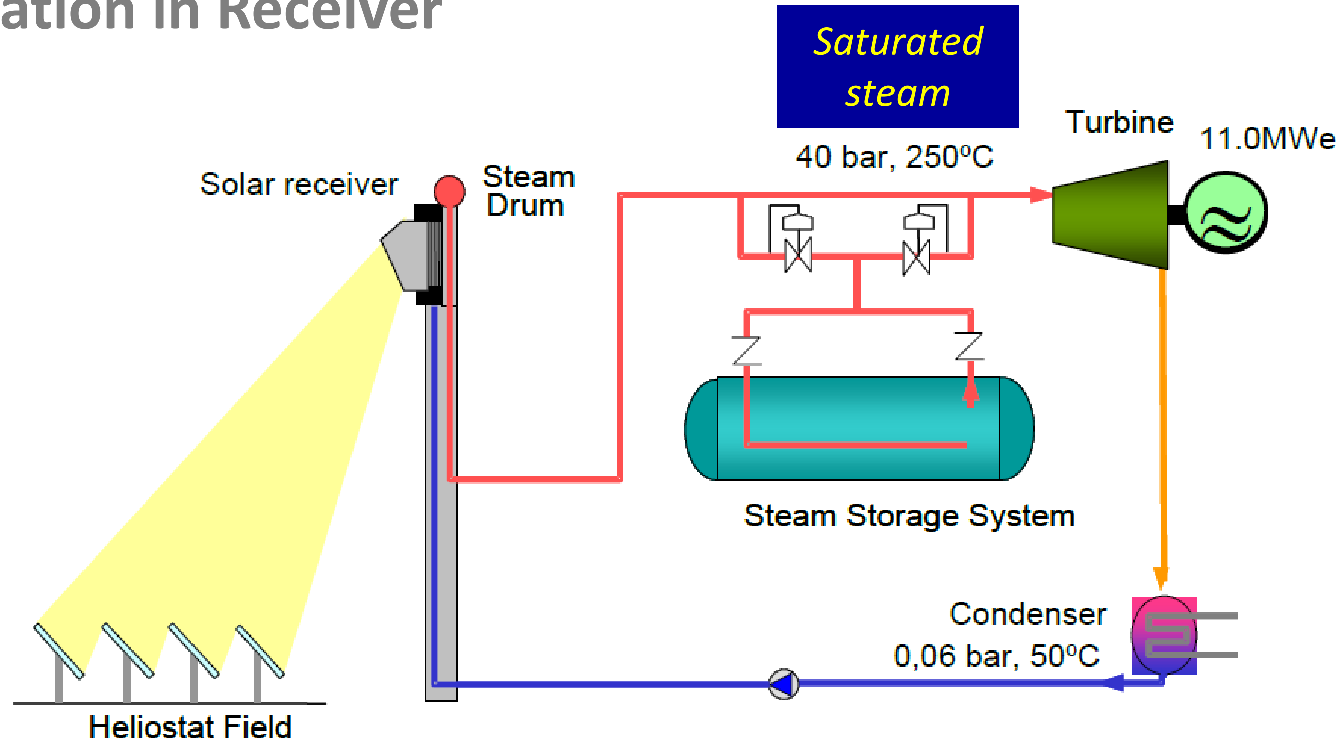

Source: Abengoa, Manuel Romero, Solar Tower Power Plants – Today and Tomorrow, Focus-Abengoa Forum on Energy and Climate Change, Sevilla Oct. 24 2007

Heliostat Field, Performance Calculation (at design conditions)

- Gross Input: Aperture Area [m²] x DNI [W/m²] = [W]

Start: 100 %

- Reflectivity, Cosine Loss, Blocking, Shading as function of hour and day for each Heliostat (60 – 80%)
  - That is the radiation power leaving the solar field (strongly dependent of day and hour)

Σ 60 -80 %

- Intercept Factor (95%)
  - That is the radiation hitting the receiver

Σ 57 - 76 %

- Absorption of Receiver (95 %) (Factor 0.95)

Σ 54 - 72 %

- Heat Losses of Receiver (8-30 %) (Factor 0.7 – 0.92)
  - This is the power available to the heat engine

Σ 38 - 66 %

Solar Tower Power Plants, Performance Calculation

- The heat engines in tower plants have higher efficiencies than in trough plants, because the tower‘s point focusing delivers higher process temperatures.
- Receiver types:
  - Direct Steam („Solar One“, „PS 10“)
  - Molten Salt („Solar Two“, „Solar Tres“ or „Gemasolar“)
  - Open Volumetric Receiver (Fluid = Air; Prototypes)
  - Pressurized Volumetric Receiver (Fluid = Air; Prototypes)
- At heat engine efficiencies of 45% we can expect total efficiencies of up to 28 % peak and 18% annual average

Solar Tower Power Plants, Performance Calculation

Parabolic Trough
(line focusing)

Tower & Dish
(point focusing)

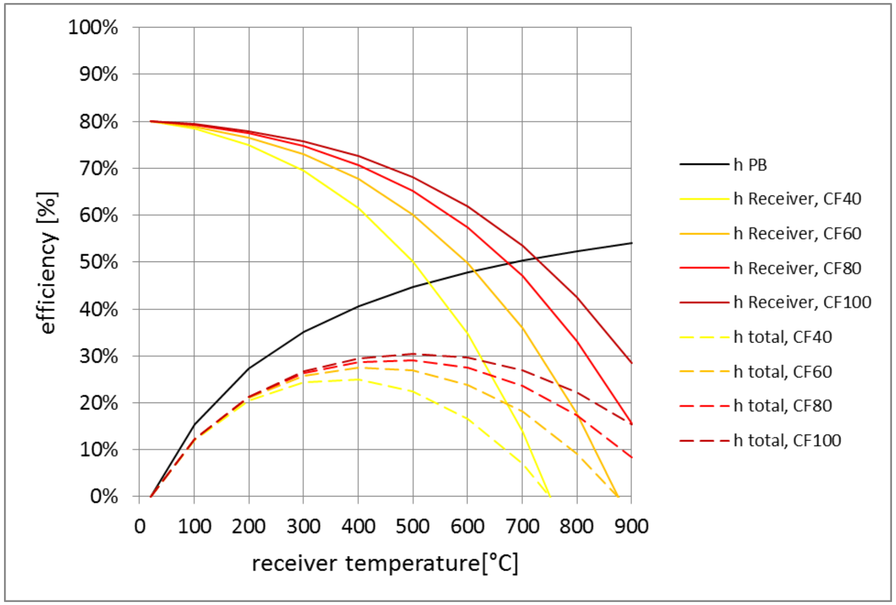

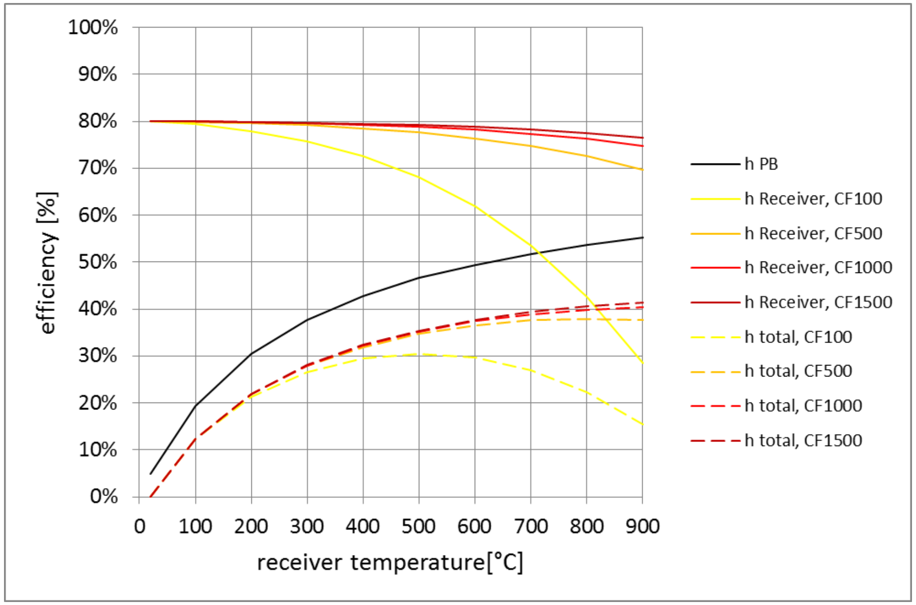

Notes: CF = concentration factor; η_{PB} = Efficiency of power block = Carnot Efficiency * 0,72; $\eta_{total} = \eta_{Receiver} * \eta_{PB}$;
$t_{ambient}$ = 20°C; $\eta_{optical}$ = 80%; DNI = 1000 W/(m² a)

Solar Tower, Status of Application

Important Pilot Plants:

- Solar One: 10 MW_{el}, Barstow, California
- Solar Two: 10 MW_{el}, Barstow, California, Salt-Receiver, TES for 24/7 operation
- CESA-1: 1 MW_{el}, PSA, Almeria, Experimental plant with 3 different receiver types
- Jülich Tower, Germany, 1.5 MW, open volumetric receiver

In commercial operation:

- PS 10 near Seville: 11 MW_{el}, operational since 2007
- PS 20 near Seville: 20 MW_{el}, operational since 2009
- Gemasolar, 19.9 MW ***with 24h/7days*** ***(spring+summer)*** ***TES***, operational since 2011
- Ivanpah, USA, 392 MW_{el}, operational since 2014

Power Tower, Picture Gallery

37° N

Solar One, California

Power Tower, Picture Gallery

Solar One, California

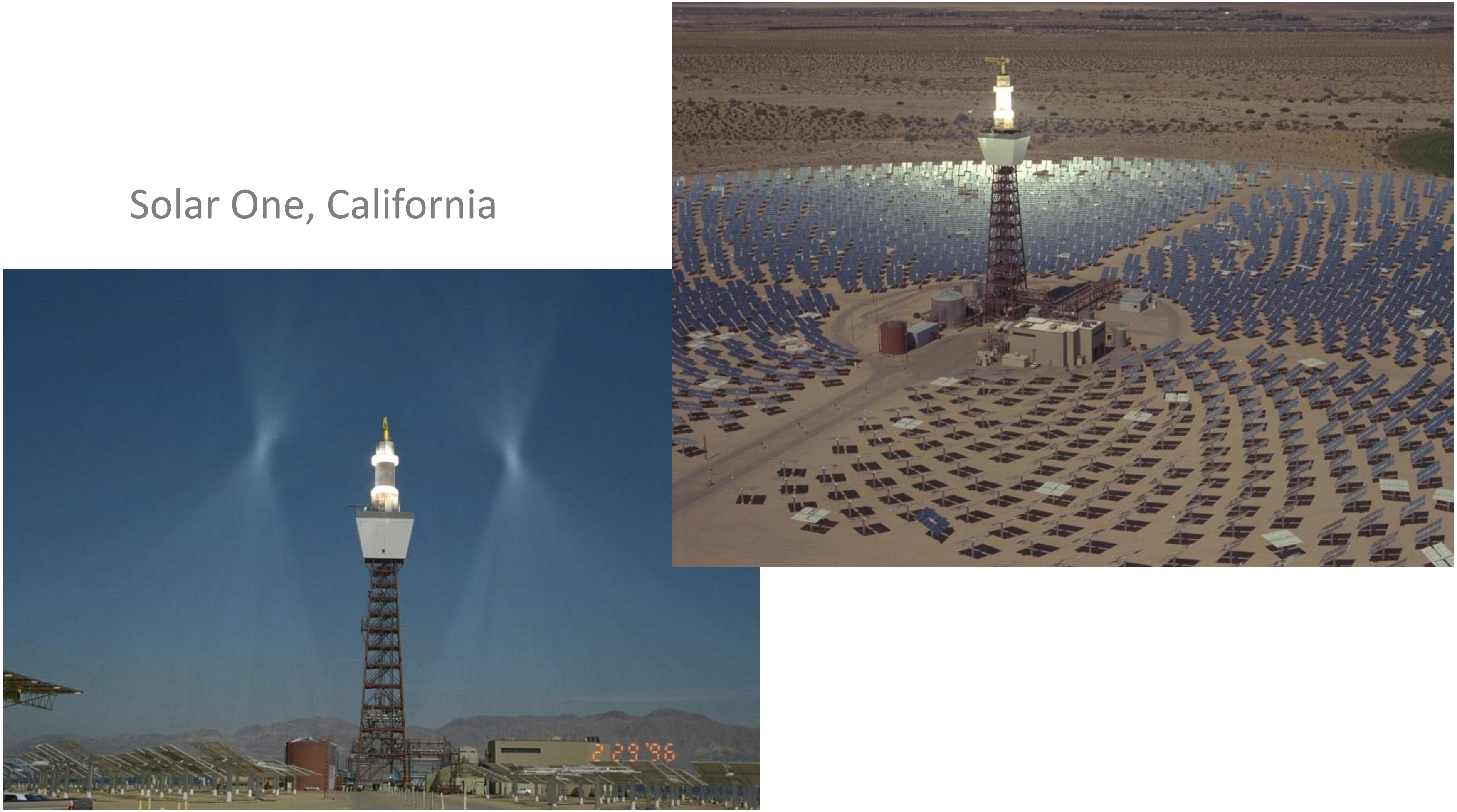

Power Tower, Picture Gallery

Gemasolar, Seville, Spain

Power Tower, Picture Gallery

37° N

Gemasolar, Seville, Spain

Power Tower, Picture Gallery

Gemasolar, Seville, Spain

General Shaikh Mohammed bin Zayed Al Nahyan, UAE National Security Advisor Shaikh Hazza bin Zayed Al Nahyan, UAE Foreign Minister Shaikh Abdullah bin Zayed Al Nayhan, Spanish King Juan Carlos, Torresol Energy's president Enrique Sendagorta and other top officials during the inauguration of the Torresol Energy Gemasolar thermasolar plant in Fuentes de Andalucia near Seville, Spain, on Tuesday. — *AFP*

Power Tower, Picture Gallery

Model, 0,4 m^2 Aperture Area

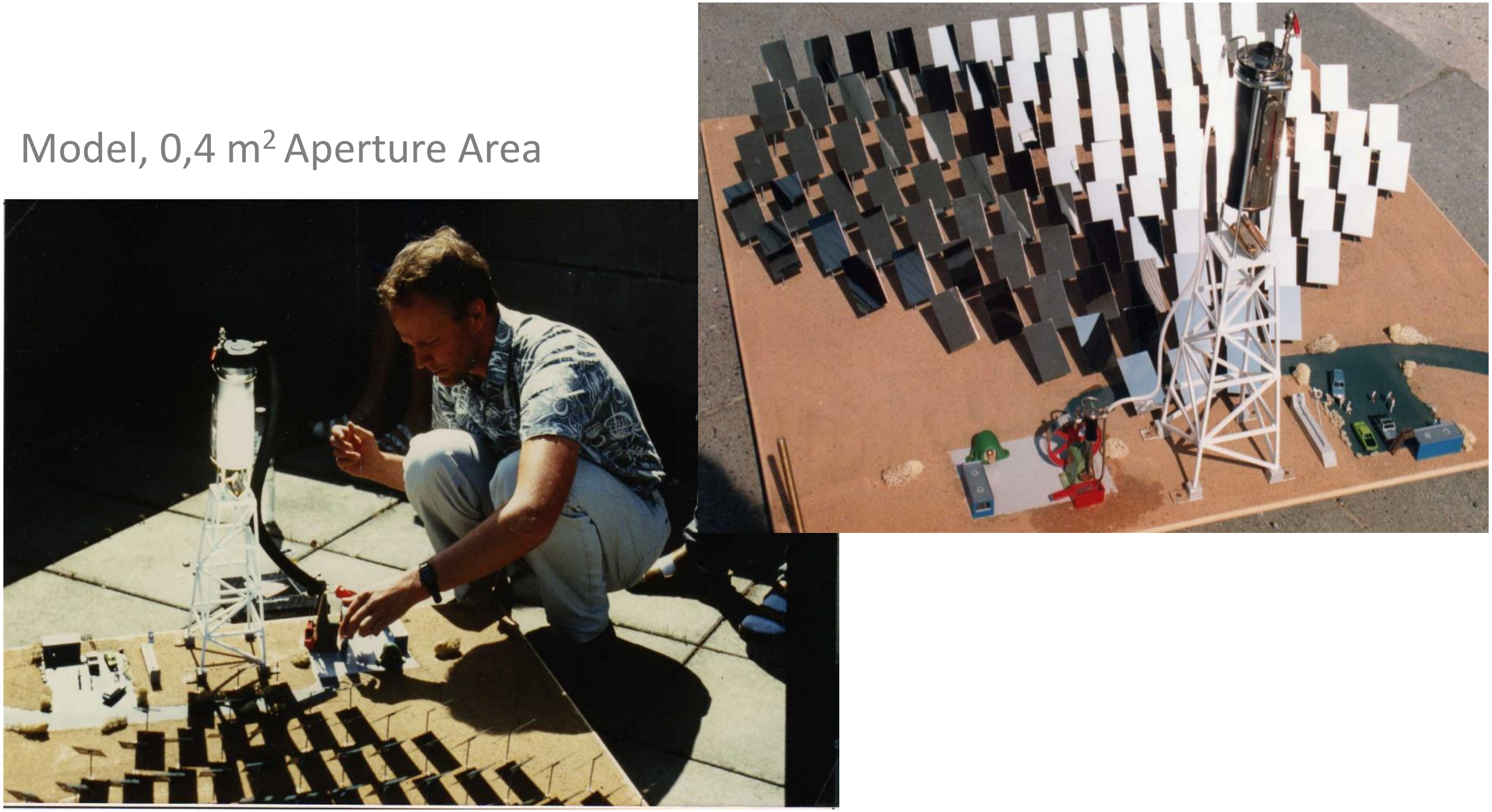

Solar Tower Power Plants, Current Developments

1) Introduction of Thermal Storage

- Pilot Plant „Solar Two“, USA
- 19.9 MW Plant „Gemasolar“ in Spain (SENER & Masdar)
- Molten Salt Storage with up to 300 K usable temperature difference *(compare to parabolic trough with 100 K only)*

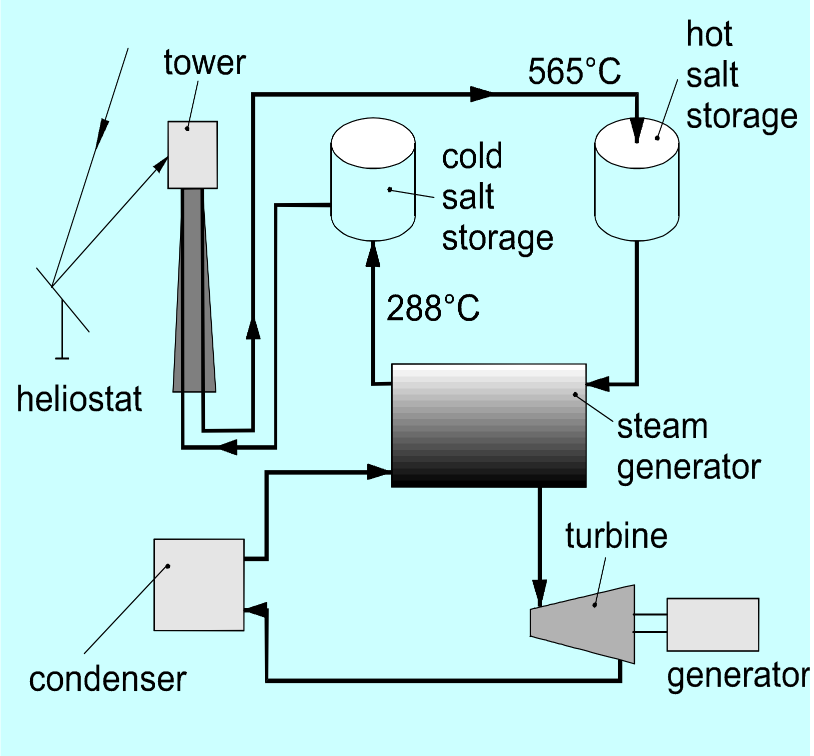

Solar Tower Power Plants, Current Developments

1) Introduction of Thermal Storage (more detailed scheme)

Source: OPERATIVE ADVANTAGES OF A CENTRAL TOWER SOLAR PLANT WITH THERMAL STORAGE SYSTEM
Juan Ignacio Burgaleta, Santiago Arias, Ibon Beñat Salbidegoitia, TORRESOL ENERGY, Solar Paces Symposium Berlin, Sept 2009

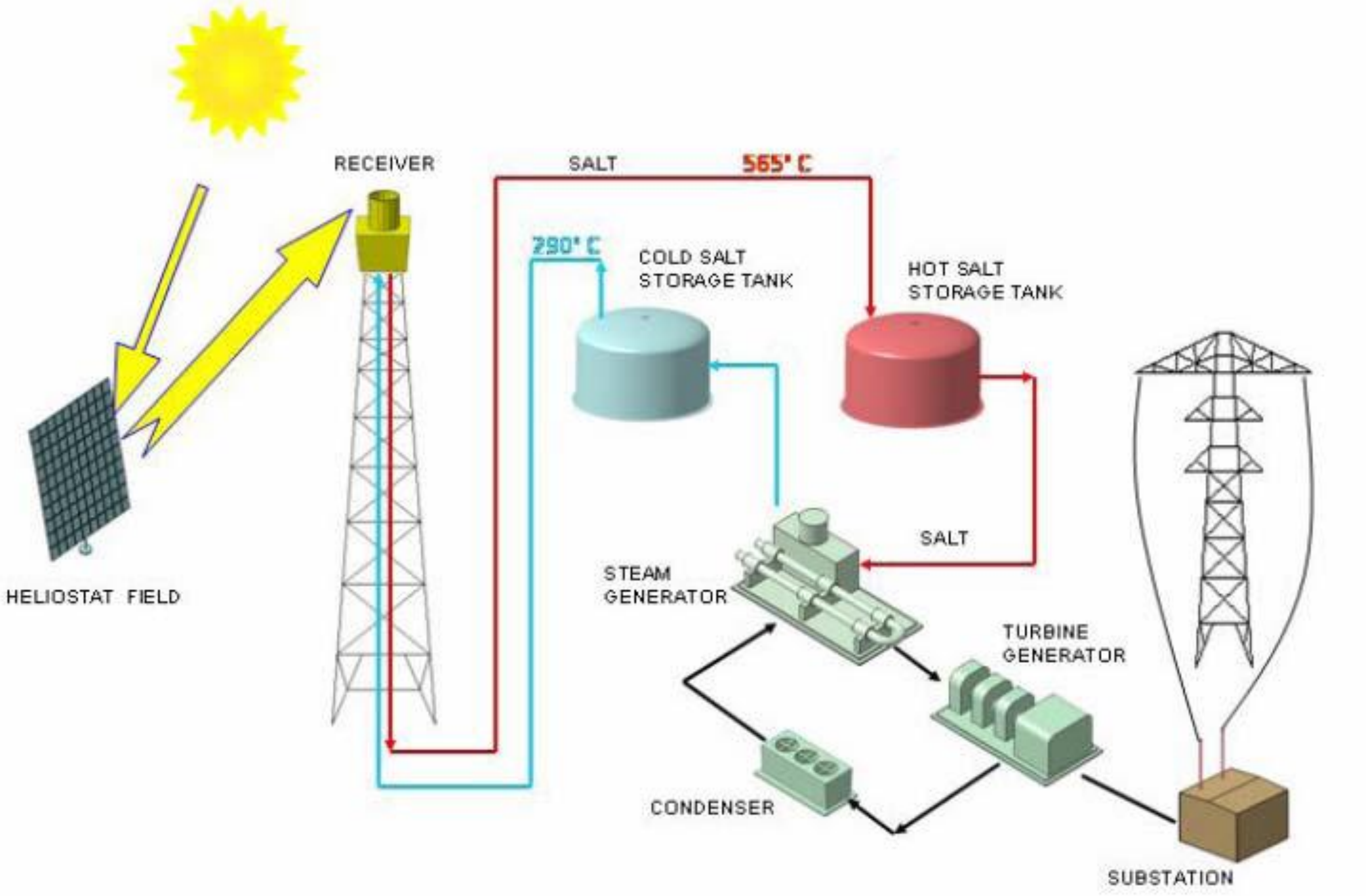

Solar Tower Power Plants, Current Developments

2) Utilization of “Combined Cycle Principle “

- The Receiver becomes the „Combustion Chamber“ of the Gas Turbine. „Pressurized Volumetric Receiver“
- Receiver needs to be pressurized (15 bar) and the window needs to let in the concentrated radiation.
- All components after the receiver are as in a conventional CC Plant
- Prototype running on PSA since 2002, Project „Solgate“

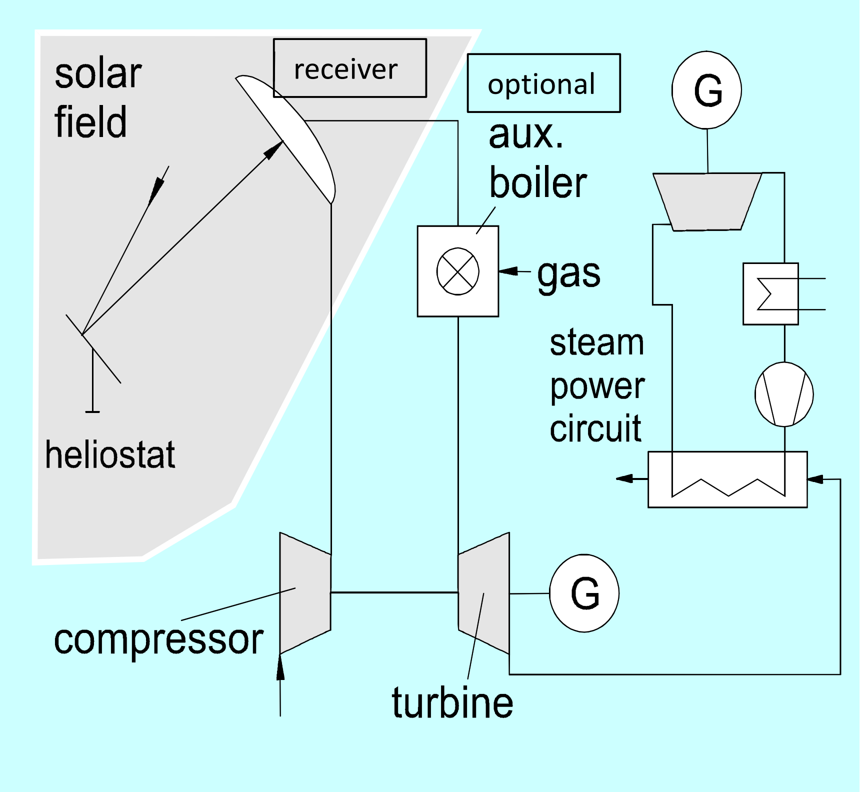

Solar Tower Power Plants, Current Developments

2) Utilization of “Combined Cycle Principle“ (more detailed scheme)

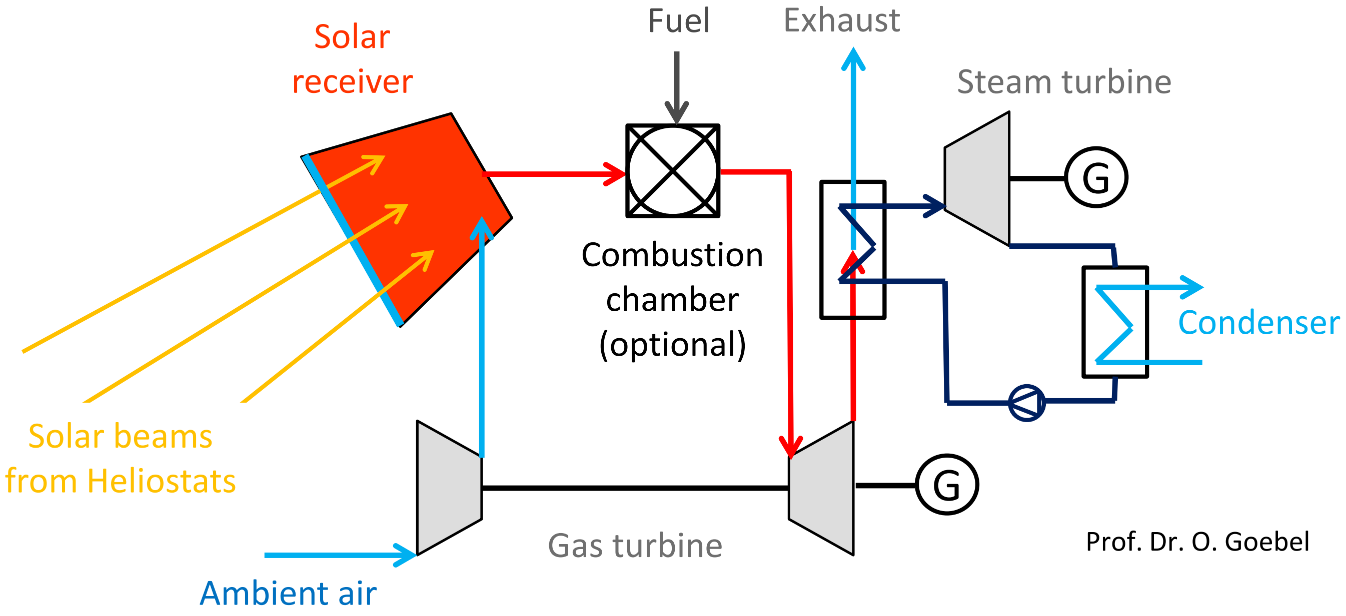

Prof. Dr. O. Goebel

Solar Tower Power Plants, Current Developments

2) Utilization of “Combined Cycle Principle“, The Receiver

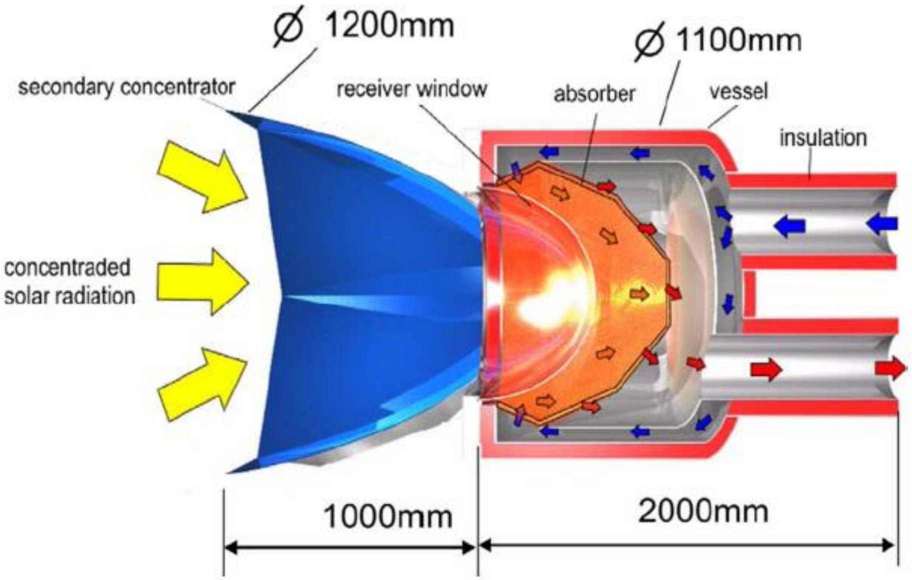

Solar Tower Power Plants, Current Developments

2) Utilization of Combined Cycle Principle (continued)

- Power Process efficiency up to 60%
- Overall total net efficiency up to 38% (peak)
    - ➢ Less area required for solar field
- Large cost saving potential because the solar field (which is cost factor no. one) is smaller
- Utilization of natural gas in hybrid mode is as efficient as in a CC plant (hence the plant can act as base load plant)
- 66% less water consumption than in SEGS plant (due to gas turbine)
- *Heat Storage not yet proven!*

Summary:

- As soon as the very sensitive pressurized volumetric receiver will work reliable, the tower with CC process will be the most efficient and cost efficient solar power technology

Solar Tower Power Plants, Current Developments

3) Open Volumetric Receiver (robust and simple)

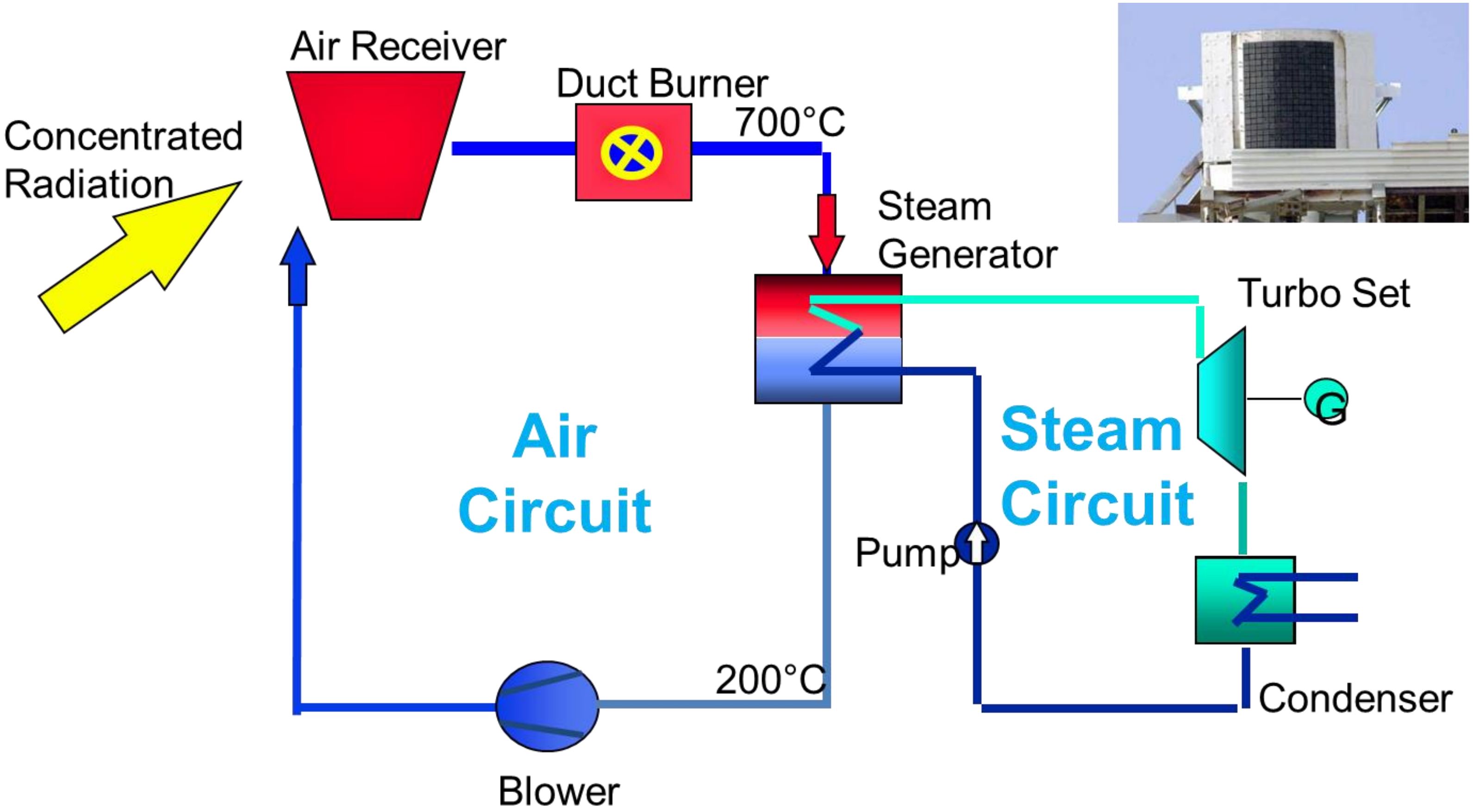

Solar Tower Power Plants, Current Developments

3) Open Volumetric Receiver (robust and simple)

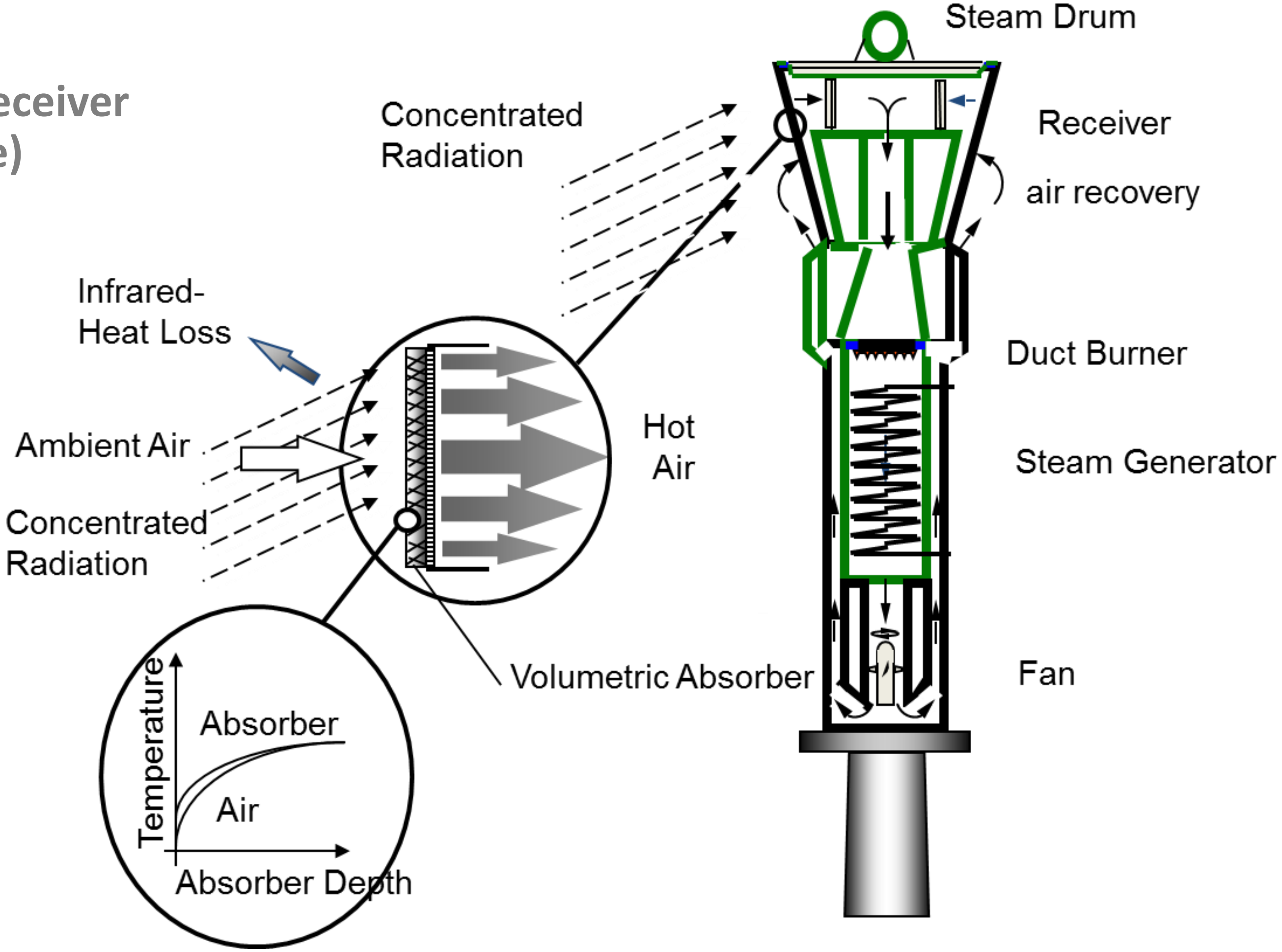

Parabolic Dish
Solar Power Plants
and Miscellaneous Technologies

Solar Dish

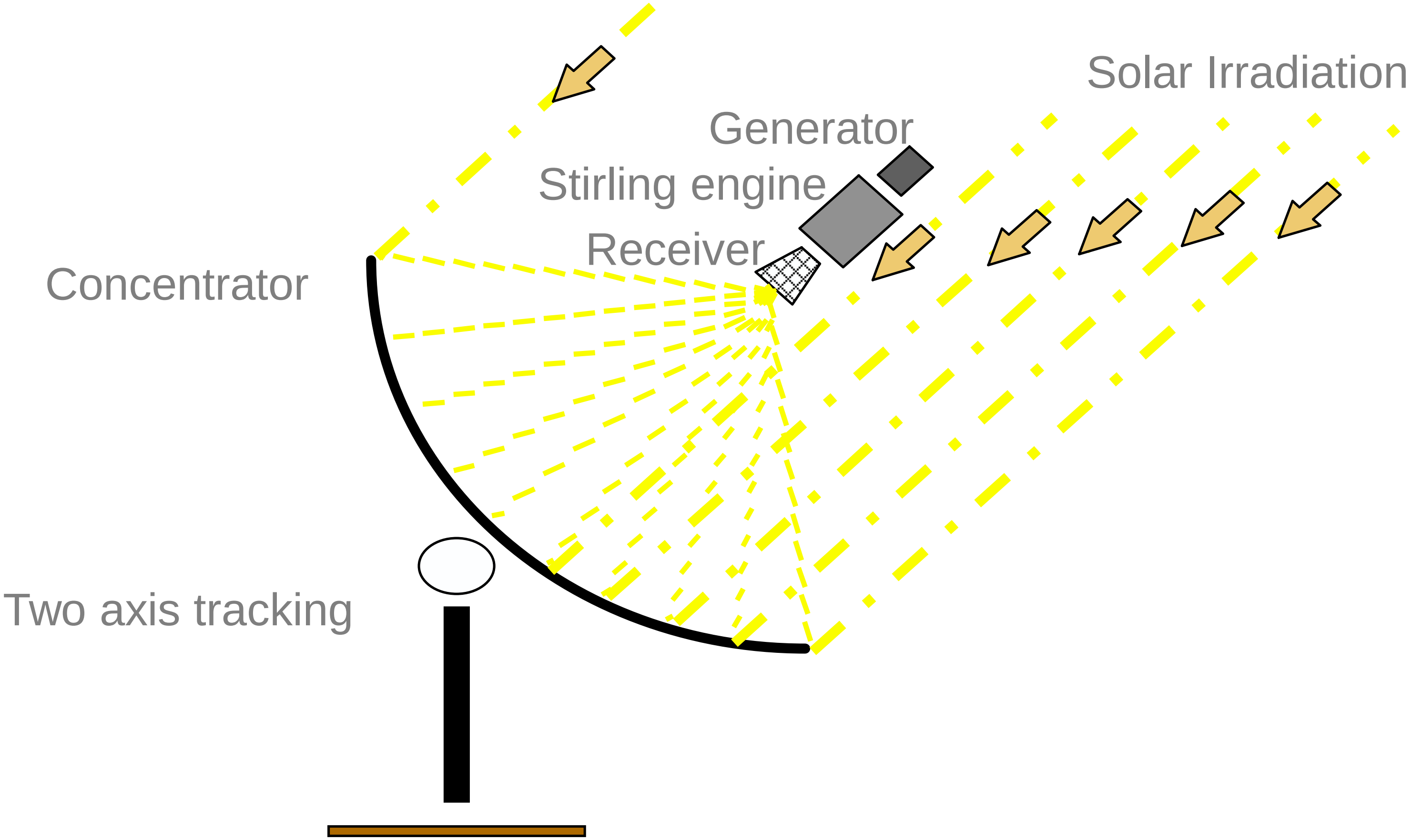
Solar Irradiation
Generator
Stirling engine
Receiver
Concentrator
Two axis tracking

Solar Dish

- Two-axis tracking with high concentration factor (> 2000)
- The heat engine is sitting in the focus and is moving together with the dish
- The generator is directly connected to the engine
- Compact and complete solar power plant
- Highest overall net efficiencies of more than 30% measured

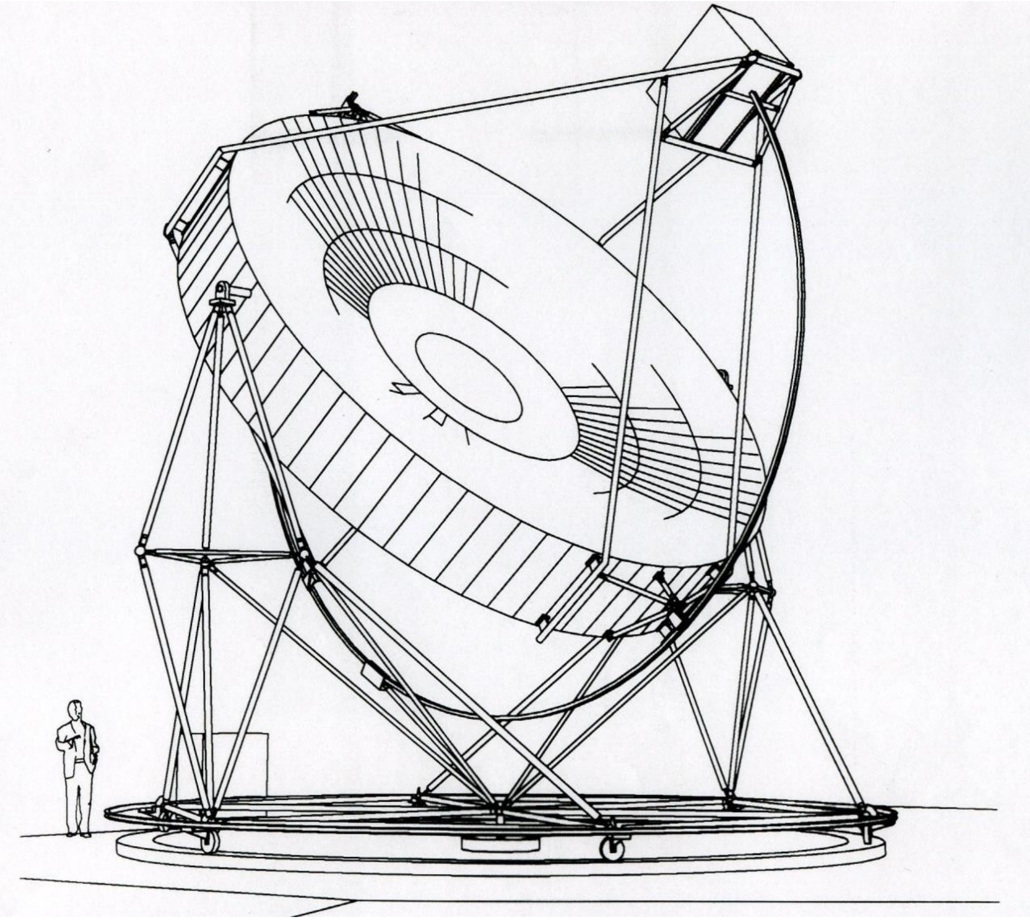

Solar Dish, Possible Heat Engines

Possible are:

- Stirling Motor (mostly used) (η = 25 - 43 %)
- (Micro-) Gas Turbine
- Steam Engine

So far used:

- Stirling Engine
- Micro Gas Turbine
- Steam Turbine (with connecting several dishes in parallel with direct steam generation in the receivers)

- Steam Turbine in single dish not feasible due to small capacity of single dish

Solar Dish, Stirling Engine

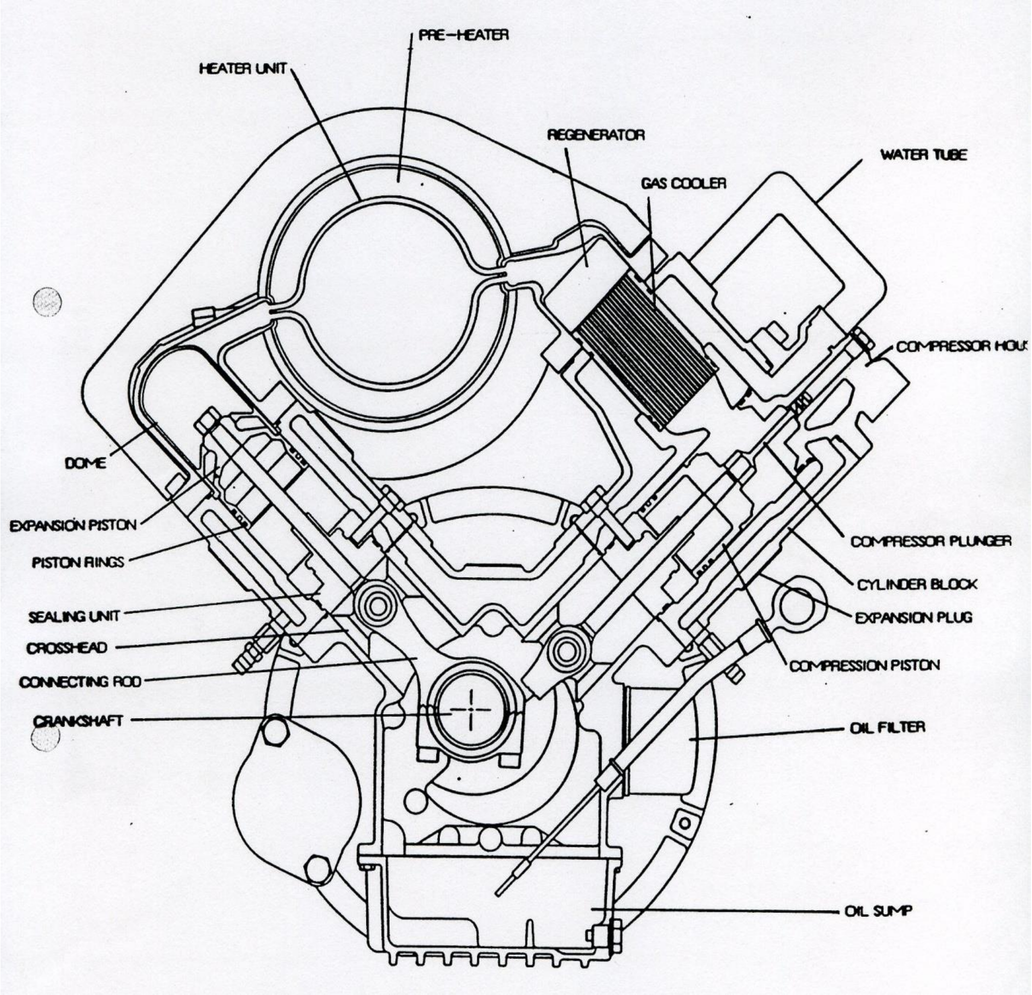

Stirling Motor SOLO V 160

- 10 KW_{el}
- 1500 rpm
- Synchronous-generator
- Working Fluid: Helium
- Gas Pressure: 100 bar
- η approx. 32 %

Solar Dish,
Receiver of Stirling Motor (SBP Dish)

SPS V-160 STIRLING RECEIVER
IM BETRIEB

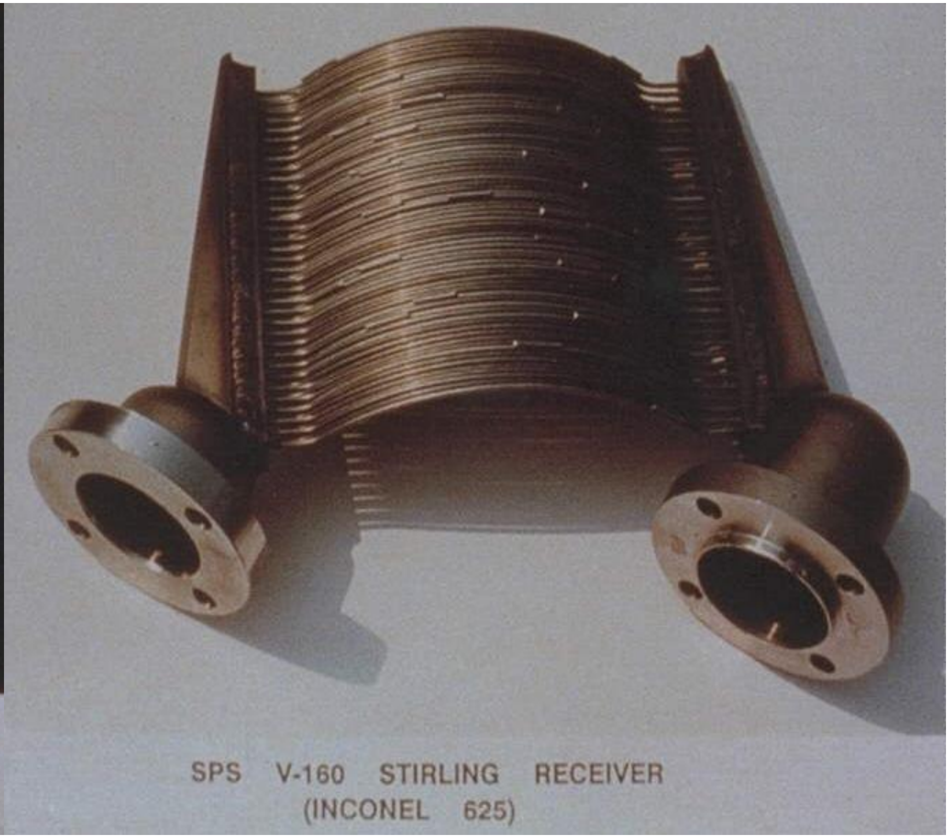

SPS V-160 STIRLING RECEIVER
(INCONEL 625)

Solar Dish, Concentrator Types

1. Dish consisting of many curved glass facets (very exact, but too expensive) (McDonnell Douglas 1985)
2. Dish consisting of few membrane reflectors (Cummins 1992)
3. Stretched Membrane Dish "Drum" with thin glass mirrors (very exact and cheap) (SBP 1984)

Solar Dish, Concentrator

- Always very high efficiency, because light is always perpendicular to aperture. => more full load hours per year!
- Tracking:

1. Polar Tracking (rotation axis parallel to earth axis)
   - Mechanics more expensive, simple algorithm
2. Azimuth – Elevation - Tracking
   - Simple mechanics, more complex algorithm

Solar Dish, Polar Tracking

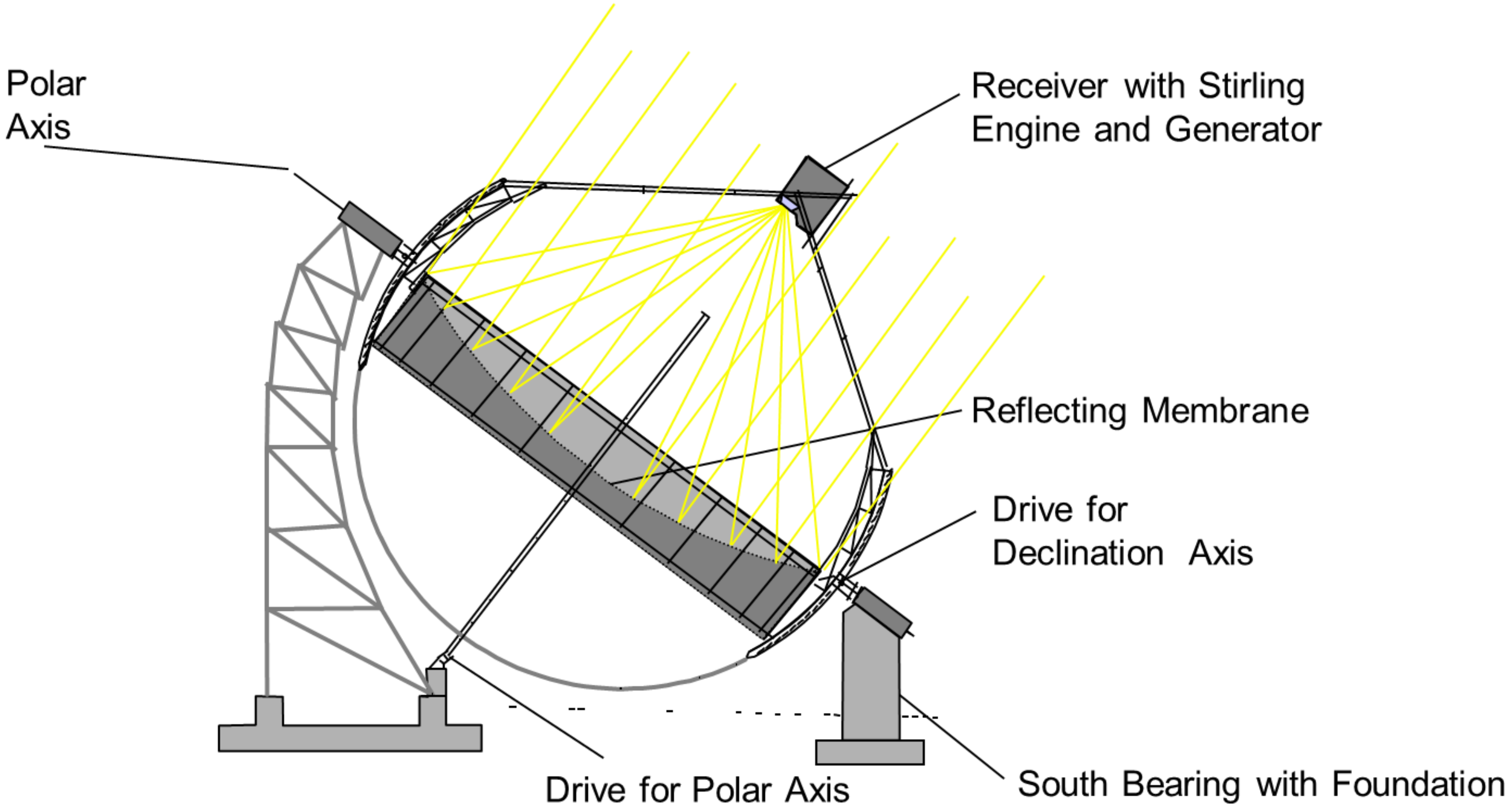

Solar Dish, Azimuth-Elevation Tracking

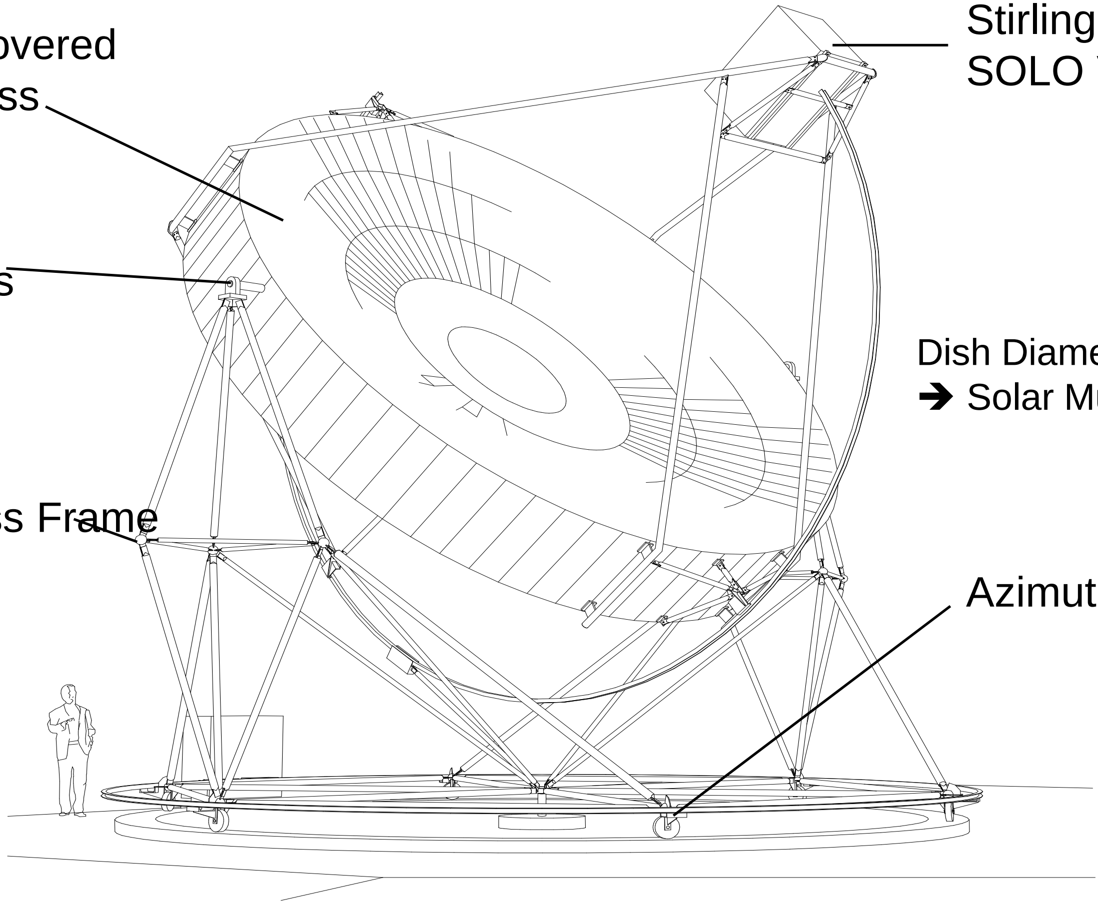

Membrane covered with Thin Glass Mirrors

Elevation Axis

Rotating Truss Frame

Stirling Engine
SOLO V161

Dish Diameter 8,5m
➔ Solar Multiple 1,3

Azimuth Tracking

Autor:	Datum: 12.3.97
File: SBP_D.ppt	Disk: I:

Solar Dish, Performance Calculation (of SBP Dish)

• Gross Input: Aperture [m^2] x DNI [W/m^2] = [W]	Start = 100 %
• Reflectivity	92 %
• Shading (5 %)	95 %
• Intercept Factor	95 %
– This is the Energy hitting the receiver	**Σ 83 %**
• Reflection and Heat Losses of the Receiver (15%)	85 %
– This is the power available to the Heat Engine	**Σ 70,5 %**
• Efficiency of Stirling (SOLO V 160)	32 %
• Overall net Efficiency, solar to electric	**Σ 22,5 %**

Solar Dish, Status of Application

So far no commercial Application

Relevant Prototypes:

- Schlaich Bergermann & Partners (SBP): 17 m Ø, 50 kW_{el}, 3 Units, 1984
- McDonell Douglas: 10,5 m Ø, 25 kW_{el}, 6 Units, 1984
- Cummins: 7,3 m Ø, 7 kW_{el}, 6 Units, 1990
- SBP: 7,5 m Ø, 9 kW_{el}, 9 Units, 1992-96
- SES: „revival“ of McDonnell Douglas unit, 6 units 2007

- The 6 SBP units are running successfully at PSA since 1996
- SES (Stirling Energy Systems, USA) has signed PPA‘s of 1,75 GW in 2008, but the respective projects didn’t happen. SES filed for bankruptcy in 2011

Solar Dish, Current Developments and Summary

1. Integration of fossil fired burners for hybrid operation
   - ➢ Prototype worked, but gas to electric efficiency very low (20%)
2. Integration of thermal storage into the receiver
   - ➢ Prototype worked, but cost is extremely high

Summary of Dish Systems:

- Initially the Dish saw its application between the large scale technologies (trough and tower) and PV. Today‘s low cost of PV and the Dish‘s non compatibility with storage and hybridization lead to a non favorable situation for the Dish concept in general.

Solar Chimney (or „updraft“), Principle

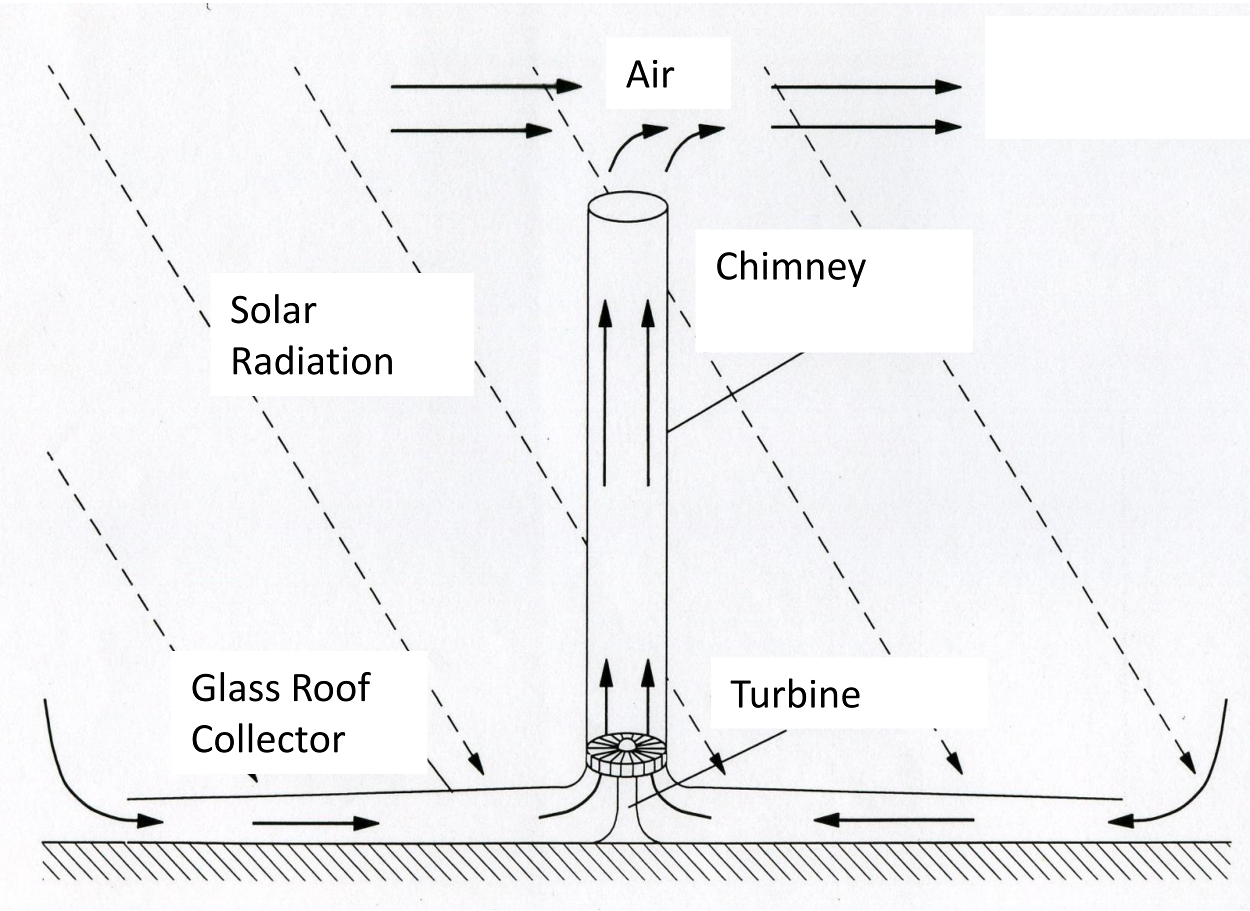

Solar Chimney

- Solar Radiation heats up air under a glass roof. In the middle of the glass roof is the entrance to a chimney, where the heated air can escape. At the bottom of the chimney is a turbine which converts the energy of the air stream into mechanical power.
- The glass roof together with the dark soil forms the solar collector, which is very cheap
- The efficiency of the process is very low:

$$\eta_{\text{total}} = \eta_{\text{Turbine}} \text{ x } \eta_{\text{ Collector}} \text{ x } g \text{ x } H_{\text{Chimney}} / (c_{\text{p, air}} \text{ x } T_{\text{ambient.}})$$

- This leads to an efficiency of 0.3 % per 100 m of tower height (at collector and turbine efficiencies of 100%)
- At realistic assumptions the efficiency is approx. 0.2 % per 100 m of tower height

Solar Chimney,
Status of Application

So far only one Prototype in

Manzanares, Spain:

- Operation: 1982 - 89
- el. Power: 50 kW
- Tower Height: 195 m
- Collector Ø: 240 m
- el. efficiency: 0,12 %

Solar Chimney, further Developments

- Since the Manzanares Prototype no more plant has been built.
- There have been some project developments, but so far none of them reached financial close.
- Generally it is doubtful whether the Solar Chimney is a useful technology. This is mainly due to its very low efficiency (2% at 1000 m chimney height). This is 10 times less than a parabolic trough plant.

Not CSP

Solar Pond

Stratification of saltwater layers very sensitive!

At this type of solar power plant a pond with a black ground and a filling with salty water functions as the receiver and as a heat storage at the same time. In the pond with a typical depth of 6 m the water forms three layers, which are stable due to the salt concentration which increases from the surface towards the ground. The lower layer with a thickness of approx. 4 m forms the absorber and the storage. The upper layer with a thickness of 0.5 m has the lowest salt content and serves as isolator against thermal losses. The layer in the middle is characterised by a high gradient of the salt concentration and serves as a separator between the upper and the lower layer.

The heat of the lower layer is transferred through a heat exchanger into an organic Rankine cycle. In the condenser of the Rankine cycle the water of the upper layer is used for cooling. With an upper process temperature of 90°C, efficiencies of 6 - 10 % are reached in the Rankine cycle. The overall efficiency of the system lies between 1.5 and 2 %. Beside plants in Australia and USA, the plant of Beith Ha' Arava (Israel) with its power output of 5 MW is the biggest prototype, built so far. In comparison to the concentrating technologies the Solar Pond Power Plant leads to low investment cost (area specific), but similar to the Solar Chimney the efficiency is pretty low.

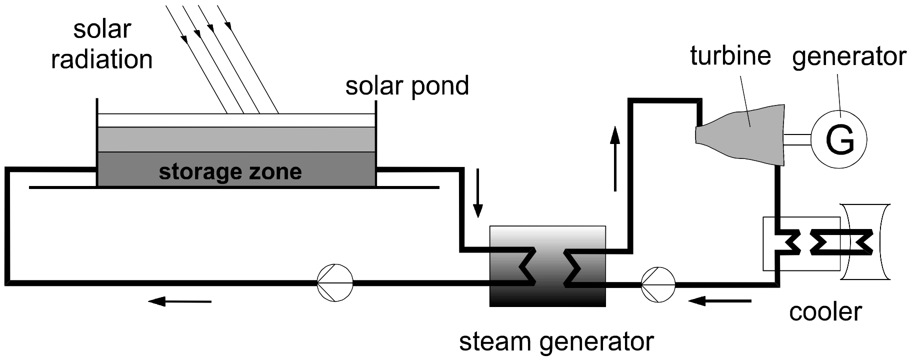

Task:
Calculate η for T_{max} = 90°C and T_{min} = 30°C, tpf = 0,5

$$\eta_{Carnot} = \frac{T_{max} - T_{min}}{T_{max}}$$

Here: T_{max} = 90°C, T_{min} = 30°C

$$\eta_{Carnot} = \frac{60K}{363K} = 16{,}5\%$$

With tpf 0,5 => η = 8,25%

Condenser Cooling and Heat Utilization

Cooling of the Condenser at Steam Power Plants

- CSP plants mostly use the Rankine Cycle to convert heat into power.
- The efficiency and power output of the turbine increase with lower pressures in the condenser (suction).
- The condenser pressure depends on the condenser temperature.
- Hence, a heat sink with the lowest possible temperature leads to the maximum efficiency and power of the process.

Cooling of the Condenser at Steam Power Plants

The 3 mostly used Cooling Principles are:

1) Water Cooling in **Once Trough** (River- or Sea Water)
    - Cheap
    - Achieves low condenser temperature
    - Huge water mass flow: $\dot{m}_{cooling\ water} \approx \dot{m}_{steam\ circuit} \cdot 60$

2) **Wet Cooling** Tower
    - High water consumption (evaporation): $\dot{m}_{evaporation} \approx \dot{m}_{steam\ circuit}$
    - Most efficient at low humidity of ambient air

3) **Air Cooled Condenser** (ACC) or “Dry Cooling”
    - Only used where no water is available
    - Relatively high condenser temperatures
    - High power demand for fans (up to 4% of gross power)
    - Most expensive- least efficient

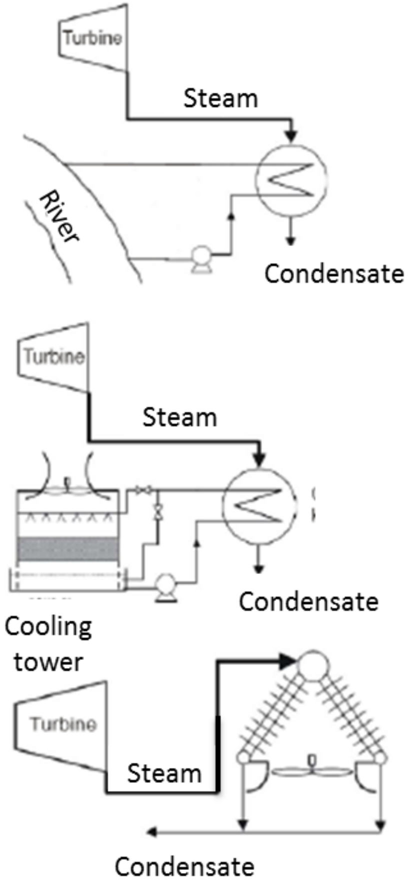

Cooling of the Condenser at Steam Power Plants

It is beneficial when the rejected heat of the condenser can be used for a second process.

Possible Utilization:

1) District Heating (only useful in regions with long heating season)
   - ➢ (usually not the case at regions with high DNI)
2) Process Heat for Industry
3) Sea Water Desalination
4) Cooling, “District Cooling“ (Absorption Chillers)

To be considered in all cases:

- Rising of Condenser Temperature required to receive usable heat
- => significant <u>reduction of electric efficiency</u> (minus 40% at Desalination)
- => overall efficiency higher, but electric efficiency reduced
- The <u>heat consumer needs to sit directly next to the CSP plant</u>, because heat cannot be transferred over longer distances.
- <u>This is unlikely</u>, because CSP plants are usually build in remote locations (cheap land)

Site Evaluation
for CSP Plants

Site and Infrastructure

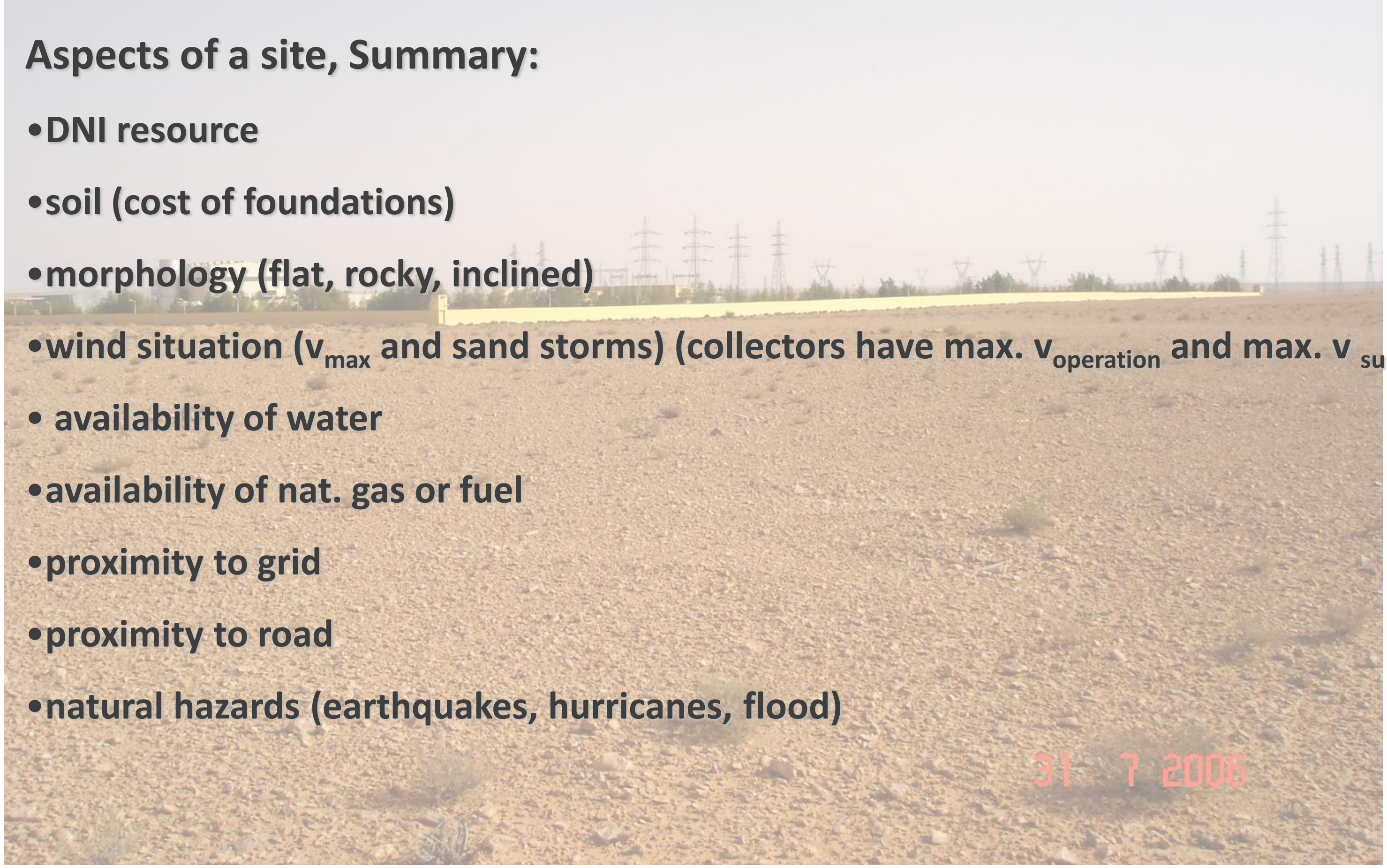

Aspects of a site, Summary:

- DNI resource
- soil (cost of foundations)
- morphology (flat, rocky, inclined)
- wind situation (v_{max} and sand storms) (collectors have max. $v_{operation}$ and max. $v_{survival}$)
- availability of water
- availability of nat. gas or fuel
- proximity to grid
- proximity to road
- natural hazards (earthquakes, hurricanes, flood)

Site Evaluation 1/4

A site for a power plant project shall be evaluated regarding the following aspects:

1. Electric Grid (High Voltage (HV) grid):
   - Distance to the HV grid
   - Distance to the next sub station
   - Available free capacity in the HV grid
   - Readiness of the grid operator to accept the additional power
   - Possible route for the connecting cable from the plant to the sub station
   - Power supply during construction of the plant

2. Transport Infrastructure:
   - Distance to next highway / railway / harbor
   - Carrying capacity of this transport connection chain (largest / heaviest plant component)
   - Possible route of the connecting road to the existing road network
   - Goods to be transported: plant components during construction, fuels, spare parts, people, evacuation of Soil etc.

Site Evaluation 2/4

3. Fuel Supply:
   - Distance to the next fuel supply point (oil or gas pipeline or coal harbor)
   - Possibility of fuel supply from this point (technically and commercially)
   - Possible route of the connection (pipe or road) to this point

4. Water:
   - Availability of cooling water (selection of cooling type, calculation of water demand)

5. Topography of the Site:
   - Flatness of the site
   - Cost of site levelling
   - Any stream courses on site? (flooding potential, ask for history!)

6. Soil properties at site:
   - Carrying capacity of the soil => cost for soil improvement
   - Workability of the soil (penetrability) => cost of foundation

Site Evaluation 3/4

7. Weather conditions at site:
    - Temperature profile along the year=> Which plant components will need shelter / heating / cooling?
    - Precipitation along the year => Which plant components will need shelter
    - Danger of fast flowing streams => Preparation of respective measures
    - Maximum wind speeds (strength of buildings and structures)
8. Seismology at site
9. Quality of the solar (DNI) resource
    - See Chapter at the beginning of the course

Site Evaluation 4/4

10. EIA, Environmental Impact Assessment :
    - Is the site habitat for protected plants and/or animals?
    - Does the project endanger neighboring habitats of plants and/or animals (e.g. drainage of wetlands, bird migrating routes)?
    - Endangering of ground water (lowering or contamination)
    - Noise disturbance (noise maps)
    - Visualization of the project and investigation of the visibility from sensible view points (visual impact study)

11. Social Acceptance:
    - Community representatives, local administrations, citizens' action groups, NGO‘s

12. Permits and Licenses:
    - Ownership, real estate office, land development plan, land use planning, civil engineering department (pipelines), traffic administration, police, telecommunication administration, military (concentration area, disturbance of radar, low altitude flight corridor)

Data Sources

- The site evaluation is based on the above mentioned data. It is extremely important that the data are taken from reliable sources.
- Preferably the data shall be sourced first hand.
  - Weather data from a weather institution and not from another study.
  - Soil data from a soil investigation at the site and not from another study.
- If first hand data are not available and second hand data have to be used, this shall be clearly indicated in the study report.

Calculation of Electricity Generation Cost

Electricity Generation Cost, EGC

- A widely used method for calculating EGC is the annuity method.
- How it works: The annual capital cost are kept constant (during the depreciation period) by reducing the interest payment each year and a respective increase of the pay back such that the total (pay back + interest) is constant over the years.
- This method leads to pretty good values for the EGC when the input data are correct.

Electricity Generation Cost, EGC

- A CSP plant has two main fixed cost components:
  - **Annual capital cost**
  - **Annual O&M (operation & maintenance) cost**
- The cost per kWh of electricity is calculated by dividing the annual fixed cost by the annual energy yield.

➢ $\frac{[€/a]}{[kWh/a]} = [€/kWh]$

Parameter 1

Parameter 2

- $EGC = \frac{annual\ capital\ cost + annual\ O\&M\ cost}{annual\ electricity\ generation}$

Parameter 3

Electricity Generation Cost, EGC

Parameter 1) Capital Expenditures (CAPEX):

CAPEX = EPC price + Owner's Cost

- Main components of CAPEX are:
  - Equipment
  - Transport
  - Duties
  - Installation cost
  - Initial spare parts
  - Ground preparation and foundations

EPC price (EPC = engineering procurement, construction)

  - Access roads
  - Grid connection (sub station)
  - Soft costs:
    - Financing costs (Interest during construction, fees)
    - Project development
    - Advisor fees (Lender's and Owner's Engineer, financial and legal Advisor)
    - Permits and licenses
    - Insurance before COD

Owner's cost

Electricity Generation Cost, EGC

Parameter 1) Capital Expenditures (CAPEX):

The capital for a power plant project is usually supplied by 2 sources:

1. Equity
2. Bank loan, mostly called "debt"

- The equity providers request a higher interest rate (called RoE, return on equity) than the banks ask for the debt, because they carry a higher risk.
- Typical debt / equity ratios range between 80/20 and 70/30
- The calculation of the annual capital cost is usually performed using the annuity method.
- The annuity is a combined payment of interest and repayment with a constant annual rate.

Electricity Generation Cost, EGC

EXCEL Exercise

Explanation of annuity with simple example

Loan = 100 $, payback time = 10 years, interest rate = 10%

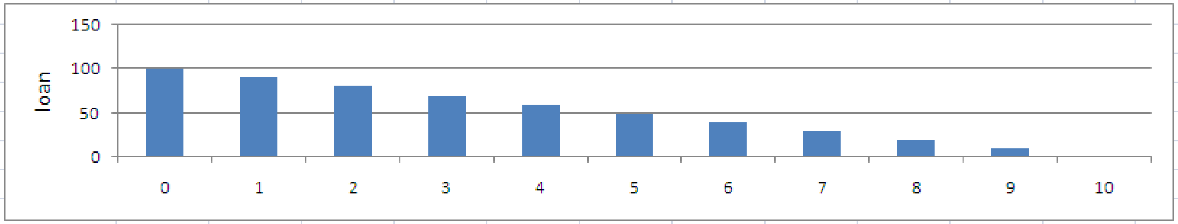

year	0	1	2	3	4	5	6	7	8	9	10	total	total avg
Loan	100	90	80	70	60	50	40	30	20	10	0		
annual pay back	0	10	10	10	10	10	10	10	10	10	10	100	10
interest payment		10	9	8	7	6	5	4	3	2	1	55	5.5
total annual payment	0	20	19	18	17	16	15	14	13	12	11	155	15.5

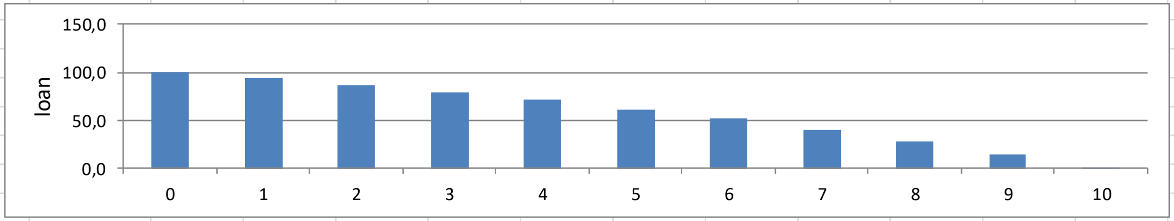

	0	1	2	3	4	5	6	7	8	9	10	total	total avg
Loan	100,0	93,73	86,83	79,25	70,90	61,72	51,62	40,52	28,30	14,86	0,07		
annual pay back	0,0	6,27	6,90	7,59	8,35	9,18	10,10	11,11	12,22	13,44	14,78	99,9	10,0
interest payment		10,00	9,37	8,68	7,92	7,09	6,17	5,16	4,05	2,83	1,49	62,8	6,3
total annual payment	0,0	16,27	16,27	16,27	16,27	16,27	16,27	16,27	16,27	16,27	16,27	162,7	16,3

Electricity Generation Cost, EGC

Parameter 1) CAPEX: annuity method, example:

- RoE: 13% p.a.
- debt rate: 6.5% p.a.
- Debt equity ratio: 70 / 30
- With this data we calculate the weighted average cost of capital WACC):
  - ➢ *WACC = 0.3 * 13% + 0.7 * 6.5% = 8.45%*
- Depreciation period: 25 a
- With this data we calculate the annuity rate: 9.7 % / a

- Equation for the annuity rate: = $\frac{WACC*(1+WACC)^n}{(1+WACC)^n-1}$ *n = depreciation period in years*
- The annual capital cost is: annuity rate * CAPEX

Electricity Generation Cost, EGC

Parameter 2) **Operation & Maintenance Cost, O&M cost:**

In a first approach O&M cost are expressed as a percentage of the CAPEX cost. Typical values are:

- Wind Farms: 3% / a
- PV: 1 - 2% / a
- CSP: 2.0 - 2.5% / a
- Coal fired plants: 2 % / a
- CC plants: 3 - 4 % /a

In a more detailed approach it is distinguished between variable and fixed O&M cost.

Electricity Generation Cost, EGC

Parameter 3) Energy Harvest:

- Energy harvest is the parameter out of the three, which is most difficult to obtain
- Energy harvest depends on technology and site condition
- For CSP plants the energy resource is DNI (Direct Normal Irradiation)

Electricity Generation Cost, EGC

Parameter 3)

Energy Harvest:

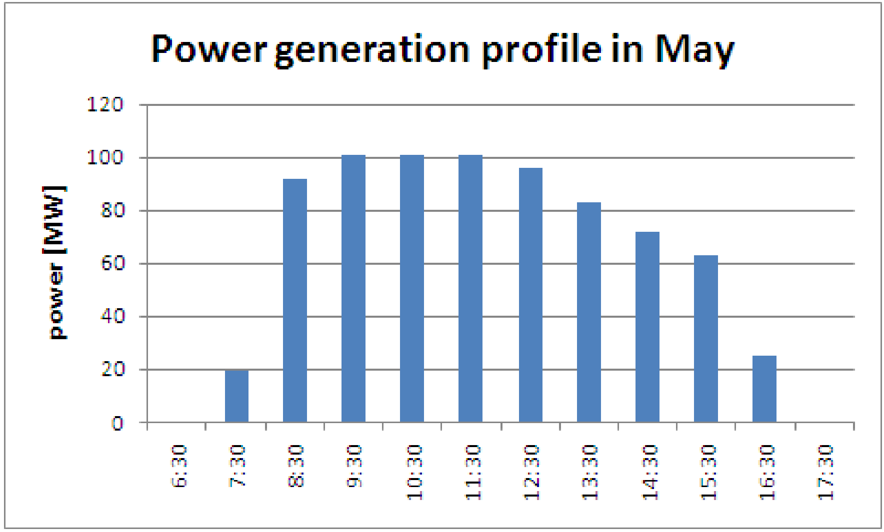

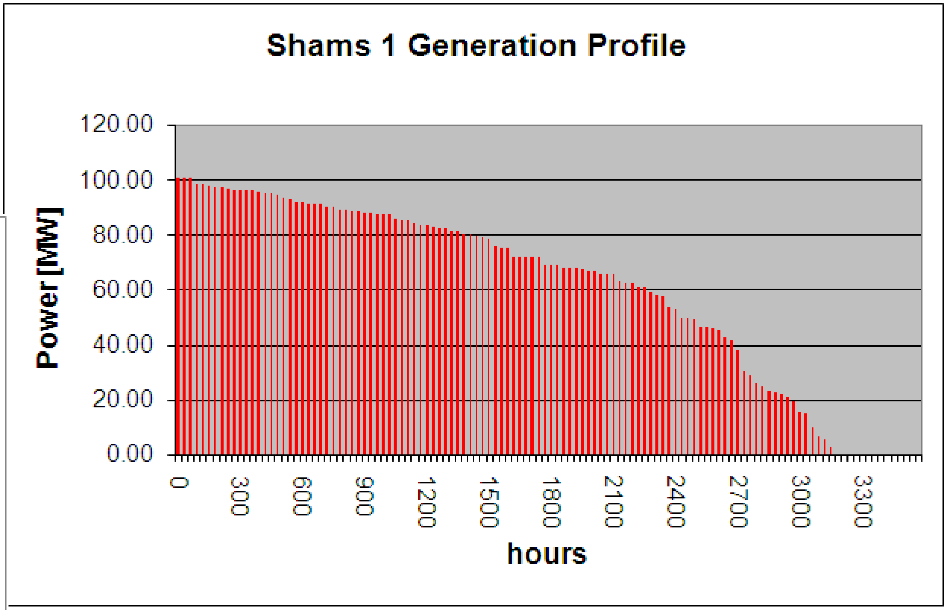

Electricity Generation Cost, EGC

Parameter 3) **Energy Harvest:** The concept of full load hours [kWh/kW/a] or [h/a]

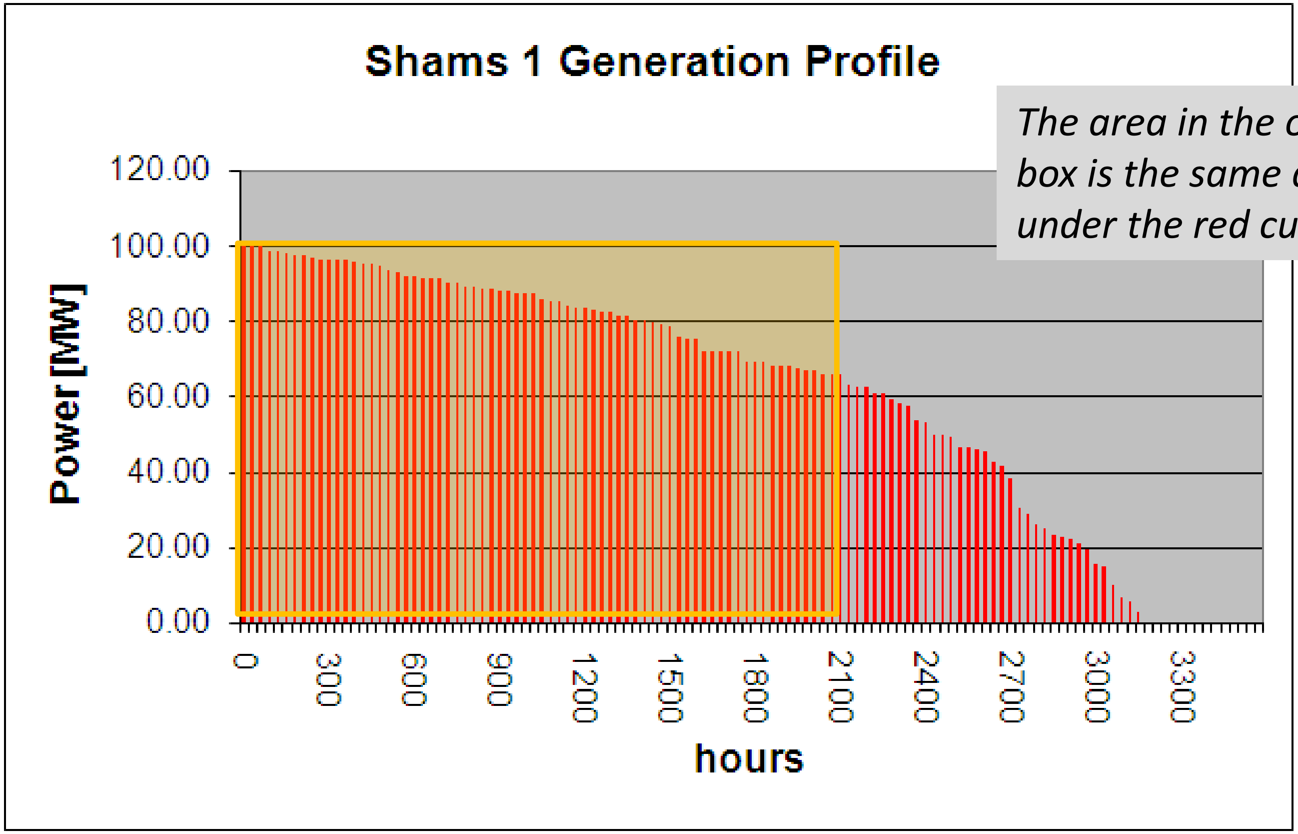

The area in the orange box is the same as under the red curve

Electricity Generation Cost, EGC

Parameter 3) **Energy Harvest:** The concept of capacity factor [% of full capacity]

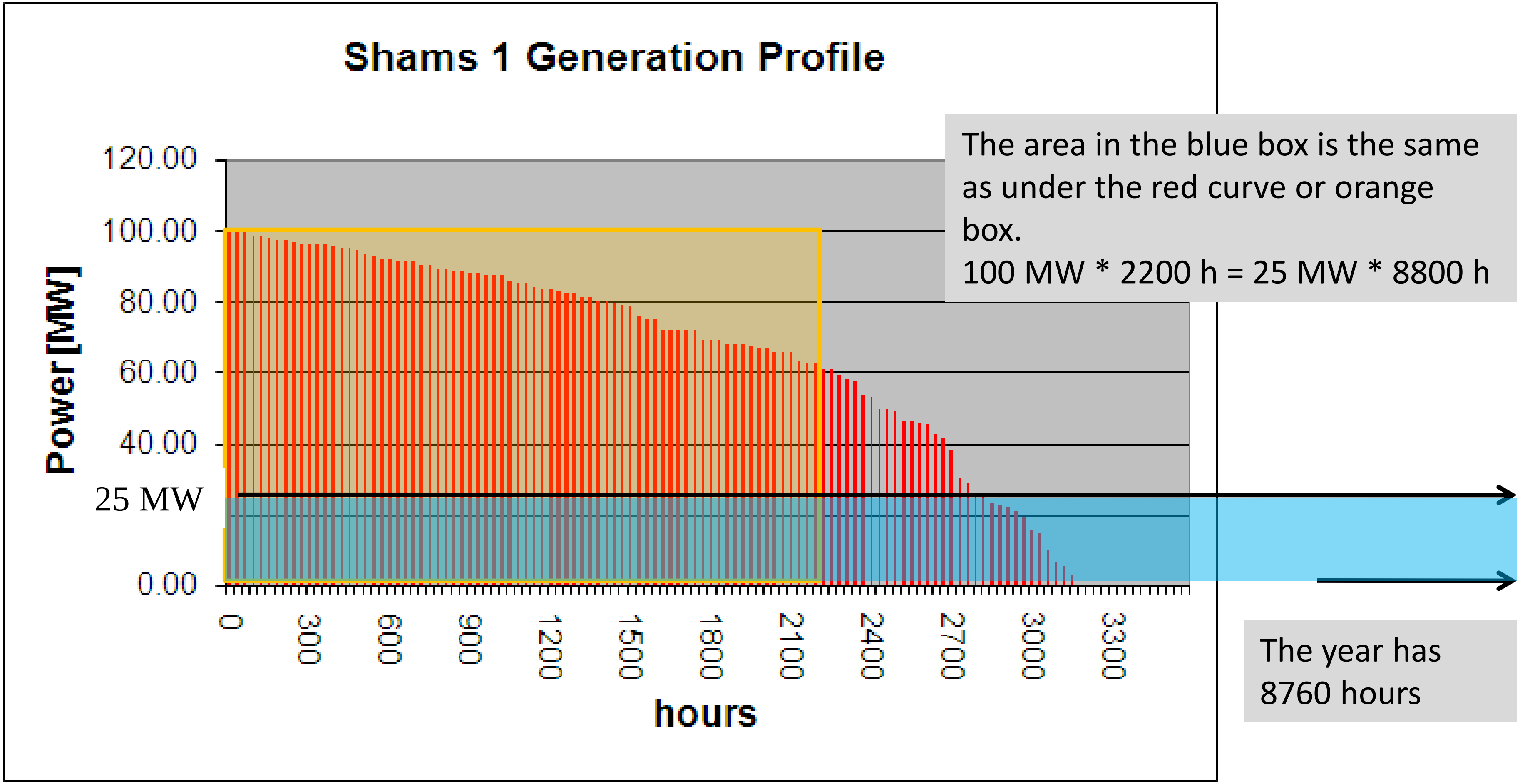

The area in the blue box is the same as under the red curve or orange box.
100 MW * 2200 h = 25 MW * 8800 h

The year has 8760 hours

Electricity Generation Cost, EGC

Parameter 3) Energy Harvest:

The impact of the Nominal Load:

- A given plant generates 220000 MWh per year
- Call it a 100 MW plant and you get 2200 h /a
- Call it a 120 MW plant and you get 1833 h / a

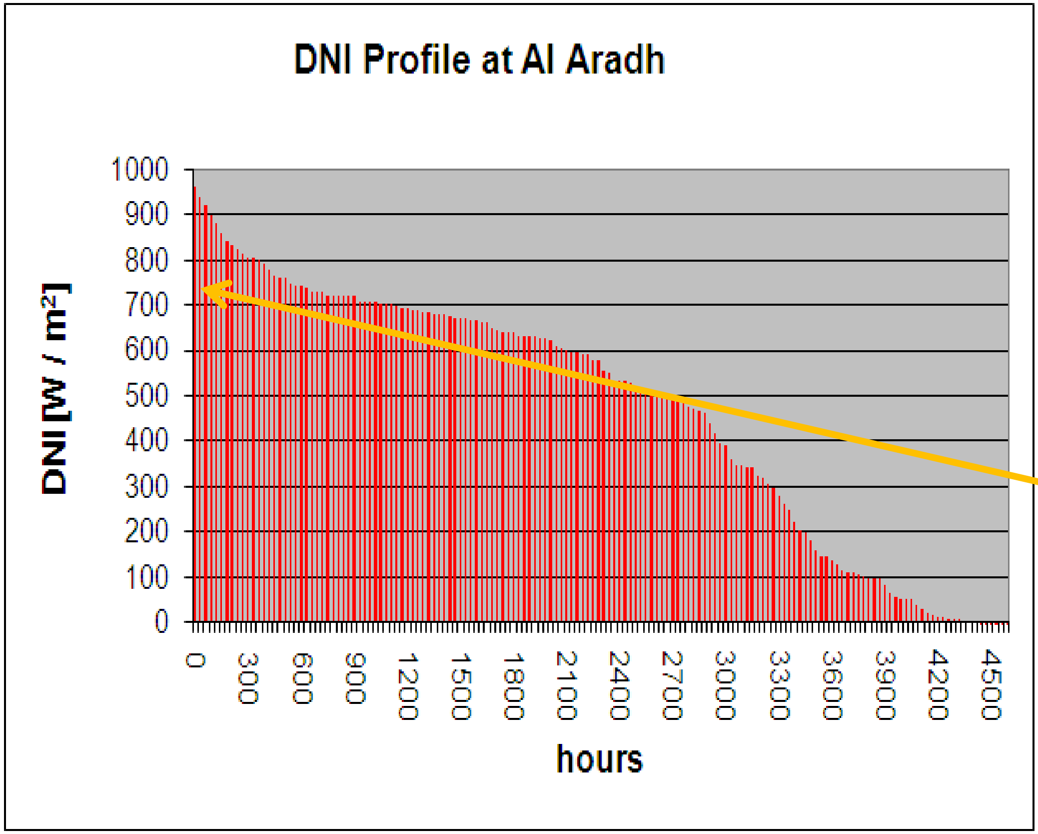

CSP plants reach their nominal load between 700 and 800 W/m^2

Electricity Generation Cost, EGC

Parameter 3) Energy Harvest:

Regardless of all theory, at the end of the day the harvest [kWh / year] can be measured for a real system or simulated with good tools (tools should be calibrated against real plant data).

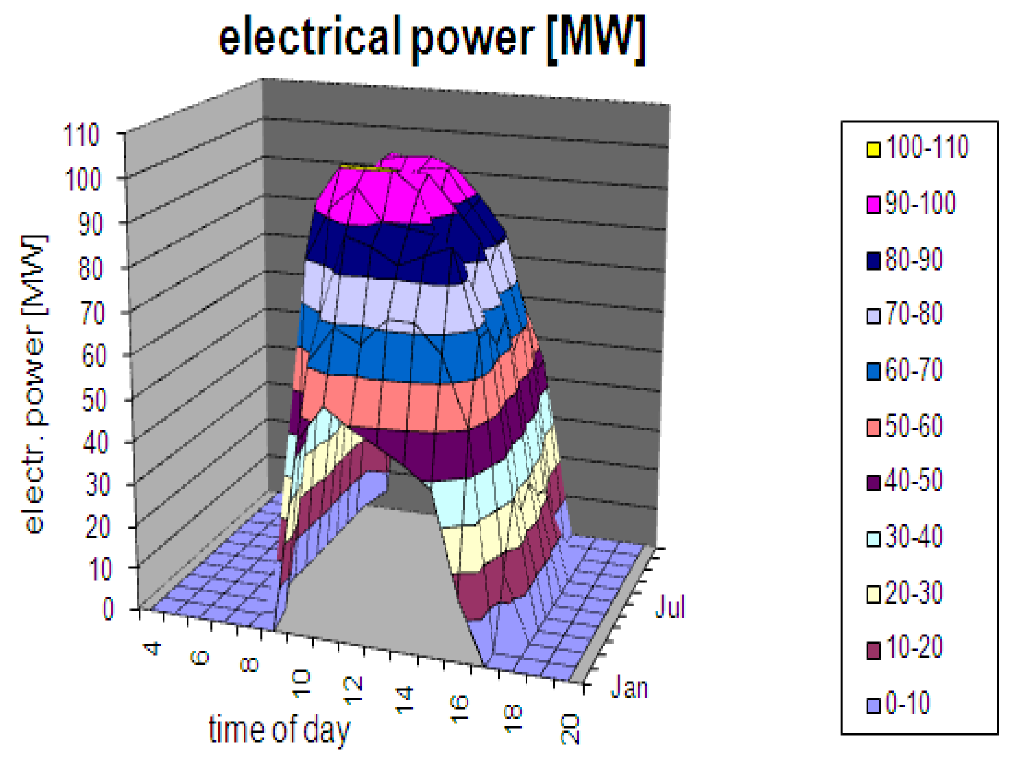

Electricity Generation Cost, EGC

4) Combining the two components in one equation:

- $EGC = \frac{annual\ capital\ cost + annual\ O\&M\ cost}{annual\ electricity\ generation}$

Or simpler: EGC= $\frac{CAPEX * (annuity + O\&M\ percentage)}{annual\ electricity\ generation}$

Example CSP plant:

Parameter 1

Parameter 2

Parameter 3

CAPEX:	400 million USD
OPEX:	2.5 % of the CAPEX p.a.
Energy yield p.a.:	100 MW * 2000 h/a = 200 GWh / a
Annuity:	9,7% p.a.

- $EGC = \frac{400 * 10^6\ (9{,}7\% /a + 2.5\% /a)}{200 * 10^6\ kWh /a}$ = 0.244 USD/kWh = **24.4 ct/kWh**

Electricity Generation Cost, EGC

The equation is easier to apply when we replace the annual electricity generation by:

Annual electricity generation = Capacity * FLH (FLH = full load hours)

Then: $EGC = \frac{CAPEX *(annuity + O\&M\ percentage)}{annual\ electricity\ generation}$

transforms to: $EGC = \frac{CAPEX/Capacity *(annuity + O\&M}{FLH}$ $\underline{\ \ percentage)}$

Example CSP plant:

- CAPEX/Capacity: 4000 USD / kW
- OPEX: 2.5 % of CAPEX p.a.
- FLH: 2000 h/a
- Annuity: 9,7% p.a.
- $EGC = \frac{4000\ /kW\ (9{,}7\%\ /a + 2\%\ /a)}{2000h/a}$ = 0.244 USD/kWh = **<u>24.4 ct/kWh</u>**

Electricity Generation Cost, EGC

Typical EPC Prices for different power plant types:

Coal fired plants:	1200 – 1600 $ / kW
Gas turbine plants:	400 – 500 $ / kW
Combined Cycle plants:	700 – 800 $ / kW
Wind power:	1200 – 1500 $ / kW
Photovoltaic:	1000 – 2000 $ / kW
CSP:	4000 $ / kW (higher when equipped with TES)

For calculating the CAPEX: When no further information is available the owner's cost can be assumed with 20% of the EPC price.

Why is Electricity of Fossil Fired Plants Cheaper?

- Fossil fired plants need much less material
- A 100 MW gas turbine (GT) contains 100 tons of steel
- The solar field of a 100 MW PT plant contains 12 000 tons of steel (120 times more than GT)
- Dimensions of a 100 MW gas turbine: 10 m x 30 m, the whole plant 100 m x 100m (1 hectare)
- Dimensions of a 100 MW solar plant: 2 km^2 (200 times more than GT)

Why is Electricity of Fossil Fired Plants Cheaper?

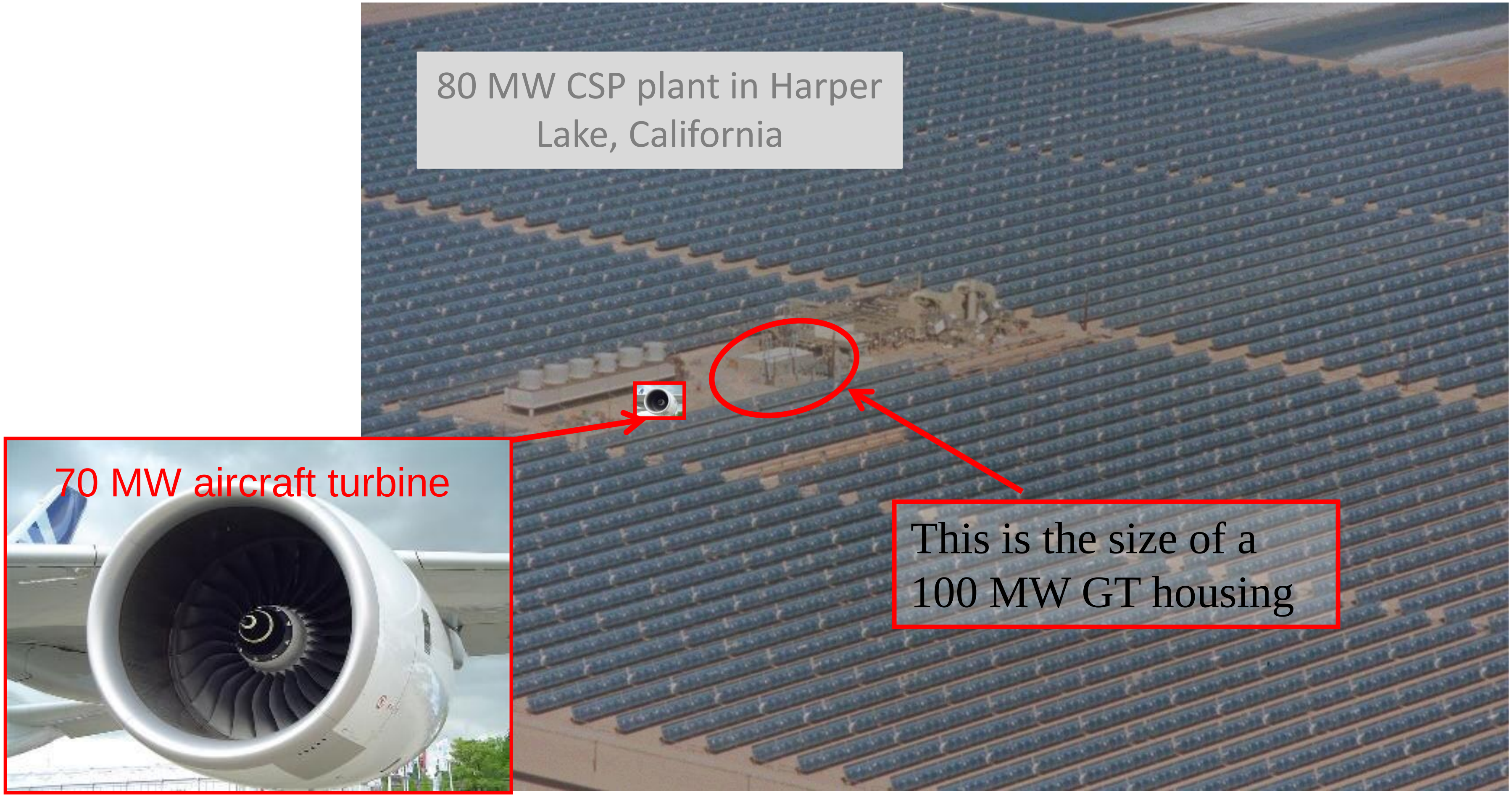

80 MW CSP plant in Harper Lake, California

70 MW aircraft turbine

This is the size of a 100 MW GT housing

Why is Electricity of Fossil Fired Plants Cheaper?

What is the message of the “Harper Lake” picture?

- EPC prices of solar plants will always be higher than EPC prices of fossil fired plants!
- The steel mass factor may go down from 120:1 to 60:1, but solar will never be cheaper in CAPEX!
- The only way to break even will be through higher fuel prices
- CSP (Californian conditions) breaks even at oil price of 70 to 120 $/barrel (depending on full load hours of fossil competitor)
- Or at coal prices of 400 $ / ton (today 80 $ / ton)
- Or at gas prices of 0.5 $ / m^3 (12 $ / MMBTU) (peaker)
- Until reaching this point, subsidies are required

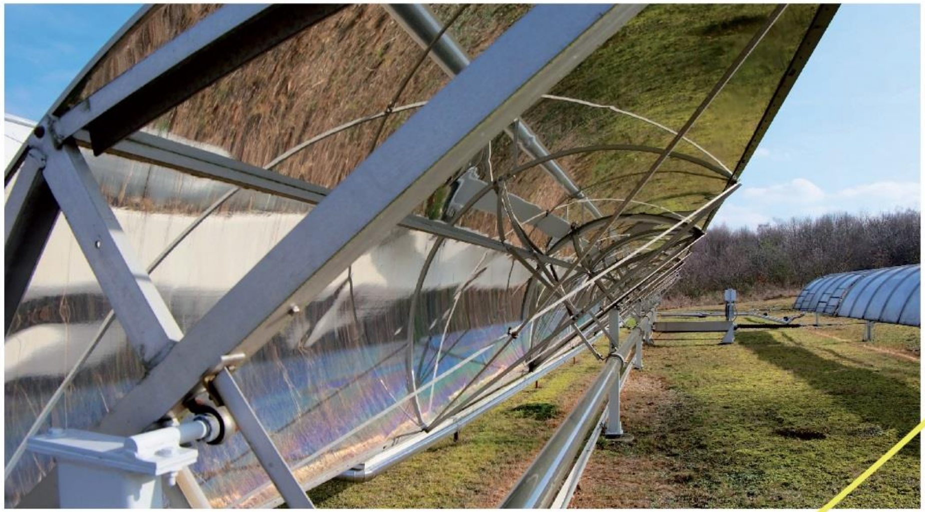

Thank you for your Attention!

Dr.-Ing. Jürgen Rheinländer
Solar Thermal Power
Engineer and Consultant

Prof. Dr.-Ing. Olaf Goebel
Hochschule Hamm-Lippstadt
Olaf.goebel@hshl.de

Ministério da
**Ciência, Tecnologia
e Inovação**

Reserve

Parabolic Trough Solar Power Plants: Integrated Solar Combined Cycle System, ISCCS

The Problem of low efficiency when running a regular Parabolic Trough Plant on gas

CC = Combined Cycle plant
SEGS = Parabolic Trough CSP plant

When a Parabolic Trough CSP Plant is operated for many hours per year on nat. gas, then it burns more gas than a CC plant of the same capacity, due to its poor gas to electric efficiency.